The Aging Brain in Semantic Cognition

Insights from fMRI & TMS

Dissertation

Zur Erlangung des akademischen Grades

Dr. rer. med.

an der Medizinischen Fakultät

der Universität Leipzig

eingereicht von

M. Sc. Sandra Martin

geboren am 01.12.1987 in Halle/Saale

angefertigt am

Max-Planck-Institut für Kognitions- und Neurowissenschaften, Leipzig

Betreuerin: Prof. Dr. Dorothee Saur

Ko-Betreuerin: PD Dr. Gesa Hartwigsen

Beschluss über die Verleihung des Doktorgrades vom:

"*I do not think of old age as an ever grimmer time that one must somehow endure and make the best of, but as a time of leisure and freedom, freed from the factitious urgencies of earlier days, free to explore whatever I wish, and to bind the thoughts and feelings of a lifetime together.*"

Oliver Sacks

Contents

1 General Introduction

Most of us have probably experienced the following situation at some point in our lives: We are in the middle of a conversation and suddenly fail to produce the intended word although we are certain we know the word and have used it before. Often, this phenomenon is related to the retrieval of factual knowledge from semantic memory, for example the name of the actor who played Forrest Gump or the name of the musical instrument that is played without physical contact by the performer. Although such transient failures to access conceptual knowledge are common across all age groups, the rate of so-called tip-of-the-tongue episodes and word retrieval problems increases with age and makes them a frequent complaint among healthy elderly (Bowles & Poon, 1985; Burke & Shafto, 2004; Lovelace & Twohig, 1990).

The age-related increase in failures to access and retrieve information from semantic memory stands in contrast to the observation, that semantic knowledge is usually preserved or even grows through adulthood into very old age (Nyberg et al., 1996; Rönnlund et al., 2005; Verhaeghen, 2003) and that general communication abilities remain largely intact in healthy aging (Kintz et al., 2016). This paradox has been explained in terms of less efficient access and retrieval processes during language processing, which rely on cognitive control functions such as working memory, attention, and inhibitory control, and are well established to steadily decline with age (Hedden & Gabrieli, 2004; Park & Reuter-Lorenz, 2009). To date, the neural mechanisms underlying those age-related changes in access to semantic memory are poorly understood. However, a better understanding of the neural reorganization processes and the neural resources that help to maintain cognitive functions would be mandatory to promote successful aging.
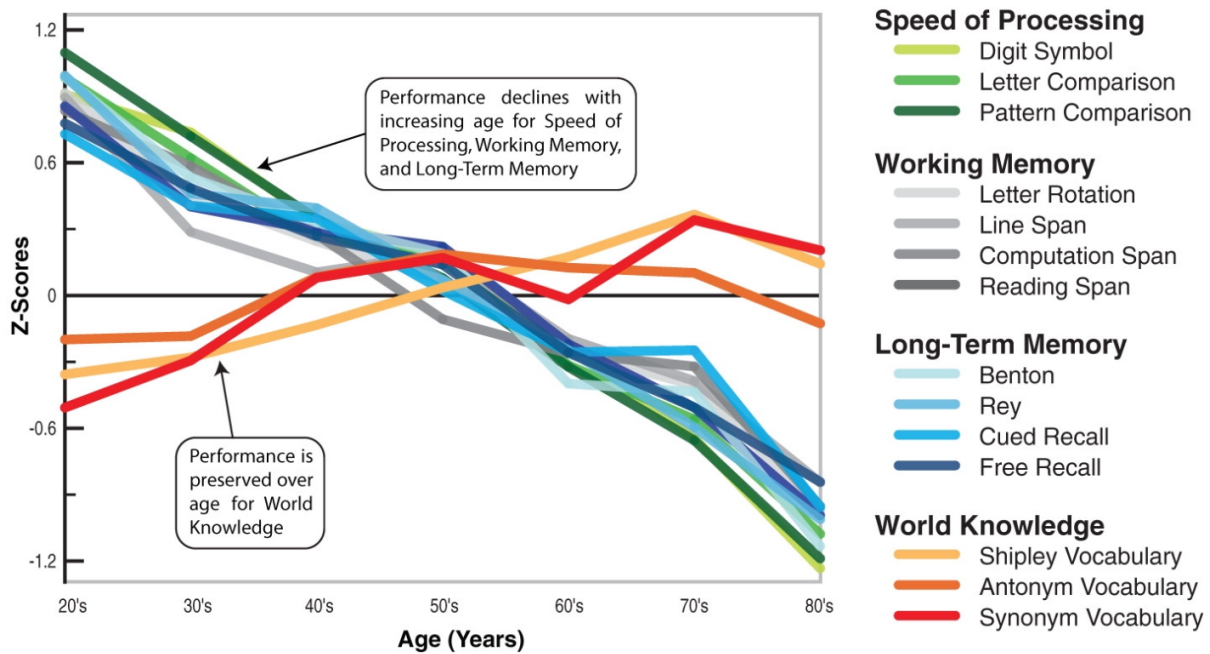
The present thesis addresses this gap by exploring age-accompanied changes in the neural network architecture during semantic processing and their impact on behavior. Using functional magnetic resonance imaging (fMRI), cognitive measures, and transcranial magnetic stimulation (TMS), the age-related interaction of domain-specific and domain-general neural networks during the retrieval and access of information from semantic memory were investigated. **Study 1**—an fMRI study—addressed the contribution of domain-general (task-positive and task-negative) networks to a semantic word retrieval task in healthy young and older adults, while **study 2** analyzed the same data set applying a whole-brain functional connectivity approach and exploring age differences in the coupling of task-relevant networks and their behavioral relevance. Graph theoretical measures of brain system integration and segregation were used to examine the network topology in young and older adults. Finally, **study 3**—a

TMS-fMRI study—tested the potential of enhancing a hub in the prefrontal cortex associated with domain-general but also semantic control processes via facilitatory stimulation in a group of healthy middle-aged to older adults. The behavioral impact of the stimulation and its neural correlates were investigated in a subsequent fMRI experiment employing a semantic language comprehension task. Overall, the findings of these studies point towards a pattern of neural reorganization in the aging brain, even when language processing abilities remain intact. We provide evidence for age-related neural dedifferentiation in semantic cognition and shed new light on the compensatory potential of such reconfiguration processes.

1.1   Cognitive Aging

Aging is accompanied by a myriad of cognitive changes. Although trajectories of cognitive aging are highly individual and inter-individual variability is striking (Cabeza et al., 2018), the steady age-related decline of cognitive control processes—also referred to as fluid intelligence—is well established (Figure 1.1; Hedden & Gabrieli, 2004). Such processes have been shown to exhibit pronounced age effects and include the domains of working memory, processing speed, mental flexibility, spatial reasoning, and inhibitory control (Hasher et al., 1991; Mitchell et al., 2000; Salthouse, 1996). Semantic memory on the other hand, which refers to the knowledge about words, concepts, and ideas we have accumulated across the lifespan (so-called crystallized intelligence), remains stable or might even increase due to the ongoing accrual of knowledge and experience across the life course (Nyberg et al., 1996; Salthouse, 2004; Verhaeghen, 2003).

   Due to the largely intact system of semantic memory in healthy aging, language processing is typically not associated with strong age-related decline. However, changes have been reported on the word, sentence, and discourse level (Kemper & Anagnopoulos, 1989; Obler & Pekkala, 2008; Peelle, 2019). On the language production side, a common complaint relates to increased word finding problems, as described in the Introduction. Longitudinal research revealed an initial decline in lexicosemantic retrieval abilities for people in their 50s, though the strongest effects have been observed from the age of 70 (Au et al., 1989; Au et al., 1995). Moreover, effects of aging on sentence and discourse production in the form of reduced local and global coherence have been observed, which becomes most evident when new information needs to be stored and incorporated (Wright et al., 2014). For language comprehension, age-related difficulties emerge when sentence processing becomes cognitively demanding (Wingfield & Stine-Morrow, 2000), for example when sentences are ambiguous, long, or complex (Goral et al., 2011; Kemper et al., 2004; Obler et al., 1991). Most cognitive accounts relate these changes to general cognitive slowing and reduced working memory and inhibition abilities. This explanation is further supported by the observation that often little or no effects of age are observed when access to semantic memory is effortless, for instance when the size of vocabulary is assessed without any time constraints (Verhaeghen, 2003), when

Figure 1.1 Changes in cognition across the adult life span. Cool colors represent cognitive domains that rely on cognitive control resources and experience a substantial decline in later life. Warm colors represent domains that rely on semantic memory and are preserved or even increase into old age. Republished with permission of Annual Reviews, Inc., from The Adaptive Brain: Aging and Neurocognitive Scaffolding, by Park, D. C., & Reuter-Lorenz, P., in Annual Review of Psychology, Vol. 60, Copyright © 2009; permission conveyed through Copyright Clearance Center, Inc.

discourse revolves around familiar and highly regularized topics (Kintz et al., 2016), or when semantic resources (larger vocabulary and world knowledge) can be used as cognitive reserve to overcome difficulties imposed through enhanced cognitive demands (Beese et al., 2019; Stine-Morrow et al., 1996). The impact of aging on language processing thus seems to the depend on the cognitive demand of a process and the individual resources in the form of domain-general cognitive abilities and semantic knowledge.

1.2   Neural Aging

In the brain, cognitive changes with age are mirrored by large-scale reorganization processes at the structural and functional levels (Cabeza et al., 2018; Grady, 2012; Morcom & Johnson, 2015). A better understanding of the neural factors that drive cognitive decline but also help preservation can help to disentangle interindividual variability and define early markers of pathological decline before they impact everyday function.

1.2.1 Structural Brain Aging

Cerebral atrophy is a hallmark of neuroanatomical changes with age. The age-accompanied reduction in gray and white matter volume along with the expansion of the ventricular system have been extensively studied in healthy and pathological aging and associated with decrements in specific cognitive functions (Fjell & Walhovd, 2010, 2020; Raz, 2004). Although a reduction in gray matter volume follows a linear time course from early adulthood onwards (Toga et al., 2006), not all cortical regions are affected to the same extent. Structural brain aging is highly heterogeneous across cortical regions with areas that mature later in life, like association cortices, being especially vulnerable to age-related loss in gray matter compared with earlier-developed areas like sensorimotor regions (McGinnis et al., 2011; Raz et al., 2005; Salat et al., 2004; Yeatman et al., 2014). Similarly, white matter tracts of association cortices, notably in the prefrontal cortex, have been shown to decline earliest, while fibers of primary sensory and motor regions are more resilient to structural changes (Bender et al., 2016; Gunning-Dixon et al., 2009). Moreover, lesions in the brain's white matter, which are known as white matter hyperintensities due to their increased signal intensity in MRI scans, have become a measure of clinical interest in aging (Brickman et al., 2009; Prins & Scheltens, 2015). Although such hyperintensities are more common in older age in general (Morris et al., 2009), numerous studies have associated a high volume of white matter hyperintensities with Alzheimer's disease, small vessel disease, and cognitive decline, making them an important clinical marker (Debette & Markus, 2010; Prins & Scheltens, 2015; Tubi et al., 2020). Despite these advances, our understanding of the relationship between structural brain aging and cognitive decline is still limited. Defining the transition from healthy to pathological aging continues to pose a major challenge and might only be solvable within a multidimensional framework incorporating life span and environmental factors, which are both known to impact morphometry and cognition (Fjell & Walhovd, 2020).

In the domain of semantic cognition, the relationship between semantic memory and pathological brain aging has been extensively studied since impaired word finding is a major symptom occurring early in neurodegenerative diseases like Alzheimer's disease and the semantic and logopenic variants of primary progressive aphasia (Bonner et al., 2010; Förstl & Kurz, 1999; Frank, 1994; Rodríguez-Aranda et al., 2016; Taler & Phillips, 2008). Deficits in accessing semantic memory have been associated with atrophy of the temporal lobes including the anterior hippocampus (D. Chan et al., 2001; Rodríguez-Aranda et al., 2016; Serra et al., 2010; Venneri et al., 2008) and in a later stage also more wide-spread atrophy of the predominantly left-lateralized frontotemporal language network (Fama et al., 2000; Rodríguez-Aranda et al., 2016). These changes are paralleled by a decline in the myelination of fiber tracts, of which the uncinate fasciculus, a pathway between inferior frontal and anterior temporal regions, and the inferior-fronto-occipital fasciculus, which runs through the extreme capsule, have been especially related to pathological deficits in semantic processing (Agosta et al., 2010;

Rodríguez-Aranda et al., 2016; Saur et al., 2008).

In comparison, much less work has focused on the relationship of structural brain aging and semantic cognition in healthy aging. Due to its high clinical relevance, healthy older adults usually serve as control participants in studies on pathological aging. Furthermore, as described earlier, semantic processing is typically less affected by age-related decline than domain-general cognitive control functions, which might be due to better preservation of the neuroanatomical correlates and successful compensatory reconfiguration of neural resources in healthy aging. However, there is some evidence that semantic processing is affected by structural brain aging in healthy older adults as well. Poorer and slower task performance has been associated with greater atrophy of gray matter in the right operculum during semantic judgment (Peelle et al., 2013; Zhu et al., 2017) and with reduced gray matter volume in bilateral prefrontal and temporal cortices as well as reduced white matter density during word retrieval (Obler et al., 2010). Moreover, research on word retrieval failures, such as the so-called tip-of-the-tongue phenomenon outlined above, suggests that neural atrophy underpins the increase in problems to access and retrieve lexicosemantic information (Shafto et al., 2007; Shafto et al., 2010).

1.2.2 Functional Brain Aging

Structural brain aging is accompanied by age-related changes in neural activity during task processing. While the most straightforward assumption might posit a reduction in neural recruitment paralleling cognitive declines and cerebral atrophy, copious research over the last decades has shown that the picture is much more complex. Functional brain aging is characterized by decreases but also increases in activity, which are mediated by the cognitive demand of a task and an individual's neural resources in the form of reserve, maintenance, and compensation.

Early research on functional brain aging focused on two frequent patterns associated with age-related changes during task processing, increased activity of bilateral frontal regions (hemispheric asymmetry reduction in older adults, HAROLD; Cabeza, 2002) and an enhanced recruitment of the prefrontal cortex alongside reduced activity in posterior brain regions (posterior-to-anterior shift in aging, PASA; Davis et al., 2008). These observations across multiple cognitive domains led to the suggestion that neurocognitive aging features a reduced specialization or distinctiveness of "core" processing areas of a task and greater activation of cognitive control regions to make up for the domain-specific under-recruitment (Park et al., 2004). It was further argued that older adults experience greater task demands at a lower level than young adults and recruit additional resources to accomplish task-related objectives (Hedden & Gabrieli, 2004). Thus, the age-accompanied over-recruitment of (bilateral) prefrontal regions, which are associated with executive functions and cognitive control, might serve a compensatory purpose. However, to prove such a compensatory mechanism, an association

between increased activation and (preserved) cognitive performance is vital. Otherwise, the over-recruitment might rather point to an inefficient pattern of age-related change in activity and thus represent neural dedifferentiation. This important distinction was outlined in the compensation-related utilization of neural circuits hypothesis (CRUNCH; Reuter-Lorenz & Cappell, 2008). According to CRUNCH, older adults can successfully compensate for processing inefficiencies by recruiting additional neural resources to maintain a similar performance level as young adults. However, when task demands increase further, brain activity in older adults might reach a plateau, leading to more errors and a pronounced drop in performance. In a similar vein, the scaffolding theory of aging and cognition (STAC; Park & Reuter-Lorenz, 2009; Reuter-Lorenz & Park, 2014) incorporates compensatory and dedifferentiation accounts of age-dependent changes in neural activity secondary to structural changes. Further, STAC tries to relate these changes to factors that influence brain activation such as life course and environmental causes but also the potential of interventions and cognitive training to reverse decline or improve the efficiency of compensatory scaffolding (Reuter-Lorenz & Park, 2014).

Notably, with the advancement of neuroimaging techniques in the study of neurocognitive aging and abundant research across cognitive domains, models like CRUNCH and STAC have become more agnostic about the particular location of compensatory recruitment, which might be domain-specific or domain-general. Additional activation of domain-specific regions has been associated with the age-related upregulation of contralateral homologous regions for domains with strong lateralization in younger adults, including the sensorimotor system (Ward, 2006), verbal working memory (Reuter-Lorenz et al., 2000; Rypma & D'Esposito, 2000), language comprehension (Peelle et al., 2010; Tyler et al., 2010), and language production (Wierenga et al., 2008). The increased recruitment of domain-general systems with age aligns with the notion of frameworks like HAROLD and PASA that the brain activation of older adults is less specialized and hence engages more cognitive control regions. However, in contrast to these early accounts, meta-analyses across cognitive domains have shown that the age-related increase in activation is not limited to the prefrontal cortex (Hoffman & Morcom, 2018; H.-J. Li et al., 2015; Spreng et al., 2010). Meta-analytic results revealed age-related additional recruitment of frontal and parietal regions which are associated with cognitive control systems such as the resting-state frontoparietal network (FPN; Damoiseaux et al., 2006; Smith et al., 2009; Yeo et al., 2011) and the task-related multiple-demand network (MDN; Duncan, 2010; Fedorenko et al., 2013). Moreover, where additional activation with age occurs is task-specific (Grady, 2012; H.-J. Li et al., 2015). For instance, meta-analytic results for studies employing memory encoding and retrieval operations demonstrated additional increases in the medial and inferior temporal lobe, posterior cingulate cortex, and inferior parietal lobe with age—areas which are typically linked to the default mode network (DMN; H.-J. Li et al., 2015). Furthermore, an age-related reduced deactivation of the DMN relative to its activation in young adults has also been reported for a number of tasks that usually rely heavily on executive systems (Grady

et al., 2010).

Whether this age-related over-recruitment of different brain regions and neural systems is compensatory or a mere consequence of reduced specialization of functional areas, remains a point of debate. While the best preservation of cognitive functions has been associated with a youth-like activation pattern due to processes of maintenance and reserve (Cabeza et al., 2018; Grady, 2012; Spreng et al., 2010), the compensatory potential of increased activity can only be assessed in relation to cognitive performance. In this regard, increased activity or the recruitment of additional brain regions can indicate successful or unsuccessful compensation, depending on the relationship with performance. If, however, such a link is missing, the over-recruitment might be described as attempted compensation and most likely indicates an age-related change in the form of neural dedifferentiation or inefficiency (Cabeza et al., 2018; Cabeza & Dennis, 2013). Finally, a better understanding of the behavioral consequences of functional brain aging might be gained through a network science approach since cognition is based on the flexible interaction of large-scale task-relevant networks.

1.2.3 Functional Network Aging

The recent conceptualization of the brain as a complex modular system (Meunier et al., 2009; Power et al., 2011) provides a unique framework to examine age-related changes in neural information processing and their consequences for behavior. The interaction of brain regions is assessed via functional connectivity, which quantifies statistical dependence between neural time series (Friston, 1994). In neuroimaging, functional connectivity is usually defined as the strength of correlation or covariance between a pair of brain structures and is based on the underlying assumption that a statistical relationship indicates a coupling of these areas (Eickhoff & Müller, 2015). Importantly, functional connectivity does not equal structural connectivity and often communication between brain regions can be observed in the absence of a direct anatomical connection. In fact, functional connectivity is often even measured without a task context during resting-state fMRI, which assesses the intrinsic connectivity of regions and thus allows inferences about the organization of large-scale brain networks (Buckner et al., 2013; Yeo et al., 2011).
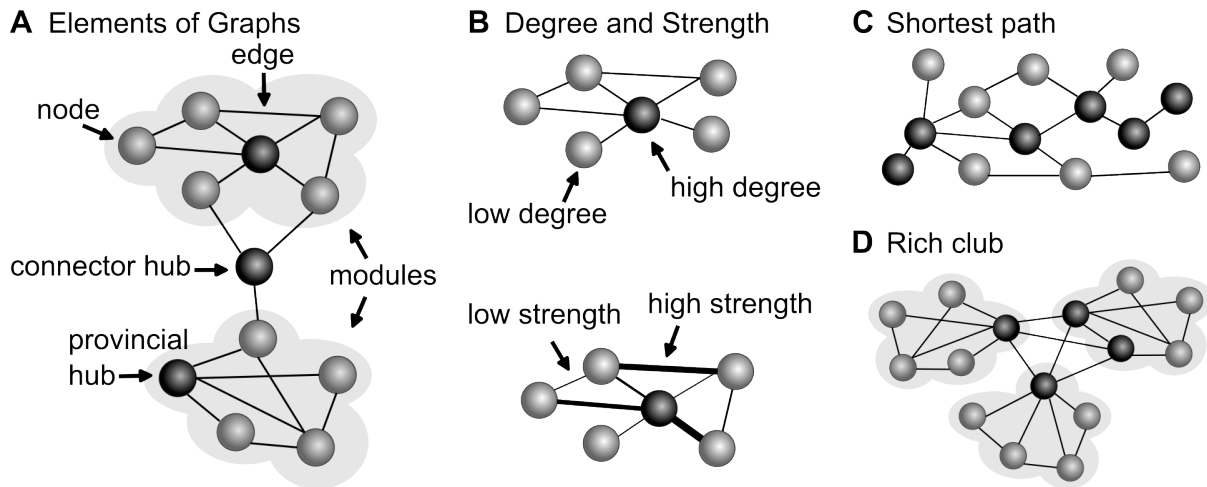
Changes in the functional connectome have become a hallmark of brain aging. Embedding age-related changes in local activity in whole-brain networks revealed universal patterns. One prominent observation in resting-state fMRI is the reduced functional connectivity within and increased connectivity between different networks with age. A decrease in connectivity has been repeatedly found for regions within the DMN (for a review, see Ferreira & Busatto, 2013)—a cognitive system which shows strong functional connectivity during rest (Greicius et al., 2003) and reduced activation during task processing in young adults (Raichle et al., 2001). Moreover, less within- and greater between-network functional connectivity at rest has also been shown for other large-scale neural systems, including dorsal attention, salience,

and sensorimotor networks (Allen et al., 2011; C.-C. Huang et al., 2015; Spreng et al., 2016; H.-Y. Zhang et al., 2014; Zonneveld et al., 2019). These changes have been interpreted as dedifferentiation of network interactions, paralleling local task-related neural changes (Grady, 2012). Longitudinal investigations confirmed the observations from cross-sectional studies and showed that within-network functional connectivity of, for instance, the DMN and FPN decreases continuously with age, while their between-network connectivity follows a u-shaped trajectory with initial declines but a steady increase from the mid-sixties (Betzel et al., 2014; Ng et al., 2016).

Further insight on the aging functional connectome can be gained by means of network science and graph theory, which offer an analytical framework to study organization principles of complex networks such as the human brain (Bullmore & Sporns, 2012; Fornito et al., 2016; Rubinov & Sporns, 2010). To this end, networks are modeled as a graph, where brain structures such as regions of interest or voxels are the *nodes* (also called *vertices*) and functional connectivity values define the *edges* (also called *links*) between them (Figure 1.2). Nodes of a graph that cluster together can be described as *modules*, which would be equivalent to individual brain networks or subnetworks. Graph theoretical measures can then be applied to understand a graph's topology and assess specific network features. The so-called "small world" organization is an important characteristic of brain graphs that has been repeatedly described for functional connectivity networks of younger adults in relation to their cognitive performance (Bassett & Bullmore, 2017; Bassett et al., 2009; Bullmore & Sporns, 2012). It describes a topological organization of the brain that combines local information processing with global information integration aimed at optimizing global cost efficiency.

Another prominent property of the human brain is the so-called "rich club" organization (Figure 1.2, Hagmann et al., 2008; van den Heuvel et al., 2012; van den Heuvel & Sporns, 2011). It pertains to the existence of *hub* nodes, which are defined by a high *degree*, i.e., a high number of connections (edges), either within their community (provincial hubs) or diversely distributed across communities (connector hubs; Bertolero et al., 2017; Hagmann et al., 2008). Connector hubs play an important role in facilitating communication between communities (modules) of a graph and previous work has highlighted their crucial role for integrative processing in resting- and task-state networks (Cohen & D'Esposito, 2016). Notably, it has been found that connector hubs tend to be more densely connected among themselves, thus forming a rich club of nodes, which are distributed among several different functional networks and serve as gatekeepers to coordinate interactions with lower-degree regions. Hence, the healthy young adult brain maintains a balance of brain system integration and segregation, which is wired for an efficient information flow across networks.

Numerous studies have revealed age-related changes to this modular organization. In line with the observation of reduced within- and increased between-network functional connectivity with age as outlined above, a general decline of functional network segregation

Figure 1.2 Fundamental graph theoretical concepts. (A) Graphs consist of a set of nodes and edges, where nodes represent brain structures, e.g., regions of interest or voxels, and edges represent measures of functional connectivity, e.g., correlation. Nodes that cluster together form modules, which have dense interconnectivity and increase the efficient information flow within such communities. Modularity is a measure of segregation. Provincial hubs are nodes with many connections within a module. To enhance global efficiency for information flow across modules, connector hubs with connections between modules exist. (B) A node's degree is defined by the number of its edges. The higher a node's degree, the more central this node is in a given community. In a weighted network, strength reflects the weight of an edge. For functional connectivity measures, such as correlation between nodes, higher values indicate higher strength. (C) The average shortest path length across all pairs of nodes of a graph is a measure of integration and indicates the efficiency for information transmission. (D) Some hubs cluster together and form a "rich club", which is characterized by dense connectivity among its nodes.

and greater integration across the lifespan has been reported in resting-state (M. Y. Chan et al., 2014; Setton et al., 2022; Stumme et al., 2020) but also task-based investigations (Deng et al., 2021; Geerligs et al., 2014; Spreng et al., 2016). Moreover, increasing age has been associated with reduced small-world organization, modularity, and local and global efficiency of functional brain networks (Betzel et al., 2014; Cao et al., 2014; Chong et al., 2019; Geerligs et al., 2015).

Association between changes in the functional network architecture and cognition with age

Importantly, these age-related reorganization processes have been associated with cognitive performance. The majority of results stems from resting-state investigations, where functional connectivity or graph theoretical results are correlated with cognitive measures assessed outside the MRI. Most studies associated network dedifferentiation with cognitive decline, especially in the domains of attention (Chong et al., 2019), episodic memory (M. Y. Chan et al., 2014), verbal and visual memory (Sala-Llonch et al., 2014), and executive functions in general (Madden et al., 2020).

Interestingly, age-accompanied differences in network topology during task processing

largely concur with reported patterns in resting-state fMRI in the form of reduced within- and stronger between-network functional connectivity and decreased segregation across multiple functional networks (Deng et al., 2021; Geerligs et al., 2014; Rieck et al., 2021; Spreng et al., 2016). However, their behavioral relevance seems to depend on the cognitive resources required for the task of interest. Most research has been conducted in domains well known to steadily decline with age, such as episodic and working memory, and reported compensational recruitment of control and attention networks for successful performance (Crowell et al., 2020; Deng et al., 2021; Gallen et al., 2016) but also maintenance processes with age to preserve neural resources despite structural deterioration (Capogna et al., 2022; Pongpipat et al., 2021).

The investigation of neural reorganization processes in cognitive abilities that remain stable with age, like language, creativity, and crystallized intelligence in general, offers a different perspective. In line with the recently proposed default-executive coupling hypothesis of aging (DECHA; Spreng & Turner, 2019; Turner & Spreng, 2015), increased connectivity between usually anti-correlated networks such as executive and default networks might be advantageous for older adults when access to semantic memory and little cognitive control are required so that they can rely on prior knowledge to maintain high performance (Adnan et al., 2019; Spreng et al., 2016). According to DECHA, the commonly reported activation increase of cognitive control regions and the attenuated suppression of the DMN co-occur and are functionally coupled in older adults. These changes of the functional network architecture reflect a shift in cognition in later life, the so-called *semanticization* of cognition: Older adults tend to rely more on their preserved semantic knowledge and less on their declining cognitive control abilities (Spreng et al., 2018; Turner & Spreng, 2015). Whether the increased default-executive coupling is advantageous or maladaptive for performance, depends on the context and cognitive demand of a task. Research on creativity and autobiographical memory confirmed the adaptive potential of increased default-executive coupling in networks of older adults (Adnan et al., 2019; Spreng et al., 2016). Thus, domains that are usually well-preserved in aging may inform the current understanding of age-accompanied changes in functional brain networks and their impact on cognition.
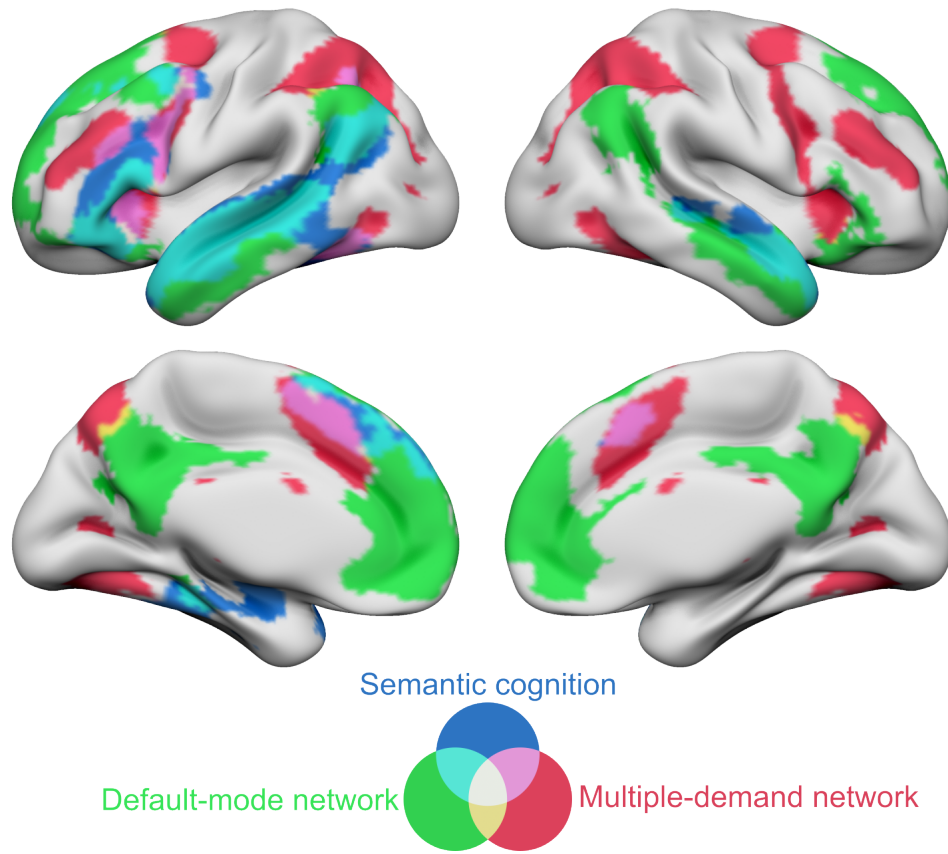
1.3 Neurocognitive Aging in Semantic Cognition

Semantic cognition has a central role in higher cognitive functions, enabling communication abilities but also recognition of and action with objects, and shaping our general understanding of the world. As outlined in section 1.1 on cognitive aging, exploring functional brain aging in the domain of semantic cognition, and more specifically language processing, might offer a differentiated perspective on successful aging since, in contrast to most other cognitive functions, semantic memory is usually well preserved in healthy aging (Nyberg et al., 1996; Rönnlund et al., 2005; Verhaeghen, 2003). Furthermore, semantic cognition has been shown to

rely on large-scale neural networks in young adults, which engage cognitive control but also default mode as well as domain-specific resources (Binder et al., 2009; Jackson, 2021; Noonan et al., 2013). Thus, age-related reorganization processes in this domain might inform current accounts on neurocognitive aging.

Semantic cognition activates a mainly left-lateralized, widespread neural network in young adults, including frontal, temporal, and parietal regions (Binder et al., 2009). This network is thought to consist of distinct, yet interacting elements: a subnetwork for semantic representation and a subnetwork for semantic control (Lambon Ralph et al., 2017). According to the Controlled Semantic Cognition framework, the semantic representation system consists of an amodal "hub", located in the bilateral anterior temporal lobes (ATL), and modality-specific "spoke" regions distributed throughout the cortex (Jefferies, 2013; Lambon Ralph et al., 2017). It is assumed that the ATL mediates between input from sensorimotor regions and output representations from spokes regions by extracting and melding information to generalizable, multimodal semantic concepts (Chiou et al., 2018; Lambon Ralph et al., 2017; Patterson et al., 2007). Although bilateral ATL areas have been linked to semantic cognition, the left ATL shows greater activation during language-specific processes such as speech comprehension and production (Rice et al., 2015). The goal-directed access and manipulation of semantic representations is realized through the semantic control system, which has been shown to rely on a distributed network of the left inferior and dorsomedial prefrontal cortex, left posterior middle and inferior temporal gyrus, and right inferior frontal gyrus (Jackson, 2021). Moreover, the left inferior parietal lobe, especially the anterior angular gyrus, has also been associated with semantic control processes as we could show in a recent analysis synthesizing multiple studies involving semantic processing (Kuhnke et al., 2022). Semantic control is critical to the flexible use of semantic knowledge, enabling the retrieval of less dominant aspects of a representation, inhibition of irrelevant information, resolution of ambiguous or incongruent meanings, and the shift between different tasks (Jackson, 2021; Jefferies, 2013).

Importantly, the network of semantic cognition shows notable overlap with domain-general networks (Figure 1.3). Semantic control regions, including the left dorsomedial prefrontal cortex, inferior temporal gyrus and some parts of bilateral inferior frontal gyrus, have been linked to the task-specific MDN. Semantic representation, on the other hand, has been associated with the DMN, which stems from the observation that some semantic "core" regions (ventral inferior parietal lobe, middle and anterior temporal lobes) are also active during resting-state fMRI when participants are engaged in semantically rich daydreaming and self-directed thought (Binder et al., 1999). Recently, it has been suggested that the DMN might play a more prominent role in higher-order cognition than previously assumed and could be central to memory retrieval (Smallwood et al., 2021). Especially the dorsal medial subsystem of the DMN overlaps with frontal, temporal, and parietal parts of the semantic cognition network derived through task-based meta-analyses (Binder et al., 1999; Jackson, 2021). It has been shown to activate

Figure 1.3 Overlaying the network of semantic cognition (including semantic control) with the multiple-demand (MD) and the default-mode network (DMN). The template for semantic cognition was taken from a meta-analysis on semantic processing (Jackson, 2021), the template for the MD network stems from Fedorenko et al. (2013), and the DM template stems from a the 7-networks resting-state parcellation (Yeo et al., 2011).

when participants can rely on their semantic knowledge during task processing, such as automatic or "overlearned" processing (Lanzoni et al., 2020; Murphy et al., 2019; Vatansever et al., 2017). Thus, the engagement of specific components of the semantic cognition network might best be understood as a gradual organization, where task contexts determine the contribution of long-term semantic knowledge and semantic control processes to guide behavior.

In line with other cognitive domains, the effect of aging on semantic cognition has been described as reduced specificity and increased dedifferentiation in task-related activation, as revealed by a recent meta-analysis (Hoffman & Morcom, 2018). Reduced specificity was most evident through less activation in semantic control regions and additional activation in the right inferior frontal gyrus, whereas dedifferentiation was characterized by stronger involvement of the domain-general MDN and attenuated suppression of the DMN (Hoffman & Morcom, 2018). Importantly, the additional activation of (bilateral) cognitive control regions was strongest in tasks, where older adults performed worse than young adults, questioning the compensatory potential of such upregulation. Moreover, due to the design of most experimental tasks, older

adults performed generally poorer than young adults, which limits the potential of these investigations to differentiate between specific (compensatory) and unspecific age-related neural changes.

As outlined in section 1.2.3 on the association of functional network aging and cognition, these open questions might be best explored through a functional network approach. However, research on age-related changes to the functional network architecture during semantic processing is sparse, which might be surprising due its central role not only in communication but our general understanding of the world. A number of studies explored such changes during semantic word retrieval, though confined to domain-specific networks (Baciu et al., 2016; Marsolais et al., 2014) or predefined regions of interest (ROIs), mainly in the prefrontal cortex (Meinzer, Flaisch, et al., 2012; Meinzer et al., 2009; Meinzer, Seeds, et al., 2012). Results showed not only reduced connectivity but a changed pattern of connections in older adults. Furthermore, a recent investigation on the organization of individually mapped semantic networks highlighted the role of semantic representation, semantic control and default mode networks during semantic processing in older adults (Ketchabaw et al., 2022), thus potentially pointing towards a stronger integration of domain-general networks with age.

1.4 The Potential of Non-Invasive Brain Stimulation in Neurocognitive Aging

In the last decades, the application of non-invasive brain stimulation (NIBS) techniques to counteract age-related cognitive decline and to promote successful aging has gained increasing interest. Similar to the use of NIBS to boost neuropsychological rehabilitation after disruption of function due to stroke, these techniques might offer the potential to support the preservation of cognitive functions in pathological but also healthy aging through modulation of cortical excitability and the enhancement of neuroplasticity. The most common methods applied to date include repetitive transcranial magnetic stimulation (rTMS), transcranial direct current stimulation (tDCS), and transcranial alternating current stimulation (tACS). The transcranial current stimulation methods, tDCS and tACS, are applied via a weak direct current on the scalp and provoke a sub-threshold modulation of neuronal excitability without triggering action potentials (Wagner et al., 2007). While tDCS is assumed to be polarity dependent, with anodal stimulation leading to a depolarization (i.e., excitation) and cathodal stimulation inducing hyperpolarization (i.e., inhibition; Nitsche & Paulus, 2000), tACS applies an alternating current that oscillates at a chosen frequency and in this way can be used to synchronize with the brain's natural cortical oscillations (Antal et al., 2008).

TMS, on the other hand, induces a local magnetic field, which in turn produces an electric field in the brain tissue (Barker et al., 1985). In contrast to tDCS and tACS, the electric field

generated via TMS is supra-threshold and thus sufficient to trigger action potentials and directly alter neural activity (Wagner et al., 2007). The magnetic field of TMS is generated through pulses of electric current that are delivered to a coil placed on the head. To produce a more sustained alteration in excitability, TMS is usually delivered in the form of repetitive TMS (rTMS) pulses. Depending on the stimulation protocol and its application during (online) or before (offline) task processing, rTMS can be used in two ways: (1) to immediately affect an area relevant to cognitive processes (online approach), which allows conclusions about the region's causal relevance, and (2) to induce neural plasticity in the targeted area for an extended period (offline approach), which allows the analysis of subsequent effects on neural activity (e.g., via fMRI or EEG) and behavior. As a therapeutic tool, the offline application of rTMS is of greatest interest since the TMS-induced changes in neuronal excitability give rise to neural reorganization processes (Hartwigsen, 2015, 2018; Siebner et al., 2009). Importantly, it has been shown that the effect of rTMS is not limited to the site of stimulation but spreads transsynaptically along cortico-cortical and cortico-subcortical connections, impacting neuronal activity throughout the targeted network (Hartwigsen & Siebner, 2013; Siebner et al., 2022; Siebner & Rothwell, 2003). Moreover, to generate longer-lasting stimulation effects on cognition, the application of patterned stimulation protocols, such as theta-burst stimulation (TBS Y.-Z. Huang et al., 2005), has gained increasing attention. TBS delivers short, high-frequency stimulation bursts at intervals which are applied intermittently (iTBS) or continuously (cTBS). ITBS is assumed to facilitate cortical excitability via long-term potentiation and cTBS to inhibit excitability via long-term depression in the cortex (Di Lazzaro et al., 2008; Y.-Z. Huang et al., 2005).

In the field of neurocognitive aging, the application of NIBS is especially relevant to improve performance in cognitive functions affected by age and potentially boost gains in interventions using cognitive training (for reviews, see Booth et al., 2022; Goldthorpe et al., 2020; Hsu et al., 2015). However, so far, findings are mixed, with some studies reporting beneficial effects, particularly in the domains of working, episodic, and associative memory (Antonenko et al., 2019; Berryhill & Jones, 2012; Manenti et al., 2013), and some studies observing no additional effect of NIBS on cognitive functions (e.g., Antonenko et al., 2022). Moreover, effect sizes are often small and show little or no transfer to untrained tasks (Booth et al., 2022; Passow et al., 2017). In the domain of semantic cognition, thus far, only a few studies explored the application of tDCS to boost semantic word retrieval in healthy older adults (Holland et al., 2011; Martin et al., 2017; Meinzer et al., 2013; Meinzer et al., 2014; Ross et al., 2011). Anodal tDCS was applied over the left inferior frontal gyrus, primary motor cortex, inferior frontal gyrus, and anterior temporal lobe, respectively, and led to improved and faster word retrieval abilities relative to sham after a single stimulation session in all studies.

Notably, most of the reported studies in healthy aging used tDCS, which might be due to its relatively easier, cheaper, and safer application compared with TMS (Gandiga et al., 2006). Moreover, tDCS can be portable, which makes it an ideal tool for the development of

treatments which can be administered at home. In contrast, TMS has the advantage that it is more focal and may reach deeper cortical regions (Lu et al., 2007), making it more appropriate for precise and less noisy stimulation. The focality of stimulation is especially relevant, when NIBS and neuroimaging techniques are combined. Examining the effects of stimulation on the neural level is of high importance considering the immense variability of stimulation approaches regarding stimulation site, duration, and intensity. Furthermore, neuroimaging results can help interpreting behavioral effects and might even be observed in the absence of a stimulation-induced behavioral change (Abellaneda-Pérez et al., 2022). For example, it has been shown that neural markers of age-related cognitive decline are detectable at earlier stages than subsequent behavioral changes (Burggren & Brown, 2014).

From the studies using tDCS to boost semantic word retrieval in older adults, only a few assessed the effect of stimulation at the neural level. Improved performance was associated with reduced activation at the stimulation site (Holland et al., 2011; Meinzer et al., 2013) and in regions that have been shown to upregulate for higher task demands in older adults (Meinzer et al., 2013). Stimulation-induced changes were also observed for functional connectivity, where increased connectivity between task-relevant regions of interest in the prefrontal cortex was observed (Holland et al., 2016) but also reduced resting-state connectivity between frontal and temporal regions indicating a more youth-like connectivity pattern after anodal tDCS (Meinzer et al., 2013). Moreover, in a different study, anodal tDCS over the left primary motor cortex led to an observable shift in laterality, with more left-lateralized language processing after active relative to sham stimulation in older adults. In summary, existing research suggests an effect of NIBS in the domain of semantic cognition not only on the behavioral but also neural level, with first evidence indicating stimulation-induced changes towards youth-like activation patterns.

So far, no study explored the potential of rTMS to modulate age-related changes in semantic cognition on the behavioral and neural level. One reason for this gap might be the relative preservation of semantic memory in healthy aging compared with other cognitive functions, as outlined in chapter 1.1, and thus a research bias toward the enhancement of declining functions with age, such as working and episodic memory. However, complaints about problems with access and retrieval of information from semantic memory prevail in healthy aging, and a recent investigation demonstrated that a more fine-grained distinction of the cognitive processes involved in semantic cognition might elucidate which components are affected by age (Hoffman, 2018). Specifically, Hoffman (2018) showed that semantic representation and retrieval processes remain intact with age but semantic control processes involved in selection and inhibition mechanisms, which are strongly correlated with executive functions, decline in older adults. Transferring this finding to the neural level would thus indicate that the stimulation of regions associated with semantic control might be most promising.

1.5 Research Questions

So far, age-related changes to the functional network architecture in semantic cognition are poorly understood. The studies presented in this thesis addressed three key issues:

(1) the age-dependent contribution of task-relevant, domain-general networks to semantic cognition,

(2) the age-related reorganization of the whole-brain functional network architecture during semantic processing, and

(3) the potential of stimulating a hub of the MDN via NIBS to facilitate semantic retrieval in healthy older adults as revealed through behavioral performance and neuroimaging.

First, it is unclear how domain-general and domain-specific networks interact during semantic cognition and how this interaction might change with age. There is evidence that functional coupling between usually anticorrelated networks increases for tasks that require cognitive control even in young adults (Shine et al., 2016) but also in older adults at rest (Krieger-Redwood et al., 2019) and during self-directed task processing, such as creative thinking (Adnan et al., 2019) and autobiographical memory (Spreng et al., 2016). To date, the change in network coupling has not been addressed during semantic processing in healthy aging. This question is especially relevant to the understanding of functional brain aging since the recently proposed DECHA framework might predict a shift towards semanticization in older adults with greater contributions of networks associated with semantic representation (Spreng & Turner, 2019; Turner & Spreng, 2015). Crucially, exploring this issue through task-based fMRI offers the opportunity to relate age-related network reorganization processes to behavioral performance and thus to inform current accounts regarding the compensatory potential of an increase in default-executive coupling with age.

To this end, **study 1** of the present thesis investigated the interaction of domain-specific and domain-general networks during semantic processing in healthy young and older adults. We used an overt semantic word retrieval task and a low-level verbal control task to assess age-related differences in functional brain activation and connectivity. One major finding of this study was the strong contribution of the domain-general MDN and DMN to semantic word retrieval in both age groups. However, the functional coupling within and between these two networks had different effects on the behavioral performance of each age group, with young adults benefiting from increased coupling in the form of better and more efficient performance.

According to the DECHA framework, older adults may profit from an increased coupling of executive and default resources when they can rely on their semantic knowledge during task processing. While my first study did not indicate such an age-related shift in network coupling during semantic word retrieval, this might have been caused by methodological choices such

as the focus on network nodes from the young adults during semantic processing. Hence, **study 2** undertook a whole-brain approach to explore age-related reorganization processes of functional networks. We combined independent component analysis (ICA) with graph theory to investigate changes to the functional network architecture with age, and related these measures to participants' in-scanner task performance and abilities of fluid and crystallized intelligence. Linking preserved performance in older adults with their reorganized network structure, enabled us to draw inferences about the compensatory potential of such network changes. One key finding of this study was the greater integration of task-relevant networks in older adults, facilitated by an increased amount of connector hubs in frontal and parietal regions. Notably, the pre-supplementary motor area (pre-SMA) emerged as a hub region, which aligned with its pronounced contribution to semantic word retrieval as revealed in study 1.

Thus, building upon these findings, **study 3** explored the potential of enhancing the pre-SMA, a hub of domain-general but also domain-specific semantic control, via facilitatory offline stimulation in a crossover study design in healthy middle-aged to older adults. We assessed the effect of stimulation on behavioral performance, task-based activation, and functional connectivity in a subsequent fMRI experiment. Relating stimulation-induced changes on the neural level with behavior allowed us to investigate the role of the pre-SMA in semantic control and its role in semantic processing in the aging brain.

2 Age-Dependent Contribution of Domain-General Networks to Semantic Cognition

Study 1

The following study explored the contribution of domain-general networks to a semantic word retrieval task in healthy young and older adults. It has been published in *Cerebral Cortex*.

ORIGINAL ARTICLE

Age-Dependent Contribution of Domain-General Networks to Semantic Cognition

Sandra Martin [iD][1,2], Dorothee Saur[2] and Gesa Hartwigsen [iD][1]

[1]Lise Meitner Research Group Cognition and Plasticity, Max Planck Institute for Human Cognitive and Brain Sciences, 04103 Leipzig, Germany and [2]Language & Aphasia Laboratory, Department of Neurology, University of Leipzig Medical Center, 04103 Leipzig, Germany

Address correspondence to Sandra Martin, Lise Meitner Research Group Cognition and Plasticity, Max Planck Institute for Human Cognitive and Brain Sciences, Stephanstr. 1a, Leipzig 04103, Germany. Email: martin@cbs.mpg.de.

Abstract

Aging is characterized by a decline of cognitive control. In semantic cognition, this leads to the paradox that older adults usually show poorer task performance than young adults despite their greater semantic knowledge. So far, the underlying neural changes of these behavioral differences are poorly understood. In the current neuroimaging study, we investigated the interaction of domain-specific and domain-general networks during verbal semantic fluency in young and older adults. Across age groups, task processing was characterized by a strong positive integration within the multiple-demand as well as between the multiple-demand and the default mode network during semantic fluency. However, the behavioral relevance of strengthened connectivity differed between groups: While within-network functional connectivity in both networks predicted greater efficiency in semantic fluency in young adults, it was associated with slower performance in older adults. Moreover, only young adults profited from connectivity between networks for their semantic memory performance. Our results suggest that the functional coupling of usually anticorrelated networks is critical for successful task processing, independent of age, when access to semantic memory is required. Furthermore, our findings lend novel support to the notion of reduced efficiency in the aging brain due to neural dedifferentiation in semantic cognition.

Key words: aging, connectivity, default mode network, language production, multiple-demand network

Introduction

Semantic cognition is a fundamental human ability that is central to communication across the life span. Key facets of semantic cognition refer to our knowledge of the world and the meaning of words and sentences. With respect to cognitive changes across the adult life span, cognitive control processes—also referred to as fluid intelligence—are well established to steadily decline with increasing age (Hedden and Gabrieli 2004), whereas semantic knowledge (so-called crystallized intelligence) has been shown to remain stable or might even increase with age due to the ongoing accrual of knowledge and experience across the life course (Verhaegen et al. 2003). In the domain of semantic cognition, the impact of aging thus seems to depend on both the specific cognitive demand of a task and the individual semantic knowledge.

At the neural level, cognitive changes with age are mirrored by large-scale reorganization processes at the structural and functional levels (Grady 2012; Morcom and Johnson 2015). Task-related performance changes in older adults have been associated with a pattern of dedifferentiation of neural activity (Li et al. 2001; Park et al. 2004) which is reflected by an under-recruitment of domain-specific regions (Lövdén et al. 2010) and reduced task-specific lateralization (Cabeza 2002). Dedifferentiation is further characterized by an increased recruitment of areas in the domain-general multiple-demand network (MDN; Lövdén et al. 2010) and a reduced deactivation of regions in the default mode network (DMN; Andrews-Hanna et al. 2007; Persson et al. 2007; Damoiseaux et al. 2008). A recent meta-analysis that investigated age-related effects on the neural substrates of semantic cognition confirmed the upregulation

of the MDN in older adults for a variety of semantic tasks (Hoffman and Morcom 2018).

In addition to local changes in task-related activity, alterations in the functional connectivity of large-scale neural networks have become a hallmark of brain aging (Li et al. 2015; Spreng et al. 2016; Damoiseaux 2017). A common observation is that functional network segregation declines with age, which is evident in the form of decreased within- and increased between-network functional connectivity (Chan et al. 2014; Geerligs et al. 2015; Spreng et al. 2016). These changes have been interpreted as dedifferentiation of network interactions, paralleling local task-related neural changes (Spreng and Turner 2019). However, the majority of studies investigated these changes at rest, and it is thus less clear how aging affects task-related functional connectivity and how this is associated with behavior.

The recently proposed default-executive coupling hypothesis of aging (DECHA; Turner and Spreng 2015; Spreng and Turner 2019) suggests that the observed activity increase in MDN regions and the reduced deactivation of the DMN co-occur and are functionally coupled in older adults. This shift in network coupling is based on the accrual of semantic knowledge and the parallel decline of cognitive control abilities. Older adults thus rely more strongly on their preserved semantic knowledge, which is reflected by a reduced deactivation of DMN regions compared with young adults. According to this hypothesis, context and cognitive demand of a task determine if this increased default-executive coupling in older adults is beneficial or maladaptive. On this basis, the framework predicts stable performance in older adults for tasks that rely on crystallized intelligence in the form of intrinsic prior knowledge and that require little cognitive control, whereas externally directed cognitive tasks result in poorer performance in older adults due to their dependence on control resources.

So far, the integration of domain-general networks in semantic word retrieval in older adulthood is poorly understood. In this context, semantic fluency tasks, which require participants to generate words that belong to a specific category within a given time, provide a unique opportunity since they require an interaction of verbal semantic and general cognitive control processes (Whiteside et al. 2016; Schmidt et al. 2017; Gordon et al. 2018). Semantic fluency tasks test a natural and important communicative ability as they rely on accessing related concepts to retrieve words. Furthermore, semantic fluency is of high ecological validity, for example, when writing a shopping list (Shao 2014), and is frequently implemented as a measure of language and neuropsychological abilities in healthy as well as clinical populations (Schmidt et al. 2017). The impact of aging on semantic fluency is especially interesting since its strong link to semantic memory would predict preserved performance for older adults. Yet, the opposite pattern is usually observed, suggesting a high load on cognitive control processes for this task (e.g., Troyer et al. 1997; Kavé and Knafo-Noam 2015; Gordon et al. 2018). Most studies that implemented semantic fluency tasks in neuroimaging experiments reported age-related changes within domain-specific networks (Marsolais et al. 2014; Baciu et al. 2016) or predefined regions of interest (ROIs), mainly in the prefrontal cortex (Meinzer et al. 2009; Meinzer, Flaisch, et al. 2012; Meinzer, Seeds, et al. 2012). However, based on the outlined changes in semantic and cognitive control abilities, older adults could show a shift in network coupling with a stronger engagement of domain-general networks, which might be additionally modulated by task demand.

The aim of the present study was to explore and compare the contribution of domain-specific and domain-general networks to a semantic language production task in healthy young and older adults. We implemented a functional magnetic resonance imaging (fMRI) study with a paced overt semantic fluency task, which included an explicit modulation of task difficulty. A counting task was used as a low-level verbal control task. First, we were interested in delineating the network for semantic fluency and its interaction with task demand. Second, we asked whether age modulates both activation patterns and behavioral performance. Finally, we were interested in task-related functional interactions between domain-specific and domain-general networks. To this end, we combined univariate whole-brain analyses with generalized psycho-physiological interaction (gPPI) analyses. We applied traditional gPPI analyses to explore the functional coupling of the strongest activation peaks for semantic fluency. This allowed us to investigate the age-related contribution of domain-general networks to language processing. Furthermore, we used modified gPPI analyses to examine functional connectivity within and between regions of domain-general networks. We were interested in age-related effects on functional connectivity patterns and how within- and between-network functional connectivity relate to behavioral performance for both age groups. We expected a language-specific, left-lateralized network for semantic fluency. We further hypothesized that increased task demand (reflected by the contrast of semantic fluency with counting as well as by the modulation of difficulty within the semantic fluency task) would affect task performance and should be accompanied by an increased recruitment of domain-general systems. With respect to task-related functional connectivity, we reasoned that older adults should demonstrate a stronger involvement of the DMN for the semantic fluency task based on their increased semantic knowledge. Moreover, a higher task load associated with general cognitive decline might further result in a stronger recruitment of the MDN in older adults. However, in line with neurocognitive theories of aging, the increased recruitment of domain-general systems might be associated with reduced specificity and efficiency; thus, overall leading to poorer performance in the older adults.

Materials and Methods

Participants

Twenty-eight healthy older adults (mean age: 65.2 years, range: 60–69 years) and 30 healthy young adults (mean age: 27.6 years, range: 21–34 years) completed our study. The data of three additional participants in the older group as well as single runs of six participants were excluded due to excessive head movement during fMRI (>1 voxel size). Groups were matched for gender. Participants in the younger group had significantly more years of education (t(55.86) = 5.2, P < 0.001). All participants were native German speakers and right-handed according to the Edinburgh Handedness Inventory (Oldfield 1971). They had normal hearing, normal or corrected-to-normal vision, and no history of neurological or psychiatric conditions or contraindication to magnetic resonance (MR) scanning. Older adults were additionally screened for cognitive impairments using the Mini-Mental State Examination (Folstein et al. 1975; all ≥26/30 points) and for depression with the Beck Depression Inventory (Beck et al. 1996; all ≤14/points). The study was approved by the local ethics committee of the University of Leipzig and was conducted

Table 1 Demographic and neuropsychological characteristics of participants

	Young adults ($n = 30$)	Older adults ($n = 28$)
Demographics		
Age (years)	27.6 (4.4)	65.2 (2.8)
Gender (F:M)	16:14	14:14
Education (years)	18.7 (2.6)	15.2 (2.5)*
Beck Depression Inventory (cutoff 18 points)	—	4.7 (4.1)
Neuropsychological		
Spot-the-word test (max. 40)	29.1 (3.2)	31.5 (2.5)*
Semantic fluency (sum surnames, hobbies)	51.2 (8.4)	40.7 (6.7)*
Reading span test (max. 6)	3.5 (1)	2.9 (0.7)*
Digit Symbol Substitution Test (max. 90 in 90 s)	72.1 (11.4)	50.2 (10.4)*
Trail Making Test A (time in s)	17.3 (5.8)	25.4 (6.4)*
Trail Making Test B (time in s)	36.1 (11.9)	61.8 (29.4)*
Mini-Mental State Examination (max. 30 points)	—	28.36 (1.2)

Note: Mean values of raw scores with SDs.
*Significant differences between age groups at $P < 0.01$.

in accordance with the Declaration of Helsinki. Participants gave written informed consent prior to the experiment. They received 10 Euro per hour for their participation.

Neuropsychological Assessment

A battery of neuropsychological tests was administered to all participants to assess cognitive functioning. Verbal knowledge and executive language functions were measured with the German version of the spot-the-word test (Wortschatztest; Schmidt and Metzler 1992; Baddeley et al. 1993), a German version of the reading span test (Daneman and Carpenter 1980), and the semantic subtest of a verbal fluency test (Regensburger Wortflüssigkeitstest; Aschenbrenner et al. 2000). The latter comprised two 1-min trials of semantic categories (surnames and hobbies) that were not part of the fMRI task. Additionally, executive functions were assessed with the Digit Symbol Substitution Test (Wechsler 1944) and the Trail Making Test A/B (Reitan 1958). Group comparisons showed that older participants only performed better than the younger group on the spot-the-word test (Table 1; Supplementary Fig. S1), which is considered to be a measure of lexical semantic knowledge and vocabulary. Consistent with our results, it has been shown to be robust to aging and cognitive decline (Baddeley et al. 1993; Law and O'Carroll 1998; Cohen-Shikora and Balota 2016). Our results confirm the maintenance of semantic memory across age (Grady 2012) and an increase in size of vocabulary with age (Verhaegen et al. 2003). All other tests showed better performance for younger participants, which is in line with the assumption of a general decline in executive functions like working memory and processing speed with age (e.g., Balota et al. 2000; Zacks et al. 2000). However, when considering age-corrected norms, the older participants performed within normal ranges on all neuropsychological tests.
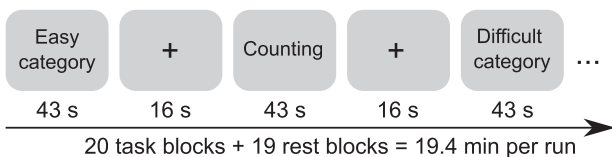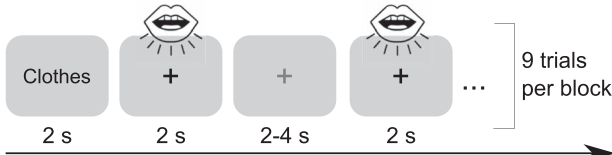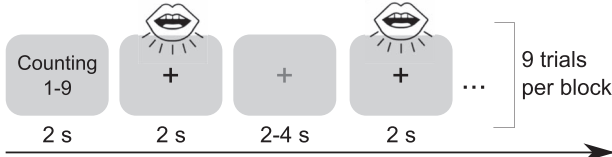
Experimental Design

All participants completed one fMRI session that was divided into two runs. Tasks consisted of a paced overt semantic fluency task and a control task of paced counting, which were implemented in a block design in the scanner. We chose a paced design for our tasks since it has been shown to be less sensitive

to motion artifacts and to yield robust brain activation patterns (Basho et al. 2007). Task blocks were 43 s long and were separated by rest blocks of 16 s (Fig. 1A). Each block started with a 2-s visual word cue indicating whether participants were expected to generate category exemplars or count forward (1–9) or backward (9–1). This was followed by nine consecutive trials of the same category or counting task, respectively. Trials within one block were separated by inter-stimulus intervals of 2–4 s. Participants were instructed to generate one exemplar for a category or one number per trial, which was indicated through a green cross on the screen, and to pause when the cross turned red (Fig. 1B,C). They were told not to repeat items and to say "next" if they could not think of an exemplar for the respective category. Each run contained 10 semantic fluency blocks, which were divided into easy and difficult categories, and 10 counting blocks, consisting of forward and backward counting, thus resulting in a total duration of 19.4 min per run. The order of blocks was counterbalanced and pseudorandomized across participants. Before the fMRI experiment, participants received instructions and practiced the task with a separate set of categories outside the scanner. Stimuli were presented using the software Presentation (Neurobehavioral Systems; version 18.0). Answers were recorded via a FOMRI III microphone (Optoacoustics).

Stimuli

Stimuli consisted of 20 semantic categories which were divided into 10 easy and 10 difficult categories. Difficulty was assessed in a separate pilot study with 24 young adults (12 males, mean age: 26 years, range: 21–32 years) and 24 older adults (10 males, mean age: 65 years, range: 60–69 years). Participants were recruited and screened using similar criteria as in the fMRI study. They generated as many exemplars as possible during 1-min trials for 30 semantic categories which were taken from German category-production norm studies (Mannhaupt 1983; Glauer et al. 2007). Responses were recorded and subsequently transcribed and analyzed. Based on the total number of correct exemplars produced for each category, the 10 categories with the largest number of produced items (colors, body parts, clothing, types of sport, animals, car parts, professions, trees, food, and musical instruments) and the 10 categories with the fewest items (flowers, insects, metals, kitchen devices, tools,

A Experimental paradigm

Easy category	+	Counting	+	Difficult category	...
43 s	16 s	43 s	16 s	43 s	

20 task blocks + 19 rest blocks = 19.4 min per run

B Overt Semantic Word Generation Task

Clothes	+	+	+	...	9 trials per block
2 s	2 s	2-4 s	2 s		

C Control task: Overt Counting

Counting 1-9	+	+	+	...	9 trials per block
2 s	2 s	2-4 s	2 s		

Figure 1. Experimental design. (A) fMRI experiment consisting of alternating blocks of a semantic fluency and a counting task separated by 16-s rest periods. (B) and (C) demonstrate the implementation of the paced design in both tasks. Procedures were identical for both tasks. Participants were instructed to produce one exemplar for a category or to say one number per green cross (here marked in dark grey), respectively, and to pause when the cross turned red (here marked in light grey). Each block contained nine trials which were separated by jittered inter-stimulus intervals.

gardening tools, fishes, cosmetics, toys, and sweets) across both age groups were chosen for the easy and difficult conditions of the semantic fluency task in the fMRI experiment, respectively. Easy ($M = 18.08$, standard deviation [SD] = 2.51) and difficult categories ($M = 10.64$, SD = 1.39) differed significantly in the mean number of generated exemplars ($t(29.66) = 11.00$, $P < 0.001$) during piloting. To ensure that there was no difference between age groups for the difficulty manipulation, we calculated a linear model with difficulty and age as predicting variables. Results revealed a significant effect of difficulty ($F = 139.67$, $P < 0.001$) but not of age group ($F = 2.46$, $P = 0.13$).

Data Acquisition and Preprocessing

MR images were collected at a 3-Tesla Prisma Scanner (Siemens) with a 32-channel head coil. For the acquisition of fMRI data, a dual gradient echo-planar imaging multiband sequence (Feinberg et al. 2010) was used for optimal blood oxygen level–dependent (BOLD) sensitivity across the whole brain (Poser et al. 2006; Halai et al. 2014). The following scanning parameters were applied: time repetition (TR) = 2000 ms; time echo (TE) = 12, 33 ms; flip angle = 90°; voxel size = 2.5 × 2.5 × 2.5 mm with an interslice gap of 0.25 mm; FOV = 204 mm; multiband acceleration factor = 2. To increase coverage of anterior temporal lobe (ATL) regions, slices were tilted by 10° of the AC-PC line. Six hundred and sixteen images consisting of 60 axial slices in interleaved order covering the whole brain were continuously acquired per run. Additionally, field maps were obtained for later distortion correction (TR = 8000 ms; TE = 50 ms). This study analyzed the data from echo 2 (TE = 33 ms) since preprocessing was performed using the software fMRIPrep (Esteban et al.

2019), which currently does not support the combination of images acquired at different echo times. We chose to use results from preprocessing with fMRIPrep since this pipeline provides state-of-the-art data processing while allowing for full transparency and reproducibility of the applied methods and a comprehensive quality assessment of each processing step, which facilitates the identification of potential outliers. We also double-checked results from preprocessing with fMRIPrep with a conventional SPM preprocessing pipeline of both echoes. The comparison of both pipelines did not reveal big differences in analysis results. A high-resolution, T1-weighted 3D volume was obtained from our in-house database (if it was not older than 2 years) or was collected after the functional scans using an MPRAGE sequence (176 slices in sagittal orientation; TR = 2300 ms; TE = 2.98 ms; flip angle = 9°; voxel size = 1 × 1 × 1 mm; no slice gap; FOV = 256 mm). Moreover, we investigated a potential resampling bias through the Montreal Neurological Institute (MNI) template. To this end, we created a study-specific template based on the structural scans of our participants. We used the Computational Anatomy Toolbox (CAT12) in SPM12 to segment the structural images. Compared with the segmentation process included in SPM12, CAT12 provides a more fine-grained, advanced segmentation that has been shown to be robust to noise and to produce reliable results (Tavares et al. 2020). We then applied the Diffeomorphic Anatomical Registration Through Exponentiated Lie Algebra (DARTEL; Ashburner 2007) toolbox to create an anatomical study-specific template (young and older adults together; for a more detailed description of the procedure see Michael et al. 2016). The coregistered functional images were normalized to this study-specific template in MNI space and were subsequently smoothed with a 5-mm full-width half-maximum (FWHM) Gaussian kernel. First- and second-level statistics were calculated analogously to the analyses using the data preprocessed with fMRIPrep. The results did not reveal major differences between the two resampling procedures for univariate within-group comparisons. All significant clusters that were found with the study-specific template approach were also found with the results based on the fMRIPrep preprocessing pipeline (resampling to the MNI template). Furthermore, the latter produced more reliable activation in the ATL in both age groups (for comparison, see unthresholded statistical maps at https://neurovault.org/collections/9072/).

Preprocessing was performed using fMRIPprep 1.2.6 (Esteban et al. 2019), which is based on Nipype 1.1.7 (Gorgolewski et al. 2017). In short, within the pipeline, anatomical images were processed using the software ANTs (Tustison et al. 2010) for bias field correction, skull stripping, coregistration, and normalization to the skull-stripped ICBM 152 Nonlinear Asymmetrical template version 2009c (Fonov et al. 2009). FreeSurfer (Dale et al. 1999) was used for brain surface reconstruction and FSL (Jenkinson et al. 2012) was used for segmentation. Functional data of each run were skull-stripped, distortion-corrected, slice-time-corrected, coregistered to the corresponding T1 weighted volume, and resampled to MNI152NLin2009cAsym standard space. Head motion parameters with respect to the BOLD reference (transformation matrices and six corresponding rotation and translation parameters) were estimated before any spatiotemporal filtering using FSL. For more details of the pipeline, see the section corresponding to workflows in fMRIPrep's documentation (https://fmriprep.org/en/1.2.6/workflows.html). After preprocessing, 29 volumes from the beginning of each run were discarded since they were collected for the combination of the

short and long TE images via an estimation of the temporal signal-to-noise ratio (Poser et al. 2006). This yielded 587 normalized images per run, which were included in further analyses. The images were smoothed with a 5-mm³ FWHM Gaussian kernel using Statistical Parametrical Mapping software (SPM12; Wellcome Trust Centre for Neuroimaging), implemented in MATLAB (version 9.3/2017b).

Data Analysis

Behavioral Data

Response recordings during the semantic fluency task were cleaned from scanner noise using Audacity (version 2.3.2, https://www.audacityteam.org/) and verbal answers and onset times were transcribed by three independent raters. Repetitions of words within a category was counted as incorrect, incomplete answers and null reactions were marked separately, and full categories that had been missed by participants (in total, 10 categories) were excluded from the analyses. Statistical analyses were performed with R via RStudio (R Core Team 2018) and the packages lme4 (Bates et al. 2015) for mixed models and ggplot2 (Wickham 2016) for visualizations. We used sum coding (ANOVA-style encoding) for all categorical predictors. In this way, the intercept represents the mean across conditions (grand mean), and the model coefficients represent the difference between the grand mean and the mean of the respective condition. For the analysis of accuracy, a generalized linear mixed-effects logistic regression was used accounting for the binary nature of the response variable (eq. 1). For response time, a linear mixed-effects model was fit to the log-transformed data (eq. 2). As fixed effects, we entered age, condition, and difficulty into the models. As random effects, we had intercepts for participants and categories. Further, education was entered as covariate of no interest to account for the difference in years of education between age groups. P values were obtained by likelihood ratio tests of the full model with the effect in question against the model without the effect in question. Post hoc comparisons were applied using the package emmeans (Lenth 2020).

$$\text{Accuracy} = \beta_0 + \beta_1 \text{Age} + \beta_2 \text{Condition} + \beta_3 \text{Difficulty}$$
$$+ \beta_4 \text{Education} + \beta_5 \text{Age} \times \text{Condition} + \beta_6 \text{Age} \times \text{Difficulty} \quad (1)$$
$$+ (1|\text{Subject}) + (1|\text{Category}) + \varepsilon,$$

$$\log(\text{Response time}) = \beta_0 + \beta_1 \text{Age} + \beta_2 \text{Condition}$$
$$+ \beta_3 \text{Difficulty} + \beta_4 \text{Education} + \beta_5 \text{Age} \times \text{Condition} \quad (2)$$
$$+ \beta_6 \text{Age} \times \text{Difficulty} + (1|\text{Subject}) + (1|\text{Category}) + \varepsilon.$$

fMRI Data

fMRI data were modeled in SPM using the two-level approach. On the first level, a general linear model (GLM) was implemented for each participant. The GLM included regressors for the task blocks of the four experimental conditions (easy categories, difficult categories, counting forward, and counting backward) and nuisance regressors consisting of the six motion parameters and individual regressors for strong volume-to-volume movement as indicated by values of framewise displacement >0.9 (Siegel et al. 2014). A two-sample t-test indicated that there was no

significant difference between older adults ($M = 15.67$, $SD = 20.04$) and young adults ($M = 7.5$, $SD = 8.35$) with respect to the number of regressed volumes ($t(28.76) = 1.66$, $P = 0.11$). Additionally, an individual regressor of no interest was included in the design matrix if a participant had missed a whole task block during the experiment ($n = 10$). Before model estimation, a high-pass filter with a cutoff at 128 s was applied to the data. Statistical parametric maps were generated by estimating the contrast for each condition against rest as well as the direct contrasts between conditions. At the second level, contrast images were entered into a random effects model. For each participant, an averaged mean-centered value of response time was entered as covariate of no interest in the design matrix. For within-group comparisons, one-sample t-tests were calculated for the main task-related contrasts, semantic fluency > counting and counting > semantic fluency. To evaluate the modulation of task difficulty within the semantic fluency task, the contrasts, easy > difficult categories and difficult > easy categories, were computed.

To investigate the effect of age on task-related activity, we conducted between-group comparisons for the interaction contrasts $c_{\text{Age} \times \text{Semantic fluency}}$ and $c_{\text{Age} \times \text{Condition}}$. Two-sample t-tests were carried out using the individual contrast images from the first-level analysis. To ensure that potential areas were indeed active in the respective group, all interactions were characterized by inclusively masking each contrast with significant voxels of the minuend (at $P < 0.001$, uncorr., cf. Noppeney et al. 2006, Meinzer, Seeds, et al. 2012). A gray matter mask which restricted statistical tests to voxels with a gray matter probability >0.3 (SPM12 tissue probability map) was applied to all second-level analyses. All results except for the interaction contrasts were corrected for multiple comparisons applying a peak level threshold at $P < 0.05$ with the family-wise error (FWE) method and a cluster-extent threshold of 20 voxels. Interaction results were thresholded at $P < 0.05$ at the cluster level with FWE correction and a voxel-wise threshold at $P < 0.001$. Anatomical locations were identified with the SPM Anatomy Toolbox (Eickhoff et al. 2005, version 2.2c) and the Harvard-Oxford cortical structural atlases distributed with FSL (https://fsl.fmrib.ox.ac.uk). Brain results were rendered by means of BrainNet Viewer (Xia et al. 2013, version 1.7) and MRIcroGL (https://www.mccauslandcenter.sc.edu/mricrogl/, version 1.2.20200331).

Since the strongest activation peaks for both tasks were found in the domain-general systems, MDN and DMN, we decided to examine the amount of activation for each condition and age group. We applied binary masks of both networks to analyses within the group of young adults to identify clusters that fell within the respective network. By basing our analysis on activity in the young adults, we ensured that more complex analyses were based on the same number of regions in both age groups. Further, this allowed us to investigate age-related differences in these regions knowing that they are relevant for task processing in young adults. For comparison, we have added an overview of the age-specific ROIs to the supplementary analyses (Supplementary Table S1). The MDN mask was based on the anatomical parcels of the MD system defined by Fedorenko et al. (2013), available at https://evlab.mit.edu/funcloc/. We decided to use the MDN parcellation since it has been shown that regions of different networks that are commonly disentangled in resting-state network parcellations (e.g., the fronto-parietal network, cingulo-opercular network, and dorsal attention network) together form a core set of MD regions for goal-directed cognitive

processing (Camilleri et al. 2018; Assem et al. 2020). For the DMN, a mask was created from the seven-network parcellation by Schaefer et al. (2018). For the contrast, semantic fluency > counting, peak global and local maxima were found in the MDN, whereas the reverse contrast identified clusters that are typically associated with the DMN. Due to the small number ($n = 3$) of peak clusters for the contrast, counting > semantic fluency with FWE correction at peak level, we decided to apply a more lenient threshold (FWE-corrected at cluster level, $P < 0.001$ at peak level) for the identification of regions associated with the DMN. This allowed us to extract a similar number of peak maxima for the MDN and the DMN and provided a much more representative picture of the DMN as a whole. In total, we identified 14 peak maxima in the MDN and 17 peak maxima in the DMN, respectively (Table 2). ROIs for these maxima were created using the MarsBar toolbox (Brett et al. 2002; version 0.44). To this end, identified clusters were extracted from contrast images, spheres of 5 mm from each maxima coordinate were created, and, in a last step, both images were combined. Subsequently, we extracted parameter estimates for these ROIs from the individual contrast images for semantic fluency > rest and counting > rest. The data were then entered into a linear mixed-effects model with network, age, and condition as fixed effects. A random intercept was included for participants (eq. 3). Categorical predictors were sum-coded. Significance values were obtained through likelihood ratio tests using the package lme4 (Bates et al. 2015). Post hoc comparisons were applied using the package emmeans (Lenth 2020).

$$\text{Beta weight} = \beta_0 + \beta_1 \text{Network} + \beta_2 \text{Age} + \beta_3 \text{Condition}$$
$$+\beta_4 \text{Network} \times \text{Age} + \beta_5 \text{Network} \times \text{Condition} + \beta_6 \text{Age} \times \quad (3)$$
$$\text{Condition} + (1|\text{Subject}) + \varepsilon.$$

Functional Connectivity Analyses
We conducted psychophysiological interaction (PPI) analyses using the gPPI toolbox for SPM12 (McLaren et al. 2012) to investigate the task-related modulation of functional connectivity, for semantic fluency. Furthermore, we applied a modified version of gPPI methods to examine the functional connections between individual ROIs during the semantic fluency task (Pongpipat et al. 2020). Seed regions were defined for all previously identified global maxima that were located within the MDN and the DMN (Table 2). For each participant, ROIs were created by searching for the individual peaks within a bounding region of 10 mm relative to the group peak and by drawing a sphere mask (5 mm in diameter) around the individual peak of a given contrast at a threshold of $P < 0.01$. To ensure that all participants had gray matter coverage of the analyzed ROIs ($n = 31$), we resampled each participant's gray matter mask to the ROIs and calculated the amount of voxels ($2 \times 2 \times 2$ mm) within the mask for each participant and ROI. We found that all participants had voxels within the gray matter mask of each ROI.

Regression models were set up for each ROI in each participant, containing the deconvolved time series of the first eigenvariate of the BOLD signal from the respective ROI as the physiological variable, the four task conditions convolved with the HRF as the psychological variable, and the interaction of both variables as the PPI term. Subsequently, first-level GLMs were calculated. For the gPPI proper methods, contrast images were then entered into a random effects model for group analyses in SPM. We restricted this analysis to the strongest peaks of

both contrasts (semantic fluency > counting and counting > semantic fluency) that fell within the MDN and DMN, respectively. This included the left pre-supplementary motor area (pre-SMA), bilateral insulae, the right temporal pole, and the right precuneus. Our main contrast of interest semantic fluency > counting was examined in within-group as well as between-group comparisons by conducting one-sample t-tests and a two-sample t-test, respectively. Multiple comparison correction was performed with the FWE method at $P < 0.05$ at peak level and a cluster-extent value of 20 voxels. A gray matter mask was applied to all group analyses as described for the task-based fMRI data analysis.

For the modified gPPI, we used the individual first-level GLMs to retrieve parameter estimates (mean regression coefficients). Estimates were extracted for the PPI variable semantic fluency > counting for each seed-to-target ROI (1 regression coefficient [PPI] * 31 seed ROIs * 30 target ROIs = 930 parameter estimates per participant). Subsequent group analyses were performed in RStudio (R Core Team 2018) with the package lme4 (Bates et al. 2015) and were visualized using the ggplot2 (Wickham 2016) and the ggeffects (Lüdecke 2018) packages. Categorical predictors were sum-coded. We were interested in the functional connectivity within and between MDN and DMN regions for each age group. To this end, we calculated intercept-only GLMs where each parameter estimate of each seed and target combination was entered into the model except when the seed and target were identical (eq. 4). The α-level (type I error) for post hoc comparisons was adjusted using the "Meff" correction (Derringer 2018). This method estimates the effective number of tests (Meff) from the correlations among tested variables and thereby allows for adjusting statistical significance thresholds for multiple comparisons without assuming independence of all tests (Derringer 2018). The Meff value for MDN and MDN variables was calculated to be 27.5. By dividing this value by the overall α of 0.05, we obtained a Meff-corrected α of 0.0018. For subsequent analyses, the individual parameter estimates of each seed-to-target combination were averaged to create one value per participant for within-MDN, within-DMN, and between-network functional connectivity (three parameter estimates per participant). To test for an effect of age group on functional connectivity, the parameter estimates were then entered into a GLM with age group as independent variable (eq. 5). We used Meff correction to adjust for multiple comparisons. A Meff value of 2.49 yielded a Meff-corrected α of 0.02. To ensure that our functional connectivity results were not confounded by head motion, we calculated the root mean square (RMS) of realignment parameters and correlated the average motion RMS per participant with each functional connectivity measure. Results did not reveal any significant correlation (see supplementary material).

$$\text{PPI}_{\text{contrast}} = \beta_0 + \varepsilon, \quad (4)$$

$$\text{PPI}_{\text{contrast}} = \beta_0 + \beta_1 \text{Age} + \varepsilon. \quad (5)$$

Furthermore, we were interested in the effect of within- and between-network functional connectivity on participants' behavioral performance during the in-scanner semantic fluency task. To this end, we calculated generalized mixed-effects logistic regressions for the accuracy data (eq. 6) and linear mixed-effects models for the log-transformed response time data (eq. 7). The mean-centered $\text{PPI}_{\text{network}}$ variables and age group as well as their interaction terms were entered as fixed effects. Random intercepts were included for participants and semantic

Table 2 ROIs within domain-general networks

ROI	Hemi	x	y	z	Region
MDN (from contrast, semantic fluency > counting)					
1	L	−31	25	2	Insula
2	L	−4	25	40	preSMA
3	L	−6	12	51	preSMA
4	R	13	27	29	dACC
5	L	4	20	40	dACC
6	L	−4	2	29	dACC
7	R	31	27	2	Insula
8	R	38	20	−4	Insula
9	L	−29	−65	51	SPL
10	L	−29	−72	43	AG
11	L	−34	−57	40	IPL
12	R	36	42	32	MFG
13	R	31	55	26	MFG
14	R	33	37	21	MFG
DMN (from contrast, counting > semantic fluency)					
15	R	51	10	−31	TP
16	R	48	−10	−15	STG
17	R	8	−65	29	Precuneus
18	R	11	−52	35	Precuneus
19	L	−9	−52	35	Precuneus
20	L	−56	2	−20	MTG
21	L	−54	10	−31	TP
22	L	−6	27	−6	ACC
23	L	−6	42	−4	ACC
24	L	−54	−62	35	AG
25	L	−41	−60	26	AG
26	L	−46	−62	18	MTG
27	L	−46	−75	35	AG
28	L	−49	−67	43	AG
29	R	51	−57	26	AG
30	R	46	−65	48	AG
31	R	43	−72	35	AG

Note: Co-ordinates are given in MNI standard space. Abbreviations: Hemi, hemisphere; IPL, inferior parietal lobe; MFG, middle frontal gyrus; SPL, superior parietal lobe; IntraCAL, Intracalcarine gyrus; TP, temporal pole; STG, superior temporal gyrus.

categories. Education was entered as covariate of no interest to account for the difference in years of education between age groups.

$$
\begin{aligned}
\text{Accuracy} = \beta_0 &+ \beta_1 \text{PPI}_{\text{MDN}} + \beta_2 \text{PPI}_{\text{DMN}} + \beta_3 \text{PPI}_{\text{MDN\_DMN}} \\
&+ \beta_4 \text{Age} + \beta_5 \text{Education} + (\beta_6 \text{PPI}_{\text{MDN}} \\
&+ \beta_7 \text{PPI}_{\text{DMN}} + \beta_8 \text{PPI}_{\text{MDN\_DMN}}) \times \text{Age} \\
&+ (1|\text{Subject}) + (1|\text{Category}) + \varepsilon,
\end{aligned} \quad (6)
$$

$$
\begin{aligned}
\log(\text{Response time}) = \beta_0 &+ \beta_1 \text{PPI}_{\text{MDN}} + \beta_2 \text{PPI}_{\text{DMN}} + \\
\beta_3 \text{PPI}_{\text{MDN\_DMN}} &+ \beta_4 \text{Age} + \beta_5 \text{Education} + (\beta_6 \text{PPI}_{\text{MDN}} \\
&+ \beta_7 \text{PPI}_{\text{DMN}} + \beta_8 \text{PPI}_{\text{MDN\_DMN}}) \times \text{Age} \\
&+ (1|\text{Subject}) + (1|\text{Category}) + \varepsilon.
\end{aligned} \quad (7)
$$
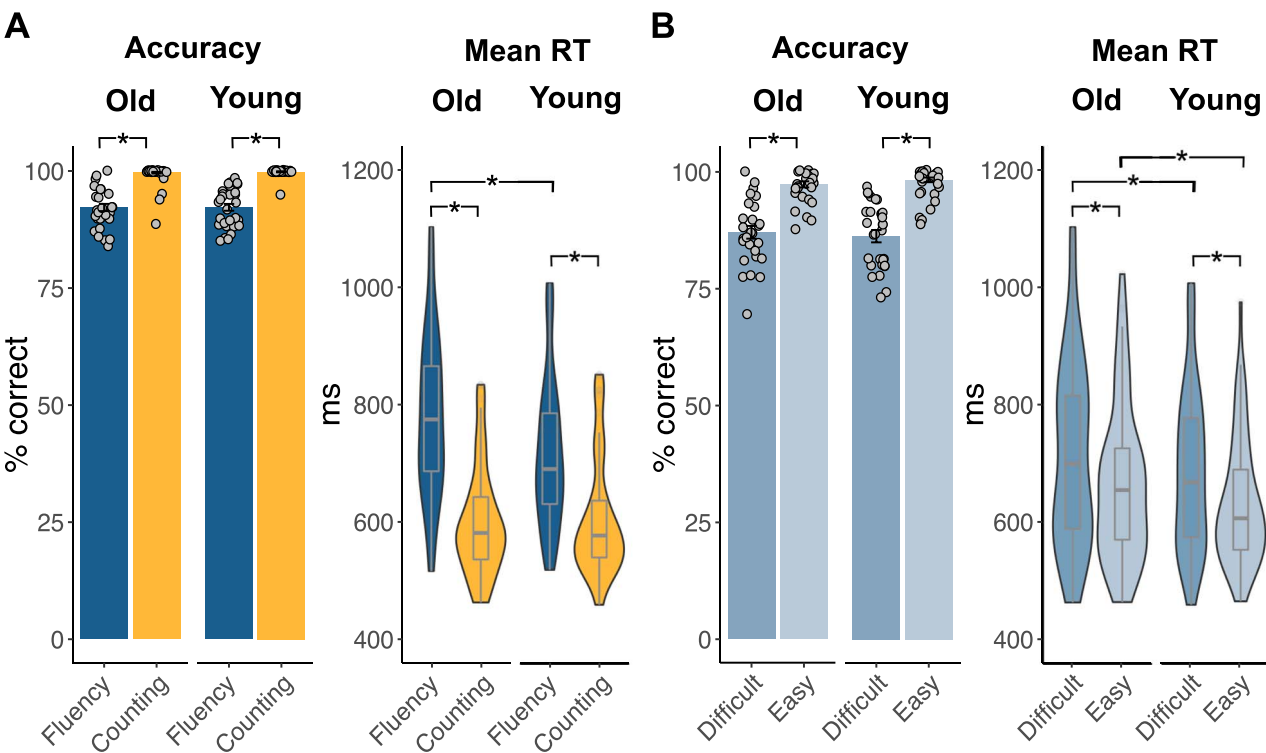
Finally, to assess how the observed changes in network properties were related to cognitive performance and semantic memory in general, we performed correlation analyses with the neuropsychological measures that had been tested outside of

the scanner. Due to the collinearity of some neuropsychological tests, we first performed a factor analysis on the standardized test scores using maximum likelihood estimation and varimax rotation in RStudio with the package stats (R Core Team 2018). Based on the hypothesis test ($\chi^2 = 14.04$, $P = 0.081$), two factors with an eigenvalue >1 were chosen. For subsequent correlations with functional connectivity measures, participant factor scores extracted via regression methods were used.

Results

Behavioral Results

For response accuracy, we fitted a generalized linear mixed-effects model for a binomial distribution. Likelihood ratio tests indicated significant main effects of condition ($\chi^2 = 21.59$, $P < 0.001$) and task difficulty ($\chi^2 = 27.47$, $P < 0.001$) but not of age group ($\chi^2 = 2.23$, $P = 0.14$). Further, we detected a significant two-way interaction between age and difficulty ($\chi^2 = 9.76$, $P = 0.002$) and condition and difficulty ($\chi^2 = 3.90$, $P = 0.048$) as well as a significant three-way interaction between age, condition, and difficulty ($\chi^2 = 9.28$, $P = 0.002$). Post hoc tests applying Bonferroni-corrected pairwise comparisons showed that both age groups produced more correct items in the counting than in the

Figure 2. Behavioral results for both age groups. Bar graphs overlaid with mean individual data points for accuracy and violin plots with box plots for mean response times for (A) both tasks (semantic fluency and counting) and (B) difficulty levels (easy and difficult) within semantic fluency. Old, older adults; young, young adults. *$P < 0.001$ (Bonferroni-corrected for pairwise comparisons).

semantic fluency task (all $P < 0.001$) and more items for the easy than the difficult semantic categories (all $P < 0.001$; Fig. 2A; Supplementary Tables S2 and S3).

Response times were analyzed fitting a linear mixed-effects model after log-transformation of the data. Likelihood ratio tests revealed main effects of condition ($\chi^2 = 21.37$, $P < 0.001$) and difficulty ($\chi^2 = 20.98$, $P < 0.001$) but not of age group ($\chi^2 = 3.25$, $P < 0.072$). There was a significant interaction between age and condition ($\chi^2 = 69.46$, $P < 0.001$). Post hoc tests using Bonferroni-corrected pairwise comparisons showed that both age groups responded significantly slower during the semantic fluency task than the counting task and during the difficult than the easy condition (all $P < 0.001$). Furthermore, young adults responded generally faster than older adults during the semantic fluency task ($P < 0.001$), independent of the level of difficulty, but not during the counting task ($P = 0.05$; Fig. 2B; Supplementary Tables S2 and S4).
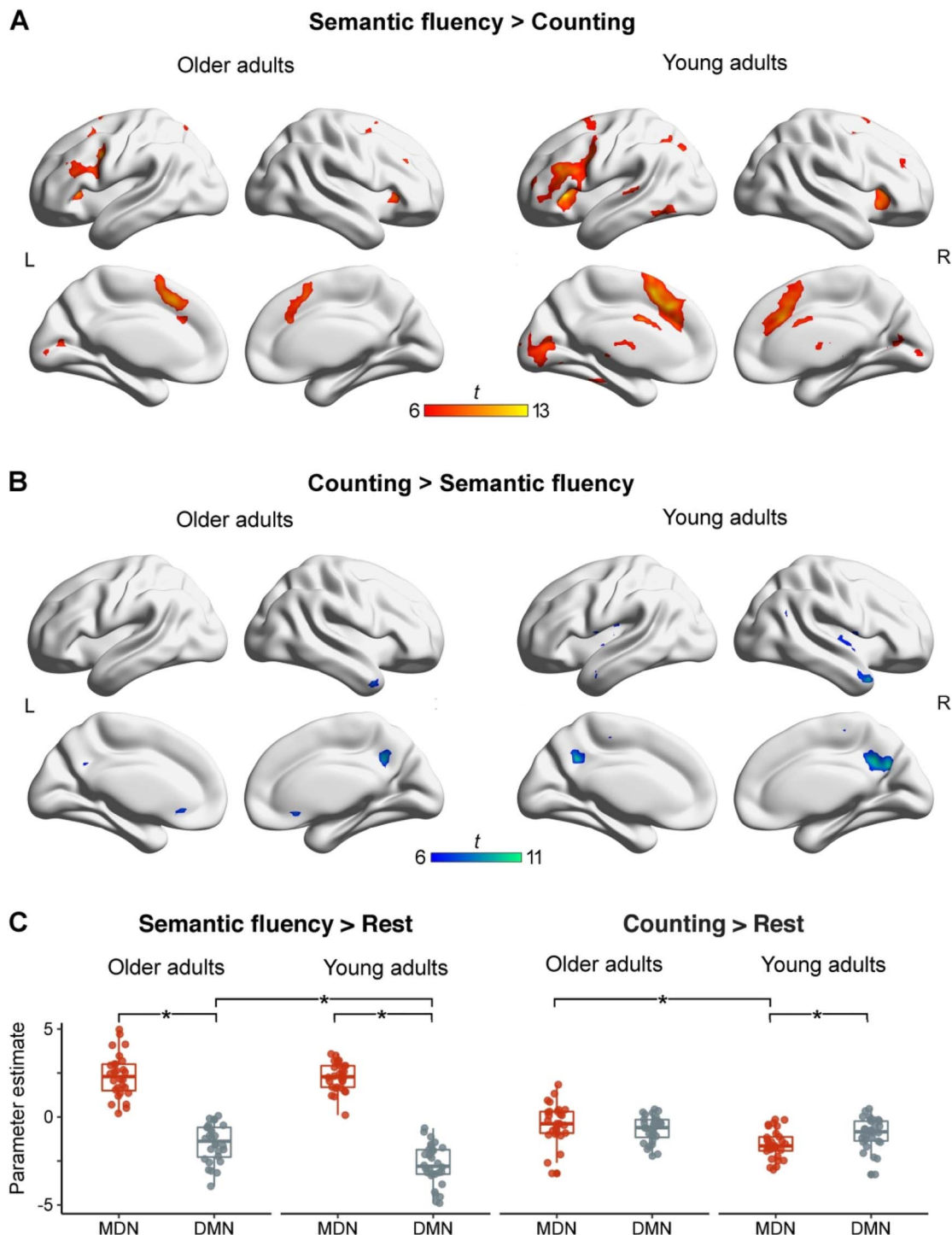
fMRI Data

The Effect of Task within Groups

Both age groups showed similar activation patterns for the main effects of our tasks compared with rest. For semantic fluency, we found a left-lateralized fronto-temporo-parietal network with additional clusters in right frontal and temporal areas, bilateral caudate nuclei, and the cerebellum (Supplementary Fig. S2; Supplementary Tables S5 and S6). The main effect of the less-demanding task counting was evident in bilateral activation of sensorimotor cortices and the cerebellum (Supplementary Fig. S2; Supplementary Tables S7 and S8).

Within each age group, we were interested in the difference in brain activation between the more demanding semantic fluency task and the automatic speech counting task as well as in the impact of the modulation of task difficulty in the semantic fluency task. For the older adults, the contrast, semantic fluency > counting, revealed a bilateral frontal network with its strongest activation peaks in middle frontal gyri, bilateral insulae extending into inferior frontal gyri, and midline structures comprising superior and medial frontal gyri. Activation in the left hemisphere was further observed in the angular gyrus and superior parietal lobe. Additional bilateral activation peaks were found in the cerebellum, caudate nuclei, calcarine gyri, and thalami (Fig. 3A; Supplementary Table S9). Younger adults demonstrated a similar pattern of activation for the contrast, semantic fluency > counting, albeit with generally larger clusters in the frontal network (Fig. 3A; Supplementary Table S10). Analyses further yielded separate clusters in the dorsal anterior cingulate cortex (dACC) and the left superior temporal gyrus for the younger group, which were not present in the older participants. The reverse contrast (counting > semantic fluency) revealed stronger activation in the right hemisphere for both groups. Results showed clusters in the right temporal pole and bilateral precunei (Fig. 3B; Supplementary Tables S11 and S12). In the younger group, additional clusters were observed in bilateral insulae and the middle temporal gyrus (MTG). When we applied a more lenient threshold of $P < 0.001$ at peak level and FWE correction ($P < 0.05$) at cluster level, additional peaks were observed in bilateral parietal lobes, including angular gyri and the anterior cingulate cortex, in the young adults (Supplementary Table S13).
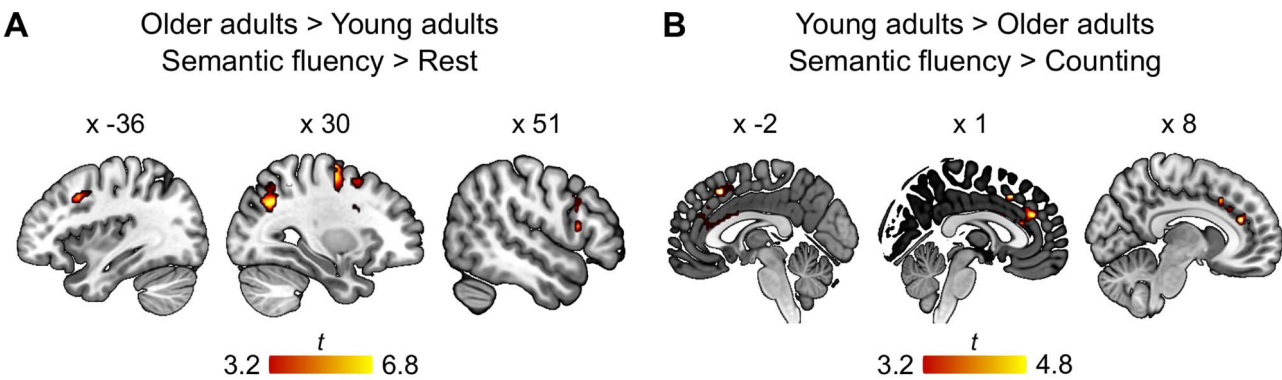
A linear mixed-effects model was fit for the mean value of parameter estimates for all peak clusters in the MDN and

Figure 3. fMRI results from univariate analyses for each age group and parameter estimates for peak maxima identified within the MDN and the DMN. (A & B) Results are FWE-corrected at $P < 0.05$ at peak level with a minimum cluster size = 20 voxel. Unthresholded statistical maps are available at https://neurovault.org/collections/9072/. (C) * Significant effects are Bonferroni-corrected.

DMN (Table 2), respectively. Likelihood ratio tests indicated significant effects for the explanatory variables network ($\chi^2 = 92.73$, $P < 0.001$), age ($\chi^2 = 11.03$, $P = 0.017$), and condition ($\chi^2 = 23.04$, $P < 0.001$). We further found a significant interaction between network and condition ($\chi^2 = 196.14$, $P < 0.001$) and a

significant three-way interaction between network, age, and condition ($\chi^2 = 18.58$, $P < 0.001$). Post hoc comparisons applying Bonferroni correction revealed an effect of age for the DMN for the contrast, semantic fluency > rest, with older adults showing stronger activity in DM regions than young adults (t = 4.89,

A Older adults > Young adults
Semantic fluency > Rest

x -36   x 30   x 51

t
3.2 ▇▇▇ 6.8

B Young adults > Older adults
Semantic fluency > Counting

x -2   x 1   x 8

t
3.2 ▇▇▇ 4.8

Figure 4. fMRI results for interaction effects. Cluster corrected at FWE $P < 0.05$ with a voxel-wise threshold at $P < 0.001$. (A) Restricted to voxels that showed a significant effect of semantic fluency in older adults and (B) restricted to voxels that showed a significant effect of semantic fluency in young adults. Statistical maps are available at https://neurovault.org/collections/9072/.

$P < 0.001$) as well as an effect of age for the MDN for the contrast, counting > rest, with older adults showing stronger activity in MD regions than young adults ($t = 4.81$, $P < 0.001$). Moreover, post hoc tests showed that, in general, the MDN was activated for the semantic fluency task across age groups, whereas the DMN showed deactivation ($t = 24.99$, $P < 0.001$). For the counting task, there was no difference in activation between both networks ($t = 0.81$, $P = 0.42$; Fig. 3C; Supplementary Tables S14 and S15).

The Effect of Task Difficulty within Groups
To investigate the effect of task difficulty on functional brain activation, we contrasted easy and difficult categories from the semantic fluency task in both age groups. We found a significant result only for young adults for the contrast, easy > difficult categories, in the right middle frontal gyrus (Supplementary Table S16).

Between-Group Comparisons
We were interested in the effect of age on task-related activations. For the interaction of both tasks compared with baseline, we found a group difference only during the semantic fluency task for older adults. We detected stronger activity in right frontal regions, including superior frontal gyrus and inferior frontal gyrus (IFG) as well as bilateral parietal lobes (Fig. 4A; Table 3). We were further interested in the interaction of age and condition. The contrast, semantic fluency > counting, revealed a significant interaction with age only for young adults. Stronger activity was observed in the paracingulate gyrus, pre-SMA, and the dACC (Fig. 4B; Table 3). The interaction of age with task difficulty (easy and difficult semantic categories) did not yield any significant results.

Generalized PPIs

Based on the activation patterns from our univariate within-group analyses, we conducted traditional gPPI analyses for the five strongest activation peaks that fell within the MDN or DMN. We asked whether and how increased semantic task demands modulate the connectivity of our ROIs.

Whole-Brain Functional Connectivity for Semantic Fluency
Three ROIs were extracted from the univariate contrast, semantic fluency > counting, the left pre-SMA and bilateral insulae. For the seeds in the left pre-SMA and left insula, analyses

revealed only significant clusters in the group of younger adults, whereas the seed in the right insula yielded only significant results for the older adults. The left pre-SMA showed increased connectivity with subcortical structures (bilateral caudate nuclei and thalami) as well as with the left precuneus and PCC in the parietal lobe (Fig. 5A; Supplementary Table S17). For the seed in the left insula, we found a similar connectivity pattern. Significant coupling was observed with bilateral caudate nuclei and the left precuneus (Fig. 5B; Supplementary Table S18). For the older adults, the right insula showed significant coupling with the precuneus and pars orbitalis in left IFG (Fig. 5C; Supplementary Table S19).

Moreover, two ROIs from the contrast, counting > semantic fluency, which were associated with the DMN, the right temporal pole, and the right precuneus, were used for traditional gPPI analyses. Seeding in the right temporal pole showed increased functional connectivity exclusively in the ipsilateral hemisphere. For the older adults, we found a significant cluster in IFG (pars opercularis) which extended into the insula (Fig. 6A; Supplementary Table S20). For the young adults, results revealed significant clusters in the IFG (pars opercularis), superior frontal gyrus, insula, and supramarginal gyrus (Fig. 6A, Supplementary Table S20). The seed in the right precuneus revealed extensive bilateral functional coupling in both age groups. For the older adults, the right precuneus showed prominent connectivity with frontal, temporal, and parietal areas in both hemispheres (Fig. 6B; Supplementary Table S21). A similar pattern emerged for the group of younger adults, albeit with a greater number of significant clusters (Fig. 6B; Supplementary Table S21). Two-sample *t*-tests did not show significant differences between groups in the PPI results for either task.

Within- and Between-Network Functional Connectivity during Semantic Fluency
To further examine the task-related connectivity within and between the domain-general systems, MDN and DMN, during the semantic fluency task compared with counting, we conducted modified gPPI analyses. For each seed-to-target combination of the ROIs in MDN and DMN (Table 2), we calculated intercept-only GLMs for each age group (Fig. 7A). For older adults, the results showed significant positive functional connectivity for regions within the MDN but not for regions within the DMN. Further, the analyses revealed strong coupling for regions between MD and DM networks. A similar pattern was observed

Table 3 Results for age-dependent differences in task-related activity

Anatomical structure	Hemi	k	t	x	y	Z
Interaction older > young adults for semantic fluency > rest (inclusively masked with [older adults: semantic fluency > rest])						
Superior frontal gyrus	**R**	**110**	**6.84**	**28**	**−8**	**65**
Precentral gyrus	R		5.53	28	-8	54
Superior parietal lobe	**R**	**263**	**6.82**	**18**	**−60**	**60**
Middle occipital gyrus	R		6.04	31	-62	35
Precuneus	R		5.93	11	-55	60
Precuneus	R		5.39	13	-67	62
Middle frontal gyrus	**L**	**74**	**5.38**	**−36**	**15**	**38**
Middle frontal gyrus	L		4.05	-46	17	38
Precentral gyrus	L		3.76	-41	2	48
Inferior parietal lobe	**L**	**109**	**5.12**	**−31**	**−45**	**54**
Superior parietal lobe	L		4.32	-19	-60	46
Precuneus	L		4.28	-11	-70	48
Superior parietal lobe	L		4.19	-16	-62	60
Middle frontal gyrus	**R**	**132**	**4.96**	**36**	**5**	**38**
IFG, p.tr.	R		4.53	36	17	24
IFG, p.op.	R		4.07	48	17	13
IFG, p.op.	R		3.73	51	15	26
Middle frontal gyrus	**R**	**74**	**4.47**	**26**	**12**	**51**
Interaction young > older adults for semantic fluency > counting (inclusively masked with [young adults: semantic fluency > counting])						
Pre-SMA	**L**	**79**	**4.84**	**−1**	**20**	**46**
Pre-SMA	R		3.81	11	27	32
Pre-SMA	L		3.55	-1	10	48
Anterior cingulate cortex	**R**	**114**	**4.58**	**8**	**37**	**21**
Pre-SMA	R		4.36	1	37	26
Anterior cingulate cortex	L		4.13	-1	20	21
Anterior cingulate cortex	L		3.58	-4	5	29

Note: Cluster corrected at FWE $P < 0.05$ with a voxel-wise threshold at $P < 0.001$. Co-ordinates are given in MNI standard space, cluster size (k) is given in mm^3, Global cluster peaks are marked in bold. Note that no significant differences above cluster correction threshold were found for 1) interaction young > older adults for semantic fluency > rest, 2) interaction older > young adults for semantic f luency > counting. Abbreviations: p. tr., pars triangularis; p.op., pars opercularis.

for young adults, albeit with overall stronger connectivity. Compared with the counting task, results showed strengthened functional connectivity within regions of the MDN and for regions between MD and DM networks during semantic fluency.

Effect of Age on Within- and Between-Network Functional Connectivity
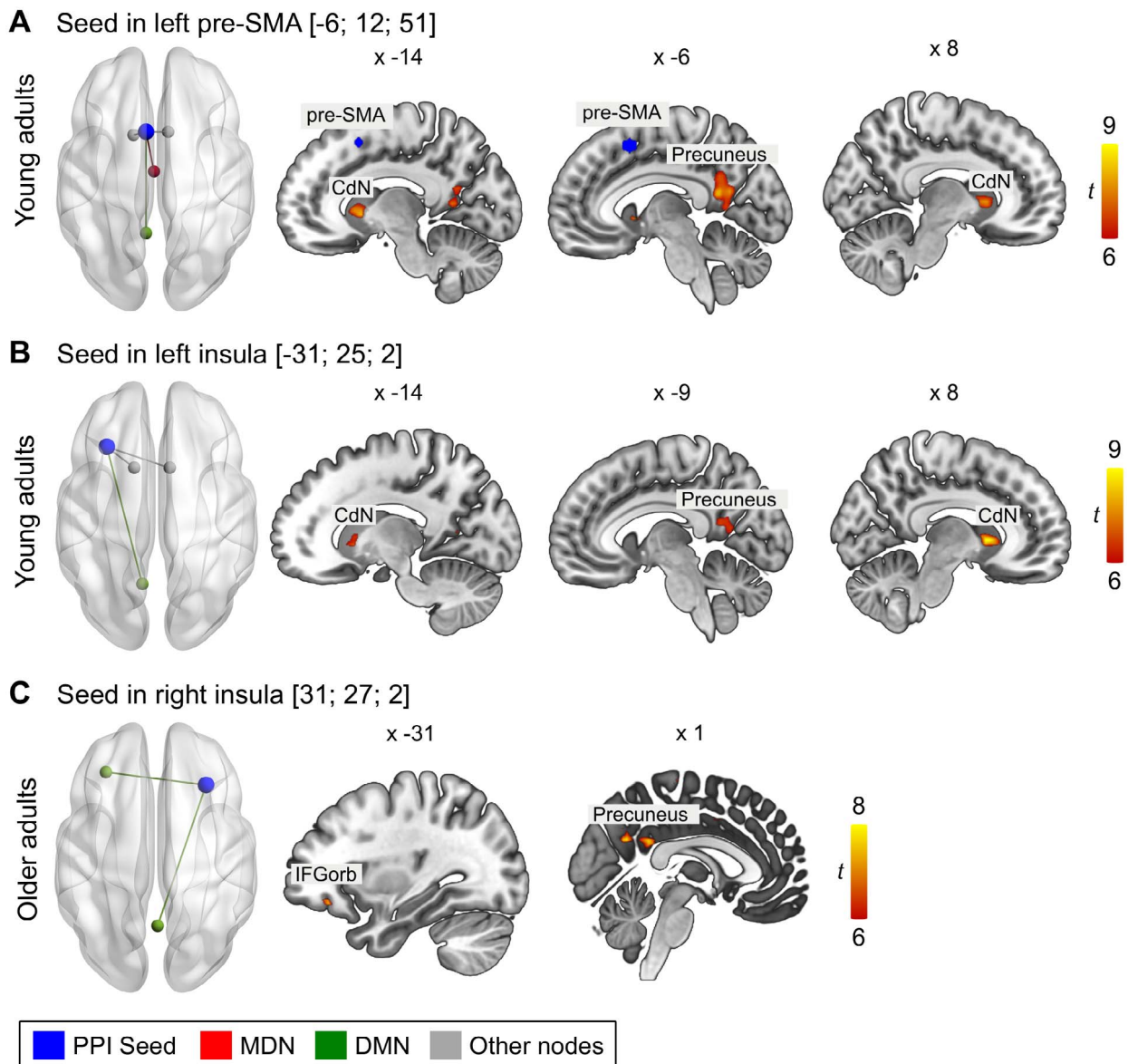
We were interested whether there was an effect of age group on the within- and between network functional connectivity. To this end, each PPI network pair (within-MDN, within-DMN, and between MDN and DMN) was regressed on age (Fig. 7B; Supplementary Table S22). Multiple-comparison correction was performed using Meff correction. The results did not show a significant effect of age on within- and between-network functional connectivity ($Ps > 0.3$), suggesting that the strength of functional connectivity was age-invariant.

Effect of Functional Connectivity on In-Scanner Task Performance

To determine whether functional connectivity within and between regions of MDN and DMN predicted participant's in-scanner task performance, we fitted generalized mixed-effects models for accuracy and response time as outcome variables and functional connectivity, age, and their interaction terms as explanatory variables. Since the functional connectivity measures were based on our contrast of interest, semantic

fluency > counting, statistical models were only fit for the behavioral results for the semantic fluency and not for the counting task. The results did not indicate significant effects of functional connectivity on accuracy (Supplementary Table S23). However, analyses revealed significant effects of functional network connectivity on response time (Fig. 7C; Supplementary Table S23 and S24). We identified main effects of within-DMN ($\chi^2 = 15.16$, $P < 0.001$) and between-network functional connectivity ($\chi^2 = 31.44$, $P < 0.001$) as well as of age ($\chi^2 = 20.26$, $P < 0.001$). Beta coefficients indicated that, across networks, strengthened functional connectivity was associated with slower response times and that young adults performed generally faster than older adults, which confirmed our behavioral results.

Moreover, significant interactions between age and within-MDN ($\chi^2 = 29.01$, $P < 0.001$), within-DMN ($\chi^2 = 37.40$, $P < 0.001$), and between-network functional connectivity ($\chi^2 = 23.75$, $P < 0.001$) were found. Post hoc tests showed that age group had a different effect on within- and between-network functional connectivity. While response time increased with strengthened connectivity in the MDN and the DMN for older adults, the opposite pattern was observed for young adults who responded faster when within-network functional connectivity increased (all $P < 0.001$). For functional connectivity between MDN and DMN, stronger coupling predicted slower responses in both age groups, albeit with young adults showing a significantly steeper positive slope than older adults ($P < 0.001$; Fig. 7C).
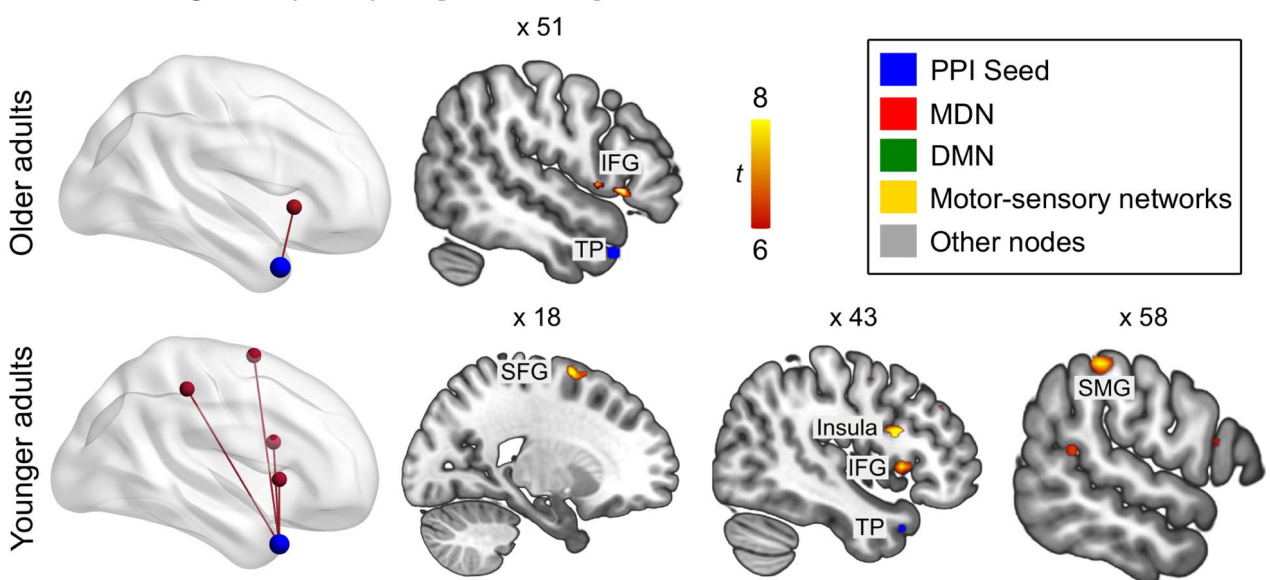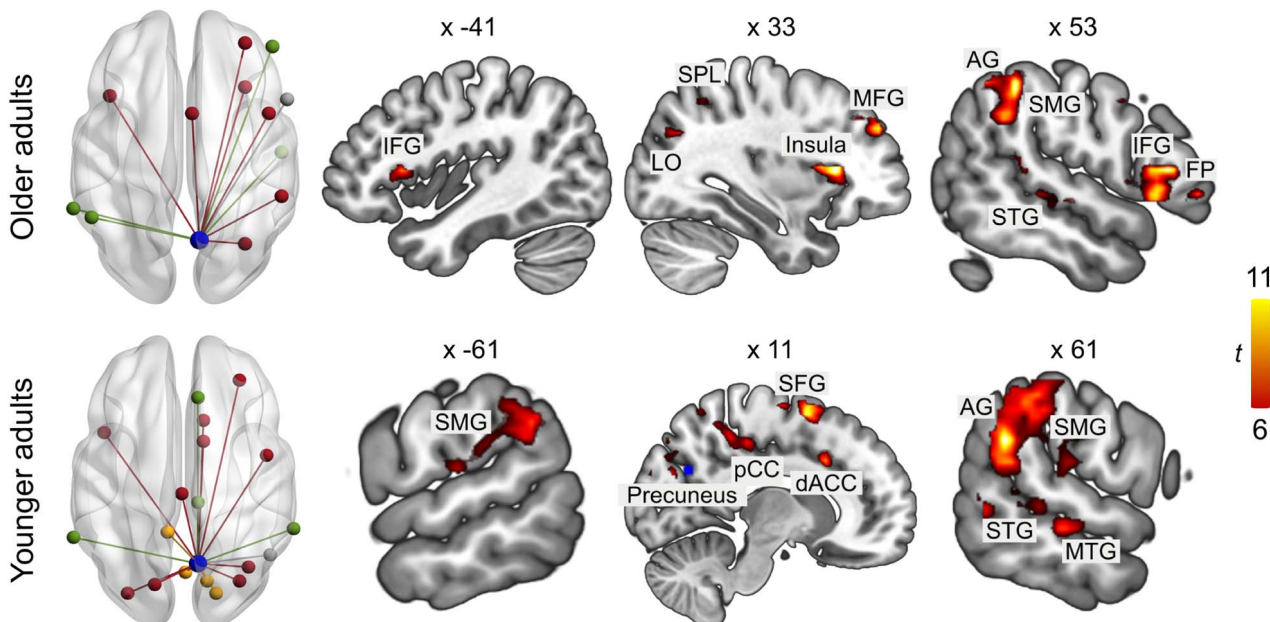
Figure 5. Functional connectivity for seeds from contrast, semantic fluency > counting. Seeds are (A) left pre-SMA, (B) left insula, and (C) right insula. All results are FWE-corrected at P < 0.05 at peak level with a minimum cluster size < 20 voxel. Abbreviations: CdN, caudate nucleus; IFGorb, inferior frontal gyrus, pars orbitalis. Unthresholded statistical maps are available at https://neurovault.org/collections/9072/.

Effect of Functional Connectivity on Cognitive Performance and Semantic Memory

We were interested in the relationship between functional connectivity and general cognitive and semantic memory performance, which were assessed via neuropsychological tests outside of the scanner. Since some tests showed high collinearity, we first performed a factor analysis on the data of both age groups together. Results identified two factors: A "cognitive performance" factor with high loadings on Trail Making Tests, A (0.8) and B (0.71), the Digit Symbol Substitution Test (0.73), the reading span test (0.45), and a "semantic memory" factor with high loadings on the spot-the-word test (0.5), and the two verbal fluency tests for hobbies (0.44) and surnames (0.98).

Individual factor scores for participants were extracted and were subsequently correlated with functional connectivity measures. The resulting P values were corrected for multiple comparisons using Bonferroni correction (P = 0.05/3 functional connectivity parameters = 0.017). First, we used partial Pearson correlations to test for a relation between connectivity and cognitive performance while controlling for the effect of age. Results revealed a significant positive correlation between executive functions and within-MDN functional connectivity (r = 0.36, P = 0.018). Second, we calculated Pearson correlations within each age group. For older adults, we found a significant positive correlation between cognitive performance and within-MDN functional connectivity (r = 0.46, P = 0.043; Fig. 7D). For young adults, results showed
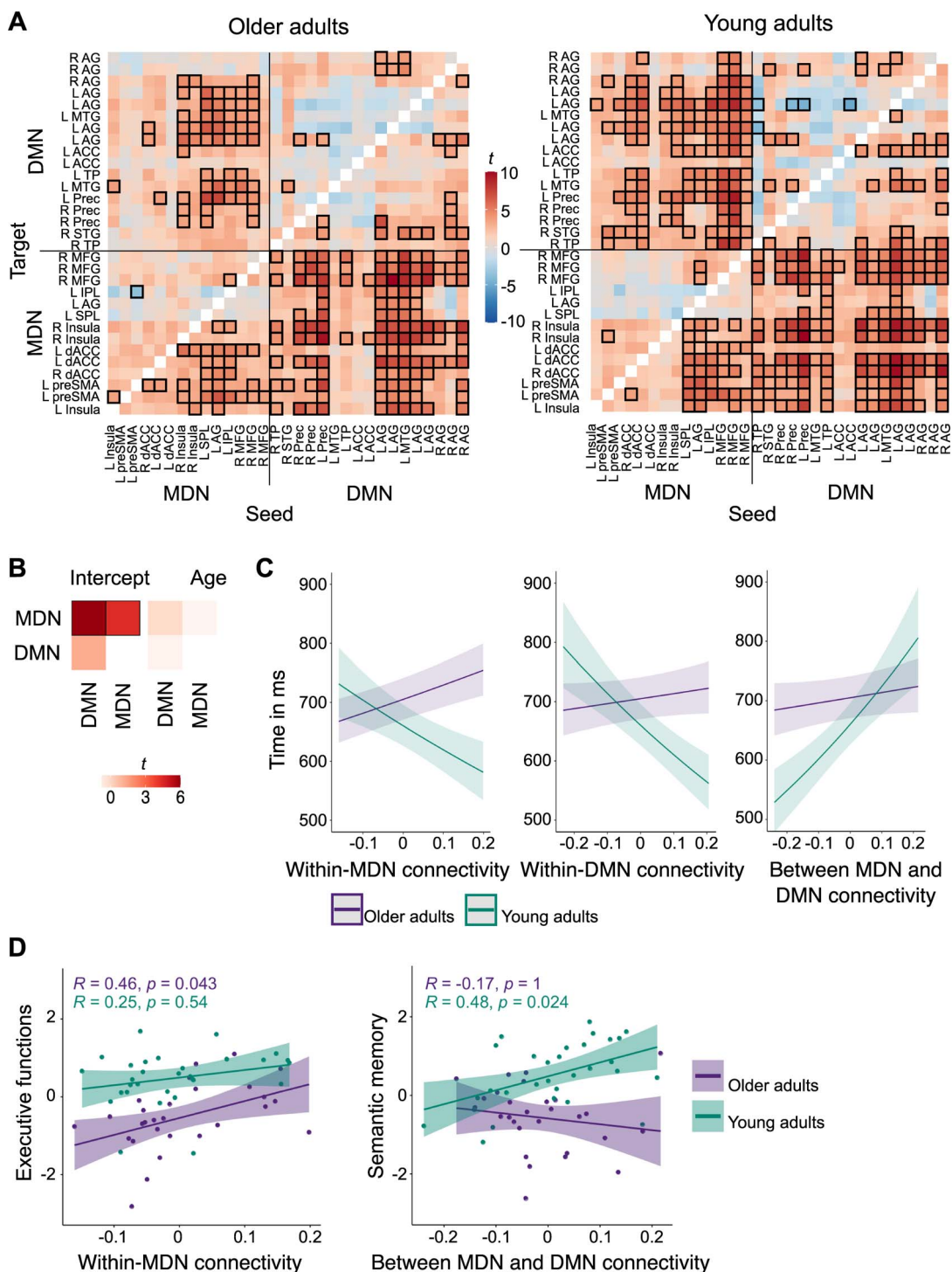
Figure 6. Functional connectivity for seeds from contrast, counting > semantic fluency. Seeds are (A) right temporal pole and (B) right precuneus. All results are FWE-corrected at $P < 0.05$ at peak level with a minimum cluster size > 20 voxel. Abbreviations: SFG, superior frontal gyrus; SMG, supramarginal gyrus; LO, lateral occipital cortex; AG, angular gyrus; FP, frontal pole. Unthresholded statistical maps are available at https://neurovault.org/collections/9072/.

a significant positive correlation between semantic memory and functional connectivity between MDN and DMN ($r = 0.48$, $P = 0.024$; Fig. 7D).

Taken together, functional connectivity within- and between-MD and DM network regions was associated with efficiency during the experimental task as well as general cognitive and semantic performance in both age groups. The effect of functional connectivity on response time was moderated by age, with young adults profiting from a strengthened within-network connectivity, whereas older adults showed a decline in response speed. Furthermore, both age groups performed slower when functional connectivity between both domain-general systems increased. Finally, functional connectivity was differently related to out-of-scanner tasks in both age groups. While analyses revealed a positive association between cognitive performance and within-MDN functional connectivity

Figure 7. Functional connectivity of domain-general network regions during semantic fluency. (A) Within- and between-network functional connectivity for each seed to target combination for each group. Heatmaps show t values. Thresholded t values with Meff-corrected α of 0.0018 are indicated with black boxes. (B) Effect of age on functional connectivity. There were no age differences in functional connectivity between or within networks. Heatmaps show t values with Meff-corrected α of 0.02. Significant effects are indicated with black boxes. (C) Significant two-way interactions between age and functional connectivity for response time during semantic fluency. (D) Correlation analyses between functional connectivity measures and neuropsychological factors. For within-MDN connectivity, only older adults showed a significant correlation with executive functions, while only young adults showed a significant correlation between semantic memory and between-network functional connectivity. Abbreviations: R, right hemisphere; L, left hemisphere; AG, angular gyrus; ACC, anterior cingulate cortex; Prec, precuneus.

in older adults, between-network functional connectivity showed a positive effect on semantic memory in young adults.

Discussion

The current study set out to describe the effects of aging on the interplay of domain-specific and domain-general neural networks in semantic cognition. By contrasting a semantic fluency task with a low-level verbal control task in an fMRI experiment, we delineated two distinct task-related networks, which displayed strong overlap with the domain-general MD and DM systems. Using task-based connectivity analyses, our findings point toward a strong interaction of these networks during verbal semantic processing across age groups and lend support to the notion that integration between usually anticorrelated functional networks increases for tasks that require cognitive control (Shine et al. 2016). Importantly, our results provide new insights into the impact of age on the functional coupling within and between MDN and DMN regions when semantic knowledge is retrieved in a goal-directed manner from memory. In line with a recent suggestion that additional recruitment of the prefrontal cortex in older adulthood might not reflect compensation but rather reduced efficiency or specificity (Morcom and Henson 2018), we show here that increased in-phase synchronization of task-relevant networks is generally associated with a decline in task efficiency in older adults, whereas young adults capitalize more on strengthened functional connectivity. This finding sheds new light on the frequently reported pattern of strengthened between-network functional connectivity in older adults at rest (Chan et al. 2014; Geerligs et al. 2015; Spreng et al. 2016).

Our task paradigm revealed two distinct functional networks for semantic fluency and counting. The main effect of semantic fluency displayed a predominantly left-lateralized fronto-temporo-parietal network for both age groups with additional activation peaks in right frontal and temporal areas, bilateral caudate nuclei, and the cerebellum. These results align well with previous investigations that applied a semantic fluency paradigm (Vitali et al. 2005; Meinzer et al. 2009; Whitney et al. 2009; Birn et al. 2010; Meinzer, Flaisch, et al. 2012; Meinzer, Seeds, et al. 2012; Nagels et al. 2012; Marsolais et al. 2014; Wagner et al. 2014; Baciu et al. 2016). The main effect of the counting task was evident in both groups in bilateral activation of sensorimotor cortices and the cerebellum, which is consistent with previous studies that used an automated speech task (e.g., Birn et al. 2010; Geranmayeh et al. 2014; Marsolais et al. 2014). Further, older adults showed recruitment of the pre-SMA, which could reflect increased cognitive demands for this age group while keeping track of the numbers during counting. In the direct comparison of both tasks, semantic fluency elicited a network that resembled the main effect of the task minus activity in pre- and postcentral gyri in both age groups, which corroborates the functional role of this network in spoken language beyond low-level sensorimotor aspects (Geranmayeh et al. 2014). Significant activation for the counting task compared with semantic fluency was evident in a mainly right-lateralized network. Previous studies have suggested that neural networks for highly overlearned automated speech tasks are either right-lateralized in healthy participants (Vanlancker-Sidtis et al. 2003; Sidtis et al. 2009) or show less left lateralization than semantically rich language production tasks (Bookheimer et al. 2000; Petrovich Brennan et al. 2007). Further evidence stems from the common observation that automated speech (e.g., counting) is

often preserved in patients who suffer from aphasia after a left hemisphere stroke (Vanlancker-Sidtis et al. 2003).

Despite the semantic nature of the task, we found that the strongest activation clusters for semantic fluency were located in the domain-general MD system in both age groups. These results are in line with previous studies that applied a similar task (e.g., Lurito et al. 2000; Basho et al. 2007) and highlight the strong executive aspect of this paradigm. There is emerging evidence on the overlap of language-specific regions like the left IFG with networks that are implicated in domain-general executive processing (Fedorenko et al. 2012) and semantic control processes (Thompson-Schill et al. 1997; Noonan et al. 2013; Jackson et al. 2021). A recent meta-analysis demonstrated an overlap of some regions of the semantic control network with the MDN, thus emphasizing the role of domain-general control in language processing (Jackson 2021). Here, we observed that semantic fluency predominantly activated the domain-general regions of the semantic control network, like the pre-SMA and the dorsomedial prefrontal cortex, including dorsal IFG, and only a small part of domain-specific semantic control (ventral IFG). Hence, the domain-general control regions may not be language-specific but appear to strongly contribute to a task that requires goal-directed controlled access to semantic memory while monitoring the verbal articulation of words that match the semantic categories. Based on our univariate results, the scope of the present investigation was confined to the age-dependent contribution of domain-general systems to semantic cognition. Nonetheless, their interaction with the semantic network remains certainly an important question for future research. Further support for the contribution of executive functions to semantic fluency stems from behavioral studies that associated cognitive flexibility, inhibition, working memory, and attention with successful performance (Aita et al. 2018; Gordon et al. 2018; Amunts et al. 2020). For both age groups, peak clusters of counting were found in the posterior DMN, which is in line with our expectation of a low-level language production task in comparison with the more demanding semantic fluency task.

Our whole-brain functional connectivity results based on traditional gPPI analyses showed that regions in the domain-general MD and DM systems strongly interact during a semantic word retrieval task compared with counting across both age groups. This was true for seeds coming from the MDN as well as the DMN. Furthermore, we observed some interaction with regions that have been associated with semantic control, like left and right IFG, and with semantic cognition in general, like right MTG (Jackson 2021). The strong interaction of MD and DM regions is in line with previous studies that reported task-specific functional coupling of cognitive control regions with the DMN, most notably the posterior cingulate cortex (PCC)/precuneus, especially in tasks requiring controlled access to semantic memory (Krieger-Redwood et al. 2016; Smith et al. 2016). Remarkably, the PCC/precuneus was the only region in our study that showed functional connectivity with all seeds from the MDN and displayed extensive functional coupling with multiple nodes in the DMN as well as with other neural networks in both age groups. This finding stresses its role as a cortical hub connecting networks to support complex behavior (Leech et al. 2012). The functional coupling of MDN and DMN is especially interesting in light of our univariate results where we observed significant deactivation in regions of the DMN during semantic fluency in both age groups. It corroborates the notion that networks that are anticorrelated during task can still show functional integration in contextually relevant situations to facilitate

goal-directed behavior (Spreng et al. 2014; Krieger-Redwood et al. 2016).

We gained further insight into the task-related functional integration of MD and DM network regions by our analyses of phase synchronization within and between both domain-general systems. Our results show that functional coupling within the MDN and between the MDN and the DMN strengthened with an increase of task load, which was true, independent of age. First, the positive coupling within regions of the MDN is in line with our univariate results for semantic fluency: Here, we found that the strongest activation clusters were located in the MDN in both age groups, thus confirming the necessary engagement of this network for successful task performance. Second, the strong in-phase synchronicity between regions of the MD and DM networks for semantic fluency compared with the control task complement our PPI results, which showed a strong interaction of both domain-general systems. This is line with the notion that the integration of the DMN is relevant for successful task processing in memory-guided cognition (Vatansever et al. 2015; Smith et al. 2016), especially when access to semantic memory is required (Wirth et al. 2011; Krieger-Redwood et al. 2019).
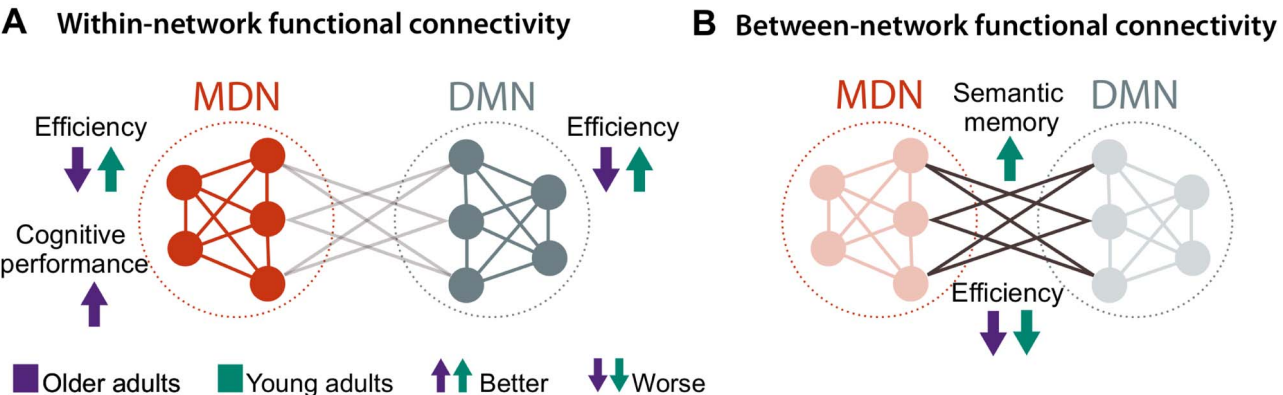
Interestingly, our results on whole-brain as well as within- and between-network functional connectivity did not reveal an effect of age. There is an extant literature describing age-related changes in connectivity in resting-state networks, with the most common observation of decreased within- and increased between-network functional connectivity (Chan et al. 2014; Geerligs et al. 2015; Ferreira et al. 2016; Grady et al. 2016;Ng et al. 2016; Zonneveld et al. 2019). However, results are more inconsistent for task-related changes in functional connectivity with age. Across a range of cognitive tasks, studies reported a similar pattern as for resting-state investigations (Geerligs et al. 2014; Spreng et al. 2016), with no changes for within- but only for between-network connectivity (Gallen et al. 2016; Grady et al. 2016), as well as for age invariance (Trelle et al. 2019; Pongpipat et al. 2020). In the domain of semantic cognition, findings are sparse with one study observing reduced within-network integration for a semantic fluency task, which was not associated with poorer performance in older adults (Marsolais et al. 2014). There are two possible explanations for the present age invariance in functional connectivity. First, the group of older adults in our study might have been too young to detect changes in functional connectivity. Longitudinal studies on cognitive aging showed that a turning point in functional coupling takes place around the age of 65–70 years (Ng et al. 2016; Zonneveld et al. 2019). Thus, although the young adults in our study displayed numerically greater and stronger functional coupling than the older adults, the overall pattern was too similar in both groups. Second, the lack of an age effect on functional connectivity might be related to the semantic nature of our fluency paradigm. Semantic tasks have been shown to require functional coupling between cognitive control as well as DM regions like the PCC/precuneus, which has been implicated in semantic cognition even in young adults (Krieger-Redwood et al. 2016). Hence, this might have aggravated the possibility of observing the frequently reported increase of between-network functional connectivity in older adults and underlines the necessity for more task-based investigations in the future to better understand the picture of neurocognitive aging.

Intriguingly, despite the observed age invariance, functional connectivity had different effects on in-scanner task performance and cognitive functioning in both age groups.

Our results show that older adults did not capitalize on strengthened functional connectivity in the same way as young adults. This was the case for functional connectivity within the MDN and the DMN where an increase of connectivity was associated with slower performance in the semantic fluency task in older adults but with faster performance in young adults (Fig. 8A). By contrast, strengthened between-network functional connectivity led to a slower performance in both age groups, with a stronger effect for young adults (Fig. 8B). Considering our whole-brain connectivity results that showed strong positive coupling between both networks during semantic fluency, this decrease in efficiency might reflect the more effortful communication between task-relevant networks compared with within-network coupling, hence leading to a slower performance across age groups. Interestingly, despite the negative effect on task efficiency, increased functional coupling between MD and DM had a positive effect on semantic memory in young but not in older adults. For the latter group, strengthened connectivity within MD regions was associated with better cognitive performance, albeit still at a significantly lower level of performance than in young adults.

Overall, our findings on the age-dependent relevance of functional connectivity to behavior are in line with theories of neurocognitive aging that suggest a reduced efficiency of neural networks with age (Davis et al. 2012; Geerligs et al. 2014; Shafto and Tyler 2014). Although older adults rely on similar neural networks as young adults for task processing, they cannot equally capitalize on them. Young adults increased their performance as well as their processing efficiency with strengthened in-phase synchronization of task-relevant networks, while older adults showed improvements in cognitive performance but not in efficiency with increased connectivity. Our results thus provide new insights into the behavioral relevance of the frequently observed pattern of neural dedifferentiation (Baltes and Lindenberger 1997; Park et al. 2004; Grady 2012), showing that older adults do not engage task-relevant networks in the same beneficial way as young adults. This is especially relevant in the context of semantic cognition where, according to the DECHA framework, increased semantic knowledge with age could lead to a performance advantage (Spreng and Turner 2019). Here, we show that this is not the case in a task that requires an efficient use of control systems while accessing semantic memory; thus, lending support to the notion that older adults are less flexible in the goal-directed functional coupling of executive and default resources (Spreng and Turner 2019).

Our findings on age-related differences in cortical activation for both tasks further underline the observed reduced efficiency of neural networks in older adults. The comparison of age groups for the semantic fluency task compared with rest revealed stronger activation only for the older adults. Significant clusters comprised hubs of the MDN as well as the right IFG, which has been emphasized in studies on semantic fluency in aging before (Meinzer et al. 2009; Meinzer, Flaisch, et al. 2012; Meinzer, Seeds, et al. 2012; Nagels et al. 2012). Remarkably, the interaction between both tasks and age revealed significant effects only for the young adults who displayed stronger activation of frontal key regions of the MDN, including the pre-SMA and dACC for semantic fluency. This finding suggests a pattern of increased processing efficiency, which was reflected by faster response times compared with the older group. It converges with previous studies on language production and comprehension that associated greater activation in the prefrontal cortex with an increased task demand in young adults

A Within-network functional connectivity

B Between-network functional connectivity

Figure 8. The different effects of within- and between-network functional connectivity on task performance in each age group. (A) Young adults improved their efficiency in the form of faster response times, whereas older adults performed slower when functional connectivity within the MDN or DMN increased. Moreover, strengthened connectivity within the MDN was related to a better performance in executive measures for older adults. (B) Strengthened between-network functional connectivity led to a decline in efficiency in both age groups. However, it was also associated with an improved performance in semantic memory only for young adults.

(Thompson-Schill et al. 1997; Fu et al. 2002; Whitney et al. 2009). The supplementary activation of MDN regions in older adults for the semantic fluency task compared with rest aligns with a meta-analysis on semantic cognition that found greater activity in areas of the MDN with older age (Hoffman and Morcom 2018). The nature of this upregulation in brain activity in older adults has been the subject of some debate (Morcom and Johnson 2015; Cabeza et al. 2018). Here, we observed additional activation in the older adults while they performed poorer than the young adults during the more demanding semantic fluency task. In light of the additional beneficial activation of frontal MDN regions in the young adults, the observed upregulation in the older adults seems to further support the idea of age-related reduced efficiency of neural responses (Nyberg et al. 2014) leading to a stronger involvement of executive control at a lower level of task demand (Hakun et al. 2015; Gallen et al. 2016). This interpretation is backed up by the observed age-related differences in the task-dependent activation of the MD and DM regions. During semantic fluency, older adults showed less deactivation of the DMN than young adults while during counting, the MDN was less deactivated in older than in young adults. Thus, in line with our functional connectivity results, older adults recruit similar neural resources as young adults, albeit at a lower level of processing efficiency, which lends additional support to the hypothesis of dedifferentiation (Park et al. 2004; Morcom and Henson 2018).

It should be noted that our results did not show a consistent effect of the intended modulation of task difficulty within the semantic fluency task on neural activation patterns. This could be related to the limited number of items participants had to produce for each category. A recent behavioral investigation on semantic fluency showed that the amount of correct responses continuously decreases with time (Gordon et al. 2018). Thus, although the effect of difficulty was present in the behavioral results in the form of reduced accuracy and slower responses, we assume that nine trials per category were not enough to establish this effect on the neural level.

Finally, it should be noted that regions for the MDN and DMN were selected from opposite contrasts and are therefore anticorrelated during the semantic fluency and counting task, respectively. However, our functional connectivity results are not a mere consequence of this selection procedure. The extracted parameter estimates of the studied ROIs are based on the PPI contrast, semantic fluency > counting, and do thus represent functional connectivity only for the language production task. Surprisingly, results from our linear regression models for these ROIs, as displayed in Figure 7A, did not only show positive connectivity between seeds and targets within the MDN, which is in line with our univariate results, but also between seeds coming from the MDN or DMN and targets in either network, which seems to contradict our univariate results where regions in the DMN were deactivated during semantic fluency. The functional connectivity results thus demonstrate a general property of network integration for usually anticorrelated networks for successful task processing.

Conclusion

In conclusion, the current study sheds light on the age-dependent contribution of the domain-general MD and DM systems during a verbal semantic fluency task. While univariate results revealed strong activity in the MDN during task processing, functional connectivity analyses demonstrated a strong interaction between the MDN and the DMN for semantic fluency. This finding corroborates the notion that usually anticorrelated networks integrate for successful task processing, especially when access to semantic memory is required. Although the strength of functional connectivity within- and between-networks was age-invariant, it had a different behavioral relevance in both age groups. Only the young adults engaged task-relevant networks in a beneficial way. This was evident in the form of better processing efficiency during semantic fluency and generally improved semantic memory. In older adults, strengthened functional connectivity within the MDN had a positive effect on cognitive performance, albeit older adults still performed at a lower level than young adults. Our results provide new insights into the concept of age-related reduced efficiency in the domain of semantic cognition and inform about the behavioral relevance of the frequently observed pattern of neural dedifferentiation.

Supplementary Material

Notes

Funding

Code and Data Availability

All behavioral data as well as extracted beta weights generated or analyzed during this study have been deposited in a public repository on Gitlab https://gitlab.gwdg.de/functionalconnectivityaging/mdn_lang. This repository also holds all self-written analysis code used for this project. Unthresholded statistical group maps for fMRI and gPPI results are made publicly available on NeuroVault: https://neurovault.org/collections/9072/. Raw and single subject neuroimaging data are protected under the General Data Protection Regulation (EU) and can only be made available from the authors upon reasonable request.

References

Aita SL, Beach JD, Taylor SE, Borgogna NC, Harrell MN, Hill BD. 2018. Executive, language, or both? An examination of the construct validity of verbal fluency measures. *Appl Neuropsychol Adult*. 26:441–451.

Amunts J, Camilleri JA, Eickhoff SB, Heim S, Weis S. 2020. Executive functions predict verbal fluency scores in healthy participants. *Sci Rep*. 10:11141.

Andrews-Hanna JR, Snyder AZ, Vincent JL, Lustig C, Head D, Raichle ME, Buckner RL. 2007. Disruption of large-scale brain systems in advanced aging. *Neuron*. 56:924–935.

Ashburner J. 2007. A fast diffeomorphic image registration algorithm. *Neuroimage*. 38:95–113.

Aschenbrenner S, Tucha O, Lange KW. 2000. *Regensburger Wortflüssigkeits-test*. Göttingen: Hogrefe.

Assem M, Glasser MF, Van Essen DC, Duncan J. 2020. A Domain-General Cognitive Core Defined in Multimodally Parcellated Human Cortex. *Cereb Cortex*. 30:4361–4380.

Baciu M, Boudiaf N, Cousin E, Perrone-Bertolotti M, Pichat C, Fournet N, Chainay H, Lamalle L, Krainik A. 2016. Functional MRI evidence for the decline of word retrieval and generation during normal aging. *Age*. 38:3.

Baddeley A, Emslie H, Nimmo-Smith I. 1993. The spot-the-word test: a robust estimate of verbal intelligence based on lexical decision. *Br J Clin Psychol*. 32:55–65.

Balota DA, Dolan PO, Duchek JM. 2000. Memory changes in healthy older adults. In: *The Oxford handbook of memory*. New York: Oxford University Press, pp. 395–409.

Baltes PB, Lindenberger U. 1997. Emergence of a powerful connection between sensory and cognitive functions across the adult life span: a new window to the study of cognitive aging? *Psychol Aging*. 12:12–21.

Basho S, Palmer ED, Rubio MA, Wulfeck B, Müller R-A. 2007. Effects of generation mode in fMRI adaptations of semantic fluency: paced production and overt speech. *Neuropsychologia*. 45:1697–1706.

Bates D, Mächler M, Bolker B, Walker S. 2015. Fitting linear mixed-effects models using lme4. *J Stat Softw*. 67:1–48.

Beck AT, Steer RA, Ball R, Ranieri W. 1996. Comparison of Beck depression inventories -IA and -II in psychiatric outpatients. *J Pers Assess*. 67:588–597.

Birn RM, Kenworthy L, Case L, Caravella R, Jones TB, Bandettini PA, Martin A. 2010. Neural systems supporting lexical search guided by letter and semantic category cues: a self-paced overt response fMRI study of verbal fluency. *Neuroimage*. 49:1099–1107.

Bookheimer SY, Zeffiro TA, Blaxton TA, Gaillard W, Theodore WH. 2000. Activation of language cortex with automatic speech tasks. *Neurology*. 55:1151–1157.

Brett M, Anton J-L, Valabregue R, Poline J-B. 2002. Region of interest analysis using an SPM toolbox. *Neuroimage*. 16:769–1198.

Cabeza R. 2002. Hemispheric asymmetry reduction in older adults: the HAROLD model. *Psychol Aging*. 17:85–100.

Cabeza R, Albert M, Belleville S, Craik FIM, Duarte A, Grady CL, Lindenberger U, Nyberg L, Park DC, Reuter-Lorenz PA, et al. 2018. Maintenance, reserve and compensation: the cognitive neuroscience of healthy ageing. *Nat Rev Neurosci*. 19: 701–710.

Camilleri JA, Müller VI, Fox P, Laird AR, Hoffstaedter F, Kalenscher T, Eickhoff SB. 2018. Definition and characterization of an extended multiple-demand network. *NeuroImage*. 165:138–147.

Chan MY, Park DC, Savalia NK, Petersen SE, Wig GS. 2014. Decreased segregation of brain systems across the healthy adult lifespan. *PNAS*. 111:E4997–E5006.

Cohen-Shikora ER, Balota DA. 2016. Visual word recognition across the adult lifespan. *Psychol Aging*. 31:488–502.

Dale AM, Fischl B, Sereno MI. 1999. Cortical surface-based analysis: I. Segmentation and surface reconstruction. *Neuroimage*. 9:179–194.

Damoiseaux JS. 2017. Effects of aging on functional and structural brain connectivity. *Neuroimage*. 160:32–40.

Damoiseaux JS, Beckmann CF, Arigita EJS, Barkhof F, Scheltens P, Stam CJ, Smith SM, RB RS A. 2008. Reduced resting-state brain activity in the "default network" in normal aging. *Cereb Cortex*. 18:1856–1864.

Daneman M, Carpenter PA. 1980. Individual differences in working memory and reading. *J Verbal Learning Verbal Behav*. 19:450–466.

Derringer J. 2018. A simple correction for non-independent tests (preprint). PsyArXiv.April 16, 2018. https://doi.org/10.31234/osf.io/f2tyw, preprint: not peer reviewed

Davis SW, Kragel JE, Madden DJ, Cabeza R. 2012. The Architecture of Cross-Hemispheric Communication in the Aging Brain: Linking Behavior to Functional and Structural Connectivity. *Cereb Cortex*. 22:232–242.

Eickhoff SB, Stephan KE, Mohlberg H, Grefkes C, Fink GR, Amunts K, Zilles K. 2005. A new SPM toolbox for combining probabilistic cytoarchitectonic maps and functional imaging data. *Neuroimage*. 25:1325–1335.

Esteban O, Markiewicz CJ, Blair RW, Moodie CA, Isik AI, Erramuzpe A, Kent JD, Goncalves M, DuPre E, Snyder M, et al. 2019. fMRIPrep: a robust preprocessing pipeline for functional MRI. *Nat Methods*. 16:111–116.

Fedorenko E, Duncan J, Kanwisher N. 2012. Language-selective and domain-general regions lie side by side within Broca's area. *Curr Biol*. 22:2059–2062.

Fedorenko E, Duncan J, Kanwisher N. 2013. Broad domain generality in focal regions of frontal and parietal cortex. *Proc Natl Acad Sci*. 110:16616–16621.

Feinberg DA, Moeller S, Smith SM, Auerbach E, Ramanna S, Glasser MF, Miller KL, Ugurbil K, Yacoub E. 2010. Multiplexed echo planar imaging for sub-second whole brain FMRI and fast diffusion imaging. *PLoS One*. 5:e15710.

Ferreira LK, Regina ACB, Kovacevic N, Martin M da GM, Santos PP, Carneiro C de G, Kerr DS, Amaro E, McIntosh AR, Busatto GF. 2016. Aging effects on whole-brain functional connectivity in adults free of cognitive and psychiatric disorders. *Cereb Cortex*. 26:3851–3865.

Folstein MF, Folstein SE, McHugh PR. 1975. "Mini-mental state": a practical method for grading the cognitive state of patients for the clinician. *J Psychiatr Res*. 12:189–198.

Fonov V, Evans A, McKinstry R, Almli C, Collins D. 2009. Unbiased nonlinear average age-appropriate brain templates from birth to adulthood. *Neuroimage*. 47:S102.

Fu CHY, Morgan K, Suckling J, Williams SCR, Andrew C, Vythelingum GN, McGuire PK. 2002. A functional magnetic resonance imaging study of overt letter verbal fluency using a clustered acquisition sequence: greater anterior cingulate activation with increased task demand. *Neuroimage*. 17:871–879.

Gallen CL, Turner GR, Adnan A, D'Esposito M. 2016. Reconfiguration of brain network architecture to support executive control in aging. *Neurobiol Aging*. 44:42–52.

Geerligs L, Maurits NM, Renken RJ, Lorist MM. 2014. Reduced specificity of functional connectivity in the aging brain during task performance. *Human Brain Mapping*. 35: 319–330.

Geerligs L, Renken RJ, Saliasi E, Maurits NM, Lorist MM. 2015. A brain-wide study of age-related changes in functional connectivity. *Cereb Cortex*. 25:1987–1999.

Geranmayeh F, Wise RJS, Mehta A, Leech R. 2014. Overlapping networks engaged during spoken language production and its cognitive control. *J Neurosci*. 34:8728–8740.

Glauer M, Häusig S, Krüger M, Betsch T, Renkewitz F, Sedlmeier P, Winkler I. 2007. Typizitätsnormen für Vertreter von 30 Kategorien. *Neurolinguistik*. 21:21–31.

Gordon JK, Young M, Garcia C. 2018. Why do older adults have difficulty with semantic fluency? *Aging Neuropsychol Cogn*. 25:803–828.

Gorgolewski KJ, Esteban O, Ellis DG, Notter MP, Ziegler E, Johnson H, Hamalainen C, Yvernault B, Burns C, Manhães-Savio A, et al. 2017. Nipype: a flexible, lightweight and extensible neuroimaging data processing framework in python. 0.13.1. *Zenodo*.

Grady C. 2012. The cognitive neuroscience of ageing. *Nat Rev Neurosci*. 13:491–505.

Grady C, Sarraf S, Saverino C, Campbell K. 2016. Age differences in the functional interactions among the default, frontoparietal control, and dorsal attention networks. *Neurobiol Aging*. 41:159–172.

Hakun JG, Zhu Z, Brown CA, Johnson NF, Gold BT. 2015. Longitudinal alterations to brain function, structure, and cognitive performance in healthy older adults: a fMRI-DTI study. *Neuropsychologia*. 71:225–235.

Halai AD, Welbourne SR, Embleton K, Parkes LM. 2014. A comparison of dual gradient-echo and spin-echo fMRI of the inferior temporal lobe. *Hum Brain Mapp*. 35:4118–4128.

Hedden T, Gabrieli JDE. 2004. Insights into the ageing mind: a view from cognitive neuroscience. *Nat Rev Neurosci*. 5:87–96.

Hoffman P, Morcom AM. 2018. Age-related changes in the neural networks supporting semantic cognition: a meta-analysis of 47 functional neuroimaging studies. *Neurosci Biobehav Rev*. 84:134–150.

Jackson RL. 2021. The neural correlates of semantic control revisited. *Neuroimage*. 224:117444.

Jenkinson M, Beckmann CF, Behrens TEJ, Woolrich MW, Smith SM. 2012. FSL. *Neuroimage*. 62:782–790.

Kavé G, Knafo-Noam A. 2015. Lifespan development of phonemic and semantic fluency: universal increase, differential decrease. *J Clin Exp Neuropsychol*. 37:751–763.

Krieger-Redwood K, Jefferies E, Karapanagiotidis T, Seymour R, Nunes A, Ang JWA, Majernikova V, Mollo G, Smallwood J. 2016. Down but not out in posterior cingulate cortex: deactivation yet functional coupling with prefrontal cortex during demanding semantic cognition. *Neuroimage*. 141:366–377.

Krieger-Redwood K, Wang H-T, Poerio G, Martinon LM, Riby LM, Smallwood J, Jefferies E. 2019. Reduced semantic control in older adults is linked to intrinsic DMN connectivity. *Neuropsychologia*. 132:107133.

Law R, O'Carroll RE. 1998. A comparison of three measures of estimating premorbid intellectual level in dementia of the Alzheimer type. *Int J Geriatr Psychiatry*. 13:727–730.

Leech R, Braga R, Sharp DJ. 2012. Echoes of the brain within the posterior cingulate cortex. *J Neurosci*. 32:215–222.

Lenth R. 2020. Emmeans: estimated marginal means, aka least-squares means. *R package version 1.4.8*.

Li H-J, Hou X-H, Liu H-H, Yue C-L, Lu G-M, Zuo X-N. 2015. Putting age-related task activation into large-scale brain networks: a meta-analysis of 114 fMRI studies on healthy aging. *Neurosci Biobehav Rev*. 57:156–174.

Li S-C, Lindenberger U, Sikström S. 2001. Aging cognition: from neuromodulation to representation. *Trends Cogn Sci*. 5:479–486.

Lövdén M, Bäckman L, Lindenberger U, Schaefer S, Schmiedek F. 2010. A theoretical framework for the study of adult cognitive plasticity. *Psychol Bull*. 136:659–676.

Lüdecke D. 2018. ggeffects: tidy data frames of marginal effects from regression models. *JOSS*. 3:772.

Lurito JT, Kareken DA, Lowe MJ, Chen SHA, Mathews VP. 2000. Comparison of rhyming and word generation with FMRI. *Hum Brain Mapp*. 10:99–106.

Mannhaupt H-R. 1983. Produktionsnormen für verbale Reaktionen zu 40 geläufigen Kategorien. *Sprache & Kognition*. 4:264–278.

Marsolais Y, Perlbarg V, Benali H, Joanette Y. 2014. Age-related changes in functional network connectivity associated with high levels of verbal fluency performance. *Cortex*. 58:123–138.

McLaren DG, Ries ML, Xu G, Johnson SC. 2012. A generalized form of context-dependent psychophysiological interactions (gPPI): a comparison to standard approaches. *Neuroimage*. 61:1277–1286.

Michael AM, Evans E, Moore GJ. 2016. Influence of Group on Individual Subject Maps in SPM Voxel Based Morphometry. *Front Neurosci*. 10:522.

Meinzer M, Flaisch T, Seeds L, Harnish S, Antonenko D, Witte V, Lindenberg R, Crosson B. 2012. Same modulation but different starting points: performance modulates age differences in inferior frontal cortex activity during word-retrieval. *PLoS One*. 7:e33631.

Meinzer M, Flaisch T, Wilser L, Eulitz C, Rockstroh B, Conway T, Gonzalez-Rothi L, Crosson B. 2009. Neural signatures of semantic and phonemic fluency in young and old adults. *J Cogn Neurosci*. 21:2007–2018.

Meinzer M, Seeds L, Flaisch T, Harnish S, Cohen ML, McGregor K, Conway T, Benjamin M, Crosson B. 2012. Impact of changed positive and negative task-related brain activity on word-retrieval in aging. *Neurobiol Aging*. 33:656–669.

Morcom AM, Henson RNA. 2018. Increased prefrontal activity with aging reflects nonspecific neural responses rather than compensation. *J Neurosci*. 38:7303–7313.

Morcom AM, Johnson W. 2015. Neural reorganization and compensation in aging. *J Cogn Neurosci*. 27:1275–1285.

Nagels A, Kircher T, Dietsche B, Backes H, Marquetand J, Krug A. 2012. Neural processing of overt word generation in healthy individuals: the effect of age and word knowledge. *Neuroimage*. 61:832–840.

Ng KK, Lo JC, Lim JKW, Chee MWL, Zhou J. 2016. Reduced functional segregation between the default mode network and the executive control network in healthy older adults: a longitudinal study. *Neuroimage*. 133:321–330.

Noonan KA, Jefferies E, Visser M, Lambon Ralph MA. 2013. Going beyond inferior prefrontal involvement in semantic control: evidence for the additional contribution of dorsal angular gyrus and posterior middle temporal cortex. *J Cogn Neurosci*. 25:1824–1850.

Noppeney U, Price CJ, Penny WD, Friston KJ. 2006. Two distinct neural mechanisms for category-selective responses. *Cereb Cortex*. 16:437–445.

Nyberg L, Andersson M, Kauppi K, Lundquist A, Persson J, Pudas S, Nilsson L-G. 2014. Age-related and genetic modulation of frontal cortex efficiency. *J Cogn Neurosci*. 26:746–754.

Oldfield RC. 1971. The assessment and analysis of handedness: the Edinburgh inventory. *Neuropsychologia*. 9:97–113.

Park DC, Polk TA, Park R, Minear M, Savage A, Smith MR, Smith EE. 2004. Aging reduces neural specialization in ventral visual cortex. *Proc Natl Acad Sci U S A*. 101:13091–13095.

Persson J, Lustig C, Nelson JK, Reuter-Lorenz PA. 2007. Age differences in deactivation: a link to cognitive control? *J Cogn Neurosci*. 19:1021–1032.

Petrovich Brennan NM, Whalen S, de Morales Branco D, O'Shea JP, Norton IH, Golby AJ. 2007. Object naming is a more sensitive measure of speech localization than number counting: converging evidence from direct cortical stimulation and fMRI. *Neuroimage*. Proceedings of the International Brain Mapping & Intraoperative Surgical Planning Society Annual Meeting, 2006. 37:S100–S108.

Pongpipat E, Kennedy K, Foster C, Boylan M, Rodrigue K. 2020. Functional connectivity within and between n-back modulated regions: An adult lifespan PPI investigation. *Brain Connect*. 11:103–118.

Poser BA, Versluis MJ, Hoogduin JM, Norris DG. 2006. BOLD contrast sensitivity enhancement and artifact reduction with multiecho EPI: parallel-acquired inhomogeneity-desensitized fMRI. *Magn Reson Med*. 55:1227–1235.

Core Team R. 2018. *R: A language and environment for statistical computing*. Vienna, Austria: R Foundation for Statistical Computing.

Reitan RM. 1958. Validity of the Trail Making Test as an indicator of organic brain damage. PMS. 8:271.

Schaefer A, Kong R, Gordon EM, Laumann TO, Zuo X-N, Holmes AJ, Eickhoff SB, Yeo BTT. 2018. Local-Global Parcellation of the Human Cerebral Cortex from Intrinsic Functional Connectivity MRI. *Cereb Cortex*. 28:3095–3114.

Shafto MA, Tyler LK. 2014. Language in the aging brain: The network dynamics of cognitive decline and preservation. *Science*. 346:583–587.

Schmidt CSM, Schumacher LV, Römer P, Leonhart R, Beume L, Martin M, Dressing A, Weiller C, Kaller CP. 2017. Are semantic and phonological fluency based on the same or distinct sets of cognitive processes? Insights from factor analyses in healthy adults and stroke patients. *Neuropsychologia*. 99:148–155.

Schmidt K-H, Metzler P. 1992. *WST-Wortschatztest*. Göttingen: Beltz Test.

Shao Z. 2014. What do verbal fluency tasks measure? Predictors of verbal fluency performance in older adults. *Front Psychol*. 5:772.

Shine JM, Bissett PG, Bell PT, Koyejo O, Balsters JH, Gorgolewski KJ, Moodie CA, Poldrack RA. 2016. The dynamics of functional brain networks: integrated network states during cognitive task performance. *Neuron*. 92:544–554.

Sidtis D, Canterucci G, Katsnelson D. 2009. Effects of neurological damage on production of formulaic language. *Clin Linguist Phon*. 23:270–284.

Siegel JS, Power JD, Dubis JW, Vogel AC, Church JA, Schlaggar BL, Petersen SE. 2014. Statistical improvements in functional magnetic resonance imaging analyses produced by censoring high-motion data points. *Hum Brain Mapp*. 35:1981–1996.

Smith DV, Gseir M, Speer ME, Delgado MR. 2016. Toward a cumulative science of functional integration: a meta-analysis of psychophysiological interactions. *Hum Brain Mapp*. 37:2904–2917.

Spreng RN, DuPre E, Selarka D, Garcia J, Gojkovic S, Mildner J, Luh W-M, Turner GR. 2014. Goal-congruent default network activity facilitates cognitive control. *J Neurosci*. 34:14108–14114.

Spreng RN, Stevens WD, Viviano JD, Schacter DL. 2016. Attenuated anticorrelation between the default and dorsal attention networks with aging: evidence from task and rest. *Neurobiol Aging*. 45:149–160.

Spreng RN, Turner GR. 2019. The shifting architecture of cognition and brain function in older adulthood. *Perspect Psychol Sci*. 14:523–542.

Tavares V, Prata D, Ferreira HA. 2020. Comparing SPM12 and CAT12 segmentation pipelines: A brain tissue volume-based age and Alzheimer's disease study. *Journal of Neuroscience Methods*. 334:108565.

Thompson-Schill SL, D'Esposito M, Aguirre GK, Farah MJ. 1997. Role of left inferior prefrontal cortex in retrieval of semantic knowledge: a reevaluation. *PNAS*. 94:14792–14797.

Trelle AN, Henson RN, Simons JS. 2019. Neural evidence for age-related differences in representational quality and strategic retrieval processes. *Neurobiol Aging*. 84:50–60.

Troyer A, Moscovitch M, Winocur G. 1997. Clustering and switching as two components of verbal fluency: evidence

from younger and older healthy adults. *Neuropsychology*. 11:138–146.

Turner GR, Spreng RN. 2015. Prefrontal engagement and reduced default network suppression co-occur and are dynamically coupled in older adults: the default–executive coupling hypothesis of aging. *J Cogn Neurosci*. 27:2462–2476.

Tustison NJ, Avants BB, Cook PA, Zheng Y, Egan A, Yushkevich PA, Gee JC. 2010. N4ITK: improved N3 bias correction. *IEEE Trans Med Imaging*. 29:1310–1320.

Vanlancker-Sidtis D, McIntosh AR, Grafton S. 2003. PET activation studies comparing two speech tasks widely used in surgical mapping. *Brain Lang*. 85:245–261.

Vatansever D, Menon DK, Manktelow AE, Sahakian BJ, Stamatakis EA. 2015. Default mode dynamics for global functional integration. *J Neurosci*. 35:15254–15262.

Verhaegen P, Borchelt M, Smith J. 2003. Relation between cardiovascular and metabolic disease and cognition in very old age: cross-sectional and longitudinal findings from the berlin aging study. *Health Psychol*. 22:559–569.

Vitali P, Abutalebi J, Tettamanti M, Rowe J, Scifo P, Fazio F, Cappa SF, Perani D. 2005. Generating animal and tool names: an fMRI study of effective connectivity. *Brain Lang*. 93:32–45.

Wagner S, Sebastian A, Lieb K, Tüscher O, Tadić A. 2014. A coordinate-based ALE functional MRI meta-analysis of brain activation during verbal fluency tasks in healthy control subjects. *BMC Neurosci*. 15:19.

Wechsler D. 1944. *The measurement of adult intelligence*. 3rd ed. Baltimore (MA): Williams & Wilkins Co.

Whiteside DM, Kealey T, Semla M, Luu H, Rice L, Basso MR, Roper B. 2016. Verbal fluency: language or executive function measure? *Appl Neuropsychol Adult*. 23(1):29–34.

Whitney C, Weis S, Krings T, Huber W, Grossman M, Kircher T. 2009. Task-dependent modulations of prefrontal and hippocampal activity during intrinsic word production. *J Cogn Neurosci*. 21:697–712.

Wickham H. 2016. *Ggplot2. Elegant Graphics for Data Analysis, Use R!* Cham, Switzerland: Springer International Publishing.

Wirth M, Jann K, Dierks T, Federspiel A, Wiest R, Horn H. 2011. Semantic memory involvement in the default mode network: a functional neuroimaging study using independent component analysis. *Neuroimage*. 54: 3057–3066.

Xia M, Wang J, He Y. 2013. Brain net viewer: a network visualization tool for human brain Connectomics. *PLoS One*. 8:e68910.

Zacks RT, Hasher L, Li KZH. 2000. Human memory. In: *The handbook of aging and cognition*. 2nd ed. Mahwah (NJ): Lawrence Erlbaum Associates Publishers, pp. 293–357.

Zonneveld HI, Pruim RHR, Bos D, Vrooman HA, Muetzel RL, Hofman A, Rombouts SARB, van der Lugt A, Niessen WJ, Ikram MA, et al. 2019. Patterns of functional connectivity in an aging population: the Rotterdam Study. *Neuroimage*. 189: 432–444.

3 Age-Related Reorganization of Functional Network Architecture in Semantic Cognition

Study 2

The following study explored age-related differences in the functional network architecture during semantic processing and their behavioral relevance. It has been published in *Cerebral Cortex.*

Age-related reorganization of functional network architecture in semantic cognition

Sandra Martin (iD)[1,2,*], Kathleen A. Williams (iD)[1], Dorothee Saur (iD)[2], Gesa Hartwigsen (iD)[1]

[1]Lise Meitner Research Group Cognition and Plasticity, Max Planck Institute for Human Cognitive and Brain Sciences, 04103 Leipzig, Germany,
[2]Language & Aphasia Laboratory, Department of Neurology, University of Leipzig Medical Center, 04103 Leipzig, Germany
*Corresponding author: Max Planck Institute for Human Cognitive and Brain Sciences, Stephanstr. 1a, 04103 Leipzig, Germany. Email: martin@cbs.mpg.de

Cognitive aging is associated with widespread neural reorganization processes in the human brain. However, the behavioral impact of such reorganization is not well understood. The current neuroimaging study investigated age differences in the functional network architecture during semantic word retrieval in young and older adults. Combining task-based functional connectivity, graph theory and cognitive measures of fluid and crystallized intelligence, our findings show age-accompanied large-scale network reorganization even when older adults have intact word retrieval abilities. In particular, functional networks of older adults were characterized by reduced decoupling between systems, reduced segregation and efficiency, and a larger number of hub regions relative to young adults. Exploring the predictive utility of these age-related changes in network topology revealed high, albeit less efficient, performance for older adults whose brain graphs showed stronger dedifferentiation and reduced distinctiveness. Our results extend theoretical accounts on neurocognitive aging by revealing the compensational potential of the commonly reported pattern of network dedifferentiation when older adults can rely on their prior knowledge for successful task processing. However, we also demonstrate the limitations of such compensatory reorganization and show that a youth-like network architecture in terms of balanced integration and segregation is associated with more economical processing.

Key words: aging; functional connectivity; graph theory; language production; semantic memory.

Introduction

Semantic memory refers to the general knowledge of words, concepts, and ideas we accumulate across the lifespan. It is a fundamental human ability and central to communication. Unlike other cognitive domains, semantic memory is usually preserved through adulthood into very old age (Verhaeghen et al. 2003), thus enabling communication abilities to remain largely intact in healthy aging. Nonetheless, memory problems in verbal communication, such as finding the right word and tip-of-the-tongue episodes, are a common complaint with increasing age (Burke and Shafto 2004). This paradox has been explained in terms of less efficient access and retrieval processes during language production that rely on semantic and cognitive control functions like working memory, attention, and inhibitory control, and are well established to steadily decline with age (Hedden and Gabrieli 2004). However, little is known about the neural mechanisms underlying those changes in access to semantic memory with age.

The field of network science provides tools to model and explore organization principles of complex systems such as the human brain (Rubinov and Sporns 2010). Studies in young adults have revealed a topological organization of the brain that combines local information processing with global information integration aimed at optimizing global cost efficiency ("small-world" organization; Bassett et al. 2009; Bullmore and Sporns 2012). Age-related changes to this modular organization have been described as general decline of network segregation in the form of decreased within- and enhanced between-network

connectivity (Chan et al. 2014; Setton et al. 2022). Moreover, increasing age has been associated with reduced small-world organization, modularity, and local and global efficiency of functional brain networks (Betzel et al. 2014; Geerligs et al. 2015; Chong et al. 2019). The impact of such reorganization on cognition remains debated. Most studies associated neural dedifferentiation with performance decline (Chan et al. 2014; Sala-Llonch et al. 2014; Chong et al. 2019), whereas some have pointed towards a pattern of compensational response (Stumme et al. 2020).

To date, most results stem from resting-state functional magnetic resonance imaging (fMRI) investigations or task-based studies in domains primarily affected by age, such as episodic and working memory. However, important insight can be gained by investigating domains, which rely on semantic cognition like language and creativity. Here, older adults might benefit from increased connectivity between usually anticorrelated networks such as executive and default networks since they can depend on prior knowledge to maintain high performance (Spreng et al. 2016; Adnan et al. 2019). In this context, semantic fluency tasks are especially valuable since they tap into semantic memory but also cognitive control and are often linked to preserved albeit slower performance with age (Gordon et al. 2018). Previous studies revealed age-related reduced functional connectivity within domain-specific networks, however, without affecting behavioral performance (Marsolais et al. 2014; Ferré et al. 2020). In addition, we recently showed that increased crosstalk between domain-general networks is essential for successful task processing,

independent of age, when access to semantic memory is required (Martin et al. 2022). Thus, domains that are usually well-preserved in aging inform the current understanding of age-accompanied changes in functional brain networks and their behavioral relevance.

The present study contributes to this field by exploring age-related reorganization of functional networks during a semantic word retrieval task. Networks of task-based functional connectivity in groups of healthy young and older adults were derived via data-driven, multivariate methods. We were interested in age differences in the coupling of task-relevant networks and their behavioral relevance. Furthermore, we applied graph-theoretical measures of brain system segregation, integration, and network hubs to investigate the network topology in young and older adults, and related these measures to participants' in-scanner task performance and abilities of fluid and crystallized intelligence. Exploring task-based network topologies as a function of cognitive performance in a domain that is usually well-preserved with age enabled us to gain key insights into age-related reorganization processes and to inform theoretical accounts regarding compensatory and detrimental effects of neurocognitive aging on behavior.

Materials and methods
Participants

Participants consisted of 31 healthy older adults (15 female; mean age = 65.5, standard deviations, SD = 2.75, range = 60–69 years) and 30 healthy young adults (16 female; mean age = 27.6, SD = 4.3, range = 21–34 years), which is the same sample as described previously (Martin et al. 2022). Data of 3 older participants as well as single runs of 6 participants had to be excluded due to strong motion during fMRI (>1 voxel size), leading to a final sample size of 28 participants in the older group. Although both groups were matched for gender, participants in the young group had significantly more years of education ($t(55.86) = 5.21$, $P < 0.001$). Inclusion criteria were native German speaker, right-handedness, normal hearing, normal or corrected-to-normal vision, no history of neurological or psychiatric conditions, and no contraindication to magnetic resonance imaging. Older adults were additionally screened for cognitive impairments with the Mini-Mental State Examination (Folstein et al. 1975; all ≥26) points and for depression with the Beck Depression Inventory (Beck et al. 1996; all ≤ 14 points). A battery of neuropsychological tests was administered probing semantic knowledge as well as verbal- and nonverbal executive functions (Fig. 1a). Differences between age groups for neuropsychological measures were determined with 2-sample *t*-tests. Consistent with previous research, older adults only performed better for the measure of semantic memory (spot-the-word test; $t(54.39) = 3.14$, $P = 0.003$), indicating a maintenance of semantic knowledge and an increase in vocabulary with age (Verhaeghen et al. 2003), whereas young adults performed better on all other tests (all at $P < 0.01$), which is consistent with the assumption of a general age-related decline of executive functions (Hedden and Gabrieli 2004). For all reported correlation analyses, neuropsychological measures were summarized via exploratory factor analysis. Results revealed an "executive functions" factor with high loadings on trail-making tests A (0.8) and B (0.71), digit symbol substitution test (0.73), and reading span test (0.45), and a "semantic memory" factor with spot-the-word test (0.5) and verbal fluency tests for hobbies (0.44) and surnames (0.98). Prior to the experiment, participants gave written informed consent. The study was approved by the local ethics committee of the University of Leipzig and conducted in accordance with the Declaration of Helsinki.
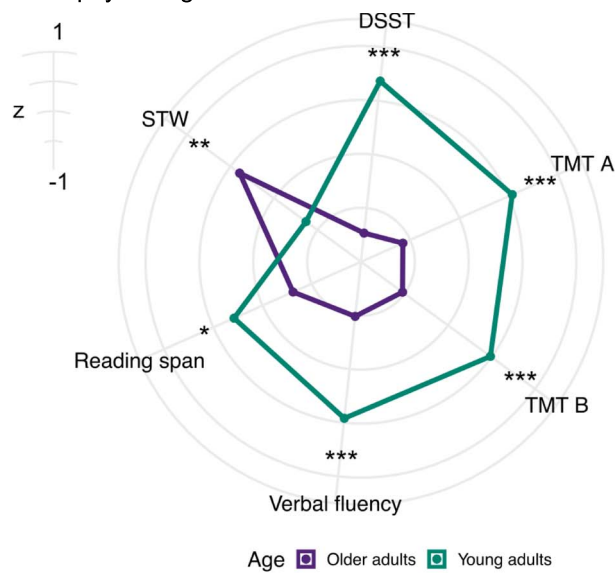
Experimental design

The experimental procedure is reported in detail in previous work (Martin et al. 2022) and briefly summarized here. Participants completed 1 experimental session, which consisted of 2 runs of the fMRI experiment and neuropsychological tests, and lasted 2 h in total. Experimental tasks consisted of a paced overt semantic fluency task and a control task of paced overt counting, which were implemented in a block design in the scanner (Fig. 1b). For the semantic fluency task, participants were asked to produce exemplars for 20 semantic categories, which were divided in 10 easy (e.g. colors) and 10 difficult (e.g. insects) categories based on a separate pilot study in healthy young and older adults (Martin et al. 2022). Task blocks were 43-s long and separated by rest blocks of 16 s. Each block started with a 2-s visual word cue indicating whether participants were expected to generate category exemplars or count forward (1–9) or backward (9–1). This was followed by 9 consecutive trials of the same category or counting task, respectively. Trials within 1 block were separated by interstimulus intervals of 2–4 s. Participants were instructed to generate 1 exemplar for a category or 1 number per trial, which was indicated by a green cross on the screen, and to pause when the cross turned red. They were told not to repeat items and to say "next" if they could not think of an exemplar for the respective category. Each run contained 10 semantic fluency blocks, divided in easy and difficult categories, and 10 counting blocks, consisting of forward and backward counting, thus resulting in a total duration of 19.4 min per run. The order of blocks was counter-balanced and pseudo-randomized across participants. Before the fMRI experiment, participants received instructions and practiced the task with a separate set of categories outside the scanner. Stimuli were presented using the software Presentation (Neurobehavioral Systems, Berkeley, United States; version 18.0). Answers were recorded via a FOMRI III microphone (Optoacoustics, Yehuda, Israel). After the experiment, response recordings were analyzed for verbal answers and onset times after being cleaned from scanner noise via Audacity software (version 2.3.2) and transcribed by 3 independent raters.
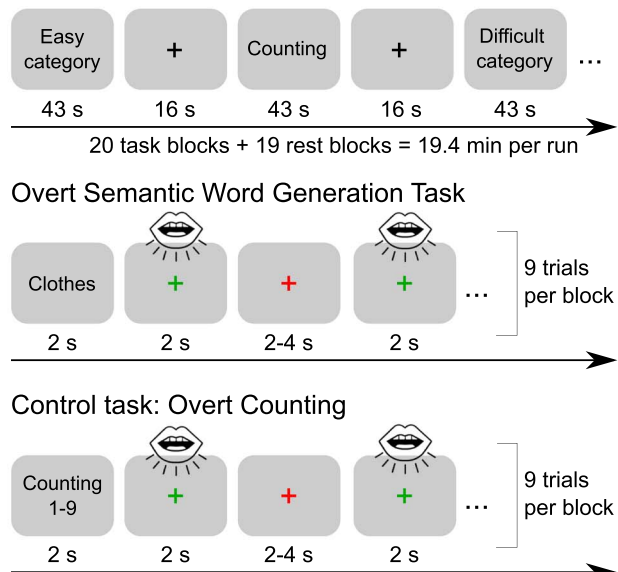
fMRI data acquisition and preprocessing

fMRI data were collected on a 3T Prisma scanner (Siemens, Erlangen, Germany) with a 32-channel head coil. For the acquisition of functional images, a multiband dual gradient-echo echo-planar imaging sequence was used for optimal blood oxygenation level-dependent (BOLD) sensitivity throughout the entire brain (Poser et al. 2006; Halai et al. 2014). The following scanning parameters were applied: time repetition (TR) = 2,000 ms; time echo (TE) = 12 ms, 33 ms; flip angle = 90°; voxel size = 2.5 × 2.5 × 2.75 mm with an inter-slice gap of 0.25 mm; field of view (FOV) = 204 mm; multiband acceleration factor = 2. To increase coverage of anterior temporal lobe (ATL) regions, slices were tilted by 10° of the AC–PC line. Six hundred sixteen images consisting of 60 axial slices in interleaved order covering the whole-brain were continuously acquired per run. In addition, field maps were obtained for later distortion correction (TR = 8,000 ms; TE = 50 ms). This study analyzed the data from echo 2 (TE = 33 ms) since preprocessing was performed using the software fMRIPrep (Esteban et al. 2019), which currently does not support the combination of images acquired at different echo times. We chose to use results from preprocessing with fMRIPrep since this pipeline provides state-of-the-art data processing

a Neuropsychological results

b Experimental paradigm

Fig. 1. Neuropsychological results and experimental design. a) Test scores were z-transformed. Higher z-values signify better performance. STW, spot-the-word test; DSST, digit symbol substitution test; and TMT trail-making test. *** P < 0.001, ** P < 0.01, and * P < 0.05. b) The fMRI experiment consisted of task blocks of overt paced semantic fluency and counting, which were presented in a pseudo-randomized order and separated by rest periods. An example for each task is shown. Participants were instructed to produce exactly one exemplar for a category or to say one number when the fixation cross turned green and to pause when the cross turned red. If they could not think of an exemplar, they were instructed to say "next." Each task block contained 9 trials of the same semantic category/counting task, which were separated by jittered interstimulus intervals.

while allowing for full transparency and reproducibility of the applied methods and a comprehensive quality assessment of each processing step that facilitates the identification of potential outliers. We also double-checked results from preprocessing with fMRIPrep with a conventional SPM preprocessing pipeline of both echoes. The results show strong overlap between both pipelines for univariate comparisons, confirming the reliability of the results independent of individual decisions during the preprocessing (Supplementary Fig. S1, see online supplementary material for a color version of this figure). A high-resolution, T1-weighted 3D volume was obtained from our in-house database (if it was not older than 2 years) or collected after the functional scans using an MPRAGE sequence (176 slices in sagittal orientation; TR = 2,300 ms; TE = 2.98 ms; flip angle = 9°; voxel size = 1 × 1 × 1 mm; no slice gap; FOV = 256 mm). Preprocessing was performed using fMRIPprep 20.2.3 (Esteban et al. 2019), which is based on Nipype 1.6.1 (Gorgolewski et al. 2011). In short, preprocessing steps included skull stripping, distortion correction, co-registration, slice timing correction, and calculation of several confounding time-series for each of the 2 BOLD runs per participant. Anatomical T1-weighted images were skull-stripped, segmented, and spatially normalized. For spatial normalization to standard space, the Montreal Neurological Institute (MNI) ICBM 152 nonlinear sixth Generation Asymmetric Average Brain Stereotaxic Registration Model (MNI152NLin6Asym) was entered as output space in fMRIPrep. For more details on the preprocessing pipeline, see the section corresponding to workflows in fMRIPrep's documentation (https://fmriprep.org/en/20.2.3/workflows.html).

Moreover, we investigated a potential resampling bias through the MNI template. To this end, we created a study-specific template based on the structural scans of our participants. We used the Computational Anatomy Toolbox (CAT12) in SPM12 to segment the structural images. Compared with the segmentation process included in SPM12, CAT12 provides a more fine-grained, advanced segmentation that has been shown to be robust to

noise and to produce reliable results (Tavares et al. 2020). We then applied the diffeomorphic anatomical registration through exponentiated lie algebra (DARTEL; Ashburner 2007) toolbox to create an anatomical study-specific template (young and older adults together; for a more detailed description of the procedure see Michael et al. 2016). The coregistered functional images were normalized to this study-specific template in MNI space and subsequently smoothed with a 5-mm full-width half-maximum (FWHM) Gaussian kernel. First- and second-level statistics were calculated analogously to the analyses using the data preprocessed with fMRIPrep. The results did not reveal major differences between the 2 resampling procedures for univariate within-group comparisons (Supplementary Fig. S2, see online supplementary material for a color version of this figure). All significant clusters that were found with the study-specific template approach were also found with the results based on the fMRIPrep preprocessing pipeline (resampling to the MNI template). Furthermore, the latter produced more reliable activation in the ATL in both age groups.

After preprocessing, 29 volumes from the beginning of each run were discarded since they were collected for the combination of the short and long TE images. This yielded 587 normalized images per run, which were included in further analyses.

Independent component analysis

We applied group independent component analysis (ICA) to define spatially independent task-active networks in a data-driven manner. ICA has been shown to decompose fMRI time series into reliable functionally connected components with the advantage of simultaneously removing non-neural fluctuations through the identification of artefactual components (Griffanti et al. 2014). Preprocessed, normalized data were smoothed with a 5-mm³ FWHM Gaussian kernel and entered into a general linear model for each participant and session using Statistical Parametrical Mapping software (SPM12; Wellcome Trust Centre for

Neuroimaging), implemented in MATLAB (version 9.10/R2021a). General linear model (GLM) included regressors for the task blocks (semantic fluency and counting) as well as nuisance regressors consisting of the 6 motion parameters and individual regressors for strong volume-to-volume movement as indicated by values of framewise displacement (FD) > 0.9 (Siegel et al. 2014). In addition, an individual regressor of no interest was included in the design matrix if a participant had missed a whole task block during the experiment ($n = 10$). Before model estimation, a high-pass filter with a cutoff at 128 s was applied to the data.

Preprocessed, normalized, and smoothed data were analyzed using the Group ICA of fMRI Toolbox (GIFT v4.0c). Dimensions were reduced to 55 using minimum description length information criteria. Icasso was repeated 50 times to ensure reliability of the decomposition, and group-level ICs were back-reconstructed to the participant level using the group-information guided ICA (GICA3) algorithm (Calhoun et al. 2001). We calculated group ICA treating all participants as 1 group to ensure that the same components were identified in both groups. We discarded those components related to banding artifacts and noise after careful visual inspection of the spatial maps according to established criteria (Griffanti et al. 2014; see Supplementary Fig. S3, see online supplementary material for a color version of this figure for an overview of all 55 ICs). From the resulting 13 non-noise components, low-level sensory components including auditory, sensorimotor, and visual networks were identified and removed since their roles were beyond the scope of our investigation. To characterize the spatial extent of the 7 remaining components at the group-level, we calculated 1-sided *t*-tests for participants' spatial maps. A gray matter mask that restricted statistical tests to voxels in the cerebrum was applied to all group-level analyses. Results were corrected for multiple comparisons using a peak level threshold at $P < 0.05$ with the family-wise error (FWE) method and a cluster-extent threshold of 10 voxels.

Brain network construction

Brain networks were constructed based on the 7 selected component maps of the ICA. To determine network labeling of the thresholded maps, we used the Jaccard index (*J*), a measure of spatial similarity (Jaccard 1912). By calculating the ratio of over-lapping voxels in 2 binary spatial network maps relative to all active voxels in either image, the Jaccard index can be used as a measure to assess the fit between a spatial component map (*A*) and a template image (*B*):

$$J = \frac{|A \cap B|}{|A \cup B|}$$

The index ranges from 0 to 1, with a high Jaccard index denoting high similarity of 2 spatial maps. It has been used previously to assess similarity of brain activation maps with template network parcellations (Jackson et al. 2019; Gordon et al. 2020). We defined a minimum threshold of $J = 0.15$ to consider a network template for a spatial component mask (Jackson et al. 2019). Next, if 2 components were best described by the same network template thereby indicating that the network might have split up in multiple components, we assessed the similarity of the combined component maps to the template. If the combined map reached a higher similarity index than each component individually, the combination was kept as a reflection of the respective network.

As template masks, we used the 17-networks functional connectivity-based parcellation scheme (Yeo et al. 2011) as

well as the network masks of general semantic cognition and semantic control defined in a meta-analysis (Jackson 2021). We included separate template masks for semantic cognition in our analysis to account for the semantic nature of our task. We also probed similarity of Jaccard indices with a 7-networks parcellation scheme (Yeo et al. 2011). Although the results for the 7-networks parcellation generally agreed with the more fine-grained parcellation, the 7-networks parcellation resulted in 3 components showing high spatial similarity with the default network template. However, differential roles have been reported for subsystems of the default network when access to semantic memory is required (Smallwood et al. 2021). Specifically, the dorsal medial subsystem of the default network ("Default B" in the 17-networks parcellation scheme) has been shown to broadly overlap with a left-lateralized temporal-frontal semantic network (Lambon Ralph et al. 2017; Smallwood et al. 2021). Since we were interested in the age-dependent interplay of domain-specific and domain-general networks in semantic cognition, the remaining analyses were based on the 17-networks parcellation scheme.

Based on the results of the Jaccard index, each thresholded component map was inclusively masked by the respective resampled template network. We were interested in the effect of age on the functional connectivity within and between selected networks. In a first step, to explore functional connectivity between networks, we extracted averaged time series across all voxels within 1 masked component, thus leading to 7 time series per participant and run. Second, networks were further parcellated into distinct regions of interest (ROIs) based on peak maxima of activated clusters. ROIs were created for all peak maxima of a significant cluster (up to 3 ROIs per cluster) using the MarsBar toolbox (Brett et al. 2002). To this end, identified clusters were extracted from the thresholded and masked component maps, spheres of 5 mm surrounding each maximum coordinate were created, and, in a last step, both images were combined. In this way, we ensured that ROIs would only contain voxels that were included in the group-level statistics. Parcellating the 7 network components based on strongest correlation peaks led to 126 cortical ROIs per participant and run.

Functional time series were extracted for the 7 ROIs and 126 ROIs parcellation schemes from non-smoothed functional data. To account for motion artifacts and other signal confounds, the following denoising pipeline was applied during time series extraction: 24 realignment parameters (6 motion parameters, temporal derivatives, and quadratic terms), global signal, and top 5 aCompCor components for white matter and cerebral spinal fluid, respectively. Censoring included a FD threshold of 0.9 mm and 18 discrete cosine-basis regressors to account for signal drifts. All these regressors were combined in a design matrix and removed from the data in a single step (Hallquist et al. 2013; Lindquist et al. 2019). The denoising strategy was based on recent recommendations (Mascali et al. 2021) that compared the performance of different denoising pipelines for analysis of task-based functional connectivity. Consistent with previous research on resting-state functional connectivity (Ciric et al. 2017; Parkes et al. 2018), the authors reported that the inclusion of global signal in a denoising pipeline markedly reduced global motion artifacts and led to more comparable results across conditions in task-based functional connectivity data (Mascali et al. 2021). Furthermore, time-series were detrended and demeaned, and functional images were masked with a subject-specific, resampled gray matter mask before denoising. During signal extraction for the set of 126 ROIs, the number of voxels per ROI and participant were extracted. ROIs for which >15% of

participants did not show any signal coverage were excluded. The resulting 121 ROIs were used for the remaining analyses.

Functional connectivity matrices

We applied correlational psychophysiological interaction analyses (cPPI; Fornito et al. 2012) to obtain connectivity terms that describe task-related interactions between our networks and regions of interest. In contrast to traditional PPI analyses, cPPI results in undirected, symmetrical connectivity matrices that are based on pairwise partial correlations between ROIs. We calculated cPPI for our contrast of interest semantic fluency > counting, separately for the 7-networks and 121-ROIs parcellations. In brief, the deconvolved time series for each ROI was multiplied with the task time course from the first-level GLM design matrix and convolved with a canonical HRF to form a PPI term. Pairwise partial correlations were estimated between PPI terms of 2 regions while controlling for the observed BOLD signal in both regions, the original task regressor, and average in-scanner head motion (mean FD). Connectivity matrices were calculated for each run separately and then averaged, resulting in a 7 × 7 and 121 × 121 correlation matrix per participant. Subsequently, correlation coefficients were Fisher-transformed to z values.

Network measures

Within- and between-network functional connectivity

Within- and between-network functional connectivity were explored for the 7-networks and 121-ROIs connectivity matrices in both age groups. Using the connectivity matrices with 7 networks allowed us to investigate the coupling and decoupling between task-relevant networks, whereas the more fine-grained parcellation provided additional insights into the coupling of regions within distinct networks. All subsequent network measures were based on the 121-ROIs connectivity matrices. For analyses of within- and between-network functional connectivity, full matrices including positive and negative correlation weights were used.

Brain system segregation

We calculated global segregation as previously implemented by Chan and colleagues (Chan et al. 2014, 2021; Wig 2017), using the unthresholded, weighted connectivity matrices. In line with previous work on functional connectivity in healthy aging (Chong et al. 2019; Chan et al. 2021), we excluded negative correlations from segregation and integration analyses by setting them to zero. Excluding negative correlations has been shown to improve the reliability of graph measures (Wang et al. 2011) and to help avoid interpretational difficulty, for example when it comes to concepts like shortest paths (Fornito et al. 2016). Building upon the network parcellation of our ICA analysis, each functional network was treated as a distinct system, and segregation was computed as the difference between mean within-system ($\overline{Z}_w$)and mean between-system ($\overline{Z}_b$)correlations divided by mean within-system correlation as shown in the following equation:

$$\text{Brain system segregation} = \frac{\overline{Z}_w - \overline{Z}_b}{\overline{Z}_w}$$

A higher ratio score denotes greater separation of functional systems.

We also calculated segregation values for each functional network individually such that within-system connectivity $\overline{Z}_w$ represents the mean of all edges (correlations) between pairwise nodes that belong to the same network and between-system connectivity $\overline{Z}_b$ reflects the mean of all edges between nodes of the respective network and all other nodes.

Edge filtering

Most graph-theoretical measures require some form of filtering to obtain a sparse graph that is more likely to represent true functional connectivity than a maximally dense graph as produced by a correlation matrix (Fornito et al. 2016). Although threshold-based filtering methods like proportional or absolute thresholding are commonly applied in network neuroscience, they are driven by an arbitrary choice of the respective threshold and suffer from low reliability (Luppi and Stamatakis 2021). To avoid these pitfalls and based on recent research on the reliability of graph construction in neuroscience (Jiang et al. 2021; Luppi and Stamatakis 2021), we calculated the orthogonalized minimum spanning tree (OMST; Dimitriadis et al. 2017) on the weighted functional connectivity matrices. Apart from its high reliability, the OMST has several advantages compared with commonly applied threshold-based methods of graph construction: It adheres to the intrinsic topological structure of the brain network by resulting in a fully connected, weighted graph and offers a data-driven method of individualized network construction accounting for each individual's optimal state of economic wiring in terms of cost and efficiency. In contrast to the original minimum spanning tree (MST), the OMST filters connectivity networks until the highest global cost efficiency (GCE) of a graph is reached while including both strong and weak connections and preserving the same mean degree across groups.

The OMST was calculated in 3 steps as described by Dimitriadis et al. (2017): (i) the MST of a graph is defined; (ii) the corresponding edges of the MST are removed from the original graph by setting edge weights to 0; (iii) steps (i) and (ii) are repeated until the GCE of the graph is optimized. GCE is defined as the global efficiency minus cost, where cost corresponds to the total weights of the selected edges of the OMST divided by the sum of the edges of the original fully weighted graph (Bassett et al. 2009). The final OMST is constructed by combining all the removed, nonoverlapping MSTs. To show that the OMST indeed results in higher GCE than other filtering methods, we compared the GCE for OMST, MST, and a method of proportional thresholding where we used a common range of 5–20% strongest edge weights of a graph (Supplementary Fig. S4, see online supplementary material for a color version of this figure). To avoid differences in graph measures caused by the number of nodes in a graph, we excluded all nodes where at least 1 participant had no signal during construction of matrices. This resulted in a 104 × 104 matrix per participant, which was used for construction of OMST and all subsequent measures.

Brain system integration

We calculated global efficiency as a measure of system-wide integration. It is defined as the average of the inverse shortest path length between all pairs of nodes in a graph and is thus a measure of efficient signal transmission (Latora and Marchiori 2001; Rubinov and Sporns 2010).

$$\text{Global efficiency} = \frac{1}{N(N-1)} \sum_{i \neq j \in G} \frac{1}{L_{i,j}}$$

Global efficiency was based on the individual OMSTs using the reciprocal edge weights to obtain a distance matrix where high weights signify short paths between nodes.

Global network hubs

We identified hubs via the normalized participation coefficient (PC; Pedersen et al. 2020). The PC provides insight into the functional role of a node. Specifically, it evaluates whether a node mainly interacts with nodes from its community or multiple communities of a network (Guimerà and Nunes Amaral 2005). In network neuroscience, PC has been applied to define nodes that are important for communication between communities (connector hubs) and nodes that are central to the communication within communities (provincial hubs; Cohen and D'Esposito 2016; Bertolero et al. 2017, 2018). Recently, it has been shown that the conventional measure of PC is strongly influenced by the size and connectedness of its community leading to a reduced interpretational value of this graph measure (Pedersen et al. 2020). Thus, a normalized version of the PC has been introduced that accounts for these differences in real-world networks while preserving its meaning though the comparison with null models. It is calculated similarly to the original PC as 1 minus the ratio between the degree k of node i with nodes in its community m and the degree of node i with all other nodes in the network. However, a normalization factor is added by subtracting the median degree of this node in a series of random networks:

$$\text{Normalized PC} = 1 - \sqrt{B_0 \sum_{m \in M} \left(\frac{k_i(m) - k_i(m)_{rand}}{k_i} \right)^2}$$

We calculated 100 random networks for each node. Connector hubs were then defined as nodes with a PC value of at least 1SD above the mean in each age group.

Statistical analyses

Age-related changes for within- and between-network functional connectivity

To assess differences between age groups for within- and between-network connectivity, we ran 2-sample t-tests for each edge of the 7-network and 121-ROIs connectivity matrices within the Network-Based Statistics toolbox (NBS; Zalesky et al. 2010). NBS applies cluster-based thresholding to correct for multiple comparisons using permutation testing. In contrast to more conventional procedures for controlling the family-wise error rate, such as the false discovery rate, NBS considers connected components in networks (graphs), which makes it especially suited for network statistics. We set an initial cluster-forming threshold at $P < 0.01$ (1-sided test; $t = 2.35$) and an FWE-corrected significance threshold at $P < 0.025$ (2 comparisons) with 10,000 permutations. Mean-centered covariates per participant for the average in-scanner head motion and mean response time were included in each model. Average head motion was defined as the mean FD based on the calculation of the root mean square deviation of the relative transformation matrices (Jenkinson et al. 2002).

Age-related changes for network measures of segregation and integration

Linear mixed-effects models were set up to examine how the dependent variables brain system segregation, individual network segregation, global efficiency, and nodal participation coefficient were predicted by age group. We included in-scanner head motion (mean FD) as covariate and a random intercept for participants.

Models were calculated as follows:

$$\text{Network measure} = \beta_0 + \beta_1 \text{Age} + \beta_2 \text{Motion} + (1|\text{Subject}) + \varepsilon$$

Significance values were obtained by likelihood-ratio tests of the full model with the effect in question against the model without the effect in question.

Association between network measures and cognitive performance

For those network measures that showed differences between young and older adults, we further examined their association with participants' cognitive performance for the in-scanner task and the neuropsychological test battery. Analyses were performed using mixed-effects models with a logistic regression for accuracy data due to their binomial nature and a linear regression for log-transformed response time data. We only analyzed response times for correct reactions for the semantic fluency task since our connectivity values were also based on our contrast of interest semantic fluency > counting. Models contained fixed effects for the respective mean-centered network measure (between-network functional connectivity, brain system segregation, individual network segregation, and global efficiency) and age group as well as their interaction term, and random intercepts for participants and semantic categories. Furthermore, mean-centered values of mean FD and education were entered as covariates. Models were set up as shown in the following equation:

$$\begin{aligned} \text{Cognitive measure} = \beta_0 &+ \beta_1 \text{Network measure} + \beta_2 \text{Age} \\ &+ \beta_3 \text{Network measure} \times \text{Age} + \beta_4 \text{Motion} \\ &+ \beta_5 \text{Education} + (1|\text{Subject}) + (1|\text{Category}) + \varepsilon \end{aligned}$$

where cognitive measure denotes accuracy and response time, respectively. Significance values were obtained via likelihood-ratio tests. We applied sum coding (analysis of variance, ANOVA-style encoding) for all categorical predictors. Results were corrected for multiple comparisons using the Bonferroni–Holm method. Where applicable, x^2 and adjusted P-values of significance testing using likelihood-ratio tests are reported. In addition, standardized effect sizes in the form of ω_p^2 for linear and odds ratio (OR) for logistic mixed-effects models are given. Tables with point estimates (b), 95% confidence intervals (CIs), t-values for linear mixed-effects models, z-values for logistic mixed-effects models, and P-values for the fixed effects coefficients are reported in the supplementary materials for each statistical model.

We performed correlation analyses with the neuropsychological tests that had been assessed outside of the scanner. Because of the collinearity of some neuropsychological tests, we ran an exploratory factor analysis on the standardized test scores using maximum likelihood estimation and varimax rotation. Based on the hypothesis test ($X^2 = 14.04$, $P = 0.081$), 2 factors with an eigenvalue > 1 were chosen. For subsequent correlations with network measures, participant factor scores extracted via regression methods were used.

All statistical models except for NBS were performed using R 4.1.0 via RStudio (R Core Team 2021) and the package lme4 (Bates et al. 2015). Effect sizes were estimated using the package parameters (Lüdecke et al. 2020) and effectsize (Ben-Shachar et al. 2020). Results were visualized using the ggplot2 (Wickham 2016) and ggeffects (Lüdecke 2018) packages. If applicable, post-hoc

Table 1. Comparison of findings for functional connectivity using different denoising strategies.

Partition	Change in methodology Denoising with GSR	Denoising without GSR
7 whole networks	• Stronger coupling for older adults • Stronger decoupling for young adults	• Stronger coupling for older adults
121 ROIs	• Stronger coupling for ROIs from different networks for older adults • Stronger coupling for ROIs within networks for young adults • Stronger decoupling for ROIs from different networks	NA

Note. ROIs: regions of interest; GSR: global signal regression.

comparisons were applied using the package emmeans (Lenth 2020). The exploratory factor analysis was calculated with the stats package (R Core Team 2021). OMSTs and all graph theory measures were calculated in Matlab using the Brain Connectivity toolbox (Rubinov and Sporns 2010) and publicly available scripts for OMST and normalized PC. Chord diagrams were generated with the circlize package (Gu et al. 2014), spring-embedded plots using the igraph package (Csardi and Nepusz 2006), and force-directed plots using the ForceAtlas2 algorithm for R available on Github (https://github.com/analyxcompany/ForceAtlas2).

Additional validation analyses

We included global signal regression in our original analyses since it has been reported to play an important factor in revealing aging effects (Ng et al. 2016; Chong et al. 2019) and has recently been shown to effectively reduce motion-related effects in task-based functional connectivity data (Mascali et al. 2021). However, the inclusion of global signal regression remains a controversial topic since it might lead to the regression of meaningful signal (Aquino et al. 2020) and can exert differential effects in group-based comparisons (Murphy and Fox 2017). Due to the underlying differences in the network architecture of young and older adults, global signal regression might have impacted our results. We thus repeated the analysis for within- and between-network functional connectivity without global signal regression.

The results of comparing both pipelines, with and without global signal regression, are summarized in Table 1, and Supplementary Fig. S5 (see online supplementary material for a color version of this figure) shows functional connectivity results for the 7-networks and 121-ROIs parcellations without global signal regression. Results show that the denoising without global signal regression led to a general shift in correlation values to a more positive range, which is expected due to the mean-centering of values around zero when global signal regression is applied. Despite the shift in correlation values, the conclusions of our findings remained the same: Networks of older adults were characterized by stronger positive coupling of different cognitive systems such as default and attention networks or semantic, control, and attention networks. It is also worth noting that we did not find significant age differences for the more fine-grained 121-ROIs parcellation for the pipeline without global signal regression (Supplementary Fig. S5b, see online supplementary material for a color version of this figure). This might point to a more pronounced effect of noise in this pipeline such that potential age differences in correlation values might be overshadowed by the greater amount of noise (most likely due to motion) in the signal.

To further investigate the motion dependence of both denoising pipelines, we calculated quality control–functional connectivity correlations (QC–FC), a common benchmark in functional connectivity studies (Ciric et al. 2017; Parkes et al. 2018; Power et al. 2018; Aquino et al. 2020). QC–FC is estimated as the correlation between functional connectivity and mean FD for each edge in a network and thus quantifies the association between gross head motion and interindividual variance in functional connectivity (Aquino et al. 2020). Lower scores denote less corruption through motion and hence more efficient denoising. We assessed QC–FC for each parcellation scheme individually. Supplementary Fig. S6 (see online supplementary material for a color version of this figure) displays the results which are summarized as the percentage of significant uncorrected edges and the full distribution of QC–FC correlations. Compared with the pipeline without global signal regression, the inclusion of global signal regression shifted the distribution of QC–FC correlations closer to zero in both parcellations. Furthermore, global signal regression reduced the percentage of (uncorrected) QC–FC correlations for the 7 networks parcellation.
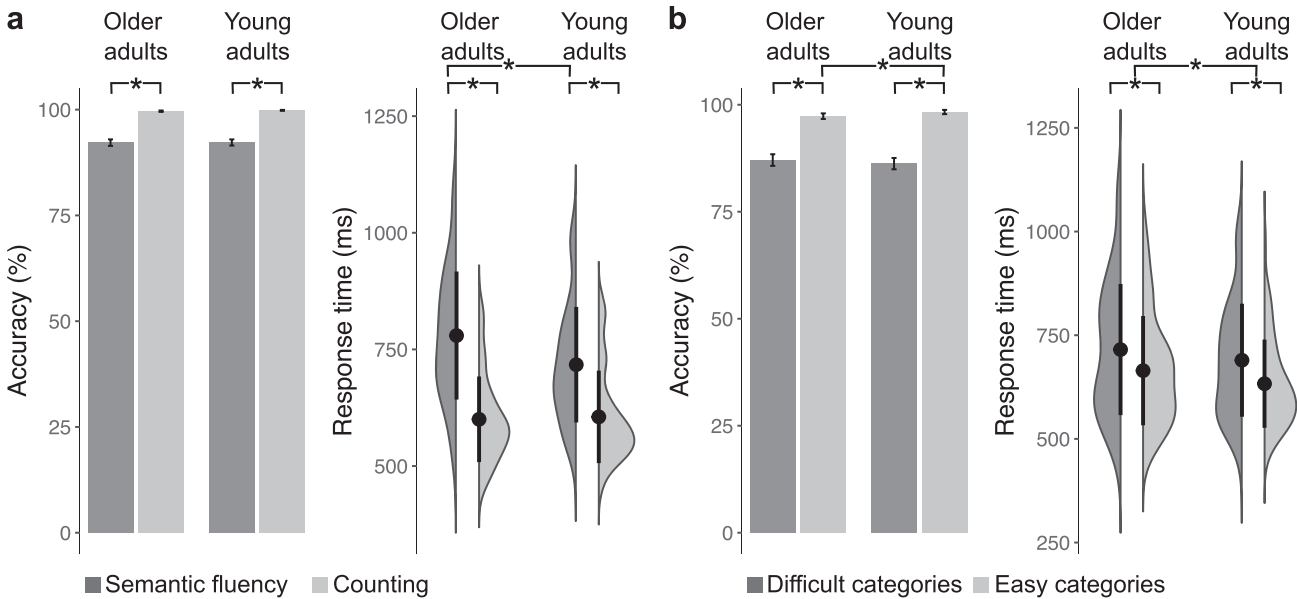
Data and code availability

All behavioral data and raw data of functional connectivity and graph-theoretical measures are available in a public repository at https://gitlab.gwdg.de/functionalconnectivityaging/mdn_lang_networkAnalysis. This repository also holds all self-written code for analyses and figures for this project. Raw neuroimaging data are protected under the General Data Protection Regulation (EU) and can only be made available from the authors upon reasonable request.

Results

The main objective of this study was to investigate age-related changes in the functional network architecture engaged during the goal-directed access to semantic memory. For the in-scanner tasks of overt semantic fluency and counting, we fitted mixed-effects models accounting for individual variance of participants and semantic categories via random effects and the difference in years of education via covariate (Supplementary Table S1). Likelihood-ratio tests showed that both age groups performed similarly (x^2 = 2.23, P = 0.14, OR = 0.51, 95% CI [0.32, 0.79]) and generally better for counting than semantic fluency (x^2 = 21.59, P < 0.001, OR = 0.04, 95% CI [0.02, 0.10]; Fig. 2a). Furthermore, we detected a main effect of difficulty (x^2 = 27.47, P < 0.001, OR = 7.43, 95% CI [4.48, 12.33]) and an interaction of difficulty with age (x^2 = 10.15, P = 0.001, OR = 0.51, 95% CI [0.34, 0.77]) indicating that more correct items were produced within each group and that young adults produced more correct items for easy (OR = 0.36, P < 0.001, 95% CI [0.21, 0.62]) but not difficult categories (OR = 0.71, P = 0.13, 95% CI [0.45, 1.10]). For response time, results showed an interaction between task and age group (x^2 = 80.01, P < 0.001, ω_p^2 = 0.004, 95% CI [0.00, 1.00]) with older adults performing slower than young adults during the semantic fluency but not the counting task (Fig. 2b). Furthermore, there was a main effect of difficulty

Fig. 2. Behavioral results. a) Both groups performed better for counting than semantic fluency. Although there was no effect of age for accuracy in either task, older adults performed slower than young adults during semantic fluency but not during counting. b) Both groups performed better for easy than difficult semantic categories, and young adults better than older adults for easy semantic categories. Furthermore, young adults were generally faster in responding during semantic fluency than older adults, independent of difficulty level. Points show mean response times with 2 standard deviations, *P < 0.05.

$(x^2 = 22.21, P < 0.001, \omega_p^2 = 0.48, 95\%$ CI [0.21, 1.00]) with generally slower responses for difficult than easy categories.

Goal-directed access to semantic memory involves default, semantic, and executive control networks
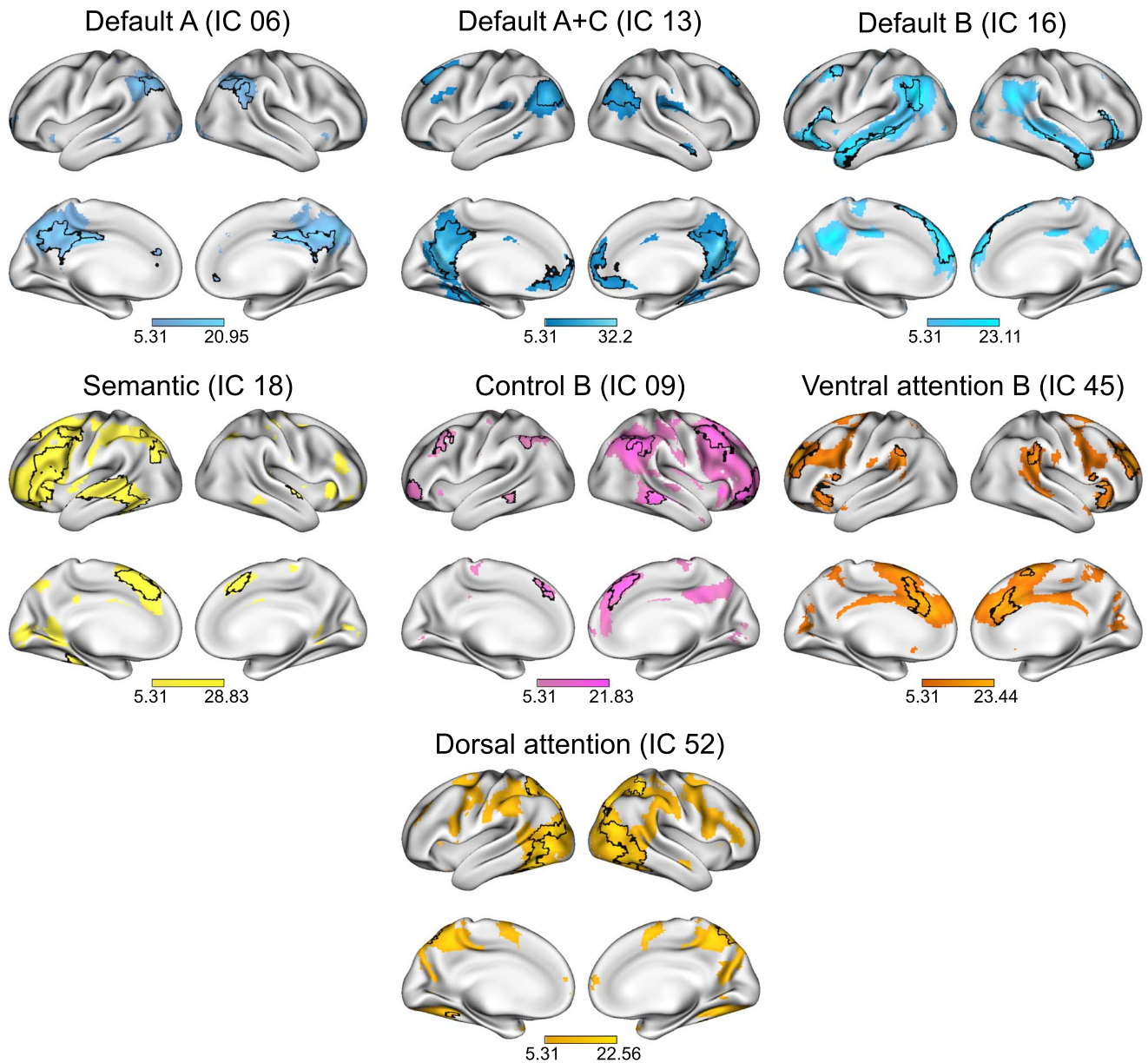
Using the data-driven method of group spatial independent component analysis (ICA) on the whole data set, we defined functional cortical networks for the semantic task. We identified 7 components of interest, which were submitted to 1-sample *t*-tests and thresholded controlling the family-wise error (FWE) rate at peak level with $P < 0.05$ and a cluster-extent threshold of 10 voxels. Figure 3 shows the thresholded maps with their original component number. To determine which cognitive network best described each component, we calculated the Jaccard similarity coefficient (*J*) between our thresholded, binarized components of interest and template masks of common resting-state (Yeo et al. 2011) and semantic cognition networks (Jackson 2021). Results showed similarity above threshold ($J = 0.15$) for all component maps with distinct cognitive networks (Table 2). For IC06, we found overlap with the frontoparietal control network C (CONT-C) and default mode network A (DMN-A). Although spatial similarity was marginally higher for CONT-C than DMN-A ($J_{Control\ C} - J_{Default\ A} = 0.01$), we refer to this component as part of the default system. Significant clusters included classic midline structures of the core default network (Smallwood et al. 2021) like posterior cingulate cortex, precuneus, and prefrontal cortex (Fig. 3). An additional analysis of similarity coefficients between the component maps and the 7-networks parcellation (Yeo et al. 2011) revealed a stronger similarity with the default network as a whole for this component ($J_{Control} - J_{Default} = -0.03$; see Supplementary Table S2 for results with the 7-networks parcellation). Furthermore, a second component (IC13) showed strong similarity with DMN-A. As described in Methods, we combined the component maps of IC06 and IC13 to assess whether this would lead to a numerical improvement of *J*. This was not the

case with $J = 0.21$ for the combined components, which was below the similarity coefficient of IC13 alone ($J = 0.26$). Thus, both components represented distinct parts of DMN-A and were hence included in subsequent analyses. For IC13, we further included default mode network C (DMN-C), which showed the second strongest overlap and was represented by significant clusters in bilateral parahippocampal gyri. Indeed, a combined template of DMN-A and DMN-C led to a numerical improvement in similarity compared to DMN-A alone ($J_{Default\ A+C} - J_{Default\ A} = 0.091$). Thus, to gain a comprehensive representation of the default network, both subsystems were combined and are referred to as default mode network A + C (DMN-A + C).

Results of Jaccard calculations further revealed the following networks for the other components: default mode network B (DMN-B; IC16) with peak activations in bilateral middle temporal gyri (MTG), inferior and superior frontal gyri (IFG and SFG), and left angular gyrus (AG); semantic network (SEM; IC18) with strong overlap with the semantic control network and peak activations in left IFG, SFG, paracingulate gyrus, posterior superior temporal gyrus (STG), and AG; frontoparietal control network B (CONT-B; IC09) with large clusters in bilateral SFG and middle frontal gyri (MFG), AG, and posterior MTG; ventral attention network B (VAN-B; IC45) with peak activation in prefrontal cortex including paracingulate gyrus, bilateral IFG and supramarginal gyri; and dorsal attention network A (DAN-A; IC52) with large clusters in bilateral AG, and temporooccipital cortex. Statistical tables with all significant clusters are reported in Supplementary Table S3.

Stronger coupling of default and executive systems predicts intact but less efficient semantic retrieval in older adults

Graphs of task-related connectivity were derived via cPPI for matrices with 7 and 121 nodes, respectively. We tested for statistically significant coupling differences between age groups by means of network-based statistics using permutation testing while controlling for in-scanner head motion (Fig. 4a). Overall, the

Fig. 3. ICA-derived networks and their overlap with cognitive networks. *T*-scores from 1-sided *t*-tests (FWE-corrected *P* < 0.05 at peak level) are displayed for the 7 selected component maps with their respective network label according to spatial similarity analysis. Overlaps between the thresholded component map and the spatially most similar cognitive network according to the Jaccard index are outlined on the surface of the brain. The areas of overlap were used for subsequent network analyses.

network of older adults showed reduced decoupling compared with young adults. Significantly stronger positive coupling was found in the graphs of older adults for the networks SEM with VAN-B, CONT-B with VAN-B, and DAN-A with VAN-B. A similar picture of age-related differences emerged for the more fine-grained graphs containing 121 nodes. Here, young adults generally showed stronger positive coupling within individual networks and between subsystems of the default network and stronger decoupling between different networks (Supplementary Fig. S7, see online supplementary material for a color version of this figure).
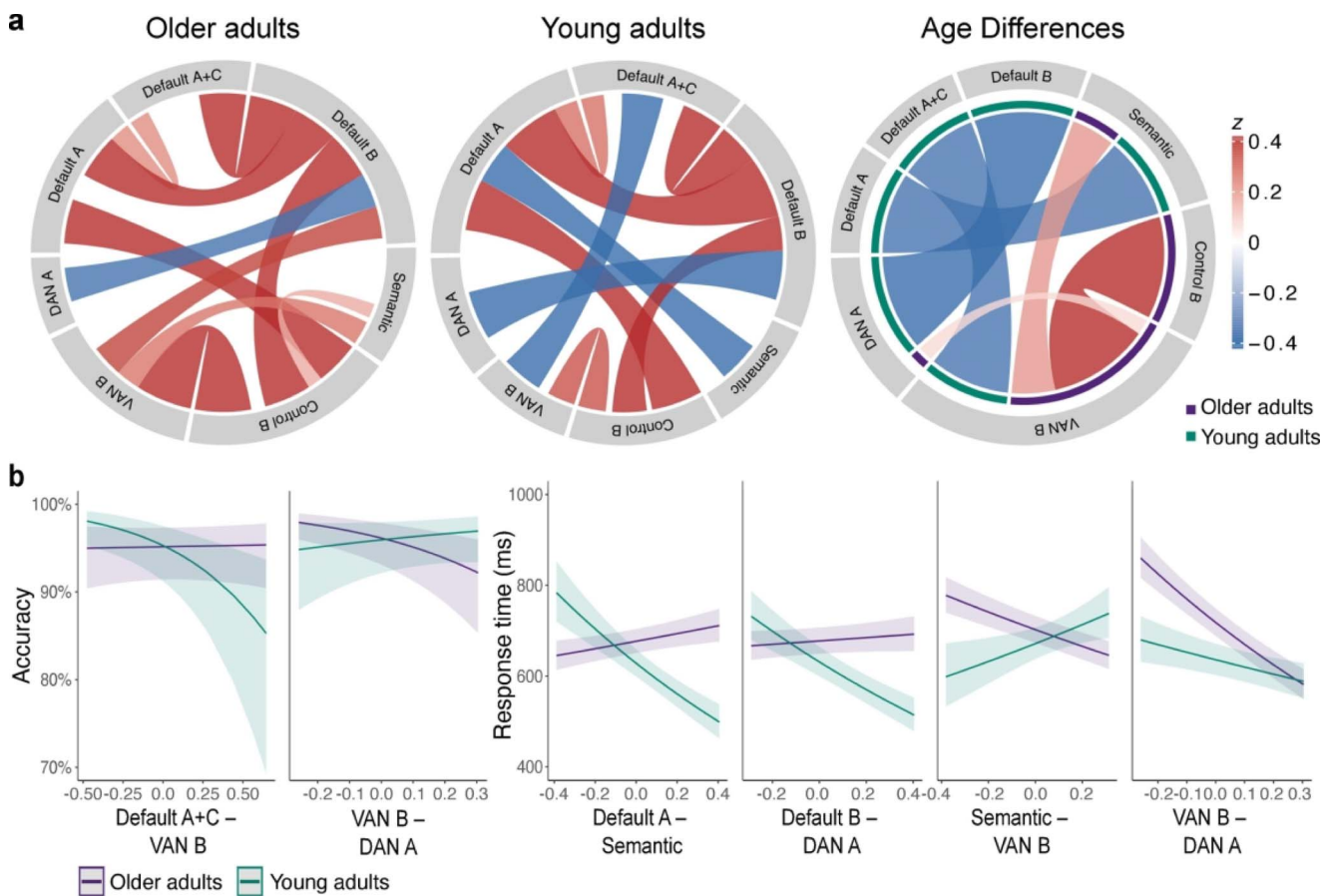
We probed the behavioral relevance of the network connection pairs that showed significant age differences by calculating mixed-effects models for accuracy and response time data (Fig. 4b; Supplementary Tables S4 and S5). For accuracy, we found significant interactions between age and between-network

connectivity for VAN-B with DMN-A + C (x^2 = 12.39, P < 0.001, OR = 1.57, 95% CI [1.22, 2.01]) and DAN-A (x^2 = 14.18, P < 0.001, OR = 0.64, 95% CI [0.51, 0.81]). Predicting response time revealed significant interactions between age and between-network connectivity for SEM with DMN-A (x^2 = 90.61, P < 0.001, ω_p^2 = 0.01, 95% CI [0.01, 1.00]) and VAN-B (x^2 = 25.75, P < 0.001, ω_p^2 = 0.02, 95% CI [0.01, 1.00]), and for DAN-A with DMN-B (x^2 = 51.76, P < 0.001, ω_p^2 = 0.008, 95% CI [0.01, 1.00]) and VAN-B (x^2 = 28.81, P < 0.001, ω_p^2 = 0.004, 95% CI [0.00, 1.00]). For older adults, increased coupling between default and attention networks predicted high but less efficient performance, whereas increased coupling of SEM and VAN-B and between both attention systems (DAN-A and VAN-B) was associated with faster responses. A different picture emerged in young adults, where stronger coupling between default and executive systems predicted faster but poorer performance, whereas increased connectivity between DAN-A and VAN-B was

Table 2. Jaccard indices for independent components and cognitive networks.

	IC06	IC09	IC13	IC16	IC18	IC45	IC52
Frontoparietal control A	0.054	0.133	0.032	0.013	0.151	0.083	0.109
Frontoparietal control B	0.091	**0.210**	0.028	0.073	0.125	0.050	0.018
Frontoparietal control C	0.168	0.020	0.066	0.010	0.010	0.028	0.044
Default A	**0.154**	0.089	**0.255**	0.149	0.040	0.054	0.019
Default B	0.039	0.069	0.031	**0.263**	0.082	0.098	0.010
Default C	0.014	0.010	**0.122**	0.008	0.026	0.001	0.020
Dorsal attention A	0.051	0.041	0.062	0.015	0.054	0.003	**0.180**
Dorsal attention B	0.008	0.038	0.006	0.006	0.071	0.053	0.123
Limbic A	0.000	0.001	0.002	0.014	0.002	0.002	0.011
Limbic B	0.001	0.007	0.015	0.004	0.009	0.005	0.002
Ventral attention A	0.042	0.012	0.023	0.015	0.033	0.124	0.065
Ventral attention B	0.014	0.074	0.001	0.031	0.059	**0.195**	0.039
Somatomotor A	0.022	0.052	0.000	0.039	0.036	0.029	0.028
Somatomotor B	0.000	0.016	0.038	0.009	0.033	0.011	0.015
Temporal parietal	0.001	0.029	0.014	0.118	0.023	0.035	0.034
Central visual	0.022	0.006	0.006	0.038	0.011	0.004	0.123
Peripheral visual	0.025	0.009	0.074	0.020	0.038	0.034	0.037
General semantic cognition	0.032	0.030	0.072	0.194	**0.201**	0.092	0.050
Semantic control	0.012	0.036	0.012	0.067	0.153	0.091	0.027

Note. The selected network labels for the respective independent components are shown in bold, whereas all cognitive networks that showed a higher similarity coefficient than $J = 0.15$ are shown in italics.

Fig. 4. Functional coupling between task-relevant networks in young and older adults and their behavioral relevance. a) Chord diagrams display significant results of functional coupling between ICA-derived networks. Connectivity values are partial correlations. The color intensity and width of a connection indicate its correlational strength. Higher z values indicate positive coupling and negative values indicate decoupling between networks. Chord diagrams of each age group are based on cPPI-derived significance values, whereas age differences were assessed using permutation testing in network-based statistics (cluster-forming threshold $P = 0.01$, FWE-corrected significance threshold $P = 0.025$ with 10,000 permutations). b) Network connections that showed significant age differences were probed for their behavioral relevance. Plots show significant 2-way interactions between age and the respective network pair for accuracy and response time data. Connectivity values were mean-centered for interaction analyses. Results were corrected for multiple comparisons using the Bonferroni–Holm method at $P = 0.05$. VAN, ventral attention network; DAN, dorsal attention network.

associated with better and faster reactions. These results suggest that both age groups showed distinct connectivity profiles, with older adults generally profiting from increased coupling between different cognitive systems and the opposite pattern for young adults.

Reduced segregation and higher integration of task-relevant networks is associated with better and more efficient performance in older adults

Next, we investigated brain system segregation and integration to get a better understanding of age-related differences in whole-brain dynamics (Fig. 5a). Segregation quantifies the presence of densely connected regions that form distinct subnetworks or communities in a global brain network (Fig. 5b). Results of a linear mixed-effects model for global brain system segregation revealed a significant effect of age ($x^2 = 11.74$, $P < 0.001$, $\omega_p^2 = 0.24$, 95% CI [0.07, 1.00]) with young adults exhibiting stronger segregation than older adults (Fig. 5c; Supplementary Table S6). Examining the predictive value of segregation for in-scanner performance and neuropsychological measures revealed significant interactions between age and segregation for accuracy ($x^2 = 9.36$, $P = 0.002$, OR = 0.62, 95% CI [0.46, 0.84]), response time ($x^2 = 64.92$, $P < 0.001$, $\omega_p^2 = 0.02$, 95% CI [0.01, 1.00]), and a significant correlation of segregation with executive functions in young adults ($r = 0.45$, $P = 0.013$). For all interactions, increasing levels of segregation predicted better and faster performance in young adults. In contrast, increasing brain-wide segregation had no effect on accuracy but predicted faster responses in older adults (Fig. 5c; Supplementary Table S7).

We used the measure of global efficiency to assess network integration. A linear mixed-effects model indicated higher global efficiency for young adults ($x^2 = 21.43$, $P < 0.001$, $\omega_p^2 = 0.38$, 95% CI [0.18, 1.00]); Fig. 5d; Supplementary Table S8). Efficiency values were then entered into regression models to assess their predictive value. Results showed a significant main effect of global efficiency for accuracy ($x^2 = 8.81$, $P = 0.003$, OR = 1.27, 95% CI [1.08, 1.48]) and a significant interaction with age for response time ($x^2 = 38.07$, $P < 0.001$, $\omega_p^2 = 0.006$, 95% CI [0.00, 1.00]). Although increasing system-wide efficiency was generally associated with better performance, it also predicted faster performance in older adults but slower responses in young adults (Fig. 5d; Supplementary Table S9).

Brain system segregation predicts age-related differences in behavior as a function of network type

We next examined whether segregation differed between networks. Previous research showed that networks exhibit differences in their patterns of age-related changes in segregation (Chan et al. 2014). Although these studies focused on a broad distinction of sensorimotor and cognitive association networks, we investigated segregation and its behavioral relevance for each network individually to explore age-accompanied differences as a function of system type. Overall, results showed that all networks were less segregated in older than young adults ($x^2 = 47.32$, $P < 0.001$, $\omega_p^2 = 0.11$, 95% CI [0.07, 1.00]; Fig. 6a; Supplementary Table S10). However, networks' increasing segregation differed in their behavioral relevance (Supplementary Table S11). For accuracy (Fig. 6b), we detected significant interactions between age and network segregation for DMN-B ($x^2 = 5.05$, $P = 0.025$, OR = 0.69, 95%CI [0.50, 0.95]) and VAN-B ($x^2 = 18.03$, $P < 0.001$, OR = 0.46, 95% CI [0.32, 0.65]). For response time (Fig. 6c), results showed significant interactions

with age and the networks DMN-A ($x^2 = 74.78$, $P < 0.001$, $\omega_p^2 = 0.02$, 95% CI [0.01, 1.00]), CONT-B ($x^2 = 16.37$, $P < 0.001$, $\omega_p^2 = 0.008$, 95% CI [0.00, 1.00]), and DAN-A ($x^2 = 79.79$, $P < 0.001$, $\omega_p^2 = 0.02$, 95% CI [0.01, 1.00]). Overall, stronger segregation of different systems was associated with better and faster performance for young adults and poorer and slower reactions in older adults. Only increasing segregation of DMN-A predicted slower reactions in young adults, which might point to a different role of this system in semantic cognition. We also explored the relationship of network segregation with neuropsychological measures (Fig. 6d). Results revealed a significant positive correlation of segregation in the VAN-B with executive measures in young adults ($r = 0.4$, $P = 0.03$) and a negative correlation of DMN-B with semantic memory in older adults ($r = -0.38$, $P = 0.045$).
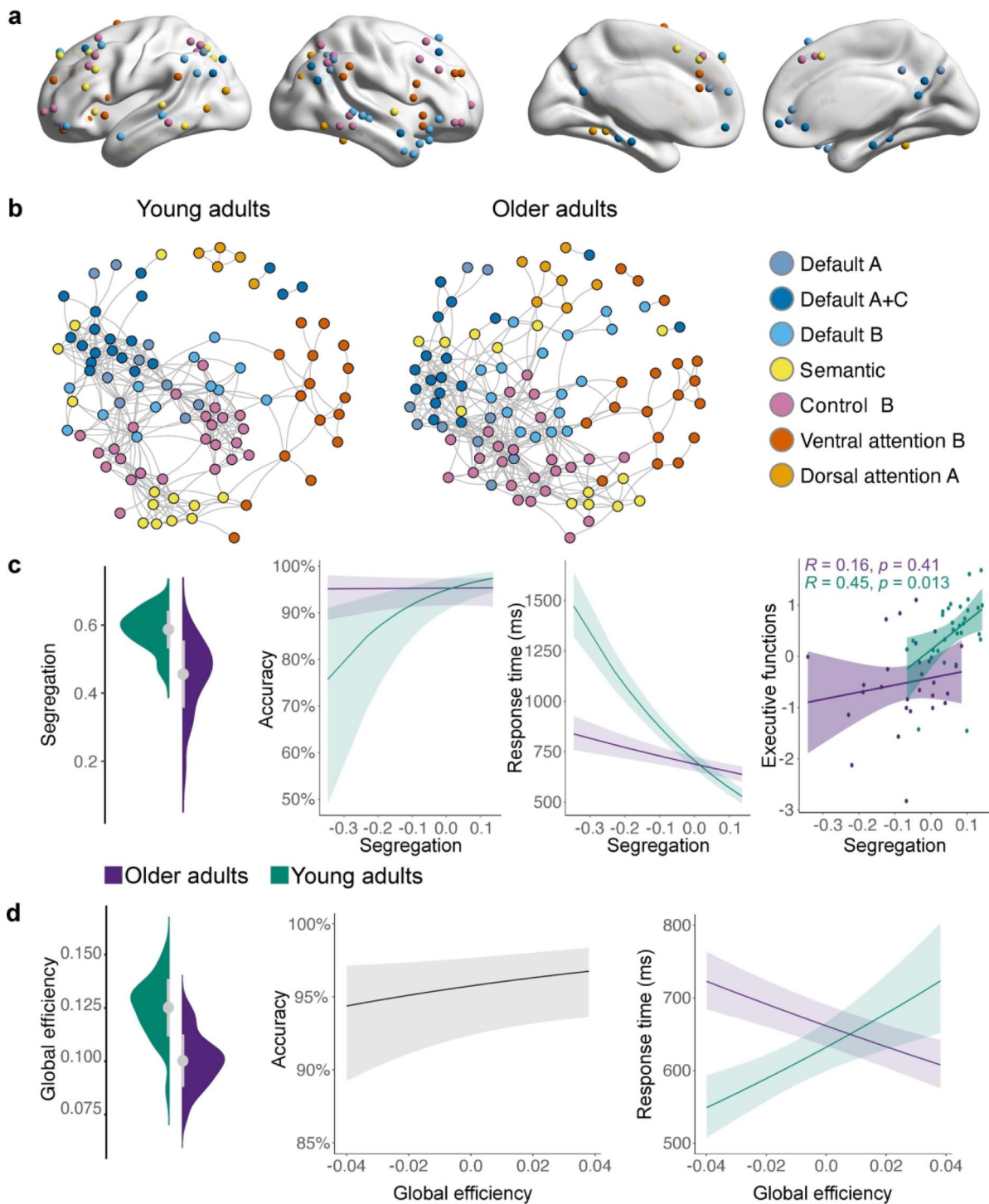
In summary, exploring brain system integration and segregation in a semantic task revealed age-specific dynamics where young adults clearly profit from a stronger modular network organization whereas increasing integration improves efficiency only in the aging brain.

Stronger system-wide integration of brain networks in older adults is facilitated by additional connector hubs in frontal and temporal regions
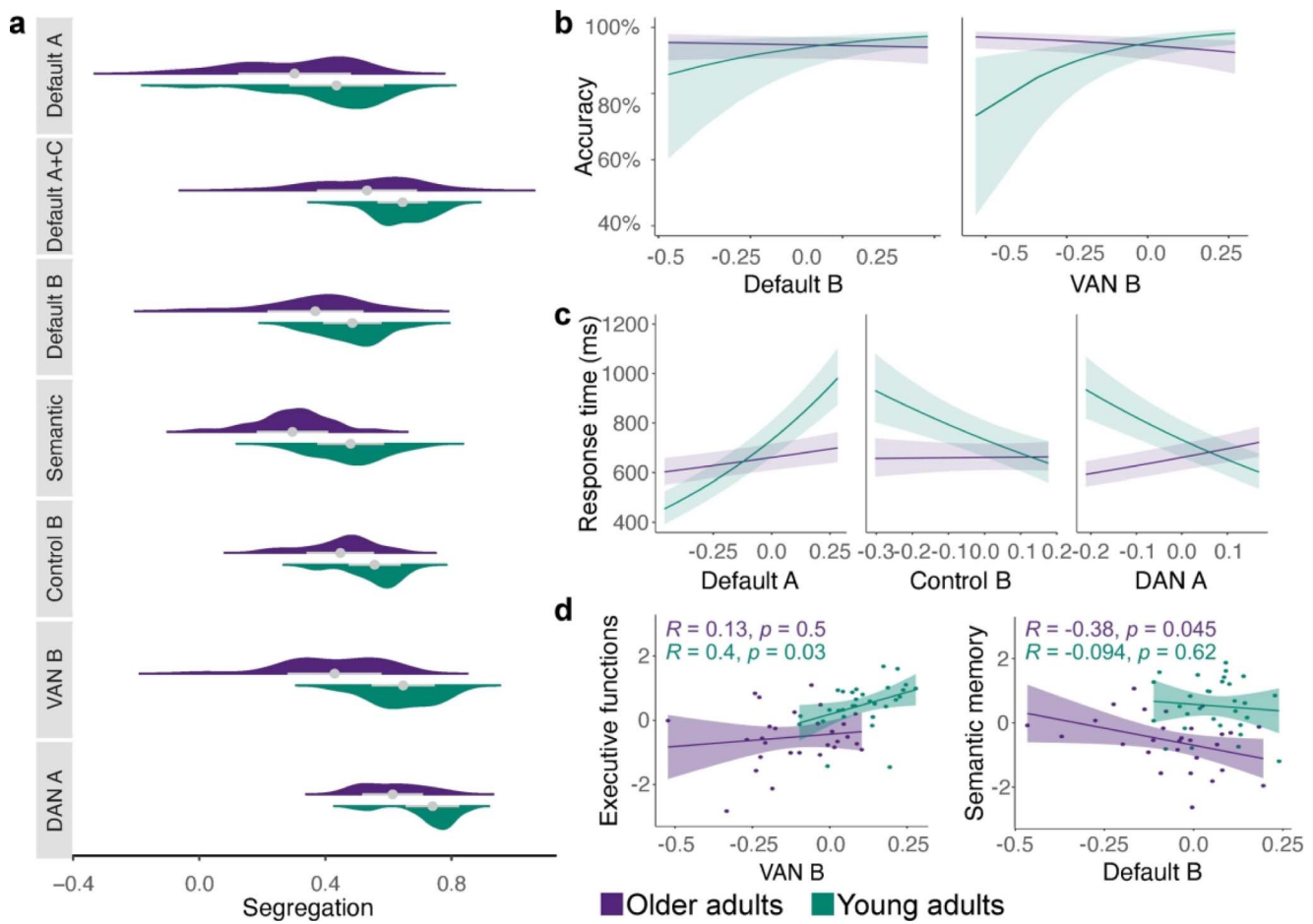
An important characteristic of large-scale brain organization is the presence of regions, or nodes, that play an important role in facilitating communication between communities of a network. These nodes, commonly referred to as connector hubs, are defined by a high number of connections (edges) diversely distributed across communities (Bertolero et al. 2017). Previous work has highlighted their crucial role for integrative processing in resting- and task-state networks (Cohen and D'Esposito 2016). We explored the existence of connector hubs via the normalized participation coefficient (PC; Pedersen et al. 2020). Results revealed connector hubs in bilateral frontal, parietal, and temporal regions in both age groups (Fig. 7a; Supplementary Tables S12 and S13). Notably, there were multiple nodes from the subsystems of the default network and CONT-B identified as connector hubs in the bilateral regions of the inferior parietal lobe and AG. Furthermore, both age groups had connector hubs in the right MTG and MFG. In older adults, additional connector hubs were found in the left SFG, pre-SMA, and frontal pole. A linear model revealed nodes with stronger PC only in the graphs of older adults: in the frontal pole and pre-SMA, which were also identified as connector hubs, STG, and bilateral fusiform gyri (Fig. 7b; Supplementary Table S14).

Discussion

The neural bases of cognitive aging remain poorly understood. It is especially debated how age-related neural reorganization impacts cognition. A better understanding of the neural resources that help to maintain cognitive functions and counteract decline would be mandatory to design efficient treatment and training protocols. In the present study, we approached this unresolved issue by investigating the functional connectome of young and older adults in semantic cognition, a key domain of human cognition largely preserved in healthy aging. Our results demonstrate a reconfigured network architecture with age even when word retrieval abilities remain intact. Overall, networks showed increased integration of task-negative and task-positive networks with age, which manifested as increased coupling between functional connectivity networks, reduced segregation of global brain systems, and a larger number of connector hubs in brain graphs

Fig. 5. Age-related differences in whole-brain segregation and integration and their behavioral relevance. a) For each participant, a task-related brain network graph was constructed using 121 nodes. The nodes were based on significant global and local peak maxima of the 7 networks derived from the ICA (see Supplementary Table S3 for exact locations of nodes). b) Spring-embedded graphs depicting age differences in the modular organization of the brain. Graphs are based on average connectivity in each age group. Stronger segregation is reflected by higher within- and lower between-network correlations. In comparison, young adults show stronger segregation than older adults for most networks. For visualization purposes, graphs are displayed at 5% graph density. c) Brain-wide system segregation was higher for young adults and had distinct effects on behavior for each age group with young adults profiting from increasing segregation. d) A different picture emerged for global efficiency. Global efficiency was calculated for individual orthogonal minimum spanning trees (OMST), which were based on weighted correlation matrices. The graphs of young adults showed stronger global efficiency than older adults. While increasing global efficiency was associated with better performance in both age groups, it predicted slower performance in young and faster performance in older adults. Note that segregation and global efficiency values were mean-centered for analyses with behavior.
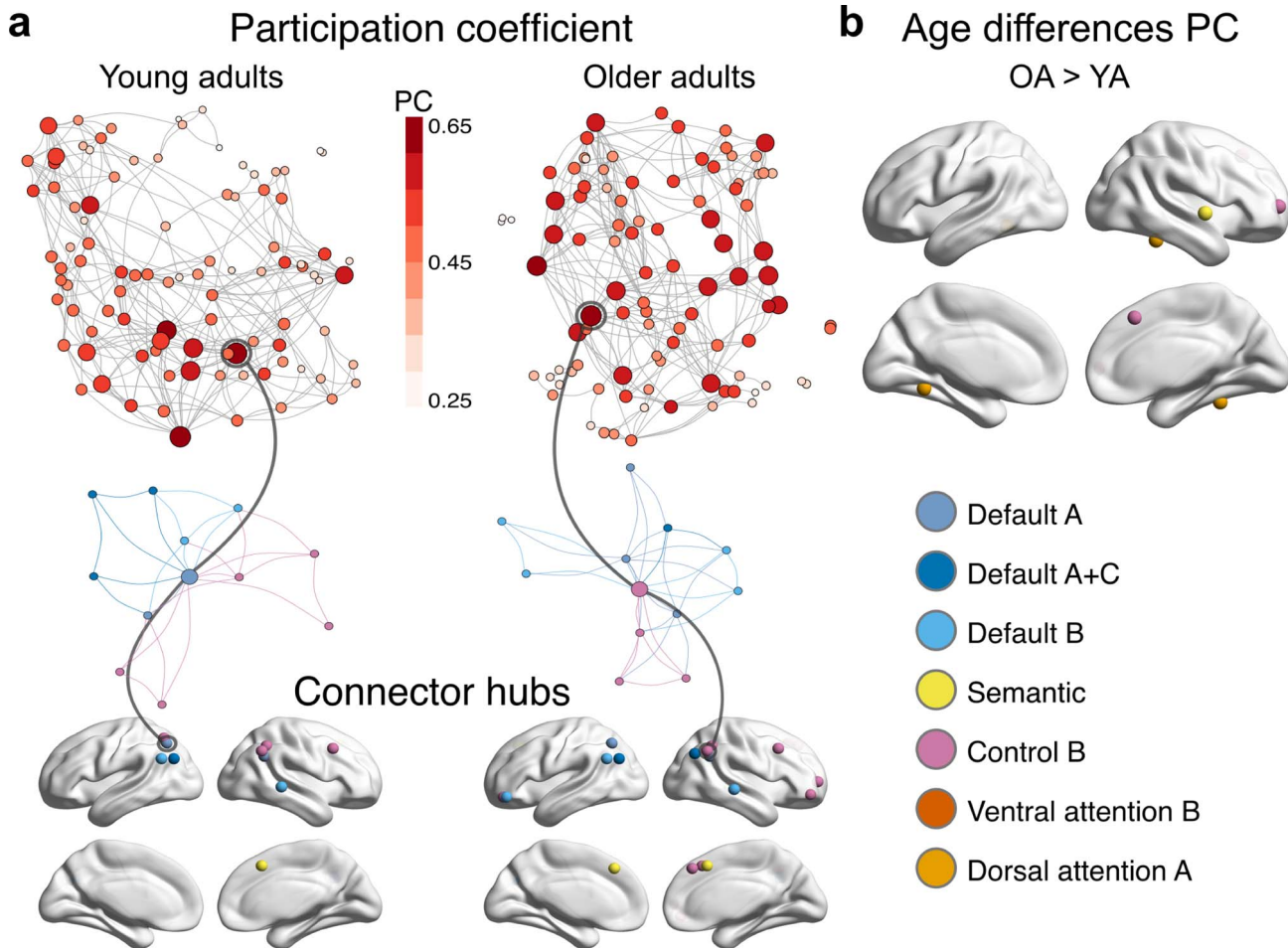
Fig. 6. Segregation of individual networks is associated with distinct behavior of older and young adults as a function of system type. a) Individual networks' segregation values by age. All networks showed stronger segregation in young adults. b) Generalized linear mixed-effects models for accuracy revealed significant interactions with age and network segregation for 2 systems, whereas c) linear mixed-effects models for response time showed significant interactions for 3 networks. For most networks, increasing segregation was associated with better and faster performance in young adults and worse and slower reactions in older adults. d) Significant correlations between network segregation and neuropsychological measures. For young adults, we detected a positive correlation of increasing segregation of VAN-B with executive functions, whereas for older adults, a negative correlation of increasing segregation of DMN-B with semantic memory was found. Note that segregation and global efficiency values were mean-centered for analyses with behavior. VAN, ventral attention network; DAN, dorsal attention network.

of older adults. Associating these network profiles with behavior revealed intact, albeit less efficient, performance for more integrated systems in older adults. These findings shed new light on the frequently reported pattern of declining brain system segregation with age and its impact on cognition (Chan et al. 2014; Geerligs et al. 2014). Our results indicate a compensatory role of increased brain system integration but also reveal its limitations in terms of economical processing.

Using task-based fMRI data and group spatial ICA, we characterized 7 higher-order large-scale functional networks relevant to semantic word retrieval. These included default, semantic, frontoparietal control, and attention networks. Notably, our analysis detected 2 networks associated with semantic processing: a network component that showed strong activity in frontal regions that have been attributed to semantic control processes (Jackson 2021) and another component overlapping with the subnetwork DMN-B (Yeo et al. 2011), which has been proposed to facilitate access to semantic knowledge (Smallwood et al. 2021). Thus, these 2 semantic sub-networks appear to represent complementary aspects of semantic cognition. Moreover, in line with our previous work (Martin et al. 2022), we detected default and cognitive control systems, lending support to the notion that networks that have

been characterized as anticorrelated during resting-state become functionally integrated for successful task processing when controlled access to semantic memory is required (Krieger-Redwood et al. 2016). Indeed, exploring task-based functional connectivity showed strong positive coupling between distinct cognitive networks in both age groups. Two subnetworks of the default network, DMN-A and DMN-B, were strongly coupled with the frontoparietal control network within each group. This finding agrees with accumulating evidence that the default network integrates with control and executive resources during goal-directed task processing (Krieger-Redwood et al. 2016), especially when complex behavior is supported by knowledge (Wang et al. 2021), and thus enables flexible cognition (Smallwood et al. 2021).

Examining age-related differences in network coupling revealed additional integration of distinct networks with age. Older adults showed stronger positive coupling of SEM, CONT-B, and DAN-A with VAN-B relative to young adults, suggesting an increased cognitive demand during semantic processing. In contrast, networks of young adults displayed stronger decoupling of default with attention and semantic control networks. Previous work indicates that young adults can benefit from a more integrated brain organization in situations of high task demand to

Fig. 7. Topology of network hubs in young and older adults. a) The normalized participation coefficient (PC) was calculated for individual orthogonal minimum spanning trees (OMST). Graphs display the PC of each node for the average OMST in each age group (top). For visualization purposes, the strongest 5% of connections are shown. Stronger PC values are reflected by color and node size. The higher the PC, the more a node is connected with nodes from other communities. The node with the highest PC value in each age group is extracted and displayed with its neighboring nodes colored by community (middle). Note that these connector hubs are connected to many different communities. Connector hubs were defined in each age group via PC values at least 1SD above the mean. In both groups, connector hubs were detected in frontal, parietal, and temporal regions (bottom). b) A linear model with age as predictor revealed nodes with stronger PC only in older adults. The top and middle graphs were plotted using the ForceAtlas2 algorithm. The force-directed layout causes nodes of the same community to cluster together and diversely connected hubs (connector hubs) to appear in the center of the graph.

facilitate information flow across components (Vatansever et al. 2015; Cohen and D'Esposito 2016; Zhang et al. 2020). Our results transfer this observation to the aging brain and demonstrate increased crosstalk between networks with age. Importantly, when we associated the differences in network coupling with behavior, we found that enhanced coupling of different cognitive systems like default and attention networks was associated with consistently high but less efficient performance in older adults. Consistent with results from different cognitive domains (Gallen et al. 2016; Adnan et al. 2019; Crowell et al. 2020; Deng et al. 2021), we demonstrate that enhanced network integration with age is linked to high accuracy but at the cost of efficiency. Although such reorganization helps older adults to maintain cognitive flexibility, it might not be the most efficient form of wiring.

Our findings are also in line with the recently proposed default-executive coupling hypothesis of aging (DECHA; Turner and Spreng 2015; Spreng and Turner 2019). According to DECHA, the age-related increase in the coupling of default and executive networks parallels the decline of cognitive control functions. Older adults rely more on their greater or preserved semantic

knowledge, which, depending on the cognitive demands of a task or situation, helps to maintain stable performance or might even lead to a performance advantage (Spreng and Turner 2019). Here, we show that in a semantic word retrieval task with a high cognitive control demand, older adults show indeed increased coupling of default and executive networks. Although this enhanced coupling helps older adults to maintain stable performance, it leads to less efficient processing. This finding further supports the notion that the flexibility in the goal-directed coupling of executive and default resources decreases with age (Spreng and Turner 2019).

We applied graph theory to further explore age-accompanied changes in the network architecture. Our results revealed global decreases in segregation and efficiency with age. The reduction of segregation in older adults is in line with previous work from resting-state (Chan et al. 2014; Sala-Llonch et al. 2014; Geerligs et al. 2015) and task-based studies (Geerligs et al. 2014; Gallen et al. 2016; Crowell et al. 2020), as well as longitudinal investigations (Betzel et al. 2014; Cao et al. 2014; Chong et al. 2019), and suggests that aging is associated with a reduced ability for specialized

processing within highly connected clusters (Rubinov and Sporns 2010). This was confirmed by our results on segregation of each individual network where young adults generally showed stronger segregation.

In terms of global efficiency, most studies reported lower global efficiency in older adults (Sala-Llonch et al. 2014; Chong et al. 2019; Gonzalez-Burgos et al. 2021), although others have also reported no changes or even increases with age (Cao et al. 2014; Chan et al. 2014; Song et al. 2014; Geerligs et al. 2015). These discrepancies might stem from methodological considerations such as the number of nodes in a brain graph since global efficiency is based on the length of its edges (Zalesky et al. 2010) or different thresholding methods of connectivity matrices like the commonly applied proportional thresholding, which has been shown to introduce spurious correlations and inflate group-related differences in graph metrics (van den Heuvel et al. 2017). To avoid these pitfalls, our calculation of global efficiency was based on the recently developed OMST (Dimitriadis et al. 2017), a data-driven approach of individualized graph construction with high reliability (Jiang et al. 2021; Luppi and Stamatakis 2021).

Reduced global efficiency implies higher wiring cost and a less efficient information flow among distributed networks of the global brain system (Bullmore and Sporns 2012). This is especially relevant for the processing of complex cognitive functions like semantic word retrieval, which require the integration of distinct networks, as revealed by our functional connectivity analyses. At the neurobiological level, these changes have been associated with reduced functional connectivity of long-range connections in older adults (Sala-Llonch et al. 2014). Thus, even though functional networks become more integrated with age, potentially due to stronger activation of more but less specialized nodes, the efficient information transfer between networks is impaired leading to slower processing in aging. This observation may represent an overall decline of cognitive attention systems in the aging brain, reflected in slower responses with similar task accuracy, which was already evident at the behavioral level in our data.

Additional evidence for this interpretation stems from the larger number of connector hubs in older adults. In the young brain, an increase of connector hubs has been linked to enhanced task demands to facilitate integration across different networks and enable better task performance (Bertolero et al. 2018; Zhang et al. 2020). Resting-state studies in healthy aging also reported more connector hubs, indicating a reduced distinctiveness of network-specific nodes (Geerligs et al. 2015; Chan et al. 2017; Chong et al. 2019). Our work confirms these findings during task processing and allows an interpretation in light of the semantic nature of our task. Nodes with a higher participation coefficient in older adults were located in frontal and temporal regions and associated with CONT-B, DAN-A, and SEM networks. This result underlines the enhanced cognitive demand during semantic word retrieval with age and provides a mechanistic explanation for the frequently reported pattern of over-activation of prefrontal control regions during demanding task processing in older adults (Davis et al. 2008). A reduced selectivity in activation of network nodes and hence an over-recruitment of less specialized brain regions leads to a decline in efficient neural processing between brain regions, and this process might form the basis of neural dedifferentiation in aging (Chan et al. 2017; Chong et al. 2019). Its effect on cognition, aberrant, or compensatory, depends on the neurocognitive requirements of a task.

Exploring the topology of task-relevant neural networks as a function of cognitive performance allowed us to directly link observed age-related differences with behavior. Results showed that young adults strongly capitalized on a more segregated system during task processing in the form of faster and better performance. In contrast, increasing whole-brain segregation predicted faster but not better performance in older adults, whereas increasing global efficiency predicted better performance across groups but faster responses only in older adults. These findings have important implications for current theories on the behavioral impact of network reorganization in aging. Although a less selective and more integrated network organization might not be the most efficient system in terms of processing speed, it enables older adults to maintain high performance. However, stronger integration does not automatically imply a more efficient system as evident by a generally reduced global efficiency in brain graphs of older adults and a predicted faster response in a more efficient system. Our findings lend support to a compensatory mechanism of age-accompanied reconfiguration in network topologies. Importantly, they also reveal the limitations of such compensatory reorganization processes and demonstrate that a youth-like network architecture in terms of balanced integration and segregation is associated with more economical processing.

Acknowledgments

Supplementary material

Supplementary material is available at *Cerebral Cortex* online.

Funding

References

Adnan A, Beaty R, Silvia P, Spreng RN, Turner GR. Creative aging: functional brain networks associated with divergent thinking in older and younger adults. *Neurobiol Aging*. 2019:75: 150–158.

Aquino KM, Fulcher BD, Parkes L, Sabaroedin K, Fornito A. Identifying and removing widespread signal deflections from fMRI data: rethinking the global signal regression problem. *NeuroImage*. 2020:212:116614.

Ashburner J. A fast diffeomorphic image registration algorithm. *NeuroImage*. 2007:38(1):95–113.

Bassett DS, Bullmore ET, Meyer-Lindenberg A, Apud JA, Weinberger DR, Coppola R. Cognitive fitness of cost-efficient brain functional networks. *Proc Natl Acad Sci*. 2009:106(28): 11747–11752.

Bates D, Mächler M, Bolker B, Walker S. Fitting linear mixed-effects models using lme4. *J Stat Softw*. 2015:67(1):1–48.

Beck AT, Steer RA, Ball R, Ranieri W. Comparison of Beck depression inventories -IA and -II in psychiatric outpatients. *J Pers Assess*. 1996:67(3):588–597.

Ben-Shachar M, Lüdecke D, Makowski D. Effectsize: estimation of effect size indices and standardized parameters. *J Open Source Softw*. 2020:5(56):2815.

Bertolero MA, Yeo BTT, D'Esposito M. The diverse club. *Nat Commun*. 2017:8(1):1277.

Bertolero MA, Yeo BTT, Bassett DS, D'Esposito M. A mechanistic model of connector hubs, modularity and cognition. *Nat Hum Behav*. 2018:2(10):765–777.

Betzel RF, Byrge L, He Y, Goñi J, Zuo X-N, Sporns O. Changes in structural and functional connectivity among resting-state networks across the human lifespan. *NeuroImage*. 2014:102:345–357.

Brett M, Anton J-L, Valabregue R, Poline J-B. Region of interest analysis using an SPM toolbox. [abstract]. Presented at the 8th International Conference on Functional Mapping of the Human Brain, June 2–6, 2002, Sendai, Japan. *NeuroImage*. 2002:16.

Bullmore E, Sporns O. The economy of brain network organization. *Nat Rev Neurosci*. 2012:13(5):336–349.

Burke DM, Shafto MA. Aging and language production. *Curr Dir Psychol Sci*. 2004:13(1):21–24.

Calhoun VD, Adali T, Pearlson GD, Pekar JJ. A method for making group inferences from functional MRI data using independent component analysis. *Hum Brain Mapp*. 2001:14(3):140–151.

Cao M, Wang J-H, Dai Z-J, Cao X-Y, Jiang L-L, Fan F-M, Song X-W, Xia M-R, Shu N, Dong Q, et al. Topological organization of the human brain functional connectome across the lifespan. *Dev Cogn Neurosci*. 2014:7:76–93.

Chan MY, Park DC, Savalia NK, Petersen SE, Wig GS. Decreased segregation of brain systems across the healthy adult lifespan. *Proc Natl Acad Sci*. 2014:111(46):E4997–E5006.

Chan MY, Alhazmi FH, Park DC, Savalia NK, Wig GS. Resting-state network topology differentiates task signals across the adult life span. *J Neurosci*. 2017:37(10):2734–2745.

Chan MY, Han L, Carreno CA, Zhang Z, Rodriguez RM, LaRose M, Hassenstab J, Wig GS. Long-term prognosis and educational determinants of brain network decline in older adult individuals. *Nat Aging*. 2021:1(11):1053–1067.

Chong JSX, Ng KK, Tandi J, Wang C, Poh J-H, Lo JC, Chee MWL, Zhou JH. Longitudinal changes in the cerebral cortex functional organization of healthy elderly. *J Neurosci*. 2019:39(28):5534–5550.

Ciric R, Wolf DH, Power JD, Roalf DR, Baum GL, Ruparel K, Shinohara RT, Elliott MA, Eickhoff SB, Davatzikos C, et al. Benchmarking of participant-level confound regression strategies for the control of motion artifact in studies of functional connectivity. *NeuroImage*. 2017:154:174–187.

Cohen JR, D'Esposito M. The segregation and integration of distinct brain networks and their relationship to cognition. *J Neurosci*. 2016:36(48):12083–12094.

Crowell CA, Davis SW, Beynel L, Deng L, Lakhlani D, Hilbig SA, Palmer H, Brito A, Peterchev AV, Luber B, et al. Older adults benefit from more widespread brain network integration during working memory. *NeuroImage*. 2020:218:116959.

Csardi G, Nepusz T. The igraph software package for complex network research. *Int J Compl Syst*. 2006:1695.

Davis SW, Dennis NA, Daselaar SM, Fleck MS, Cabeza R. Que PASA? The posterior-anterior shift in aging. *Cereb Cortex*. 2008:18(5): 1201–1209.

Deng L, Stanley ML, Monge ZA, Wing EA, Geib BR, Davis SW, Cabeza R. Age-related compensatory reconfiguration of PFC connections during episodic memory retrieval. *Cereb Cortex*. 2021:31(2): 717–730.

Dimitriadis SI, Salis C, Tarnanas I, Linden DE. Topological filtering of dynamic functional brain networks unfolds informative chronnectomics: a novel data-driven thresholding scheme based on orthogonal minimal spanning trees (OMSTs). *Front Neuroinform*. 2017:11. https://doi.org/10.3389/fninf.2017.00028.

Esteban O, Markiewicz CJ, Blair RW, Moodie CA, Isik AI, Erramuzpe A, Kent JD, Goncalves M, DuPre E, Snyder M, et al. fMRIPrep: a robust preprocessing pipeline for functional MRI. *Nat Methods*. 2019:16(1):111–116.

Ferré P, Jarret J, Brambati SM, Bellec P, Joanette Y. Task-induced functional connectivity of picture naming in healthy aging: the impacts of age and task complexity. *Neurobiol Lang (Camb)*. 2020:1(2):161–184.

Folstein MF, Folstein SE, McHugh PR. "Mini-mental state": a practical method for grading the cognitive state of patients for the clinician. *J Psychiatr Res*. 1975:12(3):189–198.

Fornito A, Harrison BJ, Zalesky A, Simons JS. Competitive and cooperative dynamics of large-scale brain functional networks supporting recollection. *Proc Natl Acad Sci*. 2012:109(31):12788–12793.

Fornito A, Zalesky A, Bullmore ET. *Fundamentals of brain network analysis*. Amsterdam; Boston: Elsevier/Academic Press; 2016.

Gallen CL, Turner GR, Adnan A, D'Esposito M. Reconfiguration of brain network architecture to support executive control in aging. *Neurobiol Aging*. 2016:44:42–52.

Geerligs L, Maurits NM, Renken RJ, Lorist MM. Reduced specificity of functional connectivity in the aging brain during task performance. *Hum Brain Mapp*. 2014:35(1):319–330.

Geerligs L, Renken RJ, Saliasi E, Maurits NM, Lorist MM. A brain-wide study of age-related changes in functional connectivity. *Cereb Cortex*. 2015:25(7):1987–1999.

Gonzalez-Burgos L, Pereira JB, Mohanty R, Barroso J, Westman E, Ferreira D. Cortical networks underpinning compensation of verbal fluency in normal aging. *Cereb Cortex*. 2021:31:3832–3845.

Gordon J, Young M, Garcia C. Why do older adults have difficulty with semantic fluency? *Aging Neuropsychol Cogn*. 2018:25(6): 803–828.

Gordon EM, Laumann TO, Marek S, Raut RV, Gratton C, Newbold DJ, Greene DJ, Coalson RS, Snyder AZ, Schlaggar BL, et al. Default-mode network streams for coupling to language and control systems. *Proc Natl Acad Sci*. 2020:117(29):17308–17319.

Gorgolewski K, Burns C, Madison C, Clark D, Halchenko Y, Waskom M, Ghosh S. Nipype: a flexible, lightweight and extensible neuroimaging data processing framework in python. *Front Neuroinform*. 2011:5:13.

Griffanti L, Salimi-Khorshidi G, Beckmann CF, Auerbach EJ, Douaud G, Sexton CE, Zsoldos E, Ebmeier KP, Filippini N, Mackay CE, et al. ICA-based artefact and accelerated fMRI acquisition for improved resting state network imaging. *NeuroImage*. 2014:95: 232–247.

Gu Z, Gu L, Eils R, Schlesner M, Brors B. Circlize implements and enhances circular visualization in R. *Bioinforma Oxf Engl*. 2014:30(19):2811–2812.

Guimerà R, Nunes Amaral LA. Functional cartography of complex metabolic networks. *Nature*. 2005:433(7028):895–900.

Halai AD, Welbourne SR, Embleton K, Parkes LM. A comparison of dual gradient-echo and spin-echo fMRI of the inferior temporal lobe. *Hum Brain Mapp*. 2014:35(8):4118–4128.

Hallquist MN, Hwang K, Luna B. The nuisance of nuisance regression: spectral misspecification in a common approach to resting-state fMRI preprocessing reintroduces noise and obscures functional connectivity. *NeuroImage*. 2013:82:208–225.

Hedden T, Gabrieli JDE. Insights into the ageing mind: a view from cognitive neuroscience. *Nat Rev Neurosci*. 2004:5(2):87–96.

Jaccard P. The distribution of the flora in the alpine zone. *New Phytol*. 1912:11(2):37–50.

Jackson RL. The neural correlates of semantic control revisited. *NeuroImage*. 2021:224:117444.

Jackson RL, Cloutman LL, Lambon Ralph MA. Exploring distinct default mode and semantic networks using a systematic ICA approach. *Cortex*. 2019:113:279–297.

Jenkinson M, Bannister P, Brady M, Smith S. Improved optimization for the robust and accurate linear registration and motion correction of brain images. *NeuroImage*. 2002:17(2):825–841.

Jiang C, Betzel R, He Y, Wang Y-S, Xing X-X, Zuo X-N. Toward reliable network neuroscience for mapping individual differences. 2021.

Krieger-Redwood K, Jefferies E, Karapanagiotidis T, Seymour R, Nunes A, Ang JWA, Majernikova V, Mollo G, Smallwood J. Down but not out in posterior cingulate cortex: deactivation yet functional coupling with prefrontal cortex during demanding semantic cognition. *NeuroImage*. 2016:141:366–377.

Lambon Ralph MA, Jefferies E, Patterson K, Rogers TT. The neural and computational bases of semantic cognition. *Nat Rev Neurosci*. 2017:18(1):42–55.

Latora V, Marchiori M. Efficient behavior of small-world networks. *Phys Rev Lett*. 2001:87(19):198701.

Lenth R. *Emmeans: estimated marginal means, aka least-squares means*; 2020. R package version 1.4.8

Lindquist MA, Geuter S, Wager TD, Caffo BS. Modular preprocessing pipelines can reintroduce artifacts into fMRI data. *Hum Brain Mapp*. 2019:40(8):2358–2376.

Lüdecke D. Ggeffects: tidy data frames of marginal effects from regression models. *J Open Source Softw*. 2018:3(26):772.

Lüdecke D, Ben-Shachar M, Patil I, Makowski D. Extracting, computing and exploring the parameters of statistical models using R. *J Open Source Softw*. 2020:5(53):2445.

Luppi AI, Stamatakis EA. Combining network topology and information theory to construct representative brain networks. *Netw Neurosci*. 2021:5(1):96–124.

Marsolais Y, Perlbarg V, Benali H, Joanette Y. Age-related changes in functional network connectivity associated with high levels of verbal fluency performance. *Cortex*. 2014:58:123–138.

Martin S, Saur D, Hartwigsen G. Age-dependent contribution of domain-general networks to semantic cognition. *Cereb Cortex*. 2022:32(4):870–890.

Mascali D, Moraschi M, DiNuzzo M, Tommasin S, Fratini M, Gili T, Wise RG, Mangia S, Macaluso E, Giove F. Evaluation of denoising strategies for task-based functional connectivity: equalizing residual motion artifacts between rest and cognitively demanding tasks. *Hum Brain Mapp*. 2021:42(6): 1805–1828.

Michael AM, Evans E, Moore GJ. Influence of group on individual subject maps in SPM voxel based morphometry. *Front Neurosci*. 2016:10:522. https://doi.org/10.3389/fnins.2016.00522.

Murphy K, Fox MD. Towards a consensus regarding global signal regression for resting state functional connectivity MRI. *NeuroImage*. 2017:154:169–173.

Ng KK, Lo JC, Lim JKW, Chee MWL, Zhou J. Reduced functional segregation between the default mode network and the executive control network in healthy older adults: a longitudinal study. *NeuroImage*. 2016:133:321–330.

Parkes L, Fulcher B, Yücel M, Fornito A. An evaluation of the efficacy, reliability, and sensitivity of motion correction strategies for resting-state functional MRI. *NeuroImage*. 2018:171:415–436.

Pedersen M, Omidvarnia A, Shine JM, Jackson GD, Zalesky A. Reducing the influence of intramodular connectivity in participation coefficient. *Netw Neurosci*. 2020:4(2):416–431.

Poser BA, Versluis MJ, Hoogduin JM, Norris DG. BOLD contrast sensitivity enhancement and artifact reduction with multiecho EPI: parallel-acquired inhomogeneity-desensitized fMRI. *Magn Reson Med*. 2006:55(6):1227–1235.

Power JD, Plitt M, Gotts SJ, Kundu P, Voon V, Bandettini PA, Martin A. Ridding fMRI data of motion-related influences: removal of signals with distinct spatial and physical bases in multiecho data. *Proc Natl Acad Sci*. 2018:115(9):E2105–E2114.

R Core Team. *R: a language and environment for statistical computing*; 2021.

Rubinov M, Sporns O. Complex network measures of brain connectivity: uses and interpretations. *NeuroImage*. 2010:52:1059–1069.

Sala-Llonch R, Junqué C, Arenaza-Urquijo EM, Vidal-Piñeiro D, Valls-Pedret C, Palacios EM, Domènech S, Salvà A, Bargalló N, Bartrés-Faz D. Changes in whole-brain functional networks and memory performance in aging. *Neurobiol Aging*. 2014:35(10):2193–2202.

Setton R, Mwilambwe-Tshilobo L, Girn M, Lockrow AW, Baracchini G, Hughes C, Lowe AJ, Cassidy BN, Li J, Luh W-M, et al. Age differences in the functional architecture of the human brain. *Cereb Cortex*. 2022:bhac056. https://doi.org/10.1093/cercor/bhac056.

Siegel JS, Power JD, Dubis JW, Vogel AC, Church JA, Schlaggar BL, Petersen SE. Statistical improvements in functional magnetic resonance imaging analyses produced by censoring high-motion data points. *Hum Brain Mapp*. 2014:35(5):1981–1996.

Smallwood J, Bernhardt BC, Leech R, Bzdok D, Jefferies E, Margulies DS. The default mode network in cognition: a topographical perspective. *Nat Rev Neurosci*. 2021:22(8):503–513.

Song J, Birn RM, Boly M, Meier TB, Nair VA, Meyerand ME, Prabhakaran V. Age-related reorganizational changes in modularity and functional connectivity of human brain networks. *Brain Connect*. 2014:4(9):662–676.

Spreng RN, Turner GR. The shifting architecture of cognition and brain function in older adulthood. *Perspect Psychol Sci*. 2019:14(4): 523–542.

Spreng RN, Stevens WD, Viviano JD, Schacter DL. Attenuated anticorrelation between the default and dorsal attention networks with aging: evidence from task and rest. *Neurobiol Aging*. 2016:45: 149–160.

Stumme J, Jockwitz C, Hoffstaedter F, Amunts K, Caspers S. Functional network reorganization in older adults: graph-theoretical analyses of age, cognition and sex. *NeuroImage*. 2020:214:116756.

Tavares V, Prata D, Ferreira HA. Comparing SPM12 and CAT12 segmentation pipelines: a brain tissue volume-based age and Alzheimer's disease study. *J Neurosci Methods*. 2020:334:108565.

Turner GR, Spreng RN. Prefrontal engagement and reduced default network suppression co-occur and are dynamically coupled in older adults: the default–executive coupling hypothesis of aging. *J Cogn Neurosci*. 2015:27(12):2462–2476.

Vatansever D, Menon DK, Manktelow AE, Sahakian BJ, Stamatakis EA. Default mode dynamics for global functional integration. *J Neurosci*. 2015:35(46):15254–15262.

van den Heuvel MP, de Lange SC, Zalesky A, Seguin C, Yeo BTT, Schmidt R. Proportional thresholding in resting-state fMRI functional connectivity networks and consequences for patient-control connectome studies: issues and recommendations. *NeuroImage*. 2017:152:437–449.

Verhaeghen P, Borchelt M, Smith J. Relation between cardiovascular and metabolic disease and cognition in very old age: cross-sectional and longitudinal findings from the berlin aging study. *Health Psychol*. 2003:22(6):559–569.

Wang J-H, Zuo X-N, Gohel S, Milham MP, Biswal BB, He Y. Graph theoretical analysis of functional brain networks: test-retest evaluation on short- and long-term resting-state functional MRI data. *PLoS One*. 2011:6(7):e21976.

Wang X, Gao Z, Smallwood J, Jefferies E. Both default and multiple-demand regions represent semantic goal information. *J Neurosci*. 2021:41(16):3679–3691.

Wickham H. Data analysis. In: *Ggplot2. Elegant graphics for data analysis, use R!* Cham: Springer International Publishing; 2016

Wig GS. Segregated systems of human brain networks. *Trends Cogn Sci*. 2017:21(12):981–996.

Yeo BT, Krienen FM, Sepulcre J, Sabuncu MR, Lashkari D, Hollinshead M, Roffman JL, Smoller JW, Zöllei L, Polimeni JR, et al. The organization of the human cerebral cortex estimated by intrinsic functional connectivity. *J Neurophysiol*. 2011:106(3): 1125–1165.

Zalesky A, Fornito A, Bullmore ET. Network-based statistic: identifying differences in brain networks. *NeuroImage*. 2010:53(4): 1197–1207.

Zhang W, Tang F, Zhou X, Li H. Dynamic reconfiguration of functional topology in human brain networks: from resting to task states. *Neural Plast*. 2020:2020:8837615–8837613.

4 Facilitatory Stimulation of the Pre-SMA in Healthy Aging has Distinct Effects on Task-Based Activity and Connectivity

Study 3

The following study explored the potential of modulating neural and behavioral correlates of semantic processing via transcranial magnetic stimulation in healthy older adults. It has been published as preprint on *bioRxiv* and has been submitted for publication to *eLife*.

Facilitatory stimulation of the pre-SMA in healthy aging has distinct effects on task-based activity and connectivity

Sandra Martin[1,2] ✉, **Regine Frieling**[1], **Dorothee Saur**[2], and **Gesa Hartwigsen**[1]

[1]Lise Meitner Research Group Cognition and Plasticity, Max Planck Institute for Human Cognitive and Brain Sciences, Leipzig, Germany; [2]Language & Aphasia Laboratory, Department of Neurology, University of Leipzig Medical Center, Leipzig, Germany

Semantic cognition is central to communication and our understanding of the world. It is usually well preserved in healthy aging. However, semantic control processes, which guide semantic access and retrieval, decline with age. The present study explored the potential of intermittent theta burst stimulation (iTBS) to enhance semantic cognition in healthy middle-aged to older adults. Using an individualized stimulation approach, we applied iTBS to the pre-supplementary motor area (pre-SMA) and assessed task-specific effects on semantic judgments in functional neuroimaging. We found increased activation after effective relative to sham stimulation only for the semantic task in visual and dorsal attention networks. Further, iTBS increased functional connectivity in domain-general executive networks. Notably, stimulation-induced changes in activation and connectivity related differently to behavior: While increased activation of the parietal dorsal attention network was linked to poorer semantic performance, its enhanced coupling with the pre-SMA was associated with more efficient semantic processing. Our findings indicate differential effects of iTBS on activity and connectivity. We show that iTBS modulates networks in a task-dependent manner and generates remote network effects. Stimulating the pre-SMA was linked to more efficient but not better performance, indicating a role in domain-general semantic control processes distinct to domain-specific semantic control.

Word count:

Abstract: 199 words
Main text: 4993 words

Introduction

Aging is accompanied by a myriad of cognitive changes. While the decline of executive functions, such as working memory, attention, and inhibitory control, and episodic memory are hallmarks of cognitive aging (Hedden and Gabrieli, 2004), functions that rely on the acquired knowledge about the world (semantic memory), such as language and creativity, usually remain well preserved and are affected by more subtle changes in healthy aging, for example increasing word retrieval problems (Henderson and Wright, 2016; Verhaeghen, 2003; Burke and Shafto, 2004). Moreover, increasing age has been associated with difficulties in language comprehension on the sentence and discourse level when processing becomes cognitively demanding, for instance through length, complexity, or ambiguity (Goral et al., 2011; Kemper et al., 2004; Obler et al., 1991). In light of the intact semantic knowledge system in healthy older adults, these changes have been attributed to declining cognitive control functions, which contribute to successful semantic processing when, for example, ambiguities need to be resolved or irrelevant information needs to be inhibited (DeDe and Knilans, 2016). In line with this notion, a recent study demonstrated an age-related decline of semantic selection processes, such as inhibiting irrelevant semantic associations, but not semantic representation and retrieval abilities (Hoffman, 2018). Notably, semantic selection was strongly correlated with non-semantic executive functions, underlining the role of domain-general cognitive control in semantic processing.

On the neural level, semantic cognition activates a mainly left-lateralized, widespread neural network in young adults, including frontal, temporal, and parietal regions (Binder et al., 2009; Jackson, 2021; Noonan et al., 2013). This network is thought to consist of distinct, yet interacting elements: a subnetwork for semantic representation and a subnetwork for semantic control (Lambon Ralph et al., 2017). Importantly, semantic control might be multidimensional as well, consisting of domain-specific semantic control, which subserves processes such as the controlled retrieval of less salient conceptual features, and domain-general control, which supports general selection and inhibition mechanisms (Hoffman, 2018). This notion is supported by the observation that brain regions that are active in tasks with high semantic control demands partially overlap with areas of the multiple-demand network (MDN), which refers to a set of frontoparietal brain regions involved in top-down cognitive control across domains (Duncan, 2010; Fedorenko et al., 2013).

In the aging brain, semantic cognition is characterized by a shift of the functional network architecture, which is reflected by increased activity of the MDN (for a review, see Hoffman and Morcom, 2018) and greater functional connectivity between domain-general networks such as the default mode network (DMN) and dorsal and ventral attention networks during semantic processing (Martin et al., 2022). This shift has also been described as reduced specialization of "core" processing areas of a task and increased neural dedifferentiation (Grady, 2012; Park et al., 2004). The behavioral relevance of these neural changes remains a point of debate. While the best preservation of cognitive functions has been associated with a youth-like pattern (Cabeza et al., 2018; Grady, 2012; Spreng et al., 2010), some changes might represent unsuccessful or attempted compensation (Hoffman and Morcom, 2018) whereas other reorganization processes have been linked to preserved, albeit less efficient semantic processing (Martin et al., 2022).

Non-invasive brain stimulation (NIBS) techniques are recognized as a promising approach to counteract age-related cognitive decline and to promote successful aging. Similar to the use of NIBS to boost neuropsychological rehabilitation after disruption of function due to stroke, these techniques might have the potential to support preservation of cognitive functions in pathological but also healthy aging through modulation of cortical excitability and the enhancement of neuroplasticity (Hartwigsen, 2018, 2015; Siebner et al., 2009). While there are some first promising results from different cognitive domains (for reviews, see Booth et al., 2022; Goldthorpe et al., 2020; Hsu et al., 2015), particularly when NIBS is coupled with training interventions, variability remains high and some studies find no beneficial effect of stimulation (e.g., Antonenko et al., 2022). Further insight into the potential of NIBS in aging can be gained by investigating the effect of stimulation on neural activity and functional connectivity. Neuroimaging results can help interpreting behavioral effects and might even be observed in the absence of a stimulation-induced behavioral change (Abellaneda-Pérez et al., 2022). In the domain of semantic cognition, only a few studies explored the effect of electrical stimulation at the neural level. These studies associated improved performance with a reduction of age-related upregulation in activity (Holland et al., 2011; Meinzer et al., 2013) and increases in functional connectivity between task-relevant regions of interest in the prefrontal cortex (Holland et al., 2016). So far, no study explored the potential of transcranial magnetic stimulation (TMS) to modulate age-related changes in semantic cognition on the behavioral and neural level.

Some studies investigated the potential of patterned repetitive transcranial magnetic stimulation to enhance performance in different cognitive tasks in healthy young brains (for a review, see Demeter, 2016). These studies report improved task performance after intermittent theta burst stimulation (iTBS; Huang et al., 2005). Fewer studies explored the modulatory effects of TBS on cognition in aging brains (Debarnot et al., 2015; Legon et al., 2016; Vidal-Piñeiro et al., 2014; Hermiller et al., 2022). The results of these studies are heterogeneous, and only one study found improved memory performance after iTBS (Debarnot et al., 2015), whereas others revealed changes in task-related activity and connectivity only (Vidal-Piñeiro et al., 2014) or non-specific effects of inhibitory stimulation (Hermiller et al., 2022). A better understanding of the modulatory effects of TBS at the neural level may help to increase the efficiency of network stimulation in aging brains. Moreover, such network approaches may be more powerful than conventional modulatory applications that target specific brain regions within specialized networks (e.g., Hartwigsen and Volz, 2021).
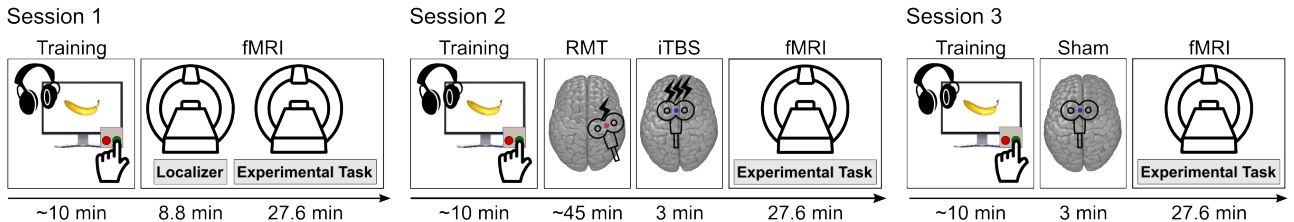
The goal of the present study was to explore the potential of iTBS to enhance semantic cognition in healthy middle-aged to older adults. We applied effective and sham iTBS to the pre-supplementary motor area (pre-SMA) and subsequently assessed the effect of stimulation using task-based functional magnetic resonance imaging (fMRI). The pre-SMA was selected as target area since it has been associated with the semantic control network and the domain-general MDN (Fedorenko et al., 2013; Jackson, 2021) emphasizing its role in mediating cognitive control across domains. Moreover, the pre-SMA contributes more to semantic processing in older relative to young adults (Martin et al., 2022) and represents a hub region in task-related functional networks of older adults, facilitating integrative processing (Martin et al., 2022). Using a semantic judgment task with varying cognitive demands and a tone judgment task as non-verbal control task, we hypothesized that iTBS might show stronger effects on the more demanding semantic condition. Further, comparing the effects of the tone with the semantic judgment task, allowed us disentangling task-specific effects of iTBS from general effects on control processes. Finally, we aimed to elucidate how stimulation-induced changes in task-related activity and functional connectivity relate to behavioral modulation.
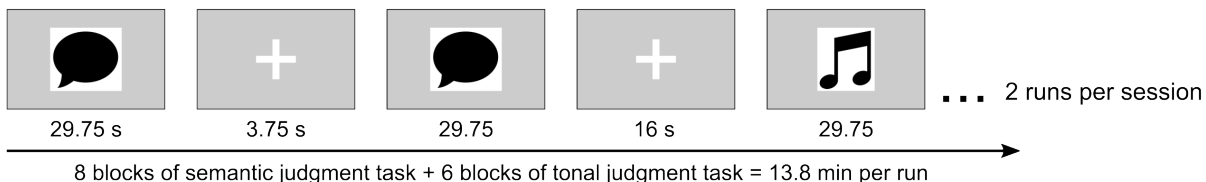
Results

We implemented a single-blind, cross-over study design with three task-based functional magnetic resonance imaging (fMRI) sessions per participant (14 female; M = 61.6, SD = 7.64, range: 45–74 years; Figure 1A). During each session, participants completed a semantic judgment task and a tone judgment task (Figure 1B & C). Using the fMRI data from the first session, we applied an individualized stimulation approach where the stimulation coordinates of each participant were based on activation patterns within a pre-defined mask of the pre-supplementary motor area (pre-SMA; Ruan et al., 2018). During the second and third session, partici-
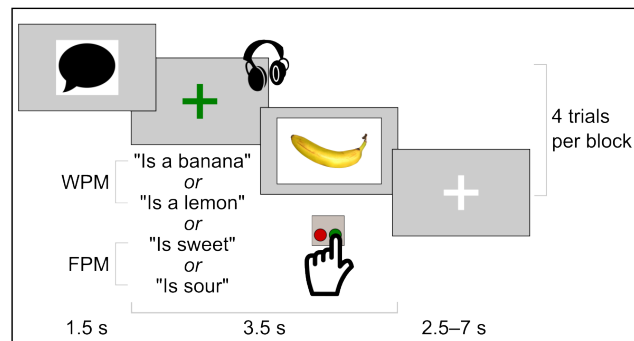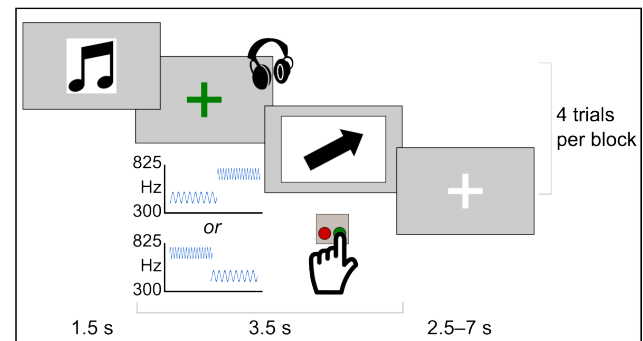
Figure 1. Experimental Design. (A) Participants completed three sessions: a baseline fMRI session and two iTBS + fMRI sessions with effective and sham stimulation. (B) Per fMRI session, two task runs were completed. Blocks of the semantic judgment and the tone judgment task were interspersed with rest blocks. (C) Example trials for the semantic and the tone judgment task are shown. Participants heard a short phrase or a sequence of two tones. At the offset of the auditory stimulus, a picture of an object or an arrow appeared. Participants indicated via button press whether auditory and visual stimuli matched. RMT: resting motor threshold, WPM: word-picture matching, FPM: feature-picture matching.
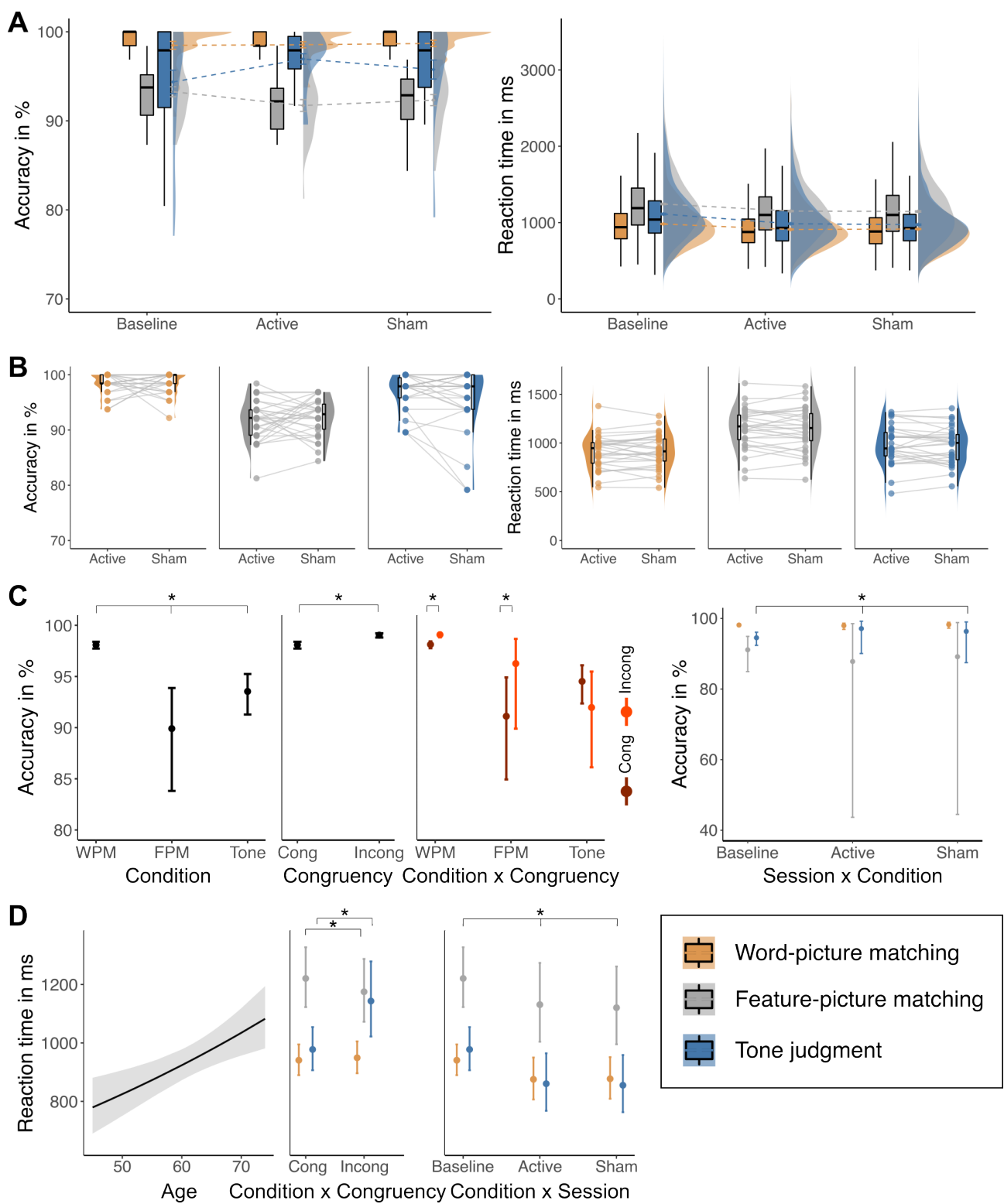
pants then received once effective and once sham iTBS over the pre-SMA prior to fMRI (Figure 1A).

Behavioral results

We were interested in potential effects of iTBS on behavioral performance (Figure 2A and B). To this end, we fitted mixed-effects models for accuracy and reaction time data of the in-scanner tasks of word-picture, feature-picture, and tone-picture matching. For accuracy, the three-way interaction between session, condition, and congruency was not significant (x^2 = 7.83, p = 0.099). However, we detected a significant interaction between condition and congruency (x^2 = 53.15, p < 0.001) and session and condition (x^2 = 21.8, p < 0.001; Figure 2C). Post-hoc tests showed that incongruent items had higher accuracy in all conditions. However, the difference between congruent and incongruent items was only significant for word-picture matching (WPM; OR = 0.38, p < 0.001) and feature-picture matching (FPM; OR = 0.31, p < 0.001). For session

and condition, post-hoc tests showed a significant difference in accuracy only for the tone judgment task, such that participants performed generally better after the baseline session (active iTBS > baseline: OR = 0.41, p < 0.001; sham iTBS > baseline: OR = 0.57, p = 0.002). Moreover, we found main effects of condition (x^2 = 279.34, p < 0.001) and congruency (x^2 = 77.32, p < 0.001) but not of session (x^2 = 2.79, p = 0.25). Post-hoc tests revealed generally better performance for word-picture than feature-picture matching (OR = 5.77, p < 0.001) and the tone-picture matching condition (OR = 3.55, p < 0.001; Figure 2C). For congruency, accuracy was higher for incongruent than congruent items (OR = 0.5, p < 0.001).

For reaction time, results showed a significant interaction of session with condition (x^2 = 44.4, p < 0.001; Figure 2D). Post-hoc tests revealed that reaction times improved for all three conditions after the baseline session (all p < 0.01). However, there was no difference in reaction time between effective and sham iTBS ses-

Figure 2. Behavioral results. (A) Results for accuracy and reaction time for each condition at each session. Boxplots show median and 1.5 x interquartile ranges. Half-violin plots display distribution and dotted lines show changes of mean values across sessions. (B) Individual data for effect of stimulation sessions on accuracy and reaction time for each condition. (C) and (D) display significant results of mixed-effects regression for accuracy and reaction time. Cong: congruent items, Incong: incongruent items.

sions. Results also showed a significant interaction between condition and congruency (x^2 = 306.53, $p <$ 0.001). Post-hoc comparisons revealed that for FPM, incongruent items were faster (p = 0.034), while for tone-picture matching, congruent items were faster (p < 0.001). Further, we found a significant effect of age on reaction time with reaction times generally increasing with age (x^2 = 9.4, p = 0.002). Full results of both models are shown in Table S4.

Univariate functional MRI data

The effect of conditions at baseline

For the semantic judgment task, we found a large left-lateralized fronto-temporo-parieto-occipital network with additional activation in the right hemisphere (Figure 3A; Table S5). An additional cluster spanned the pre-SMA. The control task of tone judgment revealed a bilateral network with clusters in frontal, temporal, parietal, and occipital regions (Figure 3A; Table S5). We were interested in the difference in brain activation between the semantic judgment and the tone judgment task. The contrast semantic judgment > tone judgment activated a mainly left-lateralized fronto-temporal network for semantic processing encompassing left inferior frontal gyrus, left anterior, middle, and superior temporal gyri, and bilateral fusiform gyri (Figure 3B; Table S5). Further, precuneus, superior frontal gyrus, and frontal pole were activated. The opposite contrast, tone judgment > semantic judgment, activated a mainly right-lateralized network including the right frontal pole, middle frontal gyrus, precuneus, and the right angular gyrus. Moreover, we found small clusters in left superior frontal gyrus and left inferior frontal lobe (Figure 3B; Table S5).

We also investigated the effect of semantic processing demand by comparing both conditions within the semantic judgment task with each other. For WPM, stronger activation in bilateral superior temporal gyri was detected when compared with FPM (Table S5). For the opposite contrast, FPM > WPM, results showed stronger activity in a left-lateralized network including inferior frontal gyrus, middle temporal gyrus, inferior parietal lobe, and superior frontal gyrus with supplementary motor area.

iTBS increases task-specific activity for semantic judgments in distributed networks

To explore the effect of iTBS and potential interactions with conditions, we contrasted effective and sham stimulation sessions. Results only revealed stronger activation after effective compared with sham sessions and only for the semantic judgment task. For semantic judgment > rest, we found stronger activation in the right posterior angular gyrus, superior temporal gyrus, middle occipital gyrus, and a cluster in left superior parietal lobe (SPL) and bilateral cuneus (Figure 4A; Table 1). This was mirrored by effects for the individual conditions of semantic judgment, WPM and FPM. For both

conditions, a cluster spanning left SPL and right cuneus was found (Table 1). Further, for FPM, an additional cluster in right angular gyrus as well as occipital and fusiform gyrus was detected. For the contrast semantic judgment > tone judgment, results showed a significant cluster in bilateral lingual gyri and left middle occipital gyrus (Figure 4B; Table 1).

Increased activity after iTBS is associated with poorer semantic performance
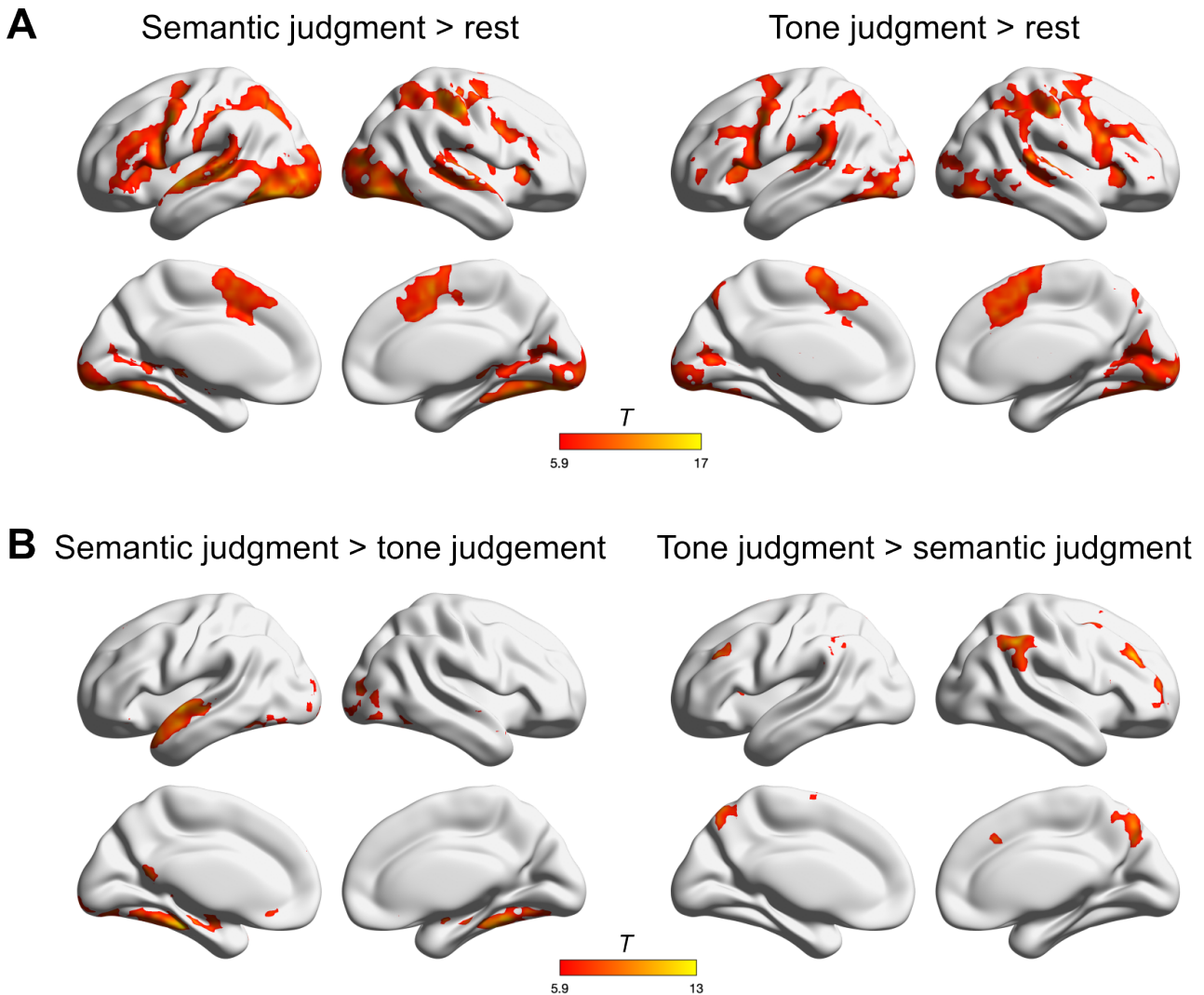
We correlated the difference in percent signal change (PSC; effective > sham iTBS) for the stimulation site pre-SMA and for cluster peaks that showed an effect of stimulation (n = 6; Table 1) with the difference in behavior. For the pre-SMA, we found that accuracy for the tone judgment task was negatively correlated with PSC (r = -0.36, p = 0.05) such that smaller PSC for effective relative to sham iTBS was associated with higher accuracy during the effective relative to the sham session (Figure 4C). Further, results showed a negative correlation for accuracy of the semantic judgment task with a cluster in left dorsal SPL (r = -0.37, p = 0.047; Figure 4D) which had shown stronger activity for semantic judgment > rest after effective relative to sham iTBS. We found that less PSC for effective compared with sham iTBS was associated with higher accuracy for effective relative to sham iTBS. This effect was further specified through the FPM condition which showed the same pattern for the cluster in left ventral SPL (r = -0.37, p = 0.044; Figure 4E). We did not detect any significant correlations for reaction time.

The effect of iTBS on subject-specific functional regions of interest (ROIs) for language processing

We extracted PSC for effective and sham iTBS sessions in the 25 subject-specific functional ROIs that were defined using a group-constrained subject-specific parcellation approach. We were interested in an effect of iTBS on PSC of the different conditions. To this end, we fitted linear mixed-effects models with predictors for session and PSC. We did not find any significant interaction between functional ROIs and session. Supplementary Figures S4-6 show the individual PSC values for both stimulation sessions for each ROI.

Effects of iTBS on functional connectivity (generalized PPIs)

Based on the activation patterns from the comparison of effective and sham iTBS, we conducted generalized psychophysiological interaction (gPPI) analyses for the significant cluster peaks. We asked whether and how effective iTBS generates changes in functional connectivity for these task-specific regions. Moreover, we were interested in a relationship between stimulation-induced changes in functional connectivity and behavior and assessed such associations for the PPI connectivity between the pre-SMA and significant cluster peaks from univariate results.

A Semantic judgment > rest   Tone judgment > rest

T
5.9   17

B Semantic judgment > tone judgement   Tone judgment > semantic judgment

T
5.9   13

Figure 3. Univariate activation results for experimental conditions during baseline session. (A) shows results for each experimental task against rest (implicit baseline) while (B) displays the results when both tasks are contrasted ahainst each other. Results are FWE-corrected at peak level p < 0.05 with a minimal cluster size k = 10 voxels.
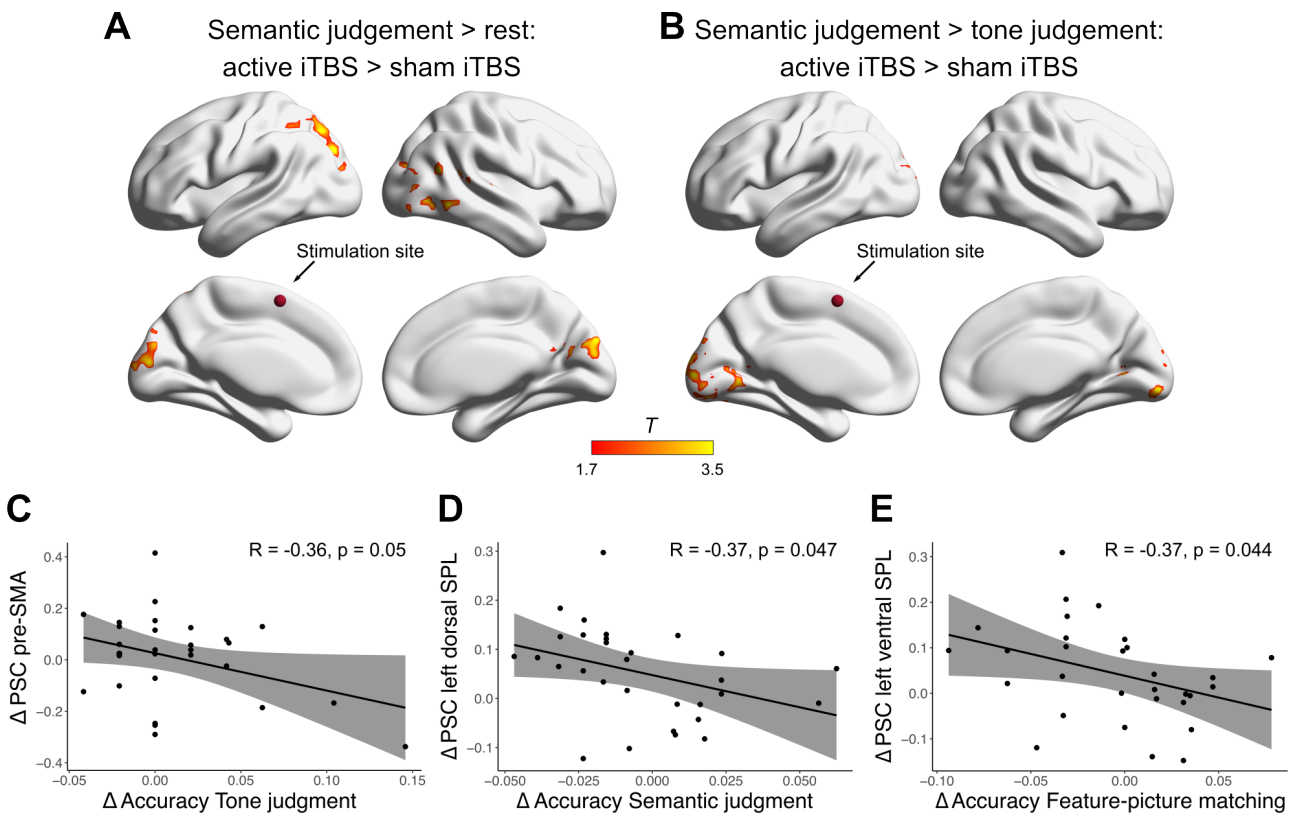
iTBS reduces task-specific connectivity for parietal areas during semantic processing

One-sample t-tests for the difference in functional connectivity between effective and sham stimulation revealed significant changes for three seed regions: the left dorsal and ventral SPL and the right cuneus. For all regions, we found reduced whole-brain connectivity after effective relative to sham iTBS for the contrast semantic judgment > tone judgment (Figure 5A; Table S6). The dorsal SPL showed reduced coupling with a cluster in the left middle frontal gyrus and frontal pole after effective stimulation. For the seed in the more ventral left SPL, we found a similar cluster in the frontal pole, which also extended into the anterior cingulate gyrus. Moreover, the ventral left SPL was negatively coupled with a cluster in the right superior frontal gyrus and pre-SMA, a region in the anterior left SPL, and the left precentral gyrus and superior frontal gyrus. The right cuneus showed greater decoupling with a cluster in the right frontal pole and middle frontal gyrus. To further

explore the interaction effect, we investigated the difference between effective and sham stimulation for the contrasts semantic judgment > rest and tone judgment > rest for the seed regions. Results showed that significant whole-brain decoupling for the cuneus was mainly driven by increased coupling of these regions during the tone judgment task (Figure S7). In the ventral SPL, a cluster in the left frontal pole was related to greater decoupling in the semantic and greater coupling in the control task after effective iTBS, thus dissociating both tasks (Figure S7).

Areas of decreased coupling belong to domain-general networks

We were interested in the representative networks of these stimulation-induced changes in functional connectivity. To this end, we plotted binary maps of the significant gPPI results together with a common seven-networks parcellation based on intrinsic functional connectivity (Yeo et al., 2011). Figure 5B shows the overlap

A Semantic judgement > rest: active iTBS > sham iTBS

B Semantic judgement > tone judgement: active iTBS > sham iTBS

Stimulation site

Stimulation site

T
1.7   3.5

C R = -0.36, p = 0.05

ΔPSC pre-SMA

ΔAccuracy Tone judgment

D R = -0.37, p = 0.047

ΔPSC left dorsal SPL

ΔAccuracy Semantic judgment

E R = -0.37, p = 0.044

ΔPSC left ventral SPL

ΔAccuracy Feature-picture matching

Figure 4. Effect of stimulation on brain activation. After effective stimulation, stronger activation was found for (A) semantic judgment > rest and for (B) semantic judgment > tone judgment. We then extracted percent signal change (PSC) for significant clusters and correlated the difference in PSC between effective and sham sessions with the difference in behavior between effective and sham sessions. (C) For Δ of accuracy of tone judgment, a negative correlation with the difference in PSC in our stimulation site pre-SMA was detected. (D) and (E): For Δ of accuracy of semantic judgment, and more specifically the FPM condition, a negative correlation with the difference in PSC in the left superior parietal lobe (SPL) was detected. fMRI results are thresholded at p < 0.05 at peak level and FWE-corrected at p < 0.05 at cluster level.

Table 1. Significant clusters for effective > sham iTBS

Anatomical structure	Hemisphere	k	t	x	y	z
Word-picture matching >Rest						
Cuneus	R	1387	3.87	9.52	-68.78	21.50
Superior parietal lobe	L		3.78	-22.82	-71.26	54.50
Superior occipital gyrus	R		3.59	21.96	-83.70	18.75
Feature-picture matching >Rest						
Angular gyrus, posterior division	R	672	4.11	54.30	-63.80	18.75
Middle occipital cortex	R		3.94	44.35	-83.70	7.75
Fusiform gyrus	R		3.36	29.42	-68.78	-6.00
Superior parietal lobe	L	763	3.45	-22.82	-71.26	46.25
Cuneus	L		3.43	-7.90	-86.19	40.75
Cuneus	R		3.32	7.03	-86.19	29.75
Semantic judgment >Rest						
Middle occipital gyrus	R	726	4.03	44.35	-81.22	7.75
Angular gyrus, posterior division	R		3.64	54.30	-63.80	18.75
Superior temporal gyrus	R		3.49	54.30	-28.97	5.00
Superior parietal lobe	L	959	3.86	-22.82	-71.26	54.50
Middle occipital gyrus	L		3.53	-25.31	-81.22	32.50
Superior parietal lobe	L		3.50	-22.82	-71.26	46.25
Semantic judgment >Tone judgment						
Lingual gyrus	L	1083	4.04	-17.85	-68.78	2.25
Middle occipital gyrus	L		3.78	-17.85	-91.17	18.75
Lingual gyrus	R		3.55	12.01	-71.26	2.25

Note. Results are thresholded at p < 0.05 at peak level and FWE-corrected at p < 0.05 at cluster level.

of the clusters that showed reduced coupling with the respective networks. Clusters in the frontal pole were associated with the DMN and in the middle frontal gyrus with the fronto-parietal control network. Furthermore, decoupled clusters from the ventral SPL were mainly linked to the ventral attention network, and in pre-central gyrus to the sensorimotor network.

Decreased coupling after iTBS is associated with slower semantic performance under effortful conditions

The change in functional connectivity between pre-SMA and left ventral SPL was associated with a change in behavior after effective stimulation (Figure 6). More specifically, a negative correlation (r = -0.49, p = 0.006) indicated that reactions for the FPM condition were slower the more those two regions were decoupled after effective iTBS.

Discussion

In light of global population aging and the associated increase in age-related diseases, new interventions are needed to counteract cognitive decline and promote successful aging. NIBS is increasingly recognized as a promising tool to boost cognitive functions in older adults. However, to design effective treatment protocols, a better understanding of the neural mechanisms of NIBS is mandatory. In particular, it remains unclear whether NIBS-induced improvements may be underpinned by decreases or increases in task-related activity and connectivity, or both. Here, we explored the effect of effective relative to sham iTBS over the pre-SMA on the behavioral and neural level during a semantic judgment task and a non-verbal control task. In the absence of direct stimulation-induced changes at the behavioral level, we found significant modulation of task-related activity and connectivity. These changes differed in their functional relevance at the behavioral level. Our main results were as follows: iTBS led to higher activation during semantic processing at remote regions in posterior areas (posterior temporal cortex, parietal, and occipital lobe). In contrast, functional connectivity results revealed reduced whole-brain connectivity of these upregulated areas during semantic processing, but increased connectivity for the tone judgment task. Strikingly, TMS-induced changes on activation and functional connectivity had differential effects on behavior. While upregulated regions were associated with poorer semantic performance, increasing connectivity between the stimulation site and a cluster in the dorsal attention network was linked to faster performance in the most demanding semantic condition. Overall, our findings indicate disparate effects of iTBS on activation and connectivity. Further, we show that iTBS modulates networks in a task-dependent manner and generates effects at regions remote to the stimulation site. Finally, our results shed new light on the role of the pre-SMA

in domain-general and semantic control processes, indicating that the pre-SMA supports executive aspects of semantic control.
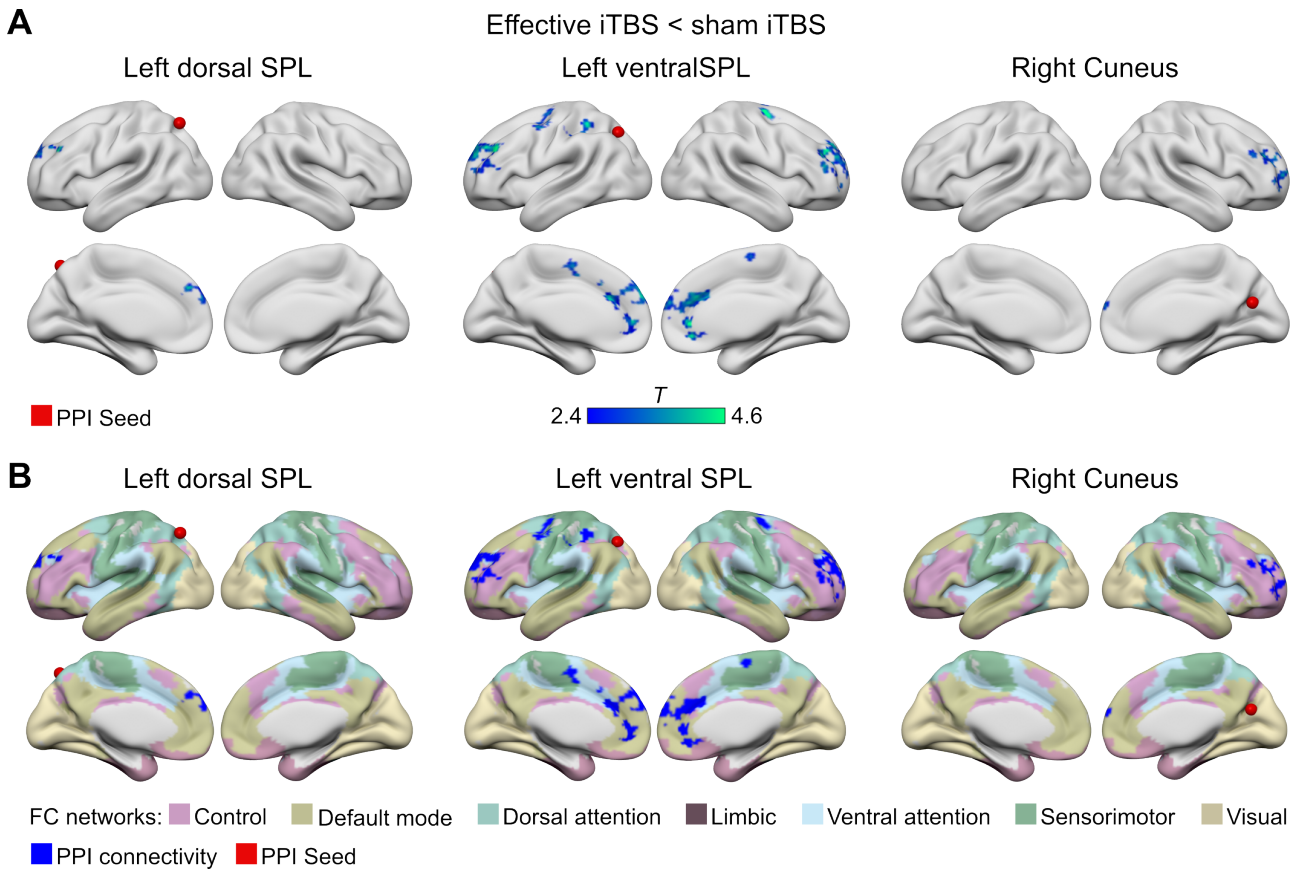
Higher-order cognitive networks for semantic judgment and tone judgment that overlap in the pre-SMA

Our task paradigm revealed two widespread functional networks for semantic judgment and non-verbal tone judgment, which overlapped in sensory-motor systems for auditory, visual and motoric processing. We delineated specific networks by contrasting both tasks with each other. Semantic processing activated a left-lateralized fronto-temporal network, which aligns well with previous investigations and meta-analyses on semantic cognition (Binder et al., 2009; Jackson, 2021; Lambon Ralph et al., 2017). Notably, the network contained core areas of semantic representation, such as the bilateral temporal poles, but also semantic control, including the left inferior frontal gyrus and posterior middle temporal gyrus. Moreover, in contrast to the tone judgment task, semantic processing activated bilateral middle and posterior fusiform gyri. While the anterior fusiform gyrus (anterior temporal lobe) has been recognized as a key area of semantic processing (Chiou et al., 2018; Lambon Ralph et al., 2017; Mion et al., 2010), less work has focused on the role of the middle and posterior fusiform gyrus in semantic cognition. Although famous for the recognition of faces (Kanwisher et al., 1997), objects in general (Grill-Spector, 2003), and visual words (Dehaene and Cohen, 2011), a recent investigation on the spatiotemporal dynamics of semantic processing linked the middle fusiform gyrus to lexical semantics, thus suggesting a role behind early visual processes (Forseth et al., 2018). This notion aligns with our results which showed pronounced bilateral activation of this region compared with the tone judgment task.

Contrasting both conditions of semantic judgment, WPM and FPM, with each other, confirmed the intended modulation of cognitive demand: While WPM showed relative greater activation in left language perception areas, which points to a focus on phonological and lexical processing during this task, FPM activated core regions of semantic but also domain-general control, indicating increased task demand. The tone judgment task, on the other hand, activated a fronto-parietal network, which was based on regions of the frontoparietal control and the dorsal attention network. Notably, all the activated regions during tone judgment also fell within the MDN, confirming the non-verbal, high executive demand of this task.

iTBS does not produce direct behavioral changes at the group level

Although univariate fMRI results from the baseline session demonstrated the contribution of the pre-SMA to the semantic judgment and the non-verbal tone
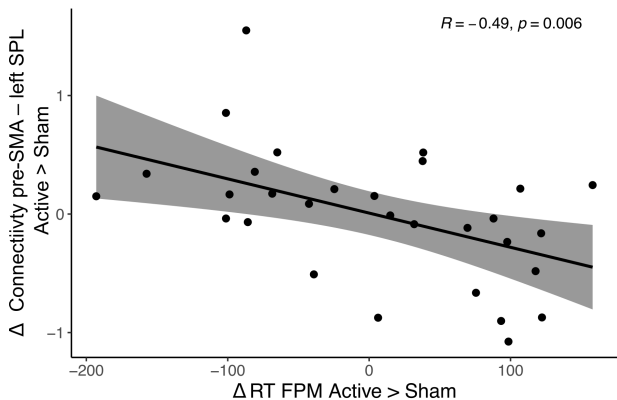
Figure 5. Functional connectivity results for cluster peaks that showed stronger activation after effective iTBS. (A) Three seeds showed stronger decoupling after effective relative to sham stimulation for the contrast semantic judgment > tone judgment. (B) Binary PPI activation maps plotted onto a seven-networks functional connectivity parcellation (Yeo et al., 2011). fMRI results are thresholded at p < 0.01 at peak level and FWE-corrected at p < 0.05 at cluster level.

judgment task, applying effective iTBS to the pre-SMA did not produce behavioral changes relative to the sham session. This result was unexpected. However, we are not the first study to observe stimulation-induced effects on the neural but not behavioral level in healthy older adults (Vidal-Piñeiro et al., 2014). The lack of a behavioral effect might be due to a number of reasons. First, in contrast to most studies, we included a separate baseline session, during which participants practiced and performed the tasks. This led to a notable improvement across all conditions, most strongly in the unfamiliar tone judgment task. Hence, familiarity with the paradigm after the baseline session might have aggravated the chance of observing a stimulation effect. This factor should be considered in future studies as well. Second, the effect of offline stimulation might not have been strong enough to induce behavioral changes. Although we took great care to minimize the time between end of stimulation and begin of task-based fMRI, this might have impeded the observation of a behavioral effect. Third, the applied tasks might have been too easy for our group of participants to observe a facilitatory effect of iTBS. This is the first study to use TBS in healthy aging in the domain of semantic cognition. While previous work successfully applied anodal transcranial direct current stimulation

to the left inferior frontal gyrus and motor cortex to enhance semantic word retrieval in healthy older adults (Holland et al., 2011; Meinzer et al., 2013, 2014), the facilitatory stimulation of an executive control hub that contributes to semantic control processes might not have been critical when task performance is already high. Nonetheless, though unintended, the absence of a stimulation effect on cognition allowed us to interpret alterations on the neural level without the confounds of behavioral changes that might make them harder to interpret otherwise (Blankenburg et al., 2010; Feredoes et al., 2011). Moreover, the behavioral relevance of these changes was demonstrated in the significant correlations between activity or connectivity increases and behavioral modulation.

iTBS over the pre-SMA increases activity in a widespread network of visual processing and cognitive control

Effective iTBS generated greater activity than sham iTBS in posterior regions but not at the stimulation site. This finding was surprising but is in line with the increasingly reported observation that TBS produces remote effects on activation in neural networks (Cárdenas-Morales et al., 2011; Halko et al., 2014; Vidal-Piñeiro

Figure 6. Relationship between stimulation-induced changes in functional connectivity and behavior. Reduced coupling of pre-SMA and left ventral SPL after effective iTBS was associated with slower reaction times (RT) during the feature-picture matching (FPM) condition.

et al., 2014). Notably, stimulation-induced changes in the BOLD signal were task-specific. Specifically, we found that activity only changed when participants were performing the semantic judgment task but not at rest or during the tone judgment task. For semantic judgments compared with the control task, increased activation was observed in the occipital cortex, including bilateral lingual gyri and medial occipital lobe, which indicates a specific role of these regions in the semantic but not the tone judgment task. This notion is supported by emerging evidence from healthy but also patient studies that the occipital cortex, particularly the lingual gyrus, supports language-related and verbal memory tasks (Amedi et al., 2004; Heath et al., 2012; Kim et al., 2011; Palejwala et al., 2021). Thus, the increased activation of these regions mediated by the pre-SMA might suggest a top-down control on visual processing regions in a task-specific manner. Moreover, comparing the semantic judgment task to rest revealed greater activation of clusters in left superior and right inferior parietal lobes apart from clusters in the occipital lobe after effective stimulation. These results were mainly driven by the FPM condition. All cluster peaks fell within the dorsal attention network, which illustrates a functional connection with focused attention, which is likely semantic-specific (Cristescu et al., 2006; Kim et al., 2011; Mahon and Caramazza, 2010).

iTBS decreases functional connectivity within cognitive control networks during semantic processing

We gained further insight into the role of the upregulated regions through functional connectivity analyses. Results showed reduced whole-brain functional connectivity for semantic judgments in dorsal and ventral SPL and the right cuneus after effective iTBS. The seeds in the left SPL showed strongest decoupling with a large prefrontal cluster in the left ventral attention network, while the cuneus was negatively coupled
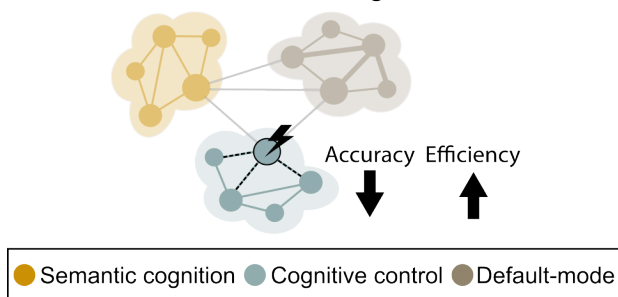
with a prefrontal cluster in the right control network. Moreover, we found reduced connectivity of the ventral SPL with our stimulation site, the pre-SMA, the parietal dorsal attention network, and a cluster in the frontal pole associated with the DMN. Notably, apart from the cluster in the DMN, all cluster peaks fell within regions of the MDN. Moreover, the majority of significant clusters were driven by increased connectivity for the tone judgment task. This finding demonstrates the potential of iTBS to generate task-specific changes in functional network coupling, which is line with previous reports (Halko et al., 2014; Singh et al., 2020; Vidal-Piñeiro et al., 2014). Further, it suggests a TMS-induced modulation of whole-brain functional connectivity in response to executive and attention demands and supports the notion of the pre-SMA as an organizing hub in the MDN, coordinating the interaction of different cognitive control regions (Camilleri et al., 2018).

iTBS-induced changes in activation and functional connectivity relate differently to behavior

Relating TMS-induced changes on activation and functional connectivity with the cognitive performance allowed us to explore the behavioral relevance of these network changes (Figure 7). While it might seem surprising that the increased activation of the parietal dorsal attention network was linked to poorer accuracy in the semantic judgment task, this finding corroborates the notion that the most efficient task processing is associated with little or no additional functional activation apart from task-specific core regions. This is a common observation in neurocognitive aging, where increased activation and reduced deactivation of domain-general regions have been associated with neural inefficiency, leading to poorer performance across a range of cognitive domains (Cabeza et al., 2018; Spreng et al., 2010). Moreover, better and more efficient behavioral performance due to training-induced activation decreases has been reported in healthy participants (Abel et al., 2012; Horner and Henson, 2008) as well as post-stroke chronic aphasia (Abel et al., 2015; Richter et al., 2008). In our study, task performance was high and remained unchanged after iTBS, indicating a stimulation-induced upregulation of remote cognitive control regions that were not necessary for efficient task processing. Though speculative, a different pattern might have emerged through the perturbation of a domain-specific node in the semantic network. A recent study from our group found a partially compensatory upregulation of MDN regions when the domain-specific semantic network was disrupted (Hartwigsen et al., 2017).

Notably, increasing functional connectivity between our stimulation site and the upregulated cluster in the parietal dorsal attention network after iTBS was associated with faster reaction times in the most demanding semantic condition. This result strengthens the idea of a task-specific coupling of cognitive control regions

Facilitatory stimulation of a domain-general hub in semantic cognition

Figure 7. Facilitatory stimulation of a hub of the domain-general multiple-demand network enhanced coupling with other cognitive control networks distal to the stimulation site. This was linked to poorer performance but increased efficiency during semantic processing in a group of middle-aged to older adults.

that have been linked to executive components of semantic processing (Kim et al., 2011; Mahon and Caramazza, 2010) and language processing in general (Geranmayeh et al., 2014; Sliwinska et al., 2017). Here, we demonstrate that such coupling can enhance the processing efficiency when cognitive demands are high but not the cognitive process per se in form of improved accuracy.

In conclusion, our results agree with the proposal of an adaptive recruitment of domain-general resources to support language processing, which, however, are less efficient than the specialized domain-specific network (Hartwigsen, 2018). Moreover, we add a new perspective to the role of the MDN in semantic cognition: Our findings indicate that the pre-SMA supports semantic-specific processes through the upregulation of and coupling with cognitive control regions that have been linked to semantic cognition. Importantly, the pre-SMA did not upregulate or couple with regions of the domain-specific network of semantic control, such as the left inferior frontal gyrus and posterior middle temporal gyrus. Together with our findings of a positive effect of pre-SMA stimulation on task efficiency but not accuracy, we propose a multidimensionality of semantic control on the neural level beyond the inferior prefrontal cortex (Badre et al., 2005; Nagel et al., 2008), consisting of a fronto-temporal domain-specific and a fronto-parietal domain-general semantic control network. Stimulating the pre-SMA with facilitatory TMS modulated domain-general semantic control but had no effect on domain-specific control regions.

Limitations and outlook

It should be noted that we did not find an effect of stimulation on the subject-specific functional ROIs for language processing. Though unexpected, this aligns with our other results, indicating a modulation of domain-general and not language-specific regions through iTBS

over the pre-SMA. A future comparison of modulation of domain-general and domain-specific semantic control hubs could help to fully explore the contribution of both control systems to semantic cognition. Moreover, we cannot rule out the possibility that our results are limited to the aging brain. Although we tested a relatively wide range from middle to older age, future studies should consider a group of young participants for comparison.

Materials and Methods

Participants

A total of 30 healthy middle-aged to older adults (14 female; M = 61.6, SD = 7.64, range: 45–74 years) participated in the experiment. Inclusion criteria were native German speaker, right-handedness, normal hearing, normal or corrected-to-normal vision, no history of neurological or psychiatric conditions, and no contraindication to magnetic resonance imaging or rTMS. Participants were also screened for cognitive impairments using the Mini-Mental State Examination (Folstein et al., 1975; all $\geq$ 26/30 points). Written informed consent was obtained from each participant prior to the experiment. The study was approved by the local ethics committee of the University of Leipzig and conducted in accordance with the Declaration of Helsinki.

Experimental Design

Figure 1 displays the experimental procedure. The study employed a single-blind, cross-over design with three sessions per participant (Figure 1A). Sessions were separated by at least one week (mean inter-session interval: 28.4 days; SD: 51.2) to prevent carry-over effects of TMS. During the first session, participants completed a short training of the experimental task followed by two runs of a language localizer task and two runs of the experimental task. The second and third session each began with a short practice of the task, after which participants were administered effective or sham iTBS over the pre-SMA. Participants then completed two runs of the experimental task. The TMS laboratory was situated close to the MR unit which enabled us to transfer participants rapidly to the MR scanner after stimulation (mean time end of stimulation until beginning of functional scan: 6.6 min). To avoid any interference of movement with the stimulation effect, participants were transferred in an MR-compatible wheelchair. During functional MRI, all stimuli were presented using the software Presentation (version 18.0, Neurobehavioral Systems, Berkeley, USA, www.neurobs.com). Visual stimuli were back-projected onto a mirror mounted on the head coil. Auditory stimuli were played via MR-compatible in-ear headphones (Sensimetrics, Gloucester, USA, http://www.sens.com/). At the beginning of each fMRI session, participants performed a short volume test in the scanner with one intact passage of the language

localizer and background scanner noise to make sure they could understand the stimuli well.

Language Localizer

The language localizer task was adapted from (Scott et al., 2016). In this task, participants listen to intact and acoustically degraded passages from Alice in Wonderland. Materials for the degraded passages as well as the experimental structure were provided by Evelina Fedorenko (`https://evlab.mit.edu/alice`). The intact passages were taken from the freely available German translation of Alice in Wonderland (`https://www.projekt-gutenberg.org/carroll/alice/alice.html`) and were recorded by a professional native German female speaker in a soundproof room. Recordings were then cut using Praat software (version 6.0.56, `https://www.praat.org`) and normalized using Audacity software (version 2.3.2, `https://www.audacityteam.org/`). In total, 24 intact and 24 acoustically degraded passages were prepared. The language localizer task is constructed as a block design. Each run consists of six intact and six degraded passages interspersed with four fixation periods. Listening passages are each 18 s long and fixation periods 12 s long, thus resulting in a total length of 4.4 min per run and 8.8 min of the whole task. Participants were instructed to lie still and quietly listen to the passages. At the beginning, participants performed a short volume test in the scanner with one intact trial and background scanner noise to make sure that they could hear the stimuli well.

Experimental Paradigm

Two tasks were implemented in the fMRI experiment in a mixed design: a semantic judgment task with varying cognitive demand and a non-verbal control task (Figure 1B). In both tasks, participants were required to decide whether an auditory stimulus matches with a presented image via yes/no-button press using the index and middle finger of their left hand. Since the experiment was planned to be also implemented in people with post-stroke aphasia, the left hand was used in all participants to avoid potential confounds through hemiparesis in the aphasia group. Further, this allowed us to shift motor activity related to the button press to the right hemisphere. The order of buttons was counterbalanced across participants. Tasks were presented in mini-blocks of four trials per task and blocks were separated by rest intervals of 3.75 s (2/3 of all intervals) or 16 s (1/3 of all intervals). Individual trials were 3.5 s long including presentation of the auditory stimulus, the object picture, and button press by the participant. Trials within blocks were interspersed with jittered inter-stimulus intervals between 2.5 and 7 s. Each run included 88 stimuli with 32 items per condition of the semantic judgment task and 24 items of the control task resulting in a total length of 13.8 min per run. Participants completed two runs per session.

Semantic judgment task

The semantic judgment task consisted of a word-picture matching (WPM) and a feature-picture matching (FPM) condition, thus varying with respect to the semantic demand of an item (Figure 1C). During both conditions, participants listened to a short phrase (e.g., "Is a banana" or "Is sour") followed by a picture of an object at the offset of the auditory stimulus. They were then asked to judge if the auditory phrase and the presented object match. Stimuli were chosen from eight categories (four living: birds, fruits, mammals, and vegetables; four non-living: clothes, furniture, tools, and vehicles) according to German norm data for semantic typicality (Schröder et al., 2012). From each category, 12 members were selected, 2/3 of them representing typical and 1/3 representing atypical items of the respective category. Hence, in total, 96 stimuli were developed. For each item, a feature from available concept property norms (Devereux et al., 2014) was chosen so that within every category, items could be paired up with regard to their grammatical gender and their feature. In this way, we made sure that every object was introduced with the appropriate gender through the indefinite article both in the congruent and incongruent condition in the auditory stimulus in the WPM condition ("Is a banana" or "Is a lemon"), thus precluding any syntactic clues on accuracy. In German, the indefinite article can take two forms: feminine "eine" and masculine and neutral "ein". Accordingly, items with male and neutral gender could be paired up together and items with female gender were paired up separately. Further, the arrangement in pairs allowed us to balance the occurrence and to control the semantic value of the features. That is, every feature property was once used as congruent and as incongruent. Since item pairs were within categories, we assured that both congruent and incongruent features were semantically associated with the items. Through this approach, we aimed at avoiding any response bias which could be introduced when an incongruent feature has a bigger semantic distance than the congruent feature from the target item. All auditory stimuli were recorded through the same professional native German female speaker as in the language localizer. Recordings were processed in the same way: They were cut using Praat and normalized via Audacity software.

Across categories, items were balanced for lexical frequency of words and lexical frequency of features using the dlexDB database (Heister et al., 2011). There was no significant difference between frequencies of words (M = 10.27, SD = 23.65) and features (M = 13.63, SD = 23.50), $t(185)$ = 0.98, p = .331). Additionally, items were also balanced across categories for length in phonemes, length in syllables, and length in seconds of the audio files of words and features respectively. In comparison, audio files of words (M = 1.24 s, SD = 0.13) were longer than those of features (M = 1.16 s, SD = 0.18), $t(176)$ = 3.81, $p < .001$). We dealt with this difference in the length of audio files by designing

the paradigm in a way that pictures of objects only appeared at the offset of each auditory stimulus, thus not depending the decision-making process on the length of the audio files. Pictures for stimulus items were taken from the freely available Bank of Standardized stimuli (Brodeur et al., 2014, 2010) and the colored picture set by Moreno-Martínez and Montoro (2012) or bought through a license of MPI CBS on Shutterstock. Objects were presented on a white background and all pictures were cropped to a size of 720 x 540 pixels. Stimuli of the semantic judgment task were investigated in a pilot experiment ($n = 50$) beforehand to confirm the intended modulation in task demand and to validate name and feature agreement for each item. Stimuli for the final set were only chosen if they showed at least 80% agreement for the word-picture and the feature-picture matching conditions.

We developed six individual stimuli lists per participant (three sessions with two runs each) such that every item appeared once in every condition across runs and sessions. Conditions and congruency were balanced across runs with pairs of congruent and incongruent stimuli never occurring in the same run. Across participants and runs, accuracy and congruency of individual items were pseudorandomized. After balancing procedures, stimuli lists were randomized.

Tone judgment task

The non-verbal control task consisted of sinewave tones at different frequencies (300–825 Hz), which were presented in a sequence of two tones (Figure 1C). Tones in a sequence always had a difference in frequency of 250 Hz. Individual tones were generated using a pure tone generator in Matlab with the following parameters: sampling frequency of 16000 Hz, duration of 450 ms, and fade-in and fade-out duration of 10 ms each. Afterwards, tones were paired up using Audacity software so that each tone once appeared first and once second in a sequence. An inter-tone interval of 300 ms was included in each sequence. Thus, each tone sequence had a length of 1200 ms which equaled the average length of all verbal stimuli. In the control task, participants heard a tone sequence and were asked to match this with a picture of an arrow pointing diagonally upwards or downwards which appeared at the offset of the auditory stimulus. Like in the semantic judgment task, participants had to indicate their choice via button press. Through this process, we aimed at keeping the task as similar as possible to the semantic judgment task but without any verbal processing involved.

Magnetic Resonance Imaging

MRI data were collected at a 3T Siemens Magnetom Skyra scanner (Siemens, Erlangen, Germany) with a 32-channel head coil. For functional scans, a gradient-echo echo-planar imaging multiband sequence (Feinberg et al., 2010) was used with the following parameters: TR: 2000 ms, TE: 22 ms, flip angle: 80°, voxel size:

2.48 x 2.48 x 2.75 mm with a 0.25 mm interslice gap, FOV: 204 mm, multiband acceleration factor: 3, number of slices per volume: 60 axial slices with interleaved order covering the whole brain. For the language localizer task, 266 volumes were acquired. For the experimental task, a total of 842 volumes per session were acquired. For distortion correction, field maps (pepolar images) were obtained at the end of each session (TR: 8000 ms, TE: 50 ms). Additionally, a high-resolution, T1-weighted 3D volume was obtained from the in-house database if available and not older than two years or was acquired after the functional scans on the first session using an MPRAGE sequence (176 slices, whole-brain coverage, TR: 2300 ms, TE: 2.98 ms, voxel size: 1 x 1 x 1 mm, matrix size: 256 x 240 mm, flip angle: 9°).

Intermittent Theta Burst Stimulation

During the second and third session, participants received once effective and once sham rTMS prior to fMRI (Figure 1A). Session order was counterbalanced across participants. rTMS was delivered using the iTBS stimulation protocol which consists of bursts of three pulses at 50 Hz given every 200 ms in two second trains, repeated every ten seconds over 190 seconds for a total of 600 pulses (Huang et al., 2005). We chose to use TBS since its high-frequency protocols have been reported to induce longer lasting after-effects with a duration of up to one hour (Chung et al., 2016). We used stereotactic neuronavigation (TMS Navigator, Localite, Bonn, Germany) based on coregistered individual T1-weighted images to precisely navigate the coil over the target area and maintain its location and orientation throughout the experiment.

iTBS was applied over the pre-SMA. We used an individualized stimulation approach where the stimulation coordinates of each participant were based on activation patterns within a pre-defined ROI for the experimental task during the first session. To this end, fMRI data from the first session were preprocessed using fMRIPrep 20.2.3 and analyzed using SPM12. A ROI mask of the pre-SMA based on a freely available probabilistic cytoarchitectonic map (Ruan et al., 2018) was created, thresholded at greater 0.3, and binarized. Activation in individuals' subject space for the contrast semantic judgment > rest was then inclusively masked using the resampled pre-SMA ROI. Significant clusters were identified after FWE-correction on peak level at $p < 0.05$. The global peak of the strongest cluster within the pre-SMA ROI was identified as the stimulation target in each participant. Figure S1 displays the individual stimulation sites within the mask. Figure S2 shows the location of individual stimulation sites with respect to two cognitive networks of interest: general semantic cognition (Jackson, 2021) and the multiple-demand network (Fedorenko et al., 2013).

iTBS was applied via a MagPro X100 stimulator (MagVenture, Farum, Denmark) equipped with a passively cooled MCFB65 figure-of-eight coil. For sham

stimulation, we used the corresponding placebo coil (MCF-P-B65), which features the same mechanical outline and acoustic noise as the effective coil but provides an effective field reduction of ~80%. During stimulation, the handle of the coil was pointed in a posterior direction (Allen et al., 2018; Taylor et al., 2007; Willacker et al., 2020). Stimulation intensity was set to 90% of individual resting motor threshold (RMT), which was determined during the second session. RMT was defined as the lowest stimulation intensity producing at least five motor evoked potentials of $\geq$ 50 µV in the relaxed first dorsal interosseous muscle when single-pulse TMS was applied to the right motor cortex ten times. The overall application of TMS pulses per sessions was well within safety limits and the whole procedure was in accordance with the current safety guidelines (Rossi et al., 2009).

Data Analyses

Behavioral data

Accuracy and reaction time data of each session were analyzed using mixed-effects models with a logistic regression for accuracy data due to their binary nature and a linear regression for log-transformed reaction time data. We only analyzed reaction times for correct responses. Contrast coding was done via sum coding where the intercept represents the grand mean across conditions and the model coefficients represent the difference between the mean of the respective condition and the grand mean. Based on the research questions of this study, session (i.e., baseline, effective or sham stimulation) and condition (WPM, FPM or tone judgment) along with their interaction term were always entered as fixed effects. Next, we used stepwise model selection to determine the best-fitting model based on the Akaike Information Criterion (AIC), where a model was considered meaningfully more informative if it decreased the AIC by at least two points (Burnham and Anderson, 2004). The AIC reduces overfitting by considering model complexity and simultaneously penalizing models with more parameters. First, the optimal random effects structure was assessed; next, which factors of congruency, stimulation order, age, and task optimized the models; and finally, interaction terms were evaluated. Table S1 displays the model selection procedure for accuracy data. The optimal model included fixed effects for session, condition, congruency, and age as well as a three-way interaction for session, condition, and congruency, and a random intercept for participants (Equation 1). Table S2 displays the model selection procedure for reaction time data. Here, the optimal model included fixed effects for session, condition, congruency, and age, and interactions between condition and congruency and session and condition. As random effects, the model included by-participant random intercepts and by-participant random slopes for session as well as random intercepts for auditory stimuli (Equation 2). P-values were obtained by likelihood ratio tests

of the full model with the effect in question against the model without the effect in question. Statistical models were performed with R (version 4.1.0; Team, 2021) and the packages lme4 (Bates et al., 2015) for mixed models and bblme (Bolker and Team, 2022) for model comparisons. Plots and result tables were generated using the packages sjPlot (Lüdecke, 2021) and ggeffects (Lüdecke, 2018).

$$
\begin{aligned}
Accuracy = \beta_0 &+ \beta_1 Session + \beta_2 Condition + \\
&\beta_3 Congruency + \beta_4 Age + \\
&\beta_5 Session \times Condition + \\
&\beta_6 Session \times Congruency + \\
&\beta_7 Condition \times Congruency + \\
&\beta_8 Session \times Condition \times Congruency + \\
&(1|Subject) + \varepsilon
\end{aligned}
\tag{1}
$$

$$
\begin{aligned}
\log(Reaction\ time) = \beta_0 &+ \beta_1 Session + \\
\beta_2 Condition &+ \beta_3 Congruency + \beta_4 Age + \\
&\beta_5 Condition \times Congruency + \\
&\beta_6 Session \times Condition + \\
&(1 + Session|Subject) + \\
&(1 + |Auditory\ stimulus) + \varepsilon
\end{aligned}
\tag{2}
$$

Preprocessing of MRI data

Preprocessing of MRI data was performed using fM-RIPrep 20.2.3 (Esteban et al., 2019) which is based on Nipype 1.6.1 (Gorgolewski et al., 2011). Preprocessing steps of functional images included slice-time correction, realignment, distortion correction, co-registration of the T1-weighted and functional EPI images, and normalization. Anatomical images were skull-stripped, segmented, and normalized to standard space. Images were normalized to the MNI152NLin6Asym template. A detailed description of the preprocessing steps is included in Supplementary Materials. After preprocessing, functional data were smoothed with an isotropic 5 mm FWHM Gaussian kernel, and analyzed in SPM12 (Wellcome Trust Centre for Neuroimaging) in Matlab (version R2021a; The MathWorks Inc., Natick, MA).

Whole-brain analyses

Functional MRI data were modelled using the two-step procedure. At the first level, data were entered into individual general linear models (GLM) for each session and participant. For the localizer, the GLM included boxcar regressors convolved with the canonical hemodynamic response function (HRF) for the task blocks of the intact and degraded listening passages. Individual thresholded (gray matter probability > 0.2) gray matter masks were used as explicit masks. For the experimental task, regressors for the three conditions and a separate regressor for error trials were included in the GLM.

Individual trials were modelled as stick functions convolved with the canonical HRF. To account for condition- and trial-specific differences in reaction time, the duration of a trial was defined as the length of the auditory stimulus plus the reaction time. For all tasks, models included regressors of no interest: six motion parameters and individual regressors for strong volume-to-volume movement as indicated by values of framewise displacement > 0.7. Further, temporal and spatial derivatives were modelled for each condition, and a high-pass filter (cutoff 128 s) was applied to remove low-frequency noise. Contrast images were generated by estimating contrasts for each condition against rest and direct contrasts between conditions.

For the experimental task, contrast images were then entered intro group-level random effects models. For the first session, one-sample t-tests were computed to define group activations for the different conditions. To assess differences in activation between effective and sham iTBS, contrast images from the sham session were subtracted from contrast images from the effective session, and the difference images were then submitted to random effects models and session effects were estimated using one-sample t-tests. For all second-level analyses, a gray matter mask was applied, which restricted statistical tests to voxels with a gray matter probability > 0.3 (SPM12 tissue probability map). Results were thresholded at $p < 0.05$ at peak level and corrected at cluster level for the family-wise error (FWE) rate at $p < 0.05$. Anatomical locations were identified with the Harvard-Oxford cortical structural atlases distributed with FSL (`https://fsl.fmrib.ox.ac.uk`).

To assess the relationship between differences in activation and differences in behavior due to iTBS, we extracted PSC for our a-priori defined stimulation site of pre-SMA and for clusters showing a significant effect of stimulation ($n = 6$; see Table 1) using the MarsBar toolbox (version 0.45; Brett et al., 2002). For the pre-SMA, PSC was extracted for a cluster centered at each individual stimulation site and containing the 10% strongest activated voxels for the contrast semantic judgment > rest, which was identical to the contrast used for the definition of the stimulation site. Data were then entered into correlation analyses where the difference in PSC for a certain condition was correlated with the difference in accuracy and reaction time between effective and sham sessions.

Analysis of subject-specific functional regions of interest

Data from the language localizer task were analyzed employing the group-constrained subject-specific approach (Julian et al., 2012). This method allows the identification of individual functional regions of interest (fROIs) sensitive to language processing (Fedorenko et al., 2010), which were then used to characterize response profiles in the independent data set of the experimental task. The definition of fROIs followed the procedure described by (Fedorenko et al., 2010) and

was done using the spm_ss toolbox (Nieto-Castañón and Fedorenko, 2012): First, individual activation maps for our contrast of interest of the localizer task (intact > acoustically degraded speech) were thresholded at a voxel-wise false discovery rate (FDR) of q < 0.05 at whole-brain level (Genovese et al., 2002) and then overlaid on top of each other. The resulting probabilistic overlap map displayed how many participants showed activation at each voxel. Next, the overlap map was smoothed (5 mm), thresholded at 3 participants (10%; cf. Fedorenko et al., 2010), and parcellated using a watershed algorithm (Meyer, 1991). The watershed algorithm resulted in 37 fROIs. Third, only those ROIs from the parcellation were retained where at least 60% of participants had any supra-threshold voxels (cf. Fedorenko et al., 2010; Julian et al., 2012). This led to a final sample of 25 parcels (Figure S3). To confirm that these parcels were indeed relevant to language processing, independent of the task, we entered them in a random-effects group-level analysis using the experimental task data. Results were calculated for the contrast language (i.e., WPM + FPM) > rest and FDR-corrected at q < 0.05. Results showed that all 25 parcels were significantly stronger activated for the language task (Table S3). Finally, subject-specific fROIs were defined as the 10% most active voxels in each participant for the localizer contrast intact > degraded speech within each parcel. Since we were interested in the potential effect of iTBS on differences in activation in the language-specific fROIs, we extracted PSC for each fROI and condition for the experimental task using the MarsBar toolbox (version 0.45; Brett et al., 2002). The data were then entered into a linear model with predictors for stimulation type (effective or sham) and fROI and their interaction term. Post-hoc comparisons were applied using the package emmeans (Lenth, 2020).

Functional connectivity analysis

We were interested in potential changes in functional connectivity induced by iTBS. To this end, we conducted psychophysiological interaction (PPI) analyses using the gPPI toolbox (McLaren et al., 2012). Seed regions were defined for significant global cluster peaks for the contrast of effective and sham session (n = 6, cf. Table 1) and for our stimulation site, bilateral pre-SMA. Binary, resampled masks were created for each seed by building a spherical ROI with a radius of 10 mm in MarsBar. Next, for each participant, individual ROIs were created by extracting the 10% most active voxels in each seed mask of a given contrast image. For the seed masks of pre-SMA, we used the contrast semantic judgment task (i.e., WPM + FPM) > rest, which was the same contrast used to define individual stimulation coordinates.

For the gPPI, individual regression models were set up for each ROI and session containing the deconvolved time series of the first eigenvariate of the BOLD signal from the respective ROI as the physiological vari-

able, regressors for the three task conditions and errors as the psychological variable, and the interaction of both variables as the PPI term. Models were adjusted for an omnibus F-test of all task regressors. Subsequently, first-level GLMs were calculated. We were specifically interested in potential differences between effective and sham iTBS sessions for the contrast semantic judgment > tone judgment. To this end, contrast images from the sham session were subtracted from contrast images from the effective session and the difference images were submitted to random-effects models for group analysis. Significant clusters were determined via one-sample t-tests. A gray matter mask was applied as described for the univariate analyses. Results were thresholded at p <0.01 at peak level and FWE-corrected p <0.05 at cluster level.

We also explored a relationship between stimulation-induced changes in functional connectivity and behavior. To this end, we extracted pre-SMA-to-ROI PPI connectivity for effective and sham sessions for the contrast semantic judgment > tone judgment where ROI refers to the six seed regions described above. We then correlated the difference between effective and sham connectivity for each pre-SMA-ROI pair with the difference between effective and sham in accuracy and reaction time.

Data Availability

All behavioral data as well as extracted beta weights generated or analyzed during this study have been deposited in a public repository on Gitlab `https://gitlab.gwdg.de/mdn-in-aging-and-aphasia/mdn_aph`. This repository also holds all self-written analysis code used for this project. Unthresholded statistical group maps for fMRI and gPPI results are made publicly available on NeuroVault: `https://neurovault.org/collections/13064/`.
Raw and single subject neuroimaging data are protected under the General Data Protection Regulation (EU) and can only be made available from the authors upon reasonable request.

Conflict of Interest

The authors declare that no competing interests exist.

Acknowledgments

Bibliography

Abel, S., Dressel, K., Weiller, C., and Huber, W. Enhancement and suppression in a lexical interference fMRI-paradigm. *Brain and Behavior*, 2(2):109–127, Mar. 2012. doi: 10.1002/brb3.31.

Abel, S., Weiller, C., Huber, W., Willmes, K., and Specht, K. Therapy-induced brain reorganization patterns in aphasia. *Brain*, 138(4):1097–1112, Apr. 2015. doi: 10.1093/brain/awv022.

Abellaneda-Pérez, K., Vaqué-Alcázar, L., Solé-Padullés, C., and Bartrés-Faz, D. Combining non-invasive brain stimulation with functional magnetic resonance imaging to investigate the neural substrates of cognitive aging. *Journal of Neuroscience Research*, 100(5): 1159–1170, 2022. doi: 10.1002/jnr.24514.

Allen, C., Singh, K. D., Verbruggen, F., and Chambers, C. D. Evidence for parallel activation of the pre-supplementary motor area and inferior frontal cortex during response inhibition: A combined MEG and TMS study. *Royal Society Open Science*, 5(2):171369, Feb. 2018. doi: 10.1098/rsos.171369.

Amedi, A., Floel, A., Knecht, S., Zohary, E., and Cohen, L. G. Transcranial magnetic stimulation of the occipital pole interferes with verbal processing in blind subjects. *Nature Neuroscience*, 7(11):1266–1270, Nov. 2004. doi: 10.1038/nn1328.

Antonenko, D., Thams, F., Grittner, U., Uhrich, J., Glöckner, F., Li, S.-C., and Flöel, A. Randomized trial of cognitive training and brain stimulation in non-demented older adults. *Alzheimer's & Dementia (New York, N. Y.)*, 8(1):e12262, 2022. doi: 10.1002/trc2.12262.

Badre, D., Poldrack, R. A., Paré-Blagoev, E. J., Insler, R. Z., and Wagner, A. D. Dissociable Controlled Retrieval and Generalized Selection Mechanisms in Ventrolateral Prefrontal Cortex. *Neuron*, 47(6):907–918, Sept. 2005. doi: 10.1016/j.neuron.2005.07.023.

Bates, D., Mächler, M., Bolker, B., and Walker, S. Fitting linear mixed-effects models using lme4. *Journal of Statistical Software*, 67(1):1–48, 2015. doi: 10.18637/jss.v067.i01.

Binder, J. R., Desai, R. H., Graves, W. W., and Conant, L. L. Where Is the Semantic System? A Critical Review and Meta-Analysis of 120 Functional Neuroimaging Studies. *Cerebral Cortex*, 19(12):2767–2796, Dec. 2009. doi: 10.1093/cercor/bhp055.

Blankenburg, F., Ruff, C. C., Bestmann, S., Bjoertomt, O., Josephs, O., Deichmann, R., and Driver, J. Studying the Role of Human Parietal Cortex in Visuospatial Attention with Concurrent TMS–fMRI. *Cerebral Cortex*, 20(11):2702–2711, Nov. 2010. doi: 10.1093/cercor/bhq015.

Bolker, B. and Team, R. C. Bbmle: Tools for General Maximum Likelihood Estimation, 2022.

Booth, S. J., Taylor, J. R., Brown, L. J. E., and Pobric, G. The effects of transcranial alternating current stimulation on memory performance in healthy adults: A systematic review. *Cortex*, 147:112–139, Feb. 2022. doi: 10.1016/j.cortex.2021.12.001.

Brett, M., Anton, J.-L., Valabregue, R., and Poline, J.-B. Region of Interest Analysis Using an SPM Toolbox. *Neuroimage*, 16, Jan. 2002. doi: 10.1016/S1053-8119(02)90013-3.

Brodeur, M. B., Dionne-Dostie, E., Montreuil, T., and Lepage, M. The Bank of Standardized Stimuli (BOSS), a New Set of 480 Normative Photos of Objects to Be Used as Visual Stimuli in Cognitive Research. *PLOS ONE*, 5(5):e10773, May 2010. doi: 10.1371/journal.pone.0010773.

Brodeur, M. B., Guérard, K., and Bouras, M. Bank of Standardized Stimuli (BOSS) Phase II: 930 New Normative Photos. *PLOS ONE*, 9(9):e106953, Sept. 2014. doi: 10.1371/journal.pone.0106953.

Burke, D. M. and Shafto, M. A. Aging and Language Production. *Current directions in psychological science*, 13(1):21, 2004. doi: 10.1111/j.0963-7214.2004.01301006.x.

Burnham, K. P. and Anderson, D. R. Multimodel Inference: Understanding AIC and BIC in Model Selection. *Sociological Methods & Research*, 33(2):261–304, Nov. 2004. doi: 10.1177/0049124104268644.

Cabeza, R., Albert, M., Belleville, S., Craik, F. I. M., Duarte, A., Grady, C. L., Lindenberger, U., Nyberg, L., Park, D. C., Reuter-Lorenz, P. A., Rugg, M. D., Steffener, J., and Rajah, M. N. Maintenance, reserve and compensation: The cognitive neuroscience of healthy ageing. *Nature Reviews Neuroscience*, 19(11):701–710, Nov. 2018. doi: 10.1038/s41583-018-0068-2.

Camilleri, J., Müller, V., Fox, P., Laird, A., Hoffstaedter, F., Kalenscher, T., and Eickhoff, S. Definition and characterization of an extended multiple-demand network. *NeuroImage*, 165:138–147, Jan. 2018. doi: 10.1016/j.neuroimage.2017.10.020.

Cárdenas-Morales, L., Grön, G., and Kammer, T. Exploring the after-effects of theta burst magnetic stimulation on the human motor cortex: A functional imaging study. *Human Brain Mapping*, 32(11):1948–1960, Nov. 2011. doi: 10.1002/hbm.21160.

Chiou, R., Humphreys, G. F., Jung, J., and Lambon Ralph, M. A. Controlled semantic cognition relies upon dynamic and flexible interactions between the executive 'semantic control' and hub-and-spoke 'semantic representation' systems. *Cortex*, 103:100–116, June 2018. doi: 10.1016/j.cortex.2018.02.018.

Chung, S. W., Hill, A. T., Rogasch, N. C., Hoy, K. E., and Fitzgerald, P. B. Use of theta-burst stimulation in changing excitability of motor cortex: A systematic review and meta-analysis. *Neuroscience & Biobehavioral Reviews*, 63:43–64, Apr. 2016. doi: 10.1016/j.neubiorev.2016.01.008.

Cristescu, T. C., Devlin, J. T., and Nobre, A. C. Orienting attention to semantic categories. *NeuroImage*, 33(4):1178–1187, Dec. 2006. doi: 10.1016/j.neuroimage.2006.08.017.

Debarnot, U., Crépon, B., Orriols, E., Abram, M., Charron, S., Lion, S., Roca, P., Oppenheim, C., Gueguen, D., Ergis, A.-M., Baron, J.-C., and Piolino, P. Intermittent theta burst stimulation over left BA10 enhances virtual reality-based prospective memory in healthy aged subjects. *Neurobiology of Aging*, 36(8):2360–2369, Aug. 2015. doi: 10.1016/j.neurobiolaging.2015.05.001.

DeDe, G. and Knilans, J. Language comprehension in aging. In Wright, H. H., editor, *Cognition, Language and Aging*, pages 107–133. John Benjamins Publishing Company, Amsterdam, Mar. 2016. ISBN 978-90-272-1232-0 978-90-272-6731-3. doi: 10.1075/z.200.05ded.

Dehaene, S. and Cohen, L. The unique role of the visual word form area in reading. *Trends in Cognitive Sciences*, 15(6):254–262, June 2011. doi: 10.1016/j.tics.2011.04.003.

Demeter, E. Enhancing Cognition with Theta Burst Stimulation. *Current Behavioral Neuroscience Reports*, 3(2):87–94, June 2016. doi: 10.1007/s40473-016-0072-7.

Devereux, B. J., Tyler, L. K., Geertzen, J., and Randall, B. The Centre for Speech, Language and the Brain (CSLB) concept property norms. *Behavior Research Methods*, 46(4):1119–1127, Dec. 2014. doi: 10.3758/s13428-013-0420-4.

Duncan, J. The multiple-demand (MD) system of the primate brain: Mental programs for intelligent behaviour. *Trends in Cognitive Sciences*, 14(4):172–179, Apr. 2010. doi: 10.1016/j.tics.2010.01.004.

Esteban, O., Markiewicz, C. J., Blair, R. W., Moodie, C. A., Isik, A. I., Erramuzpe, A., Kent, J. D., Goncalves, M., DuPre, E., Snyder, M., Oya, H., Ghosh, S. S., Wright, J., Durnez, J., Poldrack, R. A., and Gorgolewski, K. J. fMRIPrep: A robust preprocessing pipeline for functional MRI. *Nature Methods*, 16(1):111–116, Jan. 2019. doi: 10.1038/s41592-018-0235-4.

Fedorenko, E., Hsieh, P.-J., Nieto-Castañón, A., Whitfield-Gabrieli, S., and Kanwisher, N. New Method for fMRI Investigations of Language: Defining ROIs Functionally in Individual Subjects. *Journal of Neurophysiology*, 104(2):1177–1194, Apr. 2010. doi: 10.1152/jn.00032.2010.

Fedorenko, E., Duncan, J., and Kanwisher, N. Broad domain generality in focal regions of frontal and parietal cortex. *Proceedings of the National Academy of Sciences*, 110(41):16616–16621, Oct. 2013. doi: 10.1073/pnas.1315235110.

Feinberg, D. A., Moeller, S., Smith, S. M., Auerbach, E., Ramanna, S., Glasser, M. F., Miller, K. L., Ugurbil, K., and Yacoub, E. Multiplexed Echo Planar Imaging for Sub-Second Whole Brain FMRI and Fast Diffusion Imaging. *PLOS ONE*, 5(12):e15710, Dec. 2010. doi: 10.1371/journal.pone.0015710.

Feredoes, E., Heinen, K., Weiskopf, N., Ruff, C., and Driver, J. Causal evidence for frontal involvement in memory target maintenance by posterior brain areas during distracter interference of visual working memory. *Proceedings of the National Academy of Sciences*, 108(42):17510–17515, Oct. 2011. doi: 10.1073/pnas.1106439108.

Forseth, K. J., Kadipasaoglu, C. M., Conner, C. R., Hickok, G., Knight, R. T., and Tandon, N. A lexical semantic hub for heteromodal naming in middle fusiform gyrus. *Brain*, 141(7):2112–2126, July 2018. doi: 10.1093/brain/awy120.

Genovese, C. R., Lazar, N. A., and Nichols, T. Thresholding of Statistical Maps in Functional Neuroimaging Using the False Discovery Rate. *NeuroImage*, 15(4):870–878, Apr. 2002. doi: 10.1006/nimg.2001.1037.

Geranmayeh, F., Wise, R. J. S., Mehta, A., and Leech, R. Overlapping Networks Engaged during Spoken Language Production and Its Cognitive Control. *Journal of Neuroscience*, 34(26):8728–8740, June 2014. doi: 10.1523/JNEUROSCI.0428-14.2014.

Goldthorpe, R. A., Rapley, J. M., and Violante, I. R. A Systematic Review of Non-invasive Brain Stimulation Applications to Memory in Healthy Aging. *Frontiers in Neurology*, 11, 2020.

Goral, M., Clark-Cotton, M., Spiro, A., Obler, L. K., Verkuilen, J., and Albert, M. L. The Contribution of Set Switching and Working Memory to Sentence Processing in Older Adults. *Experimental aging research*, 37(5):516–538, Oct. 2011. doi: 10.1080/0361073X.2011.619858.

Gorgolewski, K., Burns, C., Madison, C., Clark, D., Halchenko, Y., Waskom, M., and Ghosh, S. Nipype: A Flexible, Lightweight and Extensible Neuroimaging Data Processing Framework in Python. *Frontiers in Neuroinformatics*, 5:13, 2011. doi: 10.3389/fninf.2011.00013.

Grady, C. L. The cognitive neuroscience of ageing. *Nature Reviews Neuroscience*, 13(7):491–505, July 2012. doi: 10.1038/nrn3256.

Grill-Spector, K. The neural basis of object perception. *Current Opinion in Neurobiology*, 13(2):159–166, Apr. 2003. doi: 10.1016/S0959-4388(03)00040-0.

Halko, M. A., Farzan, F., Eldaief, M. C., Schmahmann, J. D., and Pascual-Leone, A. Intermittent Theta-Burst Stimulation of the Lateral Cerebellum Increases Functional Connectivity of the Default Network. *The Journal of Neuroscience*, 34(36):12049–12056, Sept. 2014. doi: 10.1523/JNEUROSCI.1776-14.2014.

Hartwigsen, G. and Volz, L. J. Probing rapid network reorganization of motor and language functions via neuromodulation and neuroimaging. *NeuroImage*, 224:117449, Jan. 2021. doi: 10.1016/j.neuroimage.2020.117449.

Hartwigsen, G., Bzdok, D., Klein, M., Wawrzyniak, M., Stockert, A., Wrede, K., Classen, J., and Saur, D. Rapid short-term reorganization in the language network. *eLife*, 6, 2017. doi: 10.7554/eLife.25964.001.

Hartwigsen, G. The neurophysiology of language: Insights from non-invasive brain stimulation in the healthy human brain. *Brain and Language*, 148:81–94, Sept. 2015. doi: 10.1016/j.bandl.2014.10.007.

Hartwigsen, G. Flexible Redistribution in Cognitive Networks. *Trends in Cognitive Sciences*, 22(8):687–698, Aug. 2018. doi: 10.1016/j.tics.2018.05.008.

Heath, S., McMahon, K. L., Nickels, L., Angwin, A., MacDonald, A. D., van Hees, S., Johnson, K., McKinnon, E., and Copland, D. A. Neural mechanisms underlying the facilitation of naming in aphasia using a semantic task: An fMRI study. *BMC Neuroscience*, 13(1):98, Aug. 2012. doi: 10.1186/1471-2202-13-98.

Hedden, T. and Gabrieli, J. D. E. Insights into the ageing mind: A view from cognitive neuroscience. *Nature Reviews Neuroscience*, 5(2):87–96, Feb. 2004. doi: 10.1038/nrn1323.

Heister, J., Würzner, K.-M., Bubenzer, J., Pohl, E., Hanneforth, T., Geyken, A., and Kliegl, R. dlexDB – eine lexikalische Datenbank für die psychologische und linguistische Forschung. *Psychologische Rundschau*, 62(1):10–20, Jan. 2011. doi: 10.1026/0033-3042/a000029.

Henderson, A. and Wright, H. H. Cognition, language, and aging: An introduction. In Wright, H. H., editor, *Cognition, Language and Aging*, pages 1–11. John Benjamins Publishing Company, Amsterdam, Mar. 2016. ISBN 978-90-272-1232-0 978-90-272-6731-3. doi: 10.1075/z.200.01hen.

Hermiller, M. S., Dave, S., Wert, S. L., VanHaerents, S., Riley, M., Weintraub, S., Mesulam, M. M., and Voss, J. L. Evidence from theta-burst stimulation that age-related de-differentiation of the hippocampal network is functional for episodic memory. *Neurobiology of Aging*, 109:145–157, Jan. 2022. doi: 10.1016/j.neurobiolaging.2021.09.018.

Hoffman, P. and Morcom, A. M. Age-related changes in the neural networks supporting semantic cognition: A meta-analysis of 47 functional neuroimaging studies. *Neuroscience & Biobehavioral Reviews*, 84:134–150, Jan. 2018. doi: 10.1016/j.neubiorev.2017.11.010.

Hoffman, P. An individual differences approach to semantic cognition: Divergent effects of age on representation, retrieval and selection. *Scientific Reports*, 8(1):8145, May 2018. doi: 10.1038/s41598-018-26569-0.

Holland, R., Leff, A. P., Josephs, O., Galea, J. M., Desikan, M., Price, C. J., Rothwell, J. C., and Crinion, J. Speech Facilitation by Left Inferior Frontal Cortex Stimulation. *Current Biology*, 21(16):1403–1407, Aug. 2011. doi: 10.1016/j.cub.2011.07.021.

Holland, R., Leff, A. P., Penny, W. D., Rothwell, J. C., and Crinion, J. Modulation of frontal effective connectivity during speech. *Neuroimage*, 140:126–133, Oct. 2016. doi: 10.1016/j.neuroimage.2016.01.037.

Horner, A. J. and Henson, R. N. Priming, response learning and repetition suppression. *Neuropsychologia*, 46(7):1979–1991, June 2008. doi: 10.1016/j.neuropsychologia.2008.01.018.

Hsu, W.-Y., Ku, Y., Zanto, T. P., and Gazzaley, A. Effects of noninvasive brain stimulation on cognitive function in healthy aging and Alzheimer's disease: A systematic review and meta-analysis. *Neurobiology of Aging*, 36(8):2348–2359, Aug. 2015. doi: 10.1016/j.neurobiolaging.2015.04.016.

Huang, Y.-Z., Edwards, M. J., Rounis, E., Bhatia, K. P., and Rothwell, J. C. Theta Burst Stimulation of the Human Motor Cortex. *Neuron*, 45(2):201–206, Jan. 2005. doi: 10.1016/j.neuron.2004.12.033.

Jackson, R. L. The neural correlates of semantic control revisited. *NeuroImage*, 224:117444, Jan. 2021. doi: 10.1016/j.neuroimage.2020.117444.

Julian, J. B., Fedorenko, E., Webster, J., and Kanwisher, N. An algorithmic method for functionally defining regions of interest in the ventral visual pathway. *NeuroImage*, 60(4):2357–2364, May 2012. doi: 10.1016/j.neuroimage.2012.02.055.

Kanwisher, N., McDermott, J., and Chun, M. M. The Fusiform Face Area: A Module in Human Extrastriate Cortex Specialized for Face Perception. *Journal of Neuroscience*, 17(11):4302–4311, June 1997. doi: 10.1523/JNEUROSCI.17-11-04302.1997.

Kemper, S., Crow, A., and Kemtes, K. Eye-Fixation Patterns of High- and Low-Span Young and Older Adults: Down the Garden Path and Back Again. *Psychology and Aging*, 19(1):157–170, 2004. doi: 10.1037/0882-7974.19.1.157.

Kim, K. K., Karunanayaka, P., Privitera, M. D., Holland, S. K., and Szaflarski, J. P. Semantic association investigated with functional MRI and independent component analysis. *Epilepsy & Behavior*, 20(4):613–622, Apr. 2011. doi: 10.1016/j.yebeh.2010.11.010.

Lambon Ralph, M. A., Jefferies, E., Patterson, K., and Rogers, T. T. The neural and computational bases of semantic cognition. *Nature Reviews Neuroscience*, 18(1):42–55, Jan. 2017. doi: 10.1038/nrn.2016.150.

Legon, W., Punzell, S., Dowlati, E., Adams, S. E., Stiles, A. B., and Moran, R. J. Altered Prefrontal Excitation/Inhibition Balance and Prefrontal Output: Markers of Aging in Human Memory Networks. *Cerebral Cortex (New York, N.Y.: 1991)*, 26(11):4315–4326, Oct. 2016. doi: 10.1093/cercor/bhv200.

Lenth, R. Emmeans: Estimated Marginal Means, aka Least-Squares Means. R package version 1.4.8., 2020.

Lüdecke, D. Ggeffects: Tidy Data Frames of Marginal Effects from Regression Models. *Journal of Open Source Software*, 3(26):772, June 2018. doi: 10.21105/joss.00772.

Lüdecke, D. sjPlot - Data Visualization for Statistics in Social Science. Zenodo, 2021.

Mahon, B. Z. and Caramazza, A. Judging semantic similarity: An event-related fMRI study with auditory word stimuli. *Neuroscience*, 169(1):279–286, Aug. 2010. doi: 10.1016/j.neuroscience.2010.04.029.

Martin, S., Williams, K. A., Saur, D., and Hartwigsen, G. Age-related reorganization of functional network architecture in semantic cognition. *Cerebral Cortex*, page bhac387, Oct. 2022. doi: 10.1093/cercor/bhac387.

Martin, S., Saur, D., and Hartwigsen, G. Age-Dependent Contribution of Domain-General Networks to Semantic Cognition. *Cerebral Cortex*, 32(4):870–890, Feb. 2022. doi: 10.1093/cercor/bhab252.

McLaren, D. G., Ries, M. L., Xu, G., and Johnson, S. C. A Generalized Form of Context-Dependent Psychophysiological Interactions (gPPI): A Comparison to Standard Approaches. *Neuroimage*, 61(4):1277–1286, July 2012. doi: 10.1016/j.neuroimage.2012.03.068.

Meinzer, M., Lindenberg, R., Antonenko, D., Flaisch, T., and Floel, A. Anodal Transcranial Direct Current Stimulation Temporarily Reverses Age-Associated Cognitive Decline and Functional Brain Activity Changes. *Journal of Neuroscience*, 33(30):12470–12478, July 2013. doi: 10.1523/JNEUROSCI.5743-12.2013.

Meinzer, M., Lindenberg, R., Sieg, M. M., Nachtigall, L., Ulm, L., and Flöel, A. Transcranial direct current stimulation of the primary motor cortex improves word-retrieval in older adults. *Frontiers in Aging Neuroscience*, 6, 2014.

Meyer, F. Un algorithme optimal pour la ligne de partage des eaux. Dans 8e congrès de reconnaissance des formes et intelligence artificielle. In *8 Me Congrès de Reconnaissance Des Formes et Intelligence Artificielle*, 2, pages 847–857, Lyon, France, 1991.

Mion, M., Patterson, K., Acosta-Cabronero, J., Pengas, G., Izquierdo-Garcia, D., Hong, Y. T., Fryer, T. D., Williams, G. B., Hodges, J. R., and Nestor, P. J. What the left and right anterior fusiform gyri tell us about semantic memory. *Brain: A Journal of Neurology*, 133(11):3256–3268, Nov. 2010. doi: 10.1093/brain/awq272.

Moreno-Martínez, F. J. and Montoro, P. R. An Ecological Alternative to Snodgrass & Vanderwart: 360 High Quality Colour Images with Norms for Seven Psycholinguistic Variables. *PLoS ONE*, 7(5):e37527, May 2012. doi: 10.1371/journal.pone.0037527.

Nagel, I. E., Schumacher, E. H., Goebel, R., and D'Esposito, M. Functional MRI investigation

of verbal selection mechanisms in lateral prefrontal cortex. *NeuroImage*, 43(4):801–807, Dec. 2008. doi: 10.1016/j.neuroimage.2008.07.017.

Nieto-Castañón, A. and Fedorenko, E. Subject-specific functional localizers increase sensitivity and functional resolution of multi-subject analyses. *NeuroImage*, 63(3):1646–1669, Nov. 2012. doi: 10.1016/j.neuroimage.2012.06.065.

Noonan, K. A., Jefferies, E., Visser, M., and Lambon Ralph, M. A. Going beyond Inferior Prefrontal Involvement in Semantic Control: Evidence for the Additional Contribution of Dorsal Angular Gyrus and Posterior Middle Temporal Cortex. *Journal of Cognitive Neuroscience*, 25(11):1824–1850, July 2013. doi: 10.1162/jocn_a_00442.

Obler, L. K., Fein, D., Nicholas, M., and Albert, M. L. Auditory comprehension and aging: Decline in syntactic processing. *Applied Psycholinguistics*, 12(4):433–452, 1991. doi: 10.1017/S0142716400005865.

Palejwala, A. H., Dadario, N. B., Young, I. M., O'Connor, K., Briggs, R. G., Conner, A. K., O'Donoghue, D. L., and Sughrue, M. E. Anatomy and White Matter Connections of the Lingual Gyrus and Cuneus. *World Neurosurgery*, 151:e426–e437, July 2021. doi: 10.1016/j.wneu.2021.04.050.

Park, D. C., Polk, T. A., Park, R., Minear, M., Savage, A., Smith, M. R., and Smith, E. E. Aging Reduces Neural Specialization in Ventral Visual Cortex. *Proceedings of the National Academy of Sciences of the United States of America*, 101(35):13091–13095, 2004. doi: pnas.0405148101.

Richter, M., Miltner, W. H. R., and Straube, T. Association between therapy outcome and right-hemispheric activation in chronic aphasia. *Brain*, 131(5):1391–1401, May 2008. doi: 10.1093/brain/awn043.

Rossi, S., Hallett, M., Rossini, P. M., and Pascual-Leone, A. Safety, ethical considerations, and application guidelines for the use of transcranial magnetic stimulation in clinical practice and research. *Clinical Neurophysiology*, 120(12):2008–2039, Dec. 2009. doi: 10.1016/j.clinph.2009.08.016.

Ruan, J., Bludau, S., Palomero-Gallagher, N., Caspers, S., Mohlberg, H., Eickhoff, S. B., Seitz, R. J., and Amunts, K. Cytoarchitecture, probability maps, and functions of the human supplementary and pre-supplementary motor areas. *Brain Structure and Function*, 223(9):4169–4186, Dec. 2018. doi: 10.1007/s00429-018-1738-6.

Schröder, A., Gemballa, T., Ruppin, S., and Wartenburger, I. German norms for semantic typicality, age of acquisition, and concept familiarity. *Behavior Research Methods*, 44(2): 380–394, June 2012. doi: 10.3758/s13428-011-0164-y.

Scott, T. L., Gallée, J., and Fedorenko, E. A new fun and robust version of an fMRI localizer for the frontotemporal language system. *Cognitive Neuroscience*, 8(3):167–176, 2016. doi: 10.1080/17588928.2016.1201466.

Siebner, H. R., Hartwigsen, G., Kassuba, T., and Rothwell, J. C. How does transcranial magnetic stimulation modify neuronal activity in the brain? Implications for studies of cognition. *Cortex*, 45(9):1035–1042, Oct. 2009. doi: 10.1016/j.cortex.2009.02.007.

Singh, A., Erwin-Grabner, T., Sutcliffe, G., Paulus, W., Dechent, P., Antal, A., and Goya-Maldonado, R. Default mode network alterations after intermittent theta burst stimulation in healthy subjects. *Translational Psychiatry*, 10(1):1–10, Feb. 2020. doi: 10.1038/s41398-020-0754-5.

Sliwinska, M. W., Violante, I. R., Wise, R. J. S., Leech, R., Devlin, J. T., Geranmayeh, F., and Hampshire, A. Stimulating Multiple-Demand Cortex Enhances Vocabulary Learning. *Journal of Neuroscience*, 37(32):7606–7618, Aug. 2017. doi: 10.1523/JNEUROSCI.3857-16.2017.

Spreng, R. N., Wojtowicz, M., and Grady, C. L. Reliable differences in brain activity between young and old adults: A quantitative meta-analysis across multiple cognitive domains. *Neuroscience & Biobehavioral Reviews*, 34(8):1178–1194, July 2010. doi: 10.1016/j.neubiorev.2010.01.009.

Taylor, P. C. J., Nobre, A. C., and Rushworth, M. F. S. Subsecond Changes in Top–Down Control Exerted by Human Medial Frontal Cortex during Conflict and Action Selection: A Combined Transcranial Magnetic Stimulation–Electroencephalography Study. *Journal of Neuroscience*, 27(42):11343–11353, Oct. 2007. doi: 10.1523/JNEUROSCI.2877-07.2007.

Team, R. C. R: A language and environment for statistical computing. R Foundation for Statistical Computing, 2021.

Verhaeghen, P. Aging and vocabulary scores: A meta-analysis. *Psychology and Aging*, 18 (2):332–339, June 2003. doi: 10.1037/0882-7974.18.2.332.

Vidal-Piñeiro, D., Martin-Trias, P., Arenaza-Urquijo, E. M., Sala-Llonch, R., Clemente, I. C., Mena-Sánchez, I., Bargalló, N., Falcón, C., Pascual-Leone, Á., and Bartrés-Faz, D. Task-dependent Activity and Connectivity Predict Episodic Memory Network-based Responses to Brain Stimulation in Healthy Aging. *Brain Stimulation*, 7(2):287–296, Mar. 2014. doi: 10.1016/j.brs.2013.12.016.

Willacker, L., Roccato, M., Can, B. N., Dieterich, M., and Taylor, P. C. J. Reducing variability of perceptual decision making with offline theta-burst TMS of dorsal medial frontal cortex. *Brain Stimulation*, 13(6):1689–1696, Nov. 2020. doi: 10.1016/j.brs.2020.09.011.

Yeo, B. T., Krienen, F. M., Sepulcre, J., Sabuncu, M. R., Lashkari, D., Hollinshead, M., Roffman, J. L., Smoller, J. W., Zöllei, L., Polimeni, J. R., Fischl, B., Liu, H., and Buckner, R. L. The organization of the human cerebral cortex estimated by intrinsic functional connectivity. *Journal of Neurophysiology*, 106(3):1125–1165, Sept. 2011. doi: 10.1152/jn.00338.2011.

5 General Discussion

5.1   Summary of Main Findings
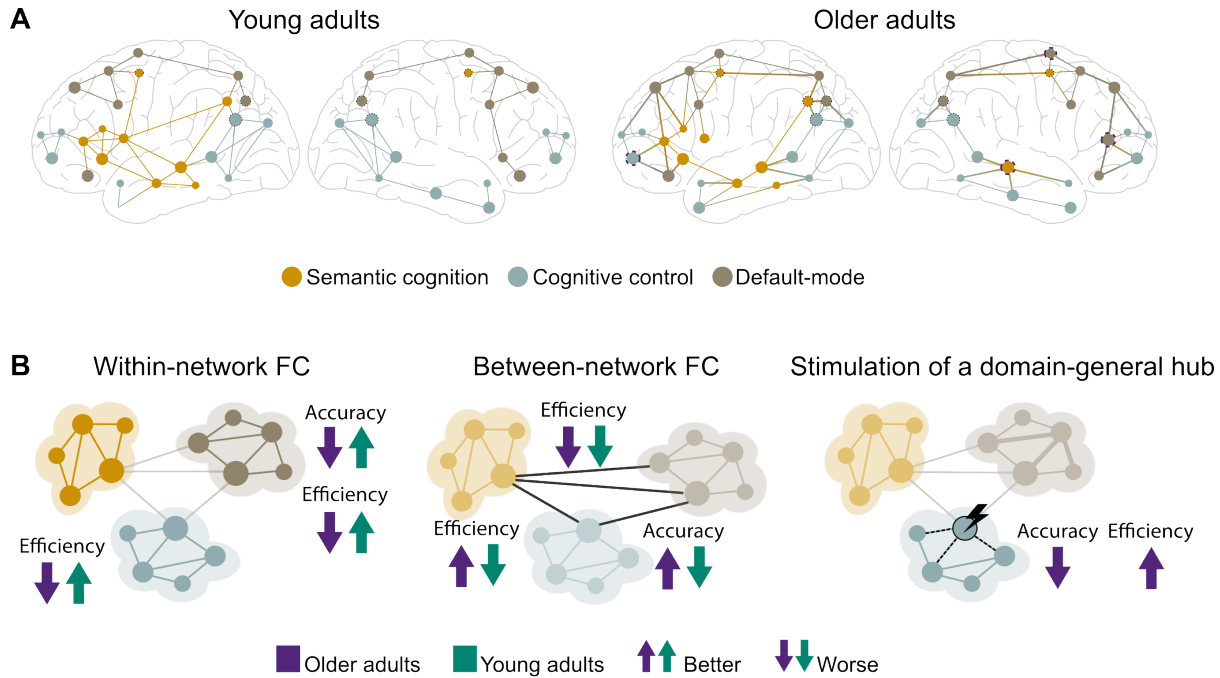
The present thesis aimed to advance our understanding of the functional network architecture in semantic cognition in the young and the aging brain. Exploring semantic processing with language production and comprehension paradigms and the combination of uni- and multivariate fMRI, task-based functional connectivity, and TMS, the presented studies approached the research questions from a comprehensive perspective and were thus able to demonstrate a relationship between age-related changes in functional networks and behavioral performance in semantic cognition.

The first two studies used a semantic word retrieval paradigm to explore age differences in the organization of task-relevant functional networks. Groups of healthy young and older adults performed a paced overt semantic fluency task and a counting task as low-level control task in an fMRI experiment. **Study 1** implemented univariate fMRI analyses and psychophysiological interaction analyses to delineate the functional networks for both tasks and to examine the functional coupling of the strongest activation peaks for the semantic task relative to the control task. Results showed that task-specific networks displayed strong overlap with the domain-general multiple-demand and default-mode system in both age groups. Using task-based connectivity analyses on the whole brain level and between regions of interest from both networks, results showed an interaction of the MDN and DMN, which was present across age groups and specific to the semantic word retrieval task. Notably, the behavioral relevance of increased coupling within and between networks differed between groups: In young adults, increased within-network connectivity was associated with faster and better performance, whereas older adults did not capitalize on strengthened functional connectivity in the same way. Together, study 1 led to two key findings. First, independent of age, integration between usually anticorrelated networks increases when controlled access to semantic memory is required to facilitate goal-directed behavior. Second, older adults do not benefit from task-relevant network coupling in the same way as young adults, which indicates a reduced efficiency of neural networks with age (Figure 5.1).

While study 1 explored the role of two task-relevant domain-general systems, the MDN and DMN, in semantic word retrieval, it remained an open question whether age-related changes to the network organization on the whole-brain level might have impacted our findings. That is, do older adults potentially rely on different functional networks during task processing, which

enables them to maintain high performance? To this end, **study 2** of this thesis combined multivariate ICA with task-based functional connectivity to assess age differences in the network architecture of semantic cognition. Moreover, we applied graph theoretical measures of brain system integration and segregation to examine age-related changes to the network topology and to relate them to our cognitive measures of fluid and crystallized intelligence. Results from the ICA revealed that task-relevant networks for semantic word retrieval include default, semantic, attention, and cognitive control networks across age groups. However, we detected fundamental changes in the coupling of networks with age. Networks of older adults showed increased integration compared with young adults. In particular, subsystems of the DMN demonstrated greater connectivity with attention and control networks, which was associated with preserved, albeit slower semantic processing in older adults. Results from graph theoretical measures underlined these findings. Graphs of older adults were less segregated, less efficient in their signal transmission, and had a larger number of connector hubs. Exploring the predictive utility of these age-related changes in network topology revealed high, albeit less efficient, performance for older adults whose brain graphs showed stronger dedifferentiation and reduced neural specificity. In summary, the findings of study 2 complement and add to the results of study 1 by demonstrating a shifted whole-brain network organization with age, which enabled participants to maintain high, albeit slower task performance during semantic word retrieval (Figure 5.1).

Results from studies 1 and 2 indicated an increased demand for cognitive control resources in older adults. Notably, the pre-SMA emerged as a hub region which contributed to semantic word retrieval. Based on this finding, **study 3** explored the potential of modulating the pre-SMA via facilitatory TMS to enhance semantic processing in a cross-over study design in healthy middle-aged to older adults. Participants completed three sessions of task-based fMRI, a baseline session, during which participants carried out the paradigm in the scanner, and two TMS sessions, during which effective or sham offline iTBS was administered, followed by the fMRI experiment. We were interested in the role of the pre-SMA in semantic control and thus implemented an auditory semantic judgment task with varying control demands (word-picture matching and feature-picture matching) and a non-verbal tone judgment task as control task. Although results did not show an effect of stimulation on accuracy and reaction time in either task, effective iTBS altered task-related activation and functional connectivity. Results showed increased activation in networks of visual processing and cognitive control during semantic processing relative to the control task. Surprisingly, these upregulated regions were associated with poorer semantic performance. Applying whole-brain and ROI-to-ROI functional connectivity analyses, we found increased whole-brain connectivity for the tone judgment compared with the semantic judgment task. However, enhanced positive coupling of the pre-SMA with a cluster in the dorsal attention network after effective iTBS was associated with faster performance in the most demanding semantic condition. In sum, the findings

Figure 5.1 Graphical abstract of main results. (A) Comparison of brain graphs of young and older adults during semantic processing. Results from studies 1 and 2 revealed reduced segregation with greater between-network functional connectivity in older adults. Brain graphs of older adults had a larger number of connector hubs (indicated by dotted lines) to facilitate information flow across networks, which were located in frontal and temporal regions. (B) Behavioral relevance of shifted network architecture in semantic cognition. Studies 1 and 2 yielded better and faster performance with increasing within-network functional connectivity (FC) in young but not older adults. Increasing FC between semantic and default networks was associated with reduced efficiency in both age groups. Increasing FC between semantic and cognitive control networks was linked to higher efficiency only in older adults. Increasing FC between default and cognitive control networks was associated with better performance only in older adults. Facilitatory stimulation of a hub of the domain-general multiple-demand network enhanced coupling with other cognitive control networks distal to the stimulation site. This was linked to poorer performance but increased efficiency during semantic processing in a group of middle-aged to older adults.

of study 3 demonstrate differential effects of iTBS on functional activation and connectivity. Stimulating the pre-SMA via facilitatory TMS was linked to more efficient but not better performance in semantic processing. The results reveal the contribution of the MDN to enhanced access to semantic memory in aging and shed new light on the role of a prefrontal hub in semantic control, indicating a dissociation between domain-general and domain-specific semantic control on the neural level (Figure 5.1).

Taken together, this thesis contributes to our knowledge of the neural correlates of semantic cognition in the young and the aging brain. The findings add to our understanding of age-related neural changes that might contribute to the increase of word retrieval problems and general difficulties in demanding language processing contexts in aging. They also open new perspectives for the development of therapeutic strategies to counteract age-related cognitive

decline and to design effective protocols for the use of NIBS in healthy and pathological aging.

5.2 Contributions and Implications

The key findings of this thesis advance our knowledge of the functional interactions of domain-general and domain-specific networks in semantic cognition and provide new evidence for a multidimensionality of the semantic control network. Furthermore, they have implications for theoretical frameworks on neurocognitive aging, especially with respect to the coupling of default and executive resources as described by the DECHA framework (Spreng & Turner, 2019; Turner & Spreng, 2015).

Domain-Specific and Domain-General Control in Semantic Cognition

Semantic cognition activates a widespread, left-lateralized network in the brain, which consists of representation and control elements (Binder et al., 2009; Jackson, 2021; Jefferies, 2013). Recent investigations have emphasized shared neural resources of semantic subsystems with domain-general networks, including an overlap of semantic representation elements with the DMN (Smallwood et al., 2021; Xu et al., 2016) and of semantic control components with the MDN (Jackson, 2021; Noonan et al., 2013) and FPN (Xu et al., 2016). The findings of studies 1 and 2 of this thesis align with these observations and add a new perspective regarding the interaction of these task-relevant networks.

Study 1 showed greatest activation in a network of frontal and superior parietal regions for the semantic word retrieval task when contrasted with the low-level counting task. These regions strongly overlapped with the MDN, thus indicating a high executive load for this task. Notably, some of these regions, such as the pre-SMA and the dorsomedial prefrontal cortex, and the dorsal angular gyrus, have also been linked to the domain-specific semantic control network (Jackson, 2021; Noonan et al., 2013). These multifaceted associations point towards a domain-general subsystem of semantic control. This interpretation was further supported by our results on increased network coupling between cognitive control regions and core regions of the DMN, which have also been associated with semantic memory and representation, including left temporal pole, ventral angular gyrus, and precuneus. Our findings corroborate the notion that cognitive control and memory-based representation networks integrate functionally when access to semantic memory is required (Krieger-Redwood et al., 2016; Spreng et al., 2014). In addition, our results offer insight into the behavioral relevance of these network interactions, which were associated with better access to semantic memory but slower semantic word retrieval in young adults, underlining the more effortful communication between task-relevant networks compared with within-network processes.

The findings of study 2 extended the results of study 1 and added a whole-brain perspective. First, brain graphs of young adults were strongly segregated, which aligns with general

observations on the organization of the brain into highly intraconnected modules with an efficient structure for global information integration (Bassett et al., 2009; Bullmore & Sporns, 2012). However, in line with study 1, graphs of both age groups showed increased connectivity between subsystems of the DMN and the fronto-parietal control network during semantic processing. Moreover, in young adults, whole-brain segregation had a pronounced effect on behavioral performance, indicating better and faster semantic word retrieval with increasing segregation. Previous work indicates that young adults can benefit from a more integrated brain organization in situations of high task demand to facilitate information flow across components (Cohen & D'Esposito, 2016; Vatansever et al., 2015; W. Zhang et al., 2020). Our results showed that semantic processing in young adults required a task-specific integration of cognitive control and default networks and was nonetheless less effortful compared with older adults.

Altogether, studies 1 and study 2 revealed an interaction of cognitive control and default resources when controlled access to semantic memory is required. Moreover, they elucidated the behavioral relevance of these network interactions. Study 3 added to these findings through the facilitatory stimulation of the pre-SMA, which was associated with semantic-specific processing in studies 1 and 2 and has also been linked to the MDN (Fedorenko et al., 2013).

The results of study 3 showed increased activation in the dorsal attention network after effective stimulation during semantic processing. Further, effective TMS enhanced the coupling of these regions with clusters in dorsal and ventral attention networks, and the FPN during the tone judgment control task. Although these result might seem at odds, they reveal an important feature of the pre-SMA, which is a role in domain-general cognitive control, extending beyond semantic cognition. The findings of study 3 are thus in line with the idea of a multidimensionality of semantic control as it has been previously suggested on the behavioral level (Hoffman, 2018) and for the left inferior prefrontal cortex (Badre et al., 2005; Krieger-Redwood et al., 2015). To prove such a domain-general contribution to semantic control, an effect on domain-general cognitive processes, such as the speed of processing, would be expected. This was confirmed by our finding that increased coupling of the pre-SMA with a parietal hub in the dorsal attention network was associated with faster reactions, thus enhancing the domain-general process of task efficiency. Hence, the role of the pre-SMA in semantic cognition might be best described as domain-general semantic control.

In conclusion, the findings of this thesis demonstrate enhanced coupling of cognitive control and default resources during semantic cognition, which contributes to better, albeit slower task processing. Furthermore, our results suggest distinct subsystems of semantic control, consisting of a fronto-temporal domain-specific and a fronto-parietal domain-general semantic control network.

Age-Related Changes in Functional Network Interactions in Semantic Cognition

The DECHA framework proposes that the frequently observed activity increase in MDN regions and the reduced deactivation of the DMN co-occur and are functionally coupled in older adults (Spreng & Turner, 2019; Turner & Spreng, 2015). This shift in the network architecture is based on the continuous accrual of semantic knowledge and the parallel decline of cognitive control abilities. Older adults thus rely more strongly on their preserved semantic knowledge, which is reflected by an attenuated suppression of DMN regions compared with young adults. Crucially, context and cognitive demand of a task determine whether the increased default-executive coupling in older adults is beneficial or maladaptive. First evidence from domains that are usually well-preserved in healthy aging, including creativity and autobiographical memory, confirmed the adaptive potential of increased default-executive coupling in older adults (Adnan et al., 2019; Spreng et al., 2016). The studies of this thesis contribute to this framework by exploring age-related changes in the interactions of control and memory networks in semantic cognition.

In line with DECHA, univariate results of study 1 revealed reduced deactivation of DMN regions in older relative to young adults during semantic word retrieval. However, functional connectivity results showed that the coupling of multiple-demand and default resources was task-relevant in both age groups, due to the high executive demand of the semantic fluency task. Relating functional connectivity with behavior, provided additional insight into the effects of network coupling. Older adults performed equally well as young adults but we did not find an age-related performance advantage in the form of higher accuracy. Increased coupling of default and executive networks was associated with slower reaction times in both groups, though much more attenuated in older adults. Our findings thus demonstrate the limitations of the age-accompanied shift towards semanticization: Tasks that require an efficient use of control systems while accessing semantic memory might not benefit from the greater semantic knowledge with age. Moreover, our results on the increase of response times with enhanced within-network coupling in older but not young adults provide striking evidence for reduced neural efficiency in aging. The finding aligns with previous work on age-related changes in semantic cognition (Hoffman & Morcom, 2018) and many other cognitive domains (Dennis & Cabeza, 2011; Park et al., 2004) and lends support to the concept of neural dedifferentiation (S.-C. Li & Lindenberger, 1999) in semantic cognition.

Neural dedifferentiation and reduced specificity are often discussed together with neural compensation, which assumes that the additional activation of domain-specific or domain-general regions might be linked to the preservation of cognitive functions in healthy aging (Cabeza et al., 2018). The results of study 2 relate the compensation account to functional network interactions in semantic cognition. Brain graphs of older adults were characterized by increased crosstalk between different networks, reduced brain system segregation, less efficient information flow among distributed networks, and a larger number of connector

hubs. Notably, these patterns of increased dedifferentiation and reduced neural efficiency (M. Y. Chan et al., 2017; Chong et al., 2019) were associated with consistently high but less efficient performance in older adults. Our findings thus show that the enhanced network integration with age helps to maintain stable performance in semantic processing. Importantly, they also reveal the limitations of such compensatory reorganization and demonstrate that a youth-like network architecture in terms of balanced integration and segregation is associated with more economical processing.

Finally, although the findings of study 3 can only be tentatively linked to accounts on neurocognitive aging, due to the within-subject study design, the results allow some first conclusions. Behavioral results showed a detrimental effect of age on reaction times, which aligns with the idea of slower processing due to reduced efficiency of cognitive control networks with age (Hedden & Gabrieli, 2004). Moreover, although the increased activation of executive and control resources after TMS over the pre-SMA was linked to poorer semantic performance, their enhanced coupling correlated with faster reactions during the most demanding semantic condition. This demonstrates the crucial role of domain-general control for efficient semantic processing as discussed in the previous section and might point towards a stimulation-induced improvement in the efficiency of executive resources in middle-aged to older adults.

In summary, the findings of this thesis inform current accounts on neurocognitive aging through the perspective of functional network interactions in semantic cognition. The results align with compensatory accounts but also reveal their limitations in terms of neural efficiency. Furthermore, they are in line with the DECHA framework and highlight the context dependency of increased coupling of default and executive networks. Our task paradigms relied on successful access to and retrieval of information from semantic memory, while requiring an efficient use of cognitive control, which was mirrored by slower behavioral performance and reduced neural efficiency in older adults. Together, our findings demonstrate poorer goal-directed behavior with age.

5.3   Future Directions

There are several implications for future research that can be derived from the present thesis. With respect to the framework of semantic control, future research on the domain-specific and the domain-general elements and their underlying neural correlates is necessary. This requires the design of paradigms that modulate both control networks and allow disentangling their individual contributions. For example, the semantic judgment task, which we designed for study 3, enabled us to contrast the semantically more demanding feature-picture matching with the lexico-semantic word-picture matching. While behavioral results confirmed the generally higher cognitive demand for feature-picture matching, evident through lower accuracy and higher response times, contrasting univariate results for both tasks revealed greater activation

during feature-picture matching in a left-lateralized network of classic domain-specific semantic control regions, such as inferior frontal gyrus and posterior middle temporal gyrus, but also domain-general semantic control areas, including middle and superior frontal gyrus with the pre-SMA, and inferior parietal lobe. Importantly, when we contrasted the non-verbal tone-judgment task with the feature-picture matching task, we found greater activation in domain-general cognitive control regions (Table C.5), which overlapped with the domain-general but not the domain-specific semantic control regions during feature-picture matching. This emphasizes the broad domain generality of these areas and lends additional support to the proposal of distinct semantic control networks. To further unwind the specificity of these networks, I am planning to use the data of the baseline session of study 3 to explore their connectivity profiles during the processing of the different tasks.

Furthermore, additional insight can be gained through the detailed analysis, for instance via synthesis or meta-analysis studies, of critical hub regions, which are likely to contribute to different cognitive domains, such as the left inferior frontal gyrus or the angular gyrus. In a recently published study, we investigated the role of the angular gyrus in semantic cognition through the synthesis of five neuroimaging studies on semantic processing (Kuhnke et al., 2022). Findings revealed distinct effects of general task difficulty and semantic processing demand on the activation of the angular gyrus and highlight separable roles of the angular gyrus in domain-general and domain-specific semantic control.

To probe the causal relevance of these regions in either domain-specific or domain-general semantic control, the application of TMS to transiently perturb a region's contribution to a cognitive process is another promising approach. In this context, previous investigations could show that the angular gyrus plays a causal role in the retrieval of specific conceptual features (Kuhnke et al., 2020) and is causally linked to the left inferior frontal gyrus during semantic processing (Hartwigsen et al., 2016). Combining TMS with neuroimaging methods can further elucidate stimulation-induced mechanisms of adaptive plasticity (Hartwigsen & Volz, 2021), as also demonstrated by study 3 of this thesis. To this end, the temporary disruption of a domain-specific semantic control hub, such as the posterior middle temporal gyrus, and the investigation of subsequent short-term reorganization in the brain could help delineate the contribution of specialized and domain-general networks to semantic cognition.

Another method to explore the relevance of a region in a specific cognitive function is through the investigation of stroke-induced reorganization processes. In this vein, the study of persons with semantic aphasia has already led to notable advances with respect to the neural correlates of semantic control and confirmed the critical role of left inferior frontal gyrus and posterior middle temporal gyrus (Jefferies & Lambon Ralph, 2006; Noonan et al., 2010). Voxel-based lesion symptom mapping (VLSM) is a useful tool to study the contribution of a region to a specific cognitive process by seeking relationships between neural tissue damage

and behavioral performance (Bates et al., 2003). To investigate the causal relevance of domain-general and domain-specific semantic control regions in our semantic judgment paradigm, we are currently collecting data from a larger sample of persons with chronic post-stroke aphasia. I am planning to apply VLSM to delineate the contribution of frontal, temporal, and parietal regions to the processing of less and more demanding semantic conditions.

On the basis of the findings regarding the age-related changes in functional networks during semantic processing, new questions arise as well. First, the first two studies of this thesis were able to demonstrate changes in the coupling of task-relevant networks with age through the comparison with a group of younger adults. Although study 3 was primarily planned as within-subject design to explore the contribution of the pre-SMA to semantic control processes, a future step would be the integration of a young group to examine a possible effect of age on stimulation-induced changes in brain activation and functional connectivity. Furthermore, in comparison to the semantic word retrieval task, the paradigm of study 3 modulates semantic demand and thus the contribution of domain-general networks to successful task processing. Based on our findings of studies 1 and 2 that older adults recruit additional domain-general resources at a lower level of task demand than young adults, the exploration of the semantic judgment paradigm in young and older adults could provide additional insight into the neural changes with respect to increased task difficulty despite intact semantic memory.

Second, the results from study 3 demonstrated the potential of TBS to generate changes in regions distal to the site of stimulation and functionally coupled networks. Exploring the functional connectivity during less (e.g., word-picture matching) and more (e.g., feature-picture matching) demanding semantic processing, might reveal hub regions of each network, which could then be used in targeted stimulation. Importantly, a recent investigation strengthened an individualized stimulation approach accounting for neuroanatomical differences between individuals (Lynch et al., 2022). Thus, targeting specific brain networks of domain-specific or domain-general processing in different age groups and applying an optimized stimulation based on individual anatomy might be the most promising approach towards efficient enhancement of functions in cognitive aging.

Third, as outlined in the Introduction, trajectories of cognitive aging are highly individual. To gain a comprehensive picture of maintenance and compensation processes in the aging brain, future studies should take both structural and functional changes into account (Cabeza et al., 2018). For instance, a recent study linked better performance to functional connectivity during memory encoding, which was related to preserved cortical thickness in the temporal lobe, thus demonstrating a relationship between cognition and structure and function in the brain (Capogna et al., 2022). Such multidimensional approaches will also help to better understand why some people appear to be more resilient to cognitive decline, probably due to maintenance or reserve of neural resources, and others show rapid deterioration (Nyberg et al., 2012; Stern et al., 2020).

Finally, mechanisms such as reserve and maintenance are best explored through a longitudinal approach since adaptive and maladaptive changes in activation and functional connectivity can only be fully evaluated over time. So far, it is unclear how much of the age-related changes in functional activation are compensatory or are better described as compensatory attempts (Cabeza et al., 2018). While the studies of the present thesis were able to relate changes in functional connectivity with behavioral performance and thus provide support for compensation, albeit not as successful as processing in the young brain, future studies should explore the development of these network alterations longitudinally and thus elucidate which patterns relate to structural maintenance over time and which are true compensation. Moreover, age-related changes in functional activation and connectivity do not follow a linear trajectory. For instance, functional connectivity between networks has been shown to change across the lifespan in resting-state (Ng et al., 2016) but also task-based investigations (Pongpipat et al., 2021). Ideally, future studies should thus incorporate middle-aged adults to gain a comprehensive picture of neurocognitive changes across the lifespan.

6 Summary of the Dissertation

Zusammenfassung der Arbeit

Dissertation zur Erlangung des akademischen Grades
Dr. rer. med.

The aging brain in semantic cognition – Insights from fMRI & TMS

eingereicht von: Sandra Martin

angefertigt am: Max-Planck-Institut für Kognitions- und Neurowissenschaften

betreut von: Prof. Dr. Dorothee Saur & PD Dr. Gesa Hartwigsen

October 2022

Aging is accompanied by a myriad of cognitive changes. Although trajectories of cognitive aging are highly individual and inter-individual variability is striking (Cabeza et al., 2018), the steady age-related decline of cognitive control processes— also referred to as fluid intelligence—is well established (Hedden & Gabrieli, 2004). Such processes have been shown to exhibit pronounced age effects and include the domains of working memory, episodic memory, processing speed, mental flexibility, spatial reasoning, and inhibitory control (Hasher et al., 1991; Salthouse, 1996). Semantic memory on the other hand, which refers to the knowledge about words, concepts, and ideas we have accumulated across the lifespan (so-called crystallized intelligence), remains stable or might even increase due to the ongoing accrual of knowledge and experience across the life course (Nyberg et al., 1996; Verhaeghen, 2003).

In the brain, cognitive changes with age are mirrored by large-scale reorganization processes at the structural and functional levels (Grady, 2012). Task-related performance changes in older adults have been associated with a pattern of dedifferentiation of neural activity (S.-C. Li et al., 2001; Park et al., 2004), which is reflected by an under-recruitment of domain-specific regions (Lövdén et al., 2010) and reduced task-specific lateralization (Cabeza, 2002). Dedifferentiation is further characterized by an increased recruitment of areas in the domain-general multiple-demand network (MDN; Fedorenko et al., 2013) and a reduced deactivation of regions in the default mode network (DMN; Andrews-Hanna et al., 2007). In line with these observations, the effect of aging on semantic cognition has been described as reduced specificity and

increased dedifferentiation in task-related activation, as revealed by a recent meta-analysis (Hoffman & Morcom, 2018).

Recently, the application of non-invasive brain stimulation techniques, such as transcranial direct current stimulation (tDCS) and repetitive transcranial magnetic stimulation (rTMS), to counteract age-related cognitive decline and to promote successful aging has gained increasing interest. However, so far, findings are mixed, with some studies reporting beneficial effects, particularly in the domains of working, episodic, and associative memory (Antonenko et al., 2019; Berryhill & Jones, 2012; Manenti et al., 2013), and some studies observing no additional effect on cognitive functions (e.g., Antonenko et al., 2022). Combining non-invasive brain stimulation with neuroimaging techniques is of high importance considering the immense variability of stimulation approaches regarding stimulation site, duration, and intensity. Furthermore, neuroimaging results can help interpreting behavioral effects and might even be observed in the absence of a stimulation-induced behavioral change (Abellaneda-Pérez et al., 2022). To date, no study explored the potential of rTMS to modulate age-related changes in semantic cognition on the behavioral and neural level.

So far, age-related changes to the functional network architecture in semantic cognition are poorly understood. The studies presented in this thesis addressed three key issues: 1) the age-dependent contribution of task-relevant, domain-general networks to semantic cognition, 2) the age-related reorganization of the whole-brain functional network architecture during semantic processing, and 3) the potential of stimulating a hub of the MDN via rTMS to facilitate semantic retrieval in healthy older adults as revealed through behavioral performance and neuroimaging.

The results of this thesis are summarized in Figure 6.1. Studies 1 and 2 applied a semantic word retrieval paradigm to explore age differences in the organization of task-relevant functional networks. Groups of healthy young and older adults performed a paced overt semantic fluency task and a counting task as low-level control task in a functional magnetic resonance imaging (fMRI) experiment. **Study 1** implemented univariate fMRI analyses and psychophysiological interaction analyses to delineate the functional networks for both tasks and to examine the functional coupling of the strongest activation peaks for the semantic task relative to the control task. Results showed that task-specific networks displayed strong overlap with the domain-general multiple-demand and default-mode system in both age groups. Using task-based connectivity analyses on the whole brain level and between regions of interest from both networks, results showed an interaction of the MDN and DMN network, which was present across age groups and specific to the semantic word retrieval task. Notably, the behavioral relevance of increased coupling within and between networks differed between groups: In young adults, increased within-network connectivity was associated with faster and better performance, whereas older adults did not capitalize on strengthened functional connectivity in the same way. Together, study 1 led to two key findings. First, independent of

age, integration between usually anticorrelated networks increases when controlled access to semantic memory is required to facilitate goal-directed behavior. Second, older adults do not benefit from task-relevant network coupling in the same way as young adults, which indicates a reduced efficiency of neural networks with age.

While study 1 explored the role of two task-relevant domain-general systems, the MDN and DMN, in semantic word retrieval, it remained an open question whether age-related changes to the network organization on the whole-brain level might have impacted our findings. That is, do older adults potentially rely on different functional networks during task processing, which enables them to maintain high performance? To this end, **study 2** of this thesis combined multivariate independent component analysis with task-based functional connectivity to assess age differences in the network architecture of semantic cognition. Moreover, we applied graph theoretical measures of brain system integration and segregation to examine age-related changes to the network topology and to relate them to our cognitive measures of fluid and crystallized intelligence. Task-relevant networks for semantic word retrieval included default, semantic, attention, and cognitive control networks across age groups. However, we detected fundamental differences in the coupling of networks with age. Networks of older adults showed increased integration compared with young adults. In particular, subsystems of the DMN demonstrated greater connectivity with attention and control networks, which was associated with preserved, albeit slower semantic processing in older adults. Results from graph theoretical measures underlined these findings. Graphs of older adults were less segregated, less efficient in their signal transmission, and had a larger number of connector hubs. Exploring the predictive utility of these age-related changes in network topology revealed high, albeit less efficient, performance for older adults whose brain graphs showed stronger dedifferentiation and reduced neural specificity. In summary, the findings of study 2 complement and add to the results of study 1 by demonstrating a shifted whole-brain network organization with age, which enabled participants to maintain high, albeit slower task performance during semantic word retrieval.

Results from studies 1 and 2 indicated an increased demand for cognitive control resources in older adults. Notably, the pre-supplementary motor area (pre-SMA) emerged as a hub region, which contributed to semantic word retrieval. Based on this finding, **study 3** explored the potential of modulating the pre-SMA via facilitatory rTMS to enhance semantic processing with a cross-over study design in healthy middle-aged to older adults. Participants completed three sessions of task-based fMRI, a baseline session, during which participants carried out the paradigm in the scanner, and two rTMS sessions, during which effective or sham offline intermittent theta-burst stimulation (iTBS) was administered, followed by the fMRI experiment. We were interested in the role of the pre-SMA in semantic control and thus implemented an auditory semantic judgment task with varying control demands (word-picture matching and feature-picture matching) and a non-verbal tone judgment task as control task. Although results

Figure 6.1 Graphical abstract of main results. (A) Comparison of brain graphs of young and older adults during semantic processing. Results from studies 1 and 2 revealed reduced segregation with greater between-network functional connectivity in older adults. Brain graphs of older adults had a larger number of connector hubs (indicated by dotted lines) to facilitate information flow across networks, which were located in frontal and temporal regions. (B) Behavioral relevance of shifted network architecture in semantic cognition. Studies 1 and 2 yielded better and faster performance with increasing within-network functional connectivity (FC) in young but not older adults. Increasing FC between semantic and default networks was associated with reduced efficiency in both age groups. Increasing FC between semantic and cognitive control networks was linked to higher efficiency only in older adults. Increasing FC between default and cognitive control networks was associated with better performance only in older adults. Facilitatory stimulation of a hub of the domain-general multiple-demand network enhanced coupling with other cognitive control networks distal to the stimulation site. This was linked to poorer performance but increased efficiency during semantic processing in a group of middle-aged to older adults.

did not show an effect of stimulation on accuracy and reaction time in either task, effective iTBS altered task-related activation and functional connectivity. Results showed increased activation in networks of visual processing and cognitive control during semantic processing relative to the control task. Surprisingly, these upregulated regions were associated with poorer semantic performance. Applying whole-brain and ROI-to-ROI functional connectivity analyses, we found increased whole-brain connectivity for the tone judgment compared with the semantic judgment task. However, enhanced positive coupling of the pre-SMA with a cluster in the dorsal attention network after effective iTBS was associated with faster performance in the most demanding semantic condition. In sum, the findings of study 3 demonstrate differential effects of iTBS on functional activation and connectivity. Stimulating the pre-SMA via facilitatory rTMS was linked to more efficient but not better performance in semantic processing. The

results reveal the contribution of the MDN to enhanced access to semantic memory in aging and shed new light on the role of a prefrontal hub in semantic control, indicating a dissociation between domain-general and domain-specific semantic control on the neural level.

Taken together, this thesis contributes to our knowledge of the neural correlates of semantic cognition in the young and the aging brain. The findings of this thesis demonstrate enhanced coupling of cognitive control and default resources during semantic cognition independent of age, which contributes to better, albeit slower task processing. Furthermore, our results suggest distinct subsystems of semantic control, consisting of a fronto-temporal domain-specific and a fronto-parietal domain-general semantic control network. Moreover, this thesis adds to our understanding of age-related neural changes that might contribute to the increase of word retrieval problems and general difficulties in demanding language processing contexts in aging. The results align with compensatory accounts of neurocognitive aging but also reveal their limitations in terms of neural efficiency. Furthermore, they are in line with the default-executive coupling hypothesis of aging (Spreng & Turner, 2019; Turner & Spreng, 2015) and highlight the context dependency of increased coupling of default and executive networks. Finally, they also open new perspectives for the development of therapeutic strategies to counteract age-related cognitive decline and to design effective protocols for the use of NIBS in healthy and pathological aging.

Bibliography

Abellaneda-Pérez, K., Vaqué-Alcázar, L., Solé-Padullés, C., & Bartrés-Faz, D. (2022). Combining non-invasive brain stimulation with functional magnetic resonance imaging to investigate the neural substrates of cognitive aging. *Journal of Neuroscience Research*, *100*(5), 1159–1170. https://doi.org/10.1002/jnr.24514

Adnan, A., Beaty, R., Silvia, P., Spreng, R. N., & Turner, G. R. (2019). Creative aging: Functional brain networks associated with divergent thinking in older and younger adults. *Neurobiology of Aging*, *75*, 150–158. https://doi.org/10.1016/j.neurobiolaging.2018.11.004

Agosta, F., Henry, R. G., Migliaccio, R., Neuhaus, J., Miller, B. L., Dronkers, N. F., Brambati, S. M., Filippi, M., Ogar, J. M., Wilson, S. M., & Gorno-Tempini, M. L. (2010). Language networks in semantic dementia. *Brain*, *133*(1), 286–299. https://doi.org/10.1093/brain/awp233

Allen, E., Erhardt, E., Damaraju, E., Gruner, W., Segall, J., Silva, R., Havlicek, M., Rachakonda, S., Fries, J., Kalyanam, R., Michael, A., Caprihan, A., Turner, J., Eichele, T., Adelsheim, S., Bryan, A., Bustillo, J., Clark, V., Feldstein Ewing, S., … Calhoun, V. (2011). A Baseline for the Multivariate Comparison of Resting-State Networks. *Frontiers in Systems Neuroscience*, *5*.

Andrews-Hanna, J. R., Snyder, A. Z., Vincent, J. L., Lustig, C., Head, D., Raichle, M. E., & Buckner, R. L. (2007). Disruption of Large-Scale Brain Systems in Advanced Aging. *Neuron*, *56*(5), 924–935. https://doi.org/10.1016/j.neuron.2007.10.038

Antal, A., Boros, K., Poreisz, C., Chaieb, L., Terney, D., & Paulus, W. (2008). Comparatively weak after-effects of transcranial alternating current stimulation (tACS) on cortical excitability in humans. *Brain Stimulation*, *1*(2), 97–105. https://doi.org/10.1016/j.brs.2007.10.001

Antonenko, D., Hayek, D., Netzband, J., Grittner, U., & Flöel, A. (2019). tDCS-induced episodic memory enhancement and its association with functional network coupling in older adults. *Scientific Reports*, *9*(1), 2273. https://doi.org/10.1038/s41598-019-38630-7

Antonenko, D., Thams, F., Grittner, U., Uhrich, J., Glöckner, F., Li, S.-C., & Flöel, A. (2022). Randomized trial of cognitive training and brain stimulation in non-demented older adults. *Alzheimer's & Dementia (New York, N. Y.)*, *8*(1), e12262. https://doi.org/10.1002/trc2.12262

Au, R., Albert, M. L., & Obler, L. K. (1989). Language in normal aging: Linguistic and neuropsychological factors. *Journal of Neurolinguistics*, *4*(3), 347–364. https://doi.org/10.1016/0911-6044(89)90026-2

Au, R., Joung, P., Nicholas, M., Obler, L. K., Kass, R., & Albert, M. L. (1995). Naming ability across the adult life span. *Aging & Cognition*, *2*(4), 300–311. https://doi.org/10.1080/13825589508256605

Baciu, M., Boudiaf, N., Cousin, E., Perrone-Bertolotti, M., Pichat, C., Fournet, N., Chainay, H., Lamalle, L., & Krainik, A. (2016). Functional MRI evidence for the decline of word retrieval and generation during normal aging. *AGE*, *38*(1), 3. https://doi.org/10.1007/s11357-015-9857-y

Badre, D., Poldrack, R. A., Paré-Blagoev, E. J., Insler, R. Z., & Wagner, A. D. (2005). Dissociable Controlled Retrieval and Generalized Selection Mechanisms in Ventrolateral Prefrontal Cortex. *Neuron*, *47*(6), 907–918. https://doi.org/10.1016/j.neuron.2005.07.023

Barker, A. T., Jalinous, R., & Freeston, I. L. (1985). Non-invasive magnetic stimulation of human motor cortex. *The Lancet*, *325*(8437), 1106–1107. https://doi.org/10.1016/S0140-6736(85)92413-4

Bassett, D. S., & Bullmore, E. T. (2017). Small-World Brain Networks Revisited. *The Neuroscientist*, *23*(5), 499–516. https://doi.org/10.1177/1073858416667720

Bassett, D. S., Bullmore, E. T., Meyer-Lindenberg, A., Apud, J. A., Weinberger, D. R., & Coppola, R. (2009). Cognitive fitness of cost-efficient brain functional networks. *Proceedings of the National Academy of Sciences*, *106*(28), 11747–11752. https://doi.org/10.1073/pnas.0903641106

Bates, E., Wilson, S. M., Saygin, A. P., Dick, F., Sereno, M. I., Knight, R. T., & Dronkers, N. F. (2003). Voxel-based lesion–symptom mapping. *Nature Neuroscience*, *6*(5), 448–450. https://doi.org/10.1038/nn1050

Beese, C., Werkle-Bergner, M., Lindenberger, U., Friederici, A. D., & Meyer, L. (2019). Adult age differences in the benefit of syntactic and semantic constraints for sentence processing. *Psychology and Aging*, *34*(1), 43–55. https://doi.org/10.1037/pag0000300

Bender, A. R., Völkle, M. C., & Raz, N. (2016). Differential aging of cerebral white matter in middle-aged and older adults: A seven-year follow-up. *NeuroImage*, *125*, 74–83. https://doi.org/10.1016/j.neuroimage.2015.10.030

Berryhill, M. E., & Jones, K. T. (2012). tDCS selectively improves working memory in older adults with more education. *Neuroscience Letters*, *521*(2), 148–151. https://doi.org/10.1016/j.neulet.2012.05.074

Bertolero, M. A., Yeo, B. T. T., & D'Esposito, M. (2017). The diverse club. *Nature Communications*, *8*(1), 1277. https://doi.org/10.1038/s41467-017-01189-w

Betzel, R. F., Byrge, L., He, Y., Goñi, J., Zuo, X.-N., & Sporns, O. (2014). Changes in structural and functional connectivity among resting-state networks across the human lifespan. *NeuroImage*, *102*, 345–357. https://doi.org/10.1016/j.neuroimage.2014.07.067

Binder, J. R., Desai, R. H., Graves, W. W., & Conant, L. L. (2009). Where Is the Semantic System? A Critical Review and Meta-Analysis of 120 Functional Neuroimaging Studies. *Cerebral Cortex*, *19*(12), 2767–2796. https://doi.org/10.1093/cercor/bhp055

Binder, J. R., Frost, J., Hammeke, T., Bellgowan, P., Rao, S., & Cox, R. (1999). Conceptual processing during the conscious resting state: A functional MRI study. *Journal of Cognitive Neuroscience*, *11*(1), 80–93. https://doi.org/10.1162/089892999563265

Bonner, M. F., Ash, S., & Grossman, M. (2010). The New Classification of Primary Progressive Aphasia into Semantic, Logopenic, or Nonfluent/Agrammatic Variants. *Current Neurology and Neuroscience Reports*, *10*(6), 484–490. https://doi.org/10.1007/s11910-010-0140-4

Booth, S. J., Taylor, J. R., Brown, L. J. E., & Pobric, G. (2022). The effects of transcranial alternating current stimulation on memory performance in healthy adults: A systematic review. *Cortex*, *147*, 112–139. https://doi.org/10.1016/j.cortex.2021.12.001

Bowles, N. L., & Poon, L. W. (1985). Aging and Retrieval of Words in Semantic Memory. *Journal of Gerontology*, *40*(1), 71–77. https://doi.org/10.1093/geronj/40.1.71

Brickman, A. M., Muraskin, J., & Zimmerman, M. E. (2009). Structural neuroimaging in Alzheimer's disease: Do white matter hyperintensities matter? *Dialogues in Clinical Neuroscience*, *11*(2), 181–190. https://doi.org/10.31887/DCNS.2009.11.2/ambrickman _eprint: https://doi.org/10.31887/DCNS.2009.11.2/ambrickman

Buckner, R. L., Krienen, F. M., & Yeo, B. T. T. (2013). Opportunities and limitations of intrinsic functional connectivity MRI. *Nature Neuroscience*, *16*(7), 832–837. https://doi.org/10.1038/nn.3423

Bullmore, E., & Sporns, O. (2012). The economy of brain network organization. *Nature Reviews Neuroscience*, *13*(5), 336–349. https://doi.org/10.1038/nrn3214

Burggren, A., & Brown, J. (2014). Imaging markers of structural and functional brain changes that precede cognitive symptoms in risk for Alzheimer's disease. *Brain Imaging and Behavior*, *8*(2), 251–261. https://doi.org/10.1007/s11682-013-9278-4

Burke, D. M., & Shafto, M. A. (2004). Aging and Language Production. *Current directions in psychological science*, *13*(1), 21. https://doi.org/10.1111/j.0963-7214.2004.01301006.x

Cabeza, R. (2002). Hemispheric asymmetry reduction in older adults: The HAROLD model. *Psychology and Aging*, *17*(1), 85–100. https://doi.org/10.1037/0882-7974.17.1.85

Cabeza, R., Albert, M., Belleville, S., Craik, F. I. M., Duarte, A., Grady, C. L., Lindenberger, U., Nyberg, L., Park, D. C., Reuter-Lorenz, P. A., Rugg, M. D., Steffener, J., & Rajah, M. N. (2018). Maintenance, reserve and compensation: The cognitive neuroscience of healthy ageing. *Nature Reviews Neuroscience*, *19*(11), 701–710. https://doi.org/10.1038/s41583-018-0068-2

Cabeza, R., & Dennis, N. A. (2013). Frontal Lobes and Aging: Deterioration and Compensation. https://doi.org/10.1093/med/9780199837755.003.0044

Cao, M., Wang, J.-H., Dai, Z.-J., Cao, X.-Y., Jiang, L.-L., Fan, F.-M., Song, X.-W., Xia, M.-R., Shu, N., Dong, Q., Milham, M. P., Castellanos, F. X., Zuo, X.-N., & He, Y. (2014). Topological organization of the human brain functional connectome across the lifespan. *Developmental Cognitive Neuroscience*, *7*, 76–93. https://doi.org/10.1016/j.dcn.2013.11.004

Capogna, E., Sneve, M. H., Raud, L., Folvik, L., Ness, H. T., Walhovd, K. B., Fjell, A. M., & Vidal-Piñeiro, D. (2022). Whole-brain connectivity during encoding: Age-related differences and associations with cognitive and brain structural decline. *Cerebral Cortex*, bhac053. https://doi.org/10.1093/cercor/bhac053

Chan, D., Fox, N. C., Scahill, R. I., Crum, W. R., Whitwell, J. L., Leschziner, G., Rossor, A. M., Stevens, J. M., Cipolotti, L., & Rossor, M. N. (2001). Patterns of temporal lobe atrophy in semantic dementia and Alzheimer's disease. *Annals of Neurology*, *49*(4), 433–442. https://doi.org/10.1002/ana.92

Chan, M. Y., Alhazmi, F. H., Park, D. C., Savalia, N. K., & Wig, G. S. (2017). Resting-State Network Topology Differentiates Task Signals across the Adult Life Span. *Journal of Neuroscience*, *37*(10), 2734–2745. https://doi.org/10.1523/JNEUROSCI.2406-16.2017

Chan, M. Y., Park, D. C., Savalia, N. K., Petersen, S. E., & Wig, G. S. (2014). Decreased segregation of brain systems across the healthy adult lifespan. *Proceedings of the National Academy of Sciences*, *111*(46), E4997–E5006. https://doi.org/10.1073/pnas.1415122111

Chiou, R., Humphreys, G. F., Jung, J., & Lambon Ralph, M. A. (2018). Controlled semantic cognition relies upon dynamic and flexible interactions between the executive 'semantic control' and hub-and-spoke 'semantic representation' systems. *Cortex*, *103*, 100–116. https://doi.org/10.1016/j.cortex.2018.02.018

Chong, J. S. X., Ng, K. K., Tandi, J., Wang, C., Poh, J.-H., Lo, J. C., Chee, M. W. L., & Zhou, J. H. (2019). Longitudinal Changes in the Cerebral Cortex Functional Organization of Healthy Elderly. *Journal of Neuroscience*, *39*(28), 5534–5550. https://doi.org/10.1523/JNEUROSCI.1451-18.2019

Cohen, J. R., & D'Esposito, M. (2016). The Segregation and Integration of Distinct Brain Networks and Their Relationship to Cognition. *Journal of Neuroscience*, *36*(48), 12083–12094. https://doi.org/10.1523/JNEUROSCI.2965-15.2016

Crowell, C. A., Davis, S. W., Beynel, L., Deng, L., Lakhlani, D., Hilbig, S. A., Palmer, H., Brito, A., Peterchev, A. V., Luber, B., Lisanby, S. H., Appelbaum, L. G., & Cabeza, R. (2020). Older adults benefit from more widespread brain network integration during working memory. *NeuroImage*, *218*, 116959. https://doi.org/10.1016/j.neuroimage.2020.116959

Damoiseaux, J. S., Rombouts, S. a. R. B., Barkhof, F., Scheltens, P., Stam, C. J., Smith, S. M., & Beckmann, C. F. (2006). Consistent resting-state networks across healthy subjects. *Proceedings of the National Academy of Sciences of the United States of America*, *103*(37), 13848–13853. https://doi.org/10.1073/pnas.0601417103

Davis, S. W., Dennis, N. A., Daselaar, S. M., Fleck, M. S., & Cabeza, R. (2008). Que PASA? The Posterior-Anterior Shift in Aging. *Cerebral Cortex*, *18*(5), 1201–1209. https://doi.org/10.1093/cercor/bhm155

Debette, S., & Markus, H. S. (2010). The clinical importance of white matter hyperintensities on brain magnetic resonance imaging: Systematic review and meta-analysis. *BMJ*, *341*, c3666. https://doi.org/10.1136/bmj.c3666

Deng, L., Stanley, M. L., Monge, Z. A., Wing, E. A., Geib, B. R., Davis, S. W., & Cabeza, R. (2021). Age-Related Compensatory Reconfiguration of PFC Connections during Episodic Memory Retrieval. *Cerebral Cortex*, *31*(2), 717–730. https://doi.org/10.1093/cercor/bhaa192

Dennis, N. A., & Cabeza, R. (2011). Age-related dedifferentiation of learning systems: An fMRI study of implicit and explicit learning. *Neurobiology of Aging*, *32*(12), 2318.e17–2318.e30. https://doi.org/10.1016/j.neurobiolaging.2010.04.004

Di Lazzaro, V., Pilato, F., Dileone, M., Profice, P., Oliviero, A., Mazzone, P., Insola, A., Ranieri, F., Meglio, M., Tonali, P. A., & Rothwell, J. C. (2008). The physiological basis of the effects of intermittent theta burst stimulation of the human motor cortex. *The Journal of Physiology*, *586*(16), 3871–3879. https://doi.org/10.1113/jphysiol.2008.152736

Duncan, J. (2010). The multiple-demand (MD) system of the primate brain: Mental programs for intelligent behaviour. *Trends in Cognitive Sciences*, *14*(4), 172–179. https://doi.org/10.1016/j.tics.2010.01.004

Eickhoff, S. B., & Müller, V. I. (2015). Functional Connectivity. In A. W. Toga (Ed.), *Brain Mapping* (pp. 187–201). Academic Press. https://doi.org/10.1016/B978-0-12-397025-1.00212-8

Fama, R., Sullivan, E. V., Shear, P. K., Cahn-Weiner, D. A., Marsh, L., Lim, K. O., Yesavage, J. A., Tinklenberg, J. R., & Pfefferbaum, A. (2000). Structural brain correlates of verbal and nonverbal fluency measures in Alzheimer's disease. *Neuropsychology*, *14*(1), 29. https://doi.org/10.1037/0894-4105.14.1.29

Fedorenko, E., Duncan, J., & Kanwisher, N. (2013). Broad domain generality in focal regions of frontal and parietal cortex. *Proceedings of the National Academy of Sciences*, *110*(41), 16616–16621. https://doi.org/10.1073/pnas.1315235110

Ferreira, L. K., & Busatto, G. F. (2013). Resting-state functional connectivity in normal brain aging. *Neuroscience & Biobehavioral Reviews*, *37*(3), 384–400. https://doi.org/10.1016/j.neubiorev.2013.01.017

Fjell, A. M., & Walhovd, K. B. (2010). Structural Brain Changes in Aging: Courses, Causes and Cognitive Consequences. *Reviews in the Neurosciences*, *21*(3), 187–222. https://doi.org/10.1515/REVNEURO.2010.21.3.187

Fjell, A. M., & Walhovd, K. B. (2020). How Age-Related Changes in the Brain Affect Cognition. In A. K. Thomas & A. Gutchess (Eds.), *The Cambridge Handbook of Cognitive Aging* (First, pp. 47–61). Cambridge University Press. https://doi.org/10.1017/9781108552684.004

Fornito, A., Zalesky, A., & Bullmore, E. T. (2016). *Fundamentals of brain network analysis.* Elsevier/Academic Press.

Förstl, H., & Kurz, A. (1999). Clinical features of Alzheimer's disease. *European Archives of Psychiatry and Clinical Neuroscience, 249*(6), 288–290. https://doi.org/10.1007/s004060050101

Frank, E. M. (1994). Effect of Alzheimer's disease on communication function. *Journal of the South Carolina Medical Association (1975), 90*(9), 417–423.

Friston, K. J. (1994). Functional and effective connectivity in neuroimaging: A synthesis. *Human Brain Mapping, 2*(1-2), 56–78. https://doi.org/10.1002/hbm.460020107

Gallen, C. L., Turner, G. R., Adnan, A., & D'Esposito, M. (2016). Reconfiguration of brain network architecture to support executive control in aging. *Neurobiology of Aging, 44,* 42–52. https://doi.org/10.1016/j.neurobiolaging.2016.04.003

Gandiga, P. C., Hummel, F. C., & Cohen, L. G. (2006). Transcranial DC stimulation (tDCS): A tool for double-blind sham-controlled clinical studies in brain stimulation. *Clinical Neurophysiology, 117*(4), 845–850. https://doi.org/10.1016/j.clinph.2005.12.003

Geerligs, L., Maurits, N. M., Renken, R. J., & Lorist, M. M. (2014). Reduced specificity of functional connectivity in the aging brain during task performance. *Human Brain Mapping, 35*(1), 319–330. https://doi.org/10.1002/hbm.22175

Geerligs, L., Renken, R. J., Saliasi, E., Maurits, N. M., & Lorist, M. M. (2015). A Brain-Wide Study of Age-Related Changes in Functional Connectivity. *Cerebral Cortex, 25*(7), 1987–1999. https://doi.org/10.1093/cercor/bhu012

Goldthorpe, R. A., Rapley, J. M., & Violante, I. R. (2020). A Systematic Review of Non-invasive Brain Stimulation Applications to Memory in Healthy Aging. *Frontiers in Neurology, 11.*

Goral, M., Clark-Cotton, M., Spiro, A., Obler, L. K., Verkuilen, J., & Albert, M. L. (2011). The Contribution of Set Switching and Working Memory to Sentence Processing in Older Adults. *Experimental aging research, 37*(5), 516–538. https://doi.org/10.1080/0361073X.2011.619858

Grady, C. L. (2012). The cognitive neuroscience of ageing. *Nature Reviews Neuroscience, 13*(7), 491–505. https://doi.org/10.1038/nrn3256

Grady, C. L., Protzner, A. B., Kovacevic, N., Strother, S. C., Afshin-Pour, B., Wojtowicz, M., Anderson, J. A. E., Churchill, N., & McIntosh, A. R. (2010). A Multivariate Analysis of Age-Related Differences in Default Mode and Task-Positive Networks across Multiple Cognitive Domains. *Cerebral Cortex, 20*(6), 1432–1447. https://doi.org/10.1093/cercor/bhp207

Greicius, M. D., Krasnow, B., Reiss, A. L., & Menon, V. (2003). Functional connectivity in the resting brain: A network analysis of the default mode hypothesis. *Proceedings of the National Academy of Sciences, 100*(1), 253–258. https://doi.org/10.1073/pnas.0135058100

Gunning-Dixon, F. M., Brickman, A. M., Cheng, J. C., & Alexopoulos, G. S. (2009). Aging of Cerebral White Matter: A Review of MRI Findings. *International journal of geriatric psychiatry, 24*(2), 109–117. https://doi.org/10.1002/gps.2087

Hagmann, P., Cammoun, L., Gigandet, X., Meuli, R., Honey, C. J., Wedeen, V. J., & Sporns, O. (2008). Mapping the Structural Core of Human Cerebral Cortex. *PLOS Biology, 6*(7), e159. https://doi.org/10.1371/journal.pbio.0060159

Hartwigsen, G. (2015). The neurophysiology of language: Insights from non-invasive brain stimulation in the healthy human brain. *Brain and Language, 148*, 81–94. https://doi.org/10.1016/j.bandl.2014.10.007

Hartwigsen, G. (2018). Flexible Redistribution in Cognitive Networks. *Trends in Cognitive Sciences, 22*(8), 687–698. https://doi.org/10.1016/j.tics.2018.05.008

Hartwigsen, G., & Siebner, H. R. (2013). Novel Methods to Study Aphasia Recovery after Stroke. In H. Naritomi & D. Krieger (Eds.), *Frontiers of Neurology and Neuroscience* (pp. 101–111). S. KARGER AG. https://doi.org/10.1159/000346431

Hartwigsen, G., & Volz, L. J. (2021). Probing rapid network reorganization of motor and language functions via neuromodulation and neuroimaging. *NeuroImage, 224*, 117449. https://doi.org/10.1016/j.neuroimage.2020.117449

Hartwigsen, G., Weigel, A., Schuschan, P., Siebner, H. R., Weise, D., Classen, J., & Saur, D. (2016). Dissociating Parieto-Frontal Networks for Phonological and Semantic Word Decisions: A Condition-and-Perturb TMS Study. *Cerebral Cortex, 26*(6), 2590–2601. https://doi.org/10.1093/cercor/bhv092

Hasher, L., Stoltzfus, E. R., Zacks, R. T., & Rypma, B. (1991). Age and inhibition. *Journal of Experimental Psychology: Learning, Memory, and Cognition, 17*(1), 163–169. https://doi.org/10.1037/0278-7393.17.1.163

Hedden, T., & Gabrieli, J. D. E. (2004). Insights into the ageing mind: A view from cognitive neuroscience. *Nature Reviews Neuroscience, 5*(2), 87–96. https://doi.org/10.1038/nrn1323

Hoffman, P. (2018). An individual differences approach to semantic cognition: Divergent effects of age on representation, retrieval and selection. *Scientific Reports, 8*(1), 8145. https://doi.org/10.1038/s41598-018-26569-0

Hoffman, P., & Morcom, A. M. (2018). Age-related changes in the neural networks supporting semantic cognition: A meta-analysis of 47 functional neuroimaging studies. *Neuroscience & Biobehavioral Reviews, 84*, 134–150. https://doi.org/10.1016/j.neubiorev.2017.11.010

Holland, R., Leff, A. P., Josephs, O., Galea, J. M., Desikan, M., Price, C. J., Rothwell, J. C., & Crinion, J. (2011). Speech Facilitation by Left Inferior Frontal Cortex Stimulation. *Current Biology, 21*(16), 1403–1407. https://doi.org/10.1016/j.cub.2011.07.021

Holland, R., Leff, A. P., Penny, W. D., Rothwell, J. C., & Crinion, J. (2016). Modulation of frontal effective connectivity during speech. *Neuroimage, 140*, 126–133. https://doi.org/10.1016/j.neuroimage.2016.01.037

Hsu, W.-Y., Ku, Y., Zanto, T. P., & Gazzaley, A. (2015). Effects of noninvasive brain stimulation on cognitive function in healthy aging and Alzheimer's disease: A systematic review and meta-analysis. *Neurobiology of Aging*, *36*(8), 2348–2359. https://doi.org/10.1016/j.neurobiolaging.2015.04.016

Huang, C.-C., Hsieh, W.-J., Lee, P.-L., Peng, L.-N., Liu, L.-K., Lee, W.-J., Huang, J.-K., Chen, L.-K., & Lin, C.-P. (2015). Age-Related Changes in Resting-State Networks of A Large Sample Size of Healthy Elderly. *CNS Neuroscience & Therapeutics*, *21*(10), 817–825. https://doi.org/10.1111/cns.12396

Huang, Y.-Z., Edwards, M. J., Rounis, E., Bhatia, K. P., & Rothwell, J. C. (2005). Theta Burst Stimulation of the Human Motor Cortex. *Neuron*, *45*(2), 201–206. https://doi.org/10.1016/j.neuron.2004.12.033

Jackson, R. L. (2021). The neural correlates of semantic control revisited. *NeuroImage*, *224*, 117444. https://doi.org/10.1016/j.neuroimage.2020.117444

Jefferies, E. (2013). The neural basis of semantic cognition: Converging evidence from neuropsychology, neuroimaging and TMS. *Cortex*, *49*(3), 611–625. https://doi.org/10.1016/j.cortex.2012.10.008

Jefferies, E., & Lambon Ralph, M. A. (2006). Semantic impairment in stroke aphasia versus semantic dementia: A case-series comparison. *Brain*, *129*(8), 2132–2147. https://doi.org/10.1093/brain/awl153

Kemper, S., & Anagnopoulos, C. (1989). Language and Aging. *Annual Review of Applied Linguistics*, *10*, 37–50. https://doi.org/10.1017/S0267190500001203

Kemper, S., Crow, A., & Kemtes, K. (2004). Eye-Fixation Patterns of High- and Low-Span Young and Older Adults: Down the Garden Path and Back Again. *Psychology and Aging*, *19*(1), 157–170. https://doi.org/10.1037/0882-7974.19.1.157

Ketchabaw, W. T., DeMarco, A. T., Paul, S., Dvorak, E., van der Stelt, C., & Turkeltaub, P. E. (2022). The organization of individually mapped structural and functional semantic networks in aging adults. *Brain Structure and Function*, *227*(7), 2513–2527. https://doi.org/10.1007/s00429-022-02544-4

Kintz, S., Fergadiotis, G., & Wright, H. H. (2016). Aging effects on discourse production. In H. H. Wright (Ed.), *Cognition, Language and Aging* (pp. 81–106). John Benjamins Publishing Company. https://doi.org/10.1075/z.200.04kin

Krieger-Redwood, K., Jefferies, E., Karapanagiotidis, T., Seymour, R., Nunes, A., Ang, J. W. A., Majernikova, V., Mollo, G., & Smallwood, J. (2016). Down but not out in posterior cingulate cortex: Deactivation yet functional coupling with prefrontal cortex during demanding semantic cognition. *NeuroImage*, *141*, 366–377. https://doi.org/10.1016/j.neuroimage.2016.07.060

Krieger-Redwood, K., Teige, C., Davey, J., Hymers, M., & Jefferies, E. (2015). Conceptual control across modalities: Graded specialisation for pictures and words in inferior frontal and

posterior temporal cortex. *Neuropsychologia*, *76*, 92–107. https://doi.org/10.1016/j. neuropsychologia.2015.02.030

Krieger-Redwood, K., Wang, H.-T., Poerio, G., Martinon, L. M., Riby, L. M., Smallwood, J., & Jefferies, E. (2019). Reduced semantic control in older adults is linked to intrinsic DMN connectivity. *Neuropsychologia*, *132*, 107133. https://doi.org/10.1016/j.neuropsychologia. 2019.107133

Kuhnke, P., Beaupain, M. C., Cheung, V. K. M., Weise, K., Kiefer, M., & Hartwigsen, G. (2020). Left posterior inferior parietal cortex causally supports the retrieval of action knowledge. *NeuroImage*, *219*, 117041. https://doi.org/10.1016/j.neuroimage.2020.117041

Kuhnke, P., Chapman, C. A., Cheung, V. K. M., Turker, S., Graessner, A., Martin, S., Williams, K. A., & Hartwigsen, G. (2022). The role of the angular gyrus in semantic cognition: A synthesis of five functional neuroimaging studies. *Brain Structure and Function*. https://doi.org/10.1007/s00429-022-02493-y

Lambon Ralph, M. A., Jefferies, E., Patterson, K., & Rogers, T. T. (2017). The neural and computational bases of semantic cognition. *Nature Reviews Neuroscience*, *18*(1), 42–55. https://doi.org/10.1038/nrn.2016.150

Lanzoni, L., Ravasio, D., Thompson, H., Vatansever, D., Margulies, D., Smallwood, J., & Jefferies, E. (2020). The role of default mode network in semantic cue integration. *NeuroImage*, *219*. https://doi.org/10.1016/j.neuroimage.2020.117019

Li, H.-J., Hou, X.-H., Liu, H.-H., Yue, C.-L., Lu, G.-M., & Zuo, X.-N. (2015). Putting age-related task activation into large-scale brain networks: A meta-analysis of 114 fMRI studies on healthy aging. *Neuroscience & Biobehavioral Reviews*, *57*, 156–174. https://doi.org/10. 1016/j.neubiorev.2015.08.013

Li, S.-C., & Lindenberger, U. (1999). Cross-level unification: A computational exploration of the link between deterioration of neurotransmitter systems and dedifferentiation of cognitive abilities in old age. In *Cognitive neuroscience of memory* (pp. 103–146). Hogrefe & Huber Publishers.

Li, S.-C., Lindenberger, U., & Sikström, S. (2001). Aging cognition: From neuromodulation to representation. *Trends in Cognitive Sciences*, *5*(11), 479–486. https://doi.org/10.1016/ S1364-6613(00)01769-1

Lövdén, M., Bäckman, L., Lindenberger, U., Schaefer, S., & Schmiedek, F. (2010). A theoretical framework for the study of adult cognitive plasticity. *Psychological Bulletin*, *136*(4), 659–676. https://doi.org/10.1037/a0020080

Lovelace, E. A., & Twohig, P. T. (1990). Healthy older adults' perceptions of their memory functioning and use of mnemonics. *Bulletin of the Psychonomic Society*, *28*(2), 115–118. https://doi.org/10.3758/BF03333979

Lu, M., Thorlin, T., Ueno, S., & Persson, M. (2007). Comparison of Maximum Induced Current and Electric Field fromTranscranial Direct Current and Magnetic Stimulations of a Human HeadModel. *PIERS Online*, *3*(2), 178–183. https://doi.org/10.2529/PIERS060906193504

Lynch, C. J., Elbau, I. G., Ng, T. H., Wolk, D., Zhu, S., Ayaz, A., Power, J. D., Zebley, B., Gunning, F. M., & Liston, C. (2022). Automated optimization of TMS coil placement for personalized functional network engagement. *Neuron*, S0896627322007449. https://doi.org/10.1016/j.neuron.2022.08.012

Madden, D. J., Jain, S., Monge, Z. A., Cook, A. D., Lee, A., Huang, H., Howard, C. M., & Cohen, J. R. (2020). Influence of structural and functional brain connectivity on age-related differences in fluid cognition. *Neurobiology of Aging*, *96*, 205–222. https://doi.org/10.1016/j.neurobiolaging.2020.09.010

Manenti, R., Brambilla, M., Petesi, M., Ferrari, C., & Cotelli, M. (2013). Enhancing verbal episodic memory in older and young subjects after non-invasive brain stimulation. *Frontiers in Aging Neuroscience*, *5*.

Marsolais, Y., Perlbarg, V., Benali, H., & Joanette, Y. (2014). Age-related changes in functional network connectivity associated with high levels of verbal fluency performance. *Cortex*, *58*, 123–138. https://doi.org/10.1016/j.cortex.2014.05.007

Martin, A. K., Meinzer, M., Lindenberg, R., Sieg, M. M., Nachtigall, L., & Flöel, A. (2017). Effects of Transcranial Direct Current Stimulation on Neural Networks Structure in Young and Older Adults. *Journal of Cognitive Neuroscience*, *29*(11), 1817–1828. https://doi.org/10.1162/jocn_a_01166

McGinnis, S. M., Brickhouse, M., Pascual, B., & Dickerson, B. C. (2011). Age-Related Changes in the Thickness of Cortical Zones in Humans. *Brain Topography*, *24*(3-4), 279–291. https://doi.org/10.1007/s10548-011-0198-6

Meinzer, M., Lindenberg, R., Antonenko, D., Flaisch, T., & Floel, A. (2013). Anodal Transcranial Direct Current Stimulation Temporarily Reverses Age-Associated Cognitive Decline and Functional Brain Activity Changes. *Journal of Neuroscience*, *33*(30), 12470–12478. https://doi.org/10.1523/JNEUROSCI.5743-12.2013

Meinzer, M., Flaisch, T., Seeds, L., Harnish, S., Antonenko, D., Witte, V., Lindenberg, R., & Crosson, B. (2012). Same Modulation but Different Starting Points: Performance Modulates Age Differences in Inferior Frontal Cortex Activity during Word-Retrieval. *PLoS ONE*, *7*(3), e33631. https://doi.org/10.1371/journal.pone.0033631

Meinzer, M., Flaisch, T., Wilser, L., Eulitz, C., Rockstroh, B., Conway, T., Gonzalez-Rothi, L., & Crosson, B. (2009). Neural Signatures of Semantic and Phonemic Fluency in Young and Old Adults. *Journal of Cognitive Neuroscience*, *21*(10), 2007–2018. https://doi.org/10.1162/jocn.2009.21219

Meinzer, M., Lindenberg, R., Sieg, M. M., Nachtigall, L., Ulm, L., & Flöel, A. (2014). Transcranial direct current stimulation of the primary motor cortex improves word-retrieval in older adults. *Frontiers in Aging Neuroscience, 6.*

Meinzer, M., Seeds, L., Flaisch, T., Harnish, S., Cohen, M. L., McGregor, K., Conway, T., Benjamin, M., & Crosson, B. (2012). Impact of changed positive and negative task-related brain activity on word-retrieval in aging. *Neurobiology of Aging, 33*(4), 656–669. https://doi.org/10.1016/j.neurobiolaging.2010.06.020

Meunier, D., Lambiotte, R., Fornito, A., Ersche, K., & Bullmore, E. (2009). Hierarchical modularity in human brain functional networks. *Frontiers in Neuroinformatics, 3.*

Mitchell, K. J., Johnson, M. K., Raye, C. L., Mather, M., & D'Esposito, M. (2000). Aging and reflective processes of working memory: Binding and test load deficits. *Psychology and Aging, 15*(3), 527–541. https://doi.org/10.1037//0882-7974.15.3.527

Morcom, A. M., & Johnson, W. (2015). Neural Reorganization and Compensation in Aging. *Journal of Cognitive Neuroscience, 27*(7), 1275–1285. https://doi.org/10.1162/jocn_a_00783

Morris, Z., Whiteley, W. N., Longstreth, W. T., Weber, F., Lee, Y.-C., Tsushima, Y., Alphs, H., Ladd, S. C., Warlow, C., Wardlaw, J. M., & Salman, R. A.-S. (2009). Incidental findings on brain magnetic resonance imaging: Systematic review and meta-analysis. *BMJ, 339*, b3016. https://doi.org/10.1136/bmj.b3016

Murphy, C., Wang, H.-T., Konu, D., Lowndes, R., Margulies, D. S., Jefferies, E., & Smallwood, J. (2019). Modes of operation: A topographic neural gradient supporting stimulus dependent and independent cognition. *NeuroImage, 186*, 487–496. https://doi.org/10.1016/j.neuroimage.2018.11.009

Ng, K. K., Lo, J. C., Lim, J. K. W., Chee, M. W. L., & Zhou, J. (2016). Reduced functional segregation between the default mode network and the executive control network in healthy older adults: A longitudinal study. *NeuroImage, 133*, 321–330. https://doi.org/10.1016/j.neuroimage.2016.03.029

Nitsche, M. A., & Paulus, W. (2000). Excitability changes induced in the human motor cortex by weak transcranial direct current stimulation. *The Journal of Physiology, 527*(3), 633–639. https://doi.org/10.1111/j.1469-7793.2000.t01-1-00633.x

Noonan, K. A., Jefferies, E., Corbett, F., & Lambon Ralph, M. A. (2010). Elucidating the Nature of Deregulated Semantic Cognition in Semantic Aphasia: Evidence for the Roles of Prefrontal and Temporo-parietal Cortices. *Journal of Cognitive Neuroscience, 22*(7), 1597–1613. https://doi.org/10.1162/jocn.2009.21289

Noonan, K. A., Jefferies, E., Visser, M., & Lambon Ralph, M. A. (2013). Going beyond Inferior Prefrontal Involvement in Semantic Control: Evidence for the Additional Contribution of Dorsal Angular Gyrus and Posterior Middle Temporal Cortex. *Journal of Cognitive Neuroscience, 25*(11), 1824–1850. https://doi.org/10.1162/jocn_a_00442

Nyberg, L., Backman, L., Erngrund, K., Olofsson, U., & Nilsson, L.-G. (1996). Age Differences in Episodic Memory, Semantic Memory, and Priming: Relationships to Demographic, Intellectual, and Biological Factors. *The Journals of Gerontology Series B: Psychological Sciences and Social Sciences*, *51B*(4), P234–P240. https://doi.org/10.1093/geronb/51B.4. P234

Nyberg, L., Lövdén, M., Riklund, K., Lindenberger, U., & Bäckman, L. (2012). Memory aging and brain maintenance. *Trends in Cognitive Sciences*, *16*(5), 292–305. https://doi.org/10. 1016/j.tics.2012.04.005

Obler, L. K., Fein, D., Nicholas, M., & Albert, M. L. (1991). Auditory comprehension and aging: Decline in syntactic processing. *Applied Psycholinguistics*, *12*(4), 433–452. https: //doi.org/10.1017/S0142716400005865

Obler, L. K., & Pekkala, S. (2008). CHAPTER 26 - Language and Communication in Aging. In B. Stemmer & H. A. Whitaker (Eds.), *Handbook of the Neuroscience of Language* (pp. 351–358). Elsevier. https://doi.org/10.1016/B978-008045352-1.00034-3

Obler, L. K., Rykhlevskaia, E., Schnyer, D., Clark-Cotton, M. R., Spiro, A., Hyun, J., Kim, D.-S., Goral, M., & Albert, M. L. (2010). Bilateral brain regions associated with naming in older adults. *Brain and Language*, *113*(3), 113–123. https://doi.org/10.1016/j.bandl.2010.03.001

Park, D. C., Polk, T. A., Park, R., Minear, M., Savage, A., Smith, M. R., & Smith, E. E. (2004). Aging Reduces Neural Specialization in Ventral Visual Cortex. *Proceedings of the National Academy of Sciences of the United States of America*, *101*(35), 13091–13095. https://doi. org/10.1073/pnas.0405148101

Park, D. C., & Reuter-Lorenz, P. (2009). The Adaptive Brain: Aging and Neurocognitive Scaffolding. *Annual Review of Psychology*, *60*, 173. https://doi.org/10.1146/annurev.psych.59. 103006.093656

Passow, S., Thurm, F., & Li, S.-C. (2017). Activating Developmental Reserve Capacity Via Cognitive Training or Non-invasive Brain Stimulation: Potentials for Promoting Fronto-Parietal and Hippocampal-Striatal Network Functions in Old Age. *Frontiers in Aging Neuroscience*, *9*, 33. https://doi.org/10.3389/fnagi.2017.00033

Patterson, K., Nestor, P. J., & Rogers, T. T. (2007). Where do you know what you know? The representation of semantic knowledge in the human brain. *Nature Reviews Neuroscience*, *8*(12), 976–987. https://doi.org/10.1038/nrn2277

Peelle, J. E. (2019). Language and Aging. In G. de Zubicaray & N. O. Schiller (Eds.), *The Oxford Handbook of Neurolinguistics*.

Peelle, J. E., Chandrasekaran, K., Powers, J., Smith, E. E., & Grossman, M. (2013). Age-related vulnerability in the neural systems supporting semantic processing. *Frontiers in Aging Neuroscience*, *5*. https://doi.org/10.3389/fnagi.2013.00046

Peelle, J. E., Troiani, V., Wingfield, A., & Grossman, M. (2010). Neural processing during older adults' comprehension of spoken sentences: Age differences in resource allocation and connectivity. *Cerebral Cortex*, *20*(4), 773–782. https://doi.org/10.1093/cercor/bhp142

Pongpipat, E. E., Kennedy, K. M., Foster, C. M., Boylan, M. A., & Rodrigue, K. M. (2021). Functional Connectivity Within and Between n-Back Modulated Regions: An Adult Lifespan Psychophysiological Interaction Investigation. *Brain Connectivity*, *11*(2), 103–118. https://doi.org/10.1089/brain.2020.0791

Power, J. D., Cohen, A. L., Nelson, S. M., Wig, G. S., Barnes, K. A., Church, J. A., Vogel, A. C., Laumann, T. O., Miezin, F. M., Schlaggar, B. L., & Petersen, S. E. (2011). Functional Network Organization of the Human Brain. *Neuron*, *72*(4), 665–678. https://doi.org/10.1016/j.neuron.2011.09.006

Prins, N. D., & Scheltens, P. (2015). White matter hyperintensities, cognitive impairment and dementia: An update. *Nature Reviews Neurology*, *11*(3), 157–165. https://doi.org/10.1038/nrneurol.2015.10

Raichle, M. E., MacLeod, A. M., Snyder, A. Z., Powers, W. J., Gusnard, D. A., & Shulman, G. L. (2001). A default mode of brain function. *Proceedings of the National Academy of Sciences*, *98*(2), 676–682. https://doi.org/10.1073/pnas.98.2.676

Raz, N. (2004). The aging brain: Structural changes and their implications for cognitive aging. https://doi.org/10.1093/acprof:oso/9780198525691.003.0006

Raz, N., Lindenberger, U., Rodrigue, K. M., Kennedy, K. M., Head, D., Williamson, A., Dahle, C., Gerstorf, D., & Acker, J. D. (2005). Regional Brain Changes in Aging Healthy Adults: General Trends, Individual Differences and Modifiers. *Cerebral Cortex*, *15*(11), 1676–1689. https://doi.org/10.1093/cercor/bhi044

Reuter-Lorenz, P. A., & Cappell, K. A. (2008). Neurocognitive Aging and the Compensation Hypothesis. *Current Directions in Psychological Science*, *17*(3), 177–182.

Reuter-Lorenz, P. A., Jonides, J., Smith, E. E., Hartley, A., Miller, A., Marshuetz, C., & Koeppe, R. A. (2000). Age Differences in the Frontal Lateralization of Verbal and Spatial Working Memory Revealed by PET. *Journal of Cognitive Neuroscience*, *12*(1), 174–187. https://doi.org/10.1162/089892900561814

Reuter-Lorenz, P. A., & Park, D. C. (2014). How Does it STAC Up? Revisiting the Scaffolding Theory of Aging and Cognition. *Neuropsychology Review*, *24*(3), 355–370. https://doi.org/10.1007/s11065-014-9270-9

Rice, G. E., Hoffman, P., & Lambon Ralph, M. A. (2015). Graded specialization within and between the anterior temporal lobes. *Annals of the New York Academy of Sciences*, *1359*, 84–97. https://doi.org/10.1111/nyas.12951

Rieck, J. R., Baracchini, G., Nichol, D., Abdi, H., & Grady, C. L. (2021). Reconfiguration and dedifferentiation of functional networks during cognitive control across the adult

lifespan. *Neurobiology of Aging*, *106*, 80–94. https://doi.org/10.1016/j.neurobiolaging. 2021.03.019

Rodríguez-Aranda, C., Waterloo, K., Johnsen, S. H., Eldevik, P., Sparr, S., Wikran, G. C., Herder, M., & Vangberg, T. R. (2016). Neuroanatomical correlates of verbal fluency in early Alzheimer's disease and normal aging. *Brain and Language*, *155–156*, 24–35. https: //doi.org/10.1016/j.bandl.2016.03.001

Rönnlund, M., Nyberg, L., Bäckman, L., & Nilsson, L.-G. (2005). Stability, growth, and decline in adult life span development of declarative memory: Cross-sectional and longitudinal data from a population-based study. *Psychology and Aging*, *20*(1), 3–18. https://doi.org/ 10.1037/0882-7974.20.1.3

Ross, L., McCoy, D., Wolk, D., Coslett, H., & Olson, I. (2011). Improved Proper Name Recall in Aging after Electrical Stimulation of the Anterior Temporal Lobes. *Frontiers in Aging Neuroscience*, *3*.

Ruan, J., Bludau, S., Palomero-Gallagher, N., Caspers, S., Mohlberg, H., Eickhoff, S. B., Seitz, R. J., & Amunts, K. (2018). Cytoarchitecture, probability maps, and functions of the human supplementary and pre-supplementary motor areas. *Brain Structure and Function*, *223*(9), 4169–4186. https://doi.org/10.1007/s00429-018-1738-6

Rubinov, M., & Sporns, O. (2010). Complex network measures of brain connectivity: Uses and interpretations. *NeuroImage*, *52*(3), 1059–1069. https://doi.org/10.1016/j.neuroimage. 2009.10.003

Rypma, B., & D'Esposito, M. (2000). Isolating the neural mechanisms of age-related changes in human working memory. *Nature Neuroscience*, *3*(5), 509–515. https://doi.org/10.1038/ 74889

Sala-Llonch, R., Junqué, C., Arenaza-Urquijo, E. M., Vidal-Piñeiro, D., Valls-Pedret, C., Palacios, E. M., Domènech, S., Salvà, A., Bargalló, N., & Bartrés-Faz, D. (2014). Changes in whole-brain functional networks and memory performance in aging. *Neurobiology of Aging*, *35*(10), 2193–2202. https://doi.org/10.1016/j.neurobiolaging.2014.04.007

Salat, D. H., Buckner, R. L., Snyder, A. Z., Greve, D. N., Desikan, R. S., Busa, E., Morris, J. C., Dale, A. M., & Fischl, B. (2004). Thinning of the Cerebral Cortex in Aging. *Cerebral Cortex*, *14*(7), 721–730. https://doi.org/10.1093/cercor/bhh032

Salthouse, T. A. (1996). The processing-speed theory of adult age differences in cognition. *Psychological Review*, *103*(3), 403–428. https://doi.org/10.1037/0033-295X.103.3.403

Salthouse, T. A. (2004). What and When of Cognitive Aging. *Current Directions in Psychological Science*, *13*(4), 140–144. https://doi.org/10.1111/j.0963-7214.2004.00293.x

Saur, D., Kreher, B. W., Schnell, S., Kümmerer, D., Kellmeyer, P., Vry, M.-S., Umarova, R., Musso, M., Glauche, V., Abel, S., Huber, W., Rijntjes, M., Hennig, J., & Weiller, C. (2008). Ventral and dorsal pathways for language. *Proceedings of the National Academy of Sciences*, *105*(46), 18035–18040. https://doi.org/10.1073/pnas.0805234105

Serra, L., Cercignani, M., Lenzi, D., Perri, R., Fadda, L., Caltagirone, C., Macaluso, E., & Bozzali, M. (2010). Grey and White Matter Changes at Different Stages of Alzheimer's Disease. *Journal of Alzheimer's Disease, 19*(1), 147–159. https://doi.org/10.3233/JAD-2010-1223

Setton, R., Mwilambwe-Tshilobo, L., Girn, M., Lockrow, A. W., Baracchini, G., Hughes, C., Lowe, A. J., Cassidy, B. N., Li, J., Luh, W.-M., Bzdok, D., Leahy, R. M., Ge, T., Margulies, D. S., Misic, B., Bernhardt, B. C., Stevens, W. D., De Brigard, F., Kundu, P., … Spreng, R. N. (2022). Age differences in the functional architecture of the human brain. *Cerebral Cortex*, bhac056. https://doi.org/10.1093/cercor/bhac056

Shafto, M. A., Burke, D. M., Stamatakis, E. A., Tam, P. P., & Tyler, L. K. (2007). On the Tip-of-the-Tongue: Neural Correlates of Increased Word-finding Failures in Normal Aging. *Journal of cognitive neuroscience, 19*(12), 2060–2070. https://doi.org/10.1162/jocn.2007.19.12.2060

Shafto, M. A., Stamatakis, E. A., Tam, P. P., & Tyler, L. K. (2010). Word Retrieval Failures in Old Age: The Relationship between Structure and Function. *Journal of Cognitive Neuroscience, 22*(7), 1530–1540. https://doi.org/10.1162/jocn.2009.21321

Shine, J. M., Bissett, P. G., Bell, P. T., Koyejo, O., Balsters, J. H., Gorgolewski, K. J., Moodie, C. A., & Poldrack, R. A. (2016). The Dynamics of Functional Brain Networks: Integrated Network States during Cognitive Task Performance. *Neuron, 92*(2), 544–554. https://doi.org/10.1016/j.neuron.2016.09.018

Siebner, H. R., Funke, K., Aberra, A. S., Antal, A., Bestmann, S., Chen, R., Classen, J., Davare, M., Di Lazzaro, V., Fox, P. T., Hallett, M., Karabanov, A. N., Kesselheim, J., Beck, M. M., Koch, G., Liebetanz, D., Meunier, S., Miniussi, C., Paulus, W., … Ugawa, Y. (2022). Transcranial magnetic stimulation of the brain: What is stimulated? – A consensus and critical position paper. *Clinical Neurophysiology, 140*, 59–97. https://doi.org/10.1016/j.clinph.2022.04.022

Siebner, H. R., Hartwigsen, G., Kassuba, T., & Rothwell, J. C. (2009). How does transcranial magnetic stimulation modify neuronal activity in the brain? Implications for studies of cognition. *Cortex, 45*(9), 1035–1042. https://doi.org/10.1016/j.cortex.2009.02.007

Siebner, H. R., & Rothwell, J. (2003). Transcranial magnetic stimulation: New insights into representational cortical plasticity. *Experimental Brain Research, 148*(1), 1–16. https://doi.org/10.1007/s00221-002-1234-2

Smallwood, J., Bernhardt, B. C., Leech, R., Bzdok, D., Jefferies, E., & Margulies, D. S. (2021). The default mode network in cognition: A topographical perspective. *Nature Reviews Neuroscience, 22*(8), 503–513. https://doi.org/10.1038/s41583-021-00474-4

Smith, S. M., Fox, P. T., Miller, K. L., Glahn, D. C., Fox, P. M., Mackay, C. E., Filippini, N., Watkins, K. E., Toro, R., Laird, A. R., & Beckmann, C. F. (2009). Correspondence of the brain's functional architecture during activation and rest. *Proceedings of the National Academy of Sciences of the United States of America, 106*(31), 13040–13045. https://doi.org/10.1073/pnas.0905267106
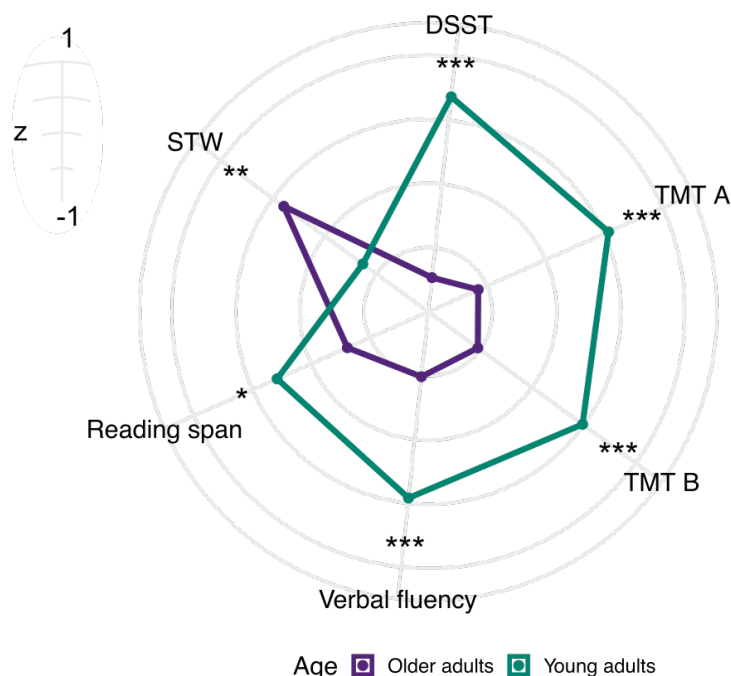
Spreng, R. N., DuPre, E., Selarka, D., Garcia, J., Gojkovic, S., Mildner, J., Luh, W.-M., & Turner, G. R. (2014). Goal-Congruent Default Network Activity Facilitates Cognitive Control. *Journal of Neuroscience*, *34*(42), 14108–14114. https://doi.org/10.1523/JNEUROSCI.2815-14.2014

Spreng, R. N., Lockrow, A. W., DuPre, E., Setton, R., Spreng, K. A. P., & Turner, G. R. (2018). Semanticized autobiographical memory and the default – executive coupling hypothesis of aging. *Neuropsychologia*, *110*, 37–43. https://doi.org/10.1016/j.neuropsychologia.2017.06.009

Spreng, R. N., Stevens, W. D., Viviano, J. D., & Schacter, D. L. (2016). Attenuated anticorrelation between the default and dorsal attention networks with aging: Evidence from task and rest. *Neurobiology of Aging*, *45*, 149–160. https://doi.org/10.1016/j.neurobiolaging.2016.05.020

Spreng, R. N., & Turner, G. R. (2019). The Shifting Architecture of Cognition and Brain Function in Older Adulthood. *Perspectives on Psychological Science*, *14*(4), 523–542. https://doi.org/10.1177/1745691619827511

Spreng, R. N., Wojtowicz, M., & Grady, C. L. (2010). Reliable differences in brain activity between young and old adults: A quantitative meta-analysis across multiple cognitive domains. *Neuroscience & Biobehavioral Reviews*, *34*(8), 1178–1194. https://doi.org/10.1016/j.neubiorev.2010.01.009

Stern, Y., Arenaza-Urquijo, E. M., Bartrés-Faz, D., Belleville, S., Cantilon, M., Chetelat, G., Ewers, M., Franzmeier, N., Kempermann, G., Kremen, W. S., Okonkwo, O., Scarmeas, N., Soldan, A., Udeh-Momoh, C., Valenzuela, M., Vemuri, P., Vuoksimaa, E., & and the Reserve, Resilience and Protective Factors PIA Empirical Definitions and Conceptual Frameworks Workgroup. (2020). Whitepaper: Defining and investigating cognitive reserve, brain reserve, and brain maintenance. *Alzheimer's & Dementia*, *16*(9), 1305–1311. https://doi.org/10.1016/j.jalz.2018.07.219

Stine-Morrow, E. A. L., Loveless, M. K., & Soederberg, L. M. (1996). Resource allocation in on-line reading by younger and older adults. *Psychology and Aging*, *11*(3), 475–486. https://doi.org/10.1037/0882-7974.11.3.475

Stumme, J., Jockwitz, C., Hoffstaedter, F., Amunts, K., & Caspers, S. (2020). Functional network reorganization in older adults: Graph-theoretical analyses of age, cognition and sex. *NeuroImage*, *214*, 116756. https://doi.org/10.1016/j.neuroimage.2020.116756

Taler, V., & Phillips, N. A. (2008). Language performance in Alzheimer's disease and mild cognitive impairment: A comparative review. *Journal of Clinical and Experimental Neuropsychology*, *30*(5), 501–556. https://doi.org/10.1080/13803390701550128

Toga, A. W., Thompson, P. M., & Sowell, E. R. (2006). Mapping brain maturation. *Trends in neurosciences*, *29*(3), 148–159. https://doi.org/10.1016/j.tins.2006.01.007

Tubi, M. A., Feingold, F. W., Kothapalli, D., Hare, E. T., King, K. S., Thompson, P. M., & Braskie, M. N. (2020). White matter hyperintensities and their relationship to cognition: Effects of segmentation algorithm. *NeuroImage*, *206*, 116327. https://doi.org/10.1016/j.neuroimage.2019.116327

Turner, G. R., & Spreng, R. N. (2015). Prefrontal Engagement and Reduced Default Network Suppression Co-occur and Are Dynamically Coupled in Older Adults: The Default–Executive Coupling Hypothesis of Aging. *Journal of Cognitive Neuroscience*, *27*(12), 2462–2476. https://doi.org/10.1162/jocn_a_00869

Tyler, L. K., Shafto, M. A., Randall, B., Wright, P., Marslen-Wilson, W. D., & Stamatakis, E. A. (2010). Preserving syntactic processing across the adult life span: The modulation of the frontotemporal language system in the context of age-related atrophy. *Cerebral Cortex (New York, N.Y.: 1991)*, *20*(2), 352–364. https://doi.org/10.1093/cercor/bhp105

van den Heuvel, M. P., Kahn, R. S., Goñi, J., & Sporns, O. (2012). High-cost, high-capacity backbone for global brain communication. *Proceedings of the National Academy of Sciences*, *109*(28), 11372–11377. https://doi.org/10.1073/pnas.1203593109

van den Heuvel, M. P., & Sporns, O. (2011). Rich-Club Organization of the Human Connectome. *Journal of Neuroscience*, *31*(44), 15775–15786. https://doi.org/10.1523/JNEUROSCI.3539-11.2011

Vatansever, D., Menon, D. K., Manktelow, A. E., Sahakian, B. J., & Stamatakis, E. A. (2015). Default Mode Dynamics for Global Functional Integration. *Journal of Neuroscience*, *35*(46), 15254–15262. https://doi.org/10.1523/JNEUROSCI.2135-15.2015

Vatansever, D., Menon, D. K., & Stamatakis, E. A. (2017). Default mode contributions to automated information processing. *Proceedings of the National Academy of Sciences*, *114*(48), 12821–12826. https://doi.org/10.1073/pnas.1710521114

Venneri, A., McGeown, W. J., Hietanen, H. M., Guerrini, C., Ellis, A. W., & Shanks, M. F. (2008). The anatomical bases of semantic retrieval deficits in early Alzheimer's disease. *Neuropsychologia*, *46*(2), 497–510. https://doi.org/10.1016/j.neuropsychologia.2007.08.026

Verhaeghen, P. (2003). Aging and vocabulary scores: A meta-analysis. *Psychology and Aging*, *18*(2), 332–339. https://doi.org/10.1037/0882-7974.18.2.332

Wagner, T., Valero-Cabre, A., & Pascual-Leone, A. (2007). Noninvasive human brain stimulation. *Annual Review of Biomedical Engineering*, *9*, 527–565. https://doi.org/10.1146/annurev.bioeng.9.061206.133100

Ward, N. S. (2006). Compensatory mechanisms in the aging motor system. *Ageing Research Reviews*, *5*(3), 239–254. https://doi.org/10.1016/j.arr.2006.04.003

Wierenga, C. E., Benjamin, M., Gopinath, K., Perlstein, W. M., Leonard, C. M., Rothi, L. J. G., Conway, T., Cato, M. A., Briggs, R., & Crosson, B. (2008). Age-related changes in word

retrieval: Role of bilateral frontal and subcortical networks. *Neurobiology of Aging*, *29*(3), 436–451. https://doi.org/10.1016/j.neurobiolaging.2006.10.024

Wingfield, A., & Stine-Morrow, E. A. L. (2000). Language and speech. In *The handbook of aging and cognition, 2nd ed* (pp. 359–416). Lawrence Erlbaum Associates Publishers.

Wright, H. H., Koutsoftas, A. D., Capilouto, G. J., & Fergadiotis, G. (2014). Global Coherence in Younger and Older Adults: Influence of Cognitive Processes and Discourse Type. *Neuropsychology, development, and cognition. Section B, Aging, neuropsychology and cognition*, *21*(2), 10.1080/13825585.2013.794894. https://doi.org/10.1080/13825585.2013. 794894

Xu, Y., Lin, Q., Han, Z., He, Y., & Bi, Y. (2016). Intrinsic functional network architecture of human semantic processing: Modules and hubs. *NeuroImage*, *132*, 542–555. https://doi.org/10.1016/j.neuroimage.2016.03.004

Yeatman, J. D., Wandell, B. A., & Mezer, A. A. (2014). Lifespan maturation and degeneration of human brain white matter. *Nature Communications*, *5*(1), 4932. https://doi.org/10.1038/ncomms5932

Yeo, B. T., Krienen, F. M., Sepulcre, J., Sabuncu, M. R., Lashkari, D., Hollinshead, M., Roffman, J. L., Smoller, J. W., Zöllei, L., Polimeni, J. R., Fischl, B., Liu, H., & Buckner, R. L. (2011). The organization of the human cerebral cortex estimated by intrinsic functional connectivity. *Journal of Neurophysiology*, *106*(3), 1125–1165. https://doi.org/10.1152/jn.00338.2011

Zhang, H.-Y., Chen, W.-X., Jiao, Y., Xu, Y., Zhang, X.-R., & Wu, J.-T. (2014). Selective Vulnerability Related to Aging in Large-Scale Resting Brain Networks. *PLOS ONE*, *9*(10), e108807. https://doi.org/10.1371/journal.pone.0108807

Zhang, W., Tang, F., Zhou, X., & Li, H. (2020). Dynamic Reconfiguration of Functional Topology in Human Brain Networks: From Resting to Task States. *Neural Plasticity*, *2020*, 8837615. https://doi.org/10.1155/2020/8837615

Zhu, Z., Yang, F., Li, D., Zhou, L., Liu, Y., Zhang, Y., & Chen, X. (2017). Age-related reduction of adaptive brain response during semantic integration is associated with gray matter reduction. *PLOS ONE*, *12*(12), e0189462. https://doi.org/10.1371/journal.pone.0189462

Zonneveld, H. I., Pruim, R. H., Bos, D., Vrooman, H. A., Muetzel, R. L., Hofman, A., Rombouts, S. A., van der Lugt, A., Niessen, W. J., Ikram, M. A., & Vernooij, M. W. (2019). Patterns of functional connectivity in an aging population: The Rotterdam Study. *NeuroImage*, *189*, 432–444. https://doi.org/10.1016/j.neuroimage.2019.01.041

A Supplementary Material for Study 1

Supplementary Methods

Figure S1. Age differences in neuropsychological tests. Test scores were z-transformed. Higher z-values signify better performance. STW Spot-the-word test, DSST Digit symbol substitution test, TMT Trail making test. *** p < 0.001, ** p < 0.01, * p < 0.05.

Table S1. Age-specific regions of interest (ROIs) within domain-general networks.

ROI	Hemi	x	y	z	Region
Older adults					
MDN (from contrast Semantic fluency > Counting)					
1	L	-9	15	51	Pre-SMA
2	L	-31	25	4	Insula
3	R	31	27	2	Insula
4	L	-34	0	57	MFGd
5	L	-44	5	35	MFGv
6	R	43	35	32	MFG

7	L	-14	-65	51	SPL
8	L	-11	-72	10	IntraCAL
9	R	18	-80	7	IntraCAL

DMN (from contrast Counting > Semantic fluency)

10	R	6	-52	38	Precuneus
11	R	51	12	-31	TP

Young adults

MDN (from contrast Semantic fluency > Counting)

1	L	-4	2	29	dACC
2	L	-31	25	2	Insula
3	R	31	27	2	Insula
4	R	36	42	32	MFG
5	L	-29	-65	51	SPL

DMN (from contrast Counting > Semantic fluency)

6	L	-56	2	-20	MTG
7	R	8	-65	29	Precuneus
8	R	51	10	-31	TP

Note. Coordinates are given in MNI standard space. Abbreviations: Hemi Hemisphere; Pre-SMA Pre-supplementary motor area; MFG/MFGd/MFGv Middle frontal gyrus dorsal/ventral; SPL Superior parietal lobe; IntraCAL Intracalcarine gyrus; TP Temporal pole; dACC Dorsal anterior cingulate cortex; MTG Middle temporal gyrus; MDN Multiple-demand network; DMN Default mode network.

Head motion and functional connectivity

We calculated the following analyses to further ensure that our results of the functional connectivity analyses were not confounded by head motion.

Firstly, we checked whether head motion was correlated with our functional connectivity measures. To this end, we calculated the root mean square (RMS) of realignment parameters for each participant (Power et al., 2014) and Pearson correlations for each functional connectivity measure and age group. Results did not reveal any significant correlation for within-MDN functional connectivity (OA: r = 0.051, p = 0.8; YA: r = 0.032, p = 0.87), within-DMN functional connectivity (OA: r = 0.058, p = 0.77; YA: r = 0.062, p = 0.75), and between-network functional connectivity (OA: r = 0.03, p = 0.88; YA: r = 0.087, p = 0.65). The script Secondly, to further rule out any potential impact of head motion on our results, we performed the following supplementary statistical analyses with motion RMS being added to the GLM as a covariate. The key statistical conclusions remain the same. (i) For within- and between-network functional connectivity (equivalent to statistical analyses for figure 7B), we found significant effects for within-MDN (β = 0.07, t = 2.01, p = 0.049) and between MDN and DMN connectivity (β = 0.12, t = 2.88, p = 0.006) which confirms our previous results. As before, there was no difference

in strength of functional connectivity between age groups (all p > 0.3). Further, there was no effect of motion RMS on any within- and between-network connectivity (all p > 0.68). (ii) For the effect of functional connectivity on task performance (equivalent to statistical analyses for figure 7C), we performed mixed-effects models with motion RMS as an additional covariate. For accuracy, we found a significant interaction between age and functional connectivity between MD and DM regions (χ^2 = 4.64, p = 0.03) which was not detected previously. Results showed that older adults' accuracy during semantic fluency decreased with strengthening functional connectivity between networks, while young adults showed the opposite pattern (Fig. 1). This finding underlines our interpretation of an age-dependent efficiency of task-relevant networks in semantic cognition. For response time data, results did not differ with respect to the statistical models that did not include a covariate for motion RMS. We found significant interactions between age and all functional connectivity measures: within-MDN functional connectivity (χ^2 = 32.29, p < 0.001), within-DMN functional connectivity (χ^2 = 35.55, p < 0.001), and between-network functional connectivity (χ^2 = 21.18, p < 0.001).

Supplementary Results

Table S2. Results for mixed-effects models for accuracy and response time.

Coefficient	Accuracy			Response time		
	Log-Odds	Conf. Int (95%)	p	Estimates	Conf. Int (95%)	p
Intercept	6.28	5.21 − 7.34	**< 0.001**	6.45	6.41 − 6.49	**< 0.001**
Age	-3.94	-5.96 − -1.92	0.136	0.01	0.00 − 0.02	0.072
Condition	-6.47	-8.58 − -4.36	**< 0.001**	0.17	0.13 − 0.22	**< 0.001**
Difficulty	4.63	2.53 − 6.73	**< 0.001**	-0.06	-0.11 − -0.01	**< 0.001**
Education	-0.11	-0.24 − 0.01	0.082	-0.01	-0.01 − 0.02	0.058
Age * Condition	7.26	3.23 − 11.29	0.162	0.08	0.06 − 0.09	**< 0.001**
Age * Difficulty	-7.99	-11.95 − -4.03	**0.002**	0.00	-0.01 − 0.02	0.7
Condition * Difficulty	-5.03	-9.22 − -0.84	0.049	-0.10	-0.20 − -0.00	0.056
Age * Condition * Difficulty	14.95	7.05 − 22.84	**0.002**	0.03	-0.00 − 0.07	0.092
Random Effects						
δ^2	3.29			0.10		
θ_{00}	0.19 Subj			0.01 Subj		
	0.22 Category			0.00 Category		
ICC	0.11			0.08		
N	58 Subj			58 Subj		
	22 Category			22 Category		
Observations	19710			19491		
Marginal R^2 / Conditional R^2	0.900 / 0.911			0.079 / 0.156		

Note. Significant effects are marked in bold. Contrasts are sum coded. P-values were obtained via likelihood ratio tests. Conf. Int. Confidence interval.

Table S3. Results of post-hoc tests for significant three-way interaction Age x Condition x Difficulty for accuracy model. P-values are Bonferroni-corrected.

Contrast	Condition	Odds Ratio	SE	df	Conf. Int (95%)	z	p
OA Easy / YA Easy	Categories	0.57	0.12	Inf	0.32 – 0.98	-2.71	**0.040**
OA Easy / OA Difficult	Categories	6.41	1.68	Inf	3.21 – 12.82	7.08	**< 0.001**
OA Easy / YA Difficult	Categories	6.10	1.65	Inf	2.98 – 12.48	6.67	**< 0.001**
YA Easy / OA Difficult	Categories	11.34	3.22	Inf	5.37 – 23.97	8.56	**< 0.001**
YA Easy / YA Difficult	Categories	10.79	2.95	Inf	5.25 – 22.17	8.71	**< 0.001**
OA Difficult / YA Difficult	Categories	0.95	0.11	Inf	0.71 – 1.28	-0.45	1
OA Easy / YA Easy	Counting	0.00	0.00	Inf	0.00 – 0.01	-3.79	**0.001**
OA Easy / OA Difficult	Counting	0.56	0.46	Inf	0.06 – 4.99	-0.71	1
OA Easy / YA Difficult	Counting	0.65	0.53	Inf	0.08 – 5.46	-0.53	1
YA Easy / OA Difficult	Counting	2461403.54	10105894.32	Inf	48.63 – 124584851753.70	3.58	**0.002**
YA Easy / YA Difficult	Counting	2896157.64	11755020.17	Inf	64.76 – 129525179185.02	3.67	**0.001**
OA Difficult / YA Difficult	Counting	1.18	0.61	Inf	0.30 – 4.67	0.31	1

Note. Significant effects are marked in bold. SE standard error; df degrees of freedom; Conf. Int confidence interval.

Table S4. Results of post-hoc tests for significant two-way interaction Age x Condition for response time model. P-values are Bonferroni-corrected.

Contrast	Condition	Odds Ratio	SE	df	Conf. Int (95%)	z	p
OA Easy / YA Easy	Categories	0.57	0.12	Inf	0.32 – 0.98	-2.71	**0.040**
OA Easy / OA Difficult	Categories	6.41	1.68	Inf	3.21 – 12.82	7.08	**< 0.001**
OA Easy / YA Difficult	Categories	6.10	1.65	Inf	2.98 – 12.48	6.67	**< 0.001**
YA Easy / OA Difficult	Categories	11.34	3.22	Inf	5.37 – 23.97	8.56	**< 0.001**
YA Easy / YA Difficult	Categories	10.79	2.95	Inf	5.25 – 22.17	8.71	**< 0.001**
OA Difficult / YA Difficult	Categories	0.95	0.11	Inf	0.71 – 1.28	-0.45	1
OA Easy / YA Easy	Counting	0.00	0.00	Inf	0.00 – 0.01	-3.79	**0.001**
OA Easy / OA Difficult	Counting	0.56	0.46	Inf	0.06 – 4.99	-0.71	1
OA Easy / YA Difficult	Counting	0.65	0.53	Inf	0.08 – 5.46	-0.53	1
YA Easy / OA Difficult	Counting	2461403.54	10105894.32	Inf	48.63 – 124584851753.70	3.58	**0.002**
YA Easy / YA Difficult	Counting	2896157.64	11755020.17	Inf	64.76 – 129525179185.02	3.67	**0.001**
OA Difficult / YA Difficult	Counting	1.18	0.61	Inf	0.30 – 4.67	0.31	1

Note. Significant effects are marked in bold. SE standard error; df degrees of freedom; Conf. Int confidence interval.

A
Semantic fluency > Rest

Older adults   Young adults

B
Counting > Rest

Older adults   Young adults

Figure S2. Functional MRI results for main effects of tasks from univariate analyses for each age group. Results are FWE-corrected at p < 0.05 at peak level.

Table S5. Older adults: Semantic fluency > Rest.

Anatomical structure	Hemi	k	t	x	y	z
Postcentral gyrus	L	899	14.26	-46	-10	35
Postcentral gyrus	L		12.75	-56	-8	29
Postcentral gyrus	L		12.01	-51	-13	46
Postcentral gyrus	L		11.13	-61	0	24
Cerebellum	L	407	13.28	-34	-57	-26
Cerebellum	L		11.9	-16	-62	-15
Cerebellum	L		9.27	-14	-60	-23
Cerebellum	L		9	-16	-75	-20
Supplementary motor cortex	L	878	13.11	-4	2	62

Supplementary motor cortex	R		12.98	4	0	68
Supplementary motor cortex	L		11.61	-9	7	57
Superior frontal gyrus	R		11.5	11	5	62
Postcentral gyrus	**R**	**370**	**12**	**53**	**-5**	**26**
Precentral gyrus	R		11.77	51	-5	35
Postcentral gyrus	R		8.46	66	-3	18
Caudate nucleus	**R**	**86**	**11.63**	**18**	**2**	**24**
Caudate nucleus	R		9.59	16	-8	21
Caudate nucleus	R		8.72	11	0	10
Cerebellum	**R**	**571**	**11.58**	**31**	**-65**	**-26**
Cerebellum	R		9.98	28	-67	-56
Cerebellum	R		9.14	21	-72	-53
Cerebellum	R		8.97	36	-55	-50
Middle frontal gyrus	**R**	**163**	**11.36**	**36**	**47**	**26**
Middle frontal gyrus	R		9.23	41	35	29
Middle frontal gyrus	R		7.43	26	35	26
Middle frontal gyrus	R		7.28	36	42	18
Insula	**L**	**122**	**9.92**	**-31**	**27**	**4**
Insula	L		8.09	-31	15	7
Inferior frontal gyrus, pars orbitalis	L		7.92	-44	37	-9
Insula	**R**	**148**	**9.91**	**31**	**27**	**2**
Insula	R		8.77	43	20	2
Inferior frontal gyrus, pars orbitalis	R		6.47	38	32	-6
Superior temporal gyrus	**R**	**78**	**9.76**	**63**	**-3**	**2**
Superior temporal gyrus	R		8.24	56	-13	2
Superior temporal gyrus	R		7.49	68	-15	2
Superior temporal gyrus	R		7.06	51	-18	7
Caudate nucleus	**L**	**45**	**9.56**	**-16**	**-10**	**24**
Caudate nucleus	L		9.11	-14	-5	16
Superior parietal lobe	**L**	**98**	**9.33**	**-19**	**-60**	**48**
Inferior parietal sulcus	L		8.5	-26	-45	38
Inferior parietal lobe	L		7.99	-26	-55	38
Inferior parietal lobe	L		7.77	-41	-40	38
Superior temporal gyrus	**L**	**54**	**8.72**	**-51**	**-28**	**10**
Superior temporal gyrus	L		7.68	-66	-23	10
Superior temporal gyrus	L		6.7	-41	-32	10
Inferior frontal gyrus, pars triangularis	**L**	**20**	**8.71**	**-36**	**40**	**4**
Superior temporal gyrus	**L**	**21**	**8.09**	**-64**	**-10**	**4**

Note. FWE-corrected (p < 0.05) at peak level, k ≥ 20 voxels.

Table S6. Young adults: Semantic fluency > Rest.

Anatomical structure	Hemi	k	t	x	y	z
Presupplementary motor cortex	**L**	**767**	**15.05**	**-4**	**12**	**51**
Supplementary motor cortex	L		13.89	-6	17	43
Supplementary motor cortex	R		12.54	4	7	62
Middle cingulate cortex	R		11.17	11	20	38
Insula	**L**	**280**	**13.95**	**-34**	**27**	**2**
Insula	L		11.74	-31	20	7
Inferior frontal gyrus, pars opercularis	L		8.61	-46	10	7
Inferior frontal gyrus, pars opercularis	L		7.01	-49	17	-4
Cerebellum	**R**	**683**	**13.82**	**33**	**-55**	**-31**
Cerebellum	R		13.01	43	-60	-28
Cerebellum	R		11.51	33	-62	-50
Cerebellum	R		11.24	26	-67	-48
Postcentral gyrus	**L**	**331**	**13.74**	**-49**	**-15**	**40**
Postcentral gyrus	L		10.89	-56	-13	46
Postcentral gyrus	L		9.93	-61	0	21
Precentral gyrus	L		8.04	-54	0	46
Cerebellum	**L**	**377**	**13.18**	**-26**	**-60**	**-26**
Cerebellum	L		12.1	-46	-62	-28
Insula	**R**	**130**	**12.01**	**33**	**22**	**7**
Inferior frontal gyrus, pars opercularis	R		9.4	46	15	4
Insula	R		9.05	41	20	-1
Cerebellum	**R**	**40**	**10.86**	**1**	**-47**	**-23**
Cerebellum	**L**	**68**	**10.41**	**-36**	**-60**	**-50**
Precentral gyrus	**R**	**208**	**10.23**	**56**	**-3**	**46**
Precentral gyrus	R		10.09	46	-10	38
Postcentral gyrus	R		8.94	56	-5	35
Rolandic operculum	R		7.71	61	-3	16
Inferior frontal gyrus, pars triangularis	**L**	**208**	**9.99**	**-44**	**32**	**24**
Inferior frontal gyrus, pars triangularis	L		8.29	-51	30	21
Inferior frontal gyrus, pars triangularis	L		8.13	-39	35	7
Inferior frontal gyrus, pars triangularis	L		7.96	-51	35	10
Thalamus	**L**	**57**	**9.31**	**-11**	**-5**	**13**

Anatomical structure	Hemi	k	t	x	y	z
Caudate nucleus	L		9.2	-16	-3	21
Inferior frontal gyrus, pars opercularis	**L**	**98**	**8.33**	**-39**	**2**	**26**
Precentral gyrus	L		7.6	-46	10	32
Precentral gyrus	L		7.16	-41	0	38
Inferior frontal gyrus, pars triangularis	L		6.5	-46	15	24
Middle frontal gyrus	**R**	**81**	**8.1**	**33**	**47**	**32**
Middle frontal gyrus	R		7.08	31	47	24
Caudate nucleus	**R**	**43**	**8.09**	**18**	**5**	**21**
Caudate nucleus	R		7.75	16	-3	24
Caudate nucleus	R		7.73	18	12	16
Middle frontal gyrus	**L**	**26**	**7.57**	**-34**	**55**	**21**
Superior temporal gyrus	**R**	**21**	**7.5**	**66**	**-30**	**7**
Superior temporal gyrus	R		6.7	56	-30	4
Superior temporal gyrus	**L**	**20**	**6.74**	**-59**	**-15**	**4**

Note. FWE-corrected (p < 0.05) at peak level, k $\geq$ 20 voxels.

Table S7. Older adults: Counting > Rest.

Anatomical structure	Hemi	k	t	x	y	z
Postcentral gyrus	**L**	**347**	**11.69**	**-46**	**-13**	**38**
Postcentral gyrus	L		11.56	-61	-3	24
Postcentral gyrus	L		11.52	-51	-13	46
Postcentral gyrus	L		11.05	-56	-8	29
Postcentral gyrus	**R**	**342**	**11.43**	**48**	**-8**	**35**
Postcentral gyrus	R		10.71	53	-3	24
Postcentral gyrus	R		9.39	63	-3	18
Supplementary motor cortex	**L**	**57**	**10.16**	**-4**	**-5**	**70**
Supplementary motor cortex	**R**	**59**	**9.96**	**4**	**0**	**68**
Cerebellum	**L**	**52**	**9.35**	**-29**	**-62**	**-23**
Cerebellum	L		7.84	-16	-65	-18
Superior temporal gyrus	**R**	**49**	**8.44**	**66**	**-10**	**2**
Superior temporal gyrus	R		7.71	63	2	-1
Superior temporal gyrus	R		6.96	68	-18	4
Superior temporal gyrus	R		6.76	53	-15	4
Superior temporal gyrus	**L**	**46**	**8.4**	**-46**	**-42**	**21**
Superior temporal gyrus	L		6.54	-46	-37	13
Superior temporal gyrus	L		6.19	-51	-28	10
Cerebellum	**R**	**26**	**6.96**	**21**	**-60**	**-23**

Cerebellum	R		6.9	11	-60	-23

Table S8. Young adults: Counting > Rest.

Anatomical structure	Hemi	*k*	*t*	*x*	*y*	*z*
Postcentral gyrus	**L**	**317**	**11.47**	**-61**	**0**	**21**
Postcentral gyrus	L		11.3	-49	-15	40
Postcentral gyrus	L		9.28	-56	-13	46
Postcentral gyrus	L		6.99	-59	-8	16
Precentral gyrus	**R**	**247**	**10.42**	**46**	**-10**	**38**
Precentral gyrus	R		9.44	56	-3	46
Rolandic operculum	R		9.35	61	2	16
Postcentral gyrus	R		8.25	56	-8	35
Cerebellum	**R**	**37**	**8.3**	**13**	**-60**	**-20**
Cerebellum	**L**	**25**	**7.37**	**-16**	**-60**	**-23**

Table S9. Older adults: Semantic fluency > Counting.

Anatomical structure	Hemi	*k*	*t*	*x*	*y*	*z*
Cerebellum	**L**	**1844**	**12.99**	**-36**	**-62**	**-26**
Cerebellum	R		12.59	28	-62	-26
Cerebellum	L		12.03	-29	-67	-26
Cerebellum	R		11.08	6	-80	-31
Middle frontal gyrus	**L**	**578**	**12.9**	**-44**	**5**	**35**
Inferior frontal gyrus, pars opercularis	L		11.2	-41	15	21
Precentral gyrus	L		10.7	-39	2	24
Middle frontal gyrus	L		8.94	-46	7	46
Superior frontal gyrus (preSMA)	**L**	**661**	**12.02**	**-9**	**15**	**51**
Presupplementary motor cortex	L		11.62	-9	20	43
Superior frontal gyrus	L		10.34	-1	10	60
Superior frontal gyrus	R		9.34	8	15	48
Insula	**L**	**269**	**10.98**	**-31**	**25**	**4**
Caudate nucleus	L		10.84	-16	0	16
Caudate nucleus	L		9.52	-16	-10	21
Superior frontal gyrus	L		8.74	-19	10	4

Insula	**R**	**113**	**10.95**	**31**	**27**	**2**
Inferior frontal gyrus. pars triangularis	R		7.25	48	22	-4
Frontal operculum	R		7.08	43	20	4
Caudate nucleus	**R**	**106**	**9.96**	**18**	**15**	**18**
Caudate nucleus	R		9.53	18	-8	21
Caudate nucleus	R		8.67	16	0	18
Thalamus	R		8.22	11	0	10
Middle frontal gyrus	**R**	**36**	**9.79**	**43**	**35**	**32**
Superior frontal gyrus	**L**	**100**	**9.12**	**-21**	**12**	**54**
Middle frontal gyrus	L		6.82	-21	-3	60
Middle frontal gyrus	L		6.57	-24	20	51
Intracalcarine cortex	**R**	**43**	**9.01**	**18**	**-80**	**7**
Occipital pole	R		7.93	13	-95	10
Intracalcarine cortex	R		6.77	13	-77	16
Angular gyrus	**L**	**27**	**8.1**	**-34**	**-72**	**43**
Middle frontal gyrus	**L**	**24**	**8.07**	**-34**	**0**	**57**
Superior parietal lobe	**L**	**61**	**7.65**	**-14**	**-65**	**51**
Superior parietal lobe	L		7.31	-21	-65	60
Angular gyrus	L		6.65	-29	-62	46
Intracalcarine cortex	**L**	**71**	**7.52**	**-11**	**-72**	**10**
Intracalcarine cortex	L		7.24	-6	-87	2
Intracalcarine cortex	L		6.96	-4	-82	10
Middle frontal gyrus	**R**	**21**	**7.39**	**23**	**60**	**-4**
Middle frontal gyrus	R		7.05	31	57	-9
Thalamus	**L**	**21**	**6.99**	**-4**	**-5**	**10**

Note. FWE-corrected (p < 0.05) at peak level, k $\geq$ 20 voxels.

Table S10. Young adults: Semantic fluency > Counting.

Anatomical structure	Hemi	*k*	*t*	*x*	*y*	*z*
Insula	**L**	**3112**	**20.03**	**-31**	**25**	**2**
Presupplementary motor cortex	L		16.85	-4	25	40
Presupplementary motor cortex	L		16.33	-6	12	51
Presupplementary motor cortex	R		14.72	13	27	29
Cerebellum	**R**	**2970**	**19.11**	**33**	**-57**	**-31**
Cerebellum	R		16.12	31	-65	-28
Cerebellum	R		13.89	28	-70	-50
Cerebellum	R		12.66	41	-60	-28

Anterior cingulate gyrus	**L**	**90**	**14.15**	**-4**	**2**	**29**
Anterior cingulate gyrus	L		9.12	-1	12	24
Anterior cingulate gyrus	R		8.89	6	7	26
Insula	**R**	**315**	**13.32**	**31**	**27**	**2**
Insula	R		12.64	38	20	-4
Caudate nucleus	**L**	**235**	**12.81**	**-9**	**5**	**2**
Caudate nucleus	L		12.02	-16	-3	21
Thalamus	L		11.32	-11	-5	13
Caudate nucleus	L		10.63	-16	7	16
Brain stem	**L**	**296**	**12.46**	**-6**	**-23**	**-18**
Thalamus	L		11.94	-9	-18	16
Thalamus	L		11.85	-4	-23	10
Thalamus	L		10.36	-4	-13	10
Superior parietal lobe	**L**	**224**	**10.49**	**-29**	**-65**	**51**
Angular gyrus	L		10.21	-29	-72	43
Inferior parietal lobe	L		8.84	-34	-57	40
Middle occipital gyrus	L		6.47	-31	-80	38
Caudate nucleus	**R**	**215**	**10.45**	**18**	**10**	**18**
Caudate nucleus	R		10.38	8	7	2
Caudate nucleus	R		9.57	13	7	10
Caudate nucleus	R		9.16	18	-3	21
Superior temporal gyrus	**L**	**54**	**9.62**	**-61**	**-30**	**7**
Planum temporale	L		6.97	-61	-15	4
Middle frontal gyrus	**R**	**176**	**8.3**	**36**	**42**	**32**
Middle frontal gyrus	R		7.56	31	55	26
Middle frontal gyrus	R		7.53	33	37	21
Middle frontal gyrus	R		7.17	41	35	40

Note. FWE-corrected ($p < 0.05$) at peak level, $k \geq 20$ voxels.

Table S11. Older adults: Counting > Semantic fluency.

Anatomical structure	Hemi	k	t	x	y	z
Temporal pole	**R**	30	9.33	51	12	-31
Precuneus	**R**	45	7.72	6	-52	38

Note. FWE-corrected ($p < 0.05$) at peak level, $k \geq 20$ voxels.

Table S12. Young adults: Counting > Semantic fluency.

Anatomical structure	Hemi	k	t	x	y	z
Temporal pole	**R**	**75**	**11.02**	**51**	**10**	**-31**
Temporal pole	R		6.93	43	20	-28
Precuneus	**R**	**312**	**9.7**	**8**	**-65**	**29**
Precuneus	R		9.59	11	-52	35
Precuneus	L		9.05	-9	-52	35
Insula	**L**	**46**	**8.62**	**-41**	**-8**	**-1**
Insula	L		7.24	-36	-18	18
Insula	L		7.02	-39	-15	2
Insula	**R**	**62**	**8.48**	**36**	**-15**	**4**
Insula	R		7.66	41	0	-6
Insula	R		7.1	38	-15	21
Middle temporal gyrus	**L**	**27**	**8.27**	**-56**	**2**	**-20**
Rolandic operculum	**R**	**22**	**8.01**	**53**	**0**	**10**
Posterior cingulate cortex	**L**	**40**	**7.9**	**-6**	**-30**	**46**
Precentral gyrus	L		6.77	-6	-25	54
Precentral gyrus	**R**	**28**	**7.42**	**1**	**-15**	**62**
Precentral gyrus	L		6.91	-4	-23	70

Note. FWE-corrected (p < 0.05) at peak level, k ≥ 20 voxels.

Table S13. Young adults: Counting > Semantic fluency (p < 0.001 uncorr., FWE-corrected p < 0.05 at cluster level).

Anatomical structure	Hemi	k	t	x	y	z
Temporal pole	**R**	**281**	**11.02**	**51**	**10**	**-31**
Temporal pole	R		6.93	43	20	-28
Middle temporal gyrus	R		5.93	61	-8	-12
Superior temporal gyrus	R		4.35	48	-10	-15
Precuneus	**R**	**3620**	**9.7**	**8**	**-65**	**29**
Precuneus	R		9.59	11	-52	35
Precuneus	L		9.05	-9	-52	35
Insula	R		8.48	36	-15	4
Central operculum	R		8.01	53	0	10
Insula	**L**	**438**	**8.62**	**-41**	**-8**	**-1**
Insula	L		7.24	-36	-18	18
Insula	L		7.02	-39	-15	2

Precentral gyrus	L		6.99	-59	2	10
Insula	L		5.22	-41	-3	-12
Middle temporal gyrus	**L**	**151**	**8.27**	**-56**	**2**	**-20**
Temporal pole	L		7.06	-54	10	-31
Temporal pole	L		4.5	-44	20	-31
Temporal pole	L		3.99	-41	7	-23
Anterior cingulate cortex	**L**	**96**	**7.36**	**-6**	**27**	**-6**
Anterior cingulate cortex	L		4.09	-6	42	-4
Angular gyrus	**L**	**281**	**7.11**	**-54**	**-62**	**35**
Angular gyrus	L		5.46	-41	-60	26
Middle temporal gyrus	L		5.05	-46	-62	18
Angular gyrus	L		4.46	-46	-75	35
Angular gyrus	L		4.03	-49	-67	43
Angular gyrus	**R**	**389**	**7.02**	**51**	**-57**	**26**
Angular gyrus	R		4.6	46	-65	48
Angular gyrus	R		4.16	43	-72	35
Lateral occipital cortex	R		4.1	46	-77	26
Lateral occipital cortex	R		3.55	56	-62	7

Note. FWE-corrected (p < 0.05) at cluster level, p < 0.001 at peak level.

Table S14. Results for linear mixed-effects model for parameter estimates from fMRI main effects.

	Beta weights		
Coefficient	*Estimates*	*Conf. Int (95%)*	*p*
Intercept	-0.39	-0.54 − -0.24	**< 0.001**
Network	1.07	0.95 − 1.19	**< 0.001**
Age	0.34	0.21 − 0.46	**< 0.001**
Condition	0.49	0.37 − 0.61	**< 0.001**
Network * Age	-0.02	-0.15 − 0.10	0.704
Network * Condition	1.14	1.02 − 1.26	**< 0.001**
Age * Condition	-0.02	-0.14 − 0.10	0.762
Network * Age * Condition	-0.27	-0.39 − -0.15	**< 0.001**
Random Effects			
δ^2	0.91		
θ_{00} Subj	0.06		
ICC	0.06		
N Subj	58		

Observations	232
Marginal R^2 / Conditional R^2	0.751 / 0.766

Note. Significant effects are marked in bold. Contrasts are sum coded. P-values were obtained via likelihood ratio tests. Conf. Int. Confidence interval.

Table S15. Results for post-hoc tests for significant three-way interaction Network x Age x Contrast for parameter estimates model. P-values are Bonferroni-corrected.

Contrast	fMRI contrast	Estimate	SE	df	Conf. Int (95%)	t	p
OA MDN - YA MDN	SF rest	0.04	0.25	196.93	-0.63 – 0.71	0.17	1
OA MDN - OA DMN	SF rest	3.83	0.25	195.3	3.15 – 4.51	15.05	**< 0.001**
OA MDN - YA DMN	SF rest	5.05	0.25	196.93	4.38 – 5.72	20.18	**< 0.001**
YA MDN - OA DMN	SF rest	3.79	0.25	196.93	3.12 – 4.45	15.12	**< 0.001**
YA MDN - YA DMN	SF rest	5.01	0.25	195.3	4.35 – 5.66	20.38	**< 0.001**
OA DMN - YA DMN	SF rest	1.22	0.25	196.93	0.56 – 1.89	4.89	**< 0.001**
OA MDN - YA MDN	Count rest	1.20	0.25	196.93	0.54 – 1.87	4.81	**< 0.001**
OA MDN - OA DMN	Count rest	0.35	0.25	195.3	-0.33 – 1.03	1.38	1
OA MDN - YA DMN	Count rest	0.57	0.25	196.93	-0.10 – 1.24	2.27	0.146
YA MDN - OA DMN	Count rest	-0.85	0.25	196.93	-1.52 – -0.19	-3.41	**0.005**
YA MDN - YA DMN	Count rest	-0.64	0.25	195.3	-1.29 – 0.02	-2.59	0.062
OA DMN - YA DMN	Count rest	0.22	0.25	196.93	-0.45 – 0.89	0.87	1

Note. Significant effects are marked in bold. SF semantic fluency; Count counting; MDN multiple-demand network; DMN default mode network; SE standard error; df degrees of freedom; Conf. Int confidence interval.

Table S16. Young adults: Easy > Difficult semantic categories.

Anatomical structure	Hemi	k	t	x	y	z
Middle frontal gyrus	**R**	**20**	**7.24**	**26**	**2**	**51**
Middle frontal gyrus	R		6.49	31	12	51

Note. FWE-corrected (p < 0.05) at peak level, k $\geq$ 20 voxels.

Table S17. PPI seed: Pre-supplementary Motor Area [-6 12 51].

Anatomical structure	Hemi	k	t	x	y	z
Older adults						
No significant clusters above threshold.						
Young adults						
Caudate nucleus	**L**	**92**	**9.89**	**-14**	**10**	**4**
Caudate nucleus	L		8.68	-16	20	4

Caudate nucleus	L		6.18	-11	7	13
Caudate nucleus	**R**	**76**	**9.19**	**8**	**12**	**2**
Caudate nucleus	R		7.72	18	22	-4
Putamen	R		7.30	18	12	-1
Caudate nucleus	R		6.93	18	25	4
Precuneus	**L**	**125**	**8.31**	**-6**	**-52**	**16**
Posterior cingulate cortex	L		7.60	-4	-55	26
Precuneus	L		7.44	-11	-55	7
Thalamus	**L**	**35**	**7.30**	**-1**	**-13**	**7**
Thalamus	R		7.29	4	-20	10
Thalamus	L		6.50	-9	-25	13

Table S18. PPI seed: Left Insula [-31 25 2].

Anatomical structure	Hemi	*k*	*t*	x	y	z
Older adults						
No significant clusters above threshold.						
Young adults						
Caudate nucleus	**R**	**36**	**10.09**	**8**	**12**	**2**
Caudate nucleus	**L**	**34**	**7.04**	**-14**	**12**	**4**
Caudate nucleus	L		6.33	-16	22	2
Precuneus	**L**	**31**	**6.88**	**-9**	**-60**	**7**
Precuneus	L		6.75	-6	-52	16

Table S19. PPI seed: Right Insula [31 27 2].

Anatomical structure	Hemi	*k*	*t*	*x*	*y*	*z*
Older adults						
Precuneus	**R**	**29**	**8.92**	**1**	**-60**	**26**
Posterior cingulate gyrus	L		8.56	-1	-45	26
Inferior frontal gyrus, pars orbitalis	**L**	**20**	**7.39**	**-31**	**35**	**-15**
Inferior frontal gyrus, pars orbitalis	L		6.46	-44	30	-12
Young adults						
No significant clusters above threshold.						

Table S20. PPI seed: Right Temporal Pole [48 15 -31].

Anatomical structure	Hemi	k	t	x	y	z
Older adults						
Inferior frontal gyrus, pars opercularis	R	24	7.33	51	17	-1
Insula	R		7.02	41	27	-1
Insula	R		6.31	41	12	-1
Young adults						
Inferior frontal gyrus, pars opercularis	R	47	8.48	43	12	21
Inferior frontal gyrus, pars opercularis	R		7.08	53	12	18
Superior frontal gyrus	R	46	8.28	18	2	65
Middle frontal gyrus	R		6.94	31	-3	62
Superior frontal gyrus	R		6.44	21	12	65
Insula	R	75	7.22	43	15	2
Frontal operculum	R		6.76	33	25	7
Frontal operculum	R		6.53	36	15	10
Supramarginal gyrus	R	23	7.21	58	-32	48

Table S21. PPI seed: Right Precuneus [8 -65 29].

Anatomical structure	Hemi	k	t	x	y	z
Older adults						
Insula	R	295	9.27	33	22	10
Inferior frontal gyrus, pars triangularis	R		9.27	53	25	10
Insula	R		8.97	41	25	-6
Inferior frontal gyrus, pars triangularis	R		8.79	46	25	4
Supramarginal gyrus	R	410	9.20	53	-40	46
Angular gyrus	R		9.18	56	-45	32
Supramarginal gyrus	R		8.91	63	-42	35
Angular gyrus	R		8.72	56	-47	48
Middle frontal gyrus	R	125	8.78	33	47	32
Middle frontal gyrus	R		8.04	41	42	29
Middle frontal gyrus	R		7.39	46	45	21
Supramarginal gyrus	L	42	8.77	-61	-47	32
Supramarginal gyrus	L		6.89	-54	-50	35
Inferior frontal gyrus, pars orbitalis	R	61	8.4	48	45	-6
Inferior frontal gyrus, pars triangularis	R		8.03	51	37	-1
Inferior frontal gyrus, pars triangularis	R		7.78	48	40	7
Inferior frontal gyrus, pars triangularis	R		7.38	41	42	-1

Anatomical structure	Hemi	k	t	x	y	z
Presupplementary motor area	**R**	**35**	**8.06**	**4**	**7**	**60**
Presupplementary motor area	R		7.44	6	10	68
Inferior frontal gyrus, pars triangularis	**L**	**70**	**8.02**	**-41**	**17**	**7**
Inferior frontal gyrus, pars triangularis	L		7.85	-36	30	4
Inferior frontal gyrus, pars opercularis	L		6.84	-46	10	7
Superior temporal gyrus	**R**	**32**	**7.86**	**53**	**-15**	**-4**
Middle temporal gyrus	R		7.03	56	-30	-1
Superior temporal gyrus	R		6.77	63	-20	-1
Precentral gyrus	**R**	**93**	**7.85**	**46**	**7**	**35**
Middle frontal gyrus	R		6.89	41	10	46
Middle frontal gyrus	R		6.88	41	15	29
Precentral gyrus	R		6.82	43	5	26
Inferior frontal gyrus, pars opercularis	**R**	**21**	**7.77**	**56**	**15**	**24**
Angular gyrus	**L**	**39**	**7.61**	**-51**	**-52**	**48**
Supramarginal gyrus	L		7.19	-59	-47	43
Lateral occipital cortex	**R**	**29**	**7.15**	**33**	**-67**	**29**
Lateral occipital cortex	R		6.78	26	-77	26
Young adults						
Supramarginal gyrus	**R**	**1300**	**9.69**	**61**	**-45**	**26**
Angular gyrus	R		8.29	63	-47	18
Supramarginal gyrus	R		8.28	51	-42	13
Supramarginal gyrus	R		8.17	58	-32	43
Superior frontal gyrus	**R**	**21**	**9.35**	**8**	**30**	**54**
Superior frontal gyrus	**R**	**185**	**9.03**	**11**	**5**	**62**
Superior frontal gyrus	R		8.40	16	12	65
Superior frontal gyrus	R		7.35	11	-10	68
Superior frontal gyrus	R		6.78	18	-3	73
Insula	**L**	**194**	**8.80**	**-44**	**10**	**-4**
Insula	L		7.86	-46	2	4
Insula	L		7.81	-34	2	0
Insula	L		6.91	-44	22	-6
Precentral gyrus	**R**	**79**	**8.36**	**46**	**-3**	**48**
Middle frontal gyrus	R		6.85	43	-3	57
Precentral gyrus	R		6.53	51	2	40
Precentral gyrus	R		6.49	33	-8	48
Anterior cingulate cortex, dorsal part	**R**	**147**	**7.97**	**11**	**17**	**35**
Anterior cingulate cortex, dorsal part	L		7.14	-1	5	43

Anatomical structure	Hemi	*k*	*t*	*x*	*y*	*z*
Anterior cingulate cortex	L		6.79	-4	25	24
Anterior cingulate cortex, dorsal part	R		6.00	4	-5	40
Middle temporal gyrus	**R**	**161**	**7.92**	**48**	**-60**	**13**
Middle temporal gyrus	R		7.44	56	-52	2
Middle temporal gyrus	R		6.88	56	-57	10
Middle temporal gyrus	R		6.34	43	-67	-1
Angular gyrus	**L**	**201**	**7.84**	**-61**	**-50**	**35**
Supramarginal gyrus	L		7.80	-64	-47	26
Supramarginal gyrus	L		7.40	-64	-40	32
Central operculum	L		6.85	-59	-23	16
Posterior cingulate cortex	**R**	**187**	**7.60**	**8**	**-30**	**46**
Precuneus	R		7.35	6	-42	51
Precentral gyrus	R		7.35	6	-18	48
Precuneus	R		7.15	8	-57	62
Posterior cingulate cortex	**L**	**24**	**7.59**	**-1**	**-25**	**26**
Posterior cingulate cortex	R		6.86	6	-28	29
Superior occipital gyrus	**L**	**24**	**7.39**	**-16**	**-77**	**43**
Lateral occipital cortex	**L**	**38**	**7.34**	**-31**	**-82**	**16**
Lateral occipital cortex	L		6.37	-29	-92	18
Cuneus	**R**	**31**	**7.32**	**18**	**-82**	**26**
Cuneus	**R**	**58**	**7.30**	**13**	**-75**	**26**
Lateral occipital cortex	R		6.51	13	-75	46
Cuneus	R		6.23	13	-75	35
Cuneus	R		6.0	8	-80	40
Lateral occipital cortex	**R**	**61**	**7.30**	**31**	**-75**	**24**
Calcarine gyrus	**R**	**50**	**7.11**	**1**	**-70**	**13**
Lingual gyrus	R		6.44	4	-80	2
Intracalcarine cortex	L		6.38	-6	-75	18
Postcentral gyrus	**L**	**20**	**6.74**	**-9**	**-47**	**57**
Precentral gyrus	L		6.33	-14	-37	43
Fusiform gyrus	**R**	**24**	**6.67**	**36**	**-67**	**-15**
Fusiform gyrus	R		6.66	28	-72	-12
Middle frontal gyrus	**R**	**23**	**6.51**	**31**	**40**	**26**
Middle frontal gyrus	R		6.22	41	42	29

Table S22. Results for linear model for within and between network connectivity.

PPI variable	FC	IV	*b*	*SE*	*t*	*p*
Semantic fluency > Counting	Within MDN	Intercept	0.05	0.02	2.70	**0.009**
		Age	0.005	0.03	0.18	0.85
	Within DMN	Intercept	-0.002	0.02	-0.07	0.95
		Age	0.02	0.03	0.50	0.63
	Between MDN and DMN	Intercept	0.10	0.02	4.47	**< 0.001**
		Age	0.04	0.03	1.25	0.22

Note. Significant effects are marked in bold: p < Meff-corrected $alpha$ of 0.018; FC Functional connectivity; IV Independent variable; MDN Multiple-demand network; DMN Default-mode network.

Table S23. Results for generalized linear mixed models for within- and between-network functional connectivity effects, age, and condition on accuracy and response time.

	Accuracy			Response time		
Coefficient	Log-Odds	*Conf. Int (95%)*	*p*	*Estimates*	*Conf. Int (95%)*	*p*
Intercept	3.09	2.48 – 3.70	**< 0.001**	6.53	6.48 – 6.58	**< 0.001**
Within-MDN FC	0.22	-1.41 – 1.84	0.592	-0.13	-0.28 – 0.03	0.493
Within-DMN FC	-0.82	-2.42 – 0.79	0.302	-0.35	-0.53 – -0.18	**< 0.001**
Between-network FC	0.56	-1.22 – 2.34	0.556	0.53	0.36 – 0.71	**< 0.001**
Age	-0.17	-0.29 – -0.01	0.11	-0.01	-0.02 – 0.01	**< 0.001**
Education	-0.15	-0.29 – -0.01	**0.028**	-0.01	-0.02 – 0.01	0.061
Within-MDN FC * Age	1.15	-1.93 – 4.23	0.469	0.94	0.60 – 1.28	**< 0.001**
Within-DMN FC * Age	2.06	-0.77 – 4.90	0.157	0.90	0.62 – 1.19	**< 0.001**
Between-network FC * Age	-2.41	-5.42 – 0.60	0.119	-0.79	-1.10 – -0.47	**< 0.001**
Random Effects						
δ^2	3.29			0.13		
θ_{00}	0.22 Subj			0.01 Subj		
	1.71 Category			0.00 Category		
ICC	0.37			0.12		
N	58 Subj			58 Subj		
	20 Category			20 Category		
Observations	9837			9675		
Marginal R^2 / Conditional R^2	0.002 / 0.371			0.027 / 0.143		
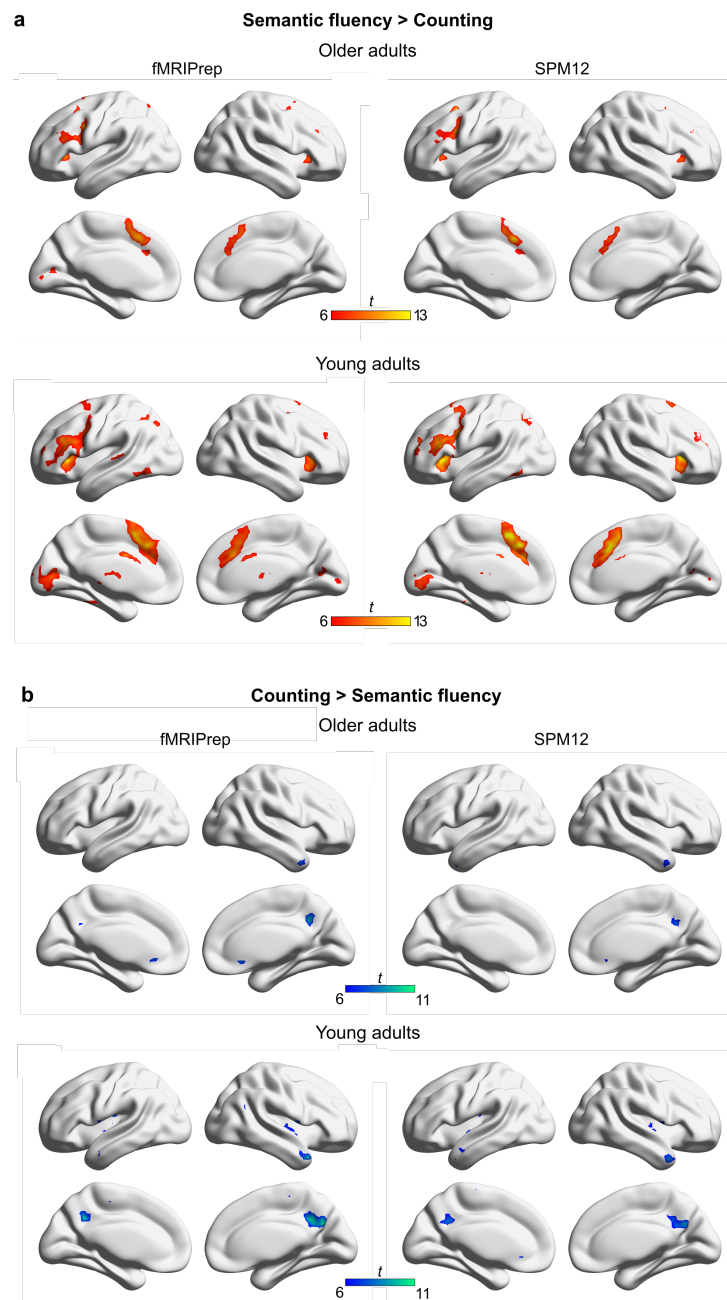
Note. Significant effects are marked in bold. Contrasts are sum coded. P-values were obtained via likelihood ratio tests. Conf. Int. Confidence interval.

Table S24. . Results of post-hoc tests for two-way interactions Age x Connectivity measure for response time model. P-values are Bonferroni-corrected.
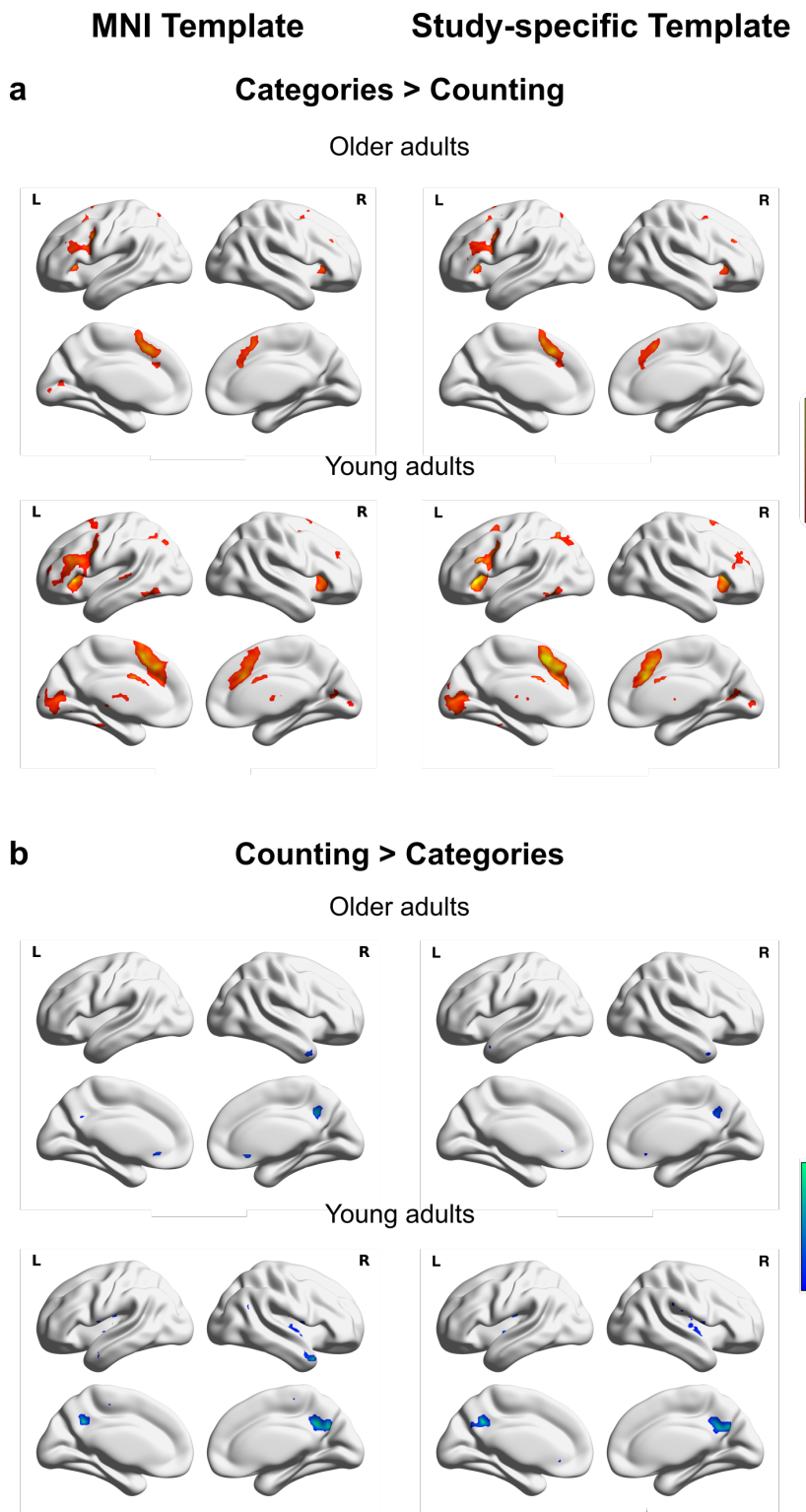
Contrast	FC	Estimate	SE	df	Conf. Int (95%)	z	p
OA – YA	Within MDN	636	118	Inf	405 – 867	5.39	**< 0.001**
	Within DMN	604	100	Inf	407 – 800	6	**< 0.001**
	Between MDN and DMN	-516	110	Inf	-732 – -301	-4.69	**< 0.001**

Note. Significant effects are marked in bold. FC functional connectivity; SE standard error; df degrees of freedom; Conf. Int confidence intervals.

B Supplementary Material for Study 2

a   **Semantic fluency > Counting**

Older adults

fMRIPrep   SPM12

t
6 ▮▮▮▮ 13

Young adults

t
6 ▮▮▮▮ 13

b   **Counting > Semantic fluency**

Older adults

fMRIPrep   SPM12

t
6 ▮▮▮▮ 11

Young adults

t
6 ▮▮▮▮ 11
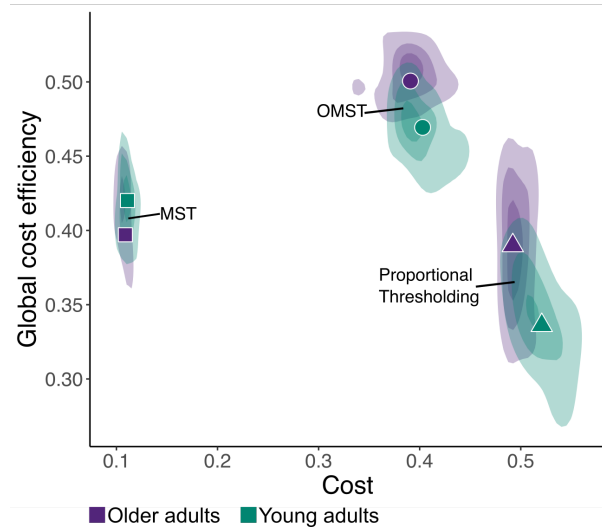
Figure S1. Comparison of different preprocessing pipelines. Plots show univariate results for preprocessing with fMRIPrep 20.2.3 and SPM12 in each age group for contrasts (A) Semantic fluency > Counting and (B) Counting > Semantic fluency. Results are FWE-corr. p < 0.05 at peak-level with a minimum cluster size of k = 10 voxels.

MNI Template　　　**Study-specific Template**

a　　　　　**Categories > Counting**

Older adults

Young adults

b　　　　　**Counting > Categories**

Older adults

Young adults
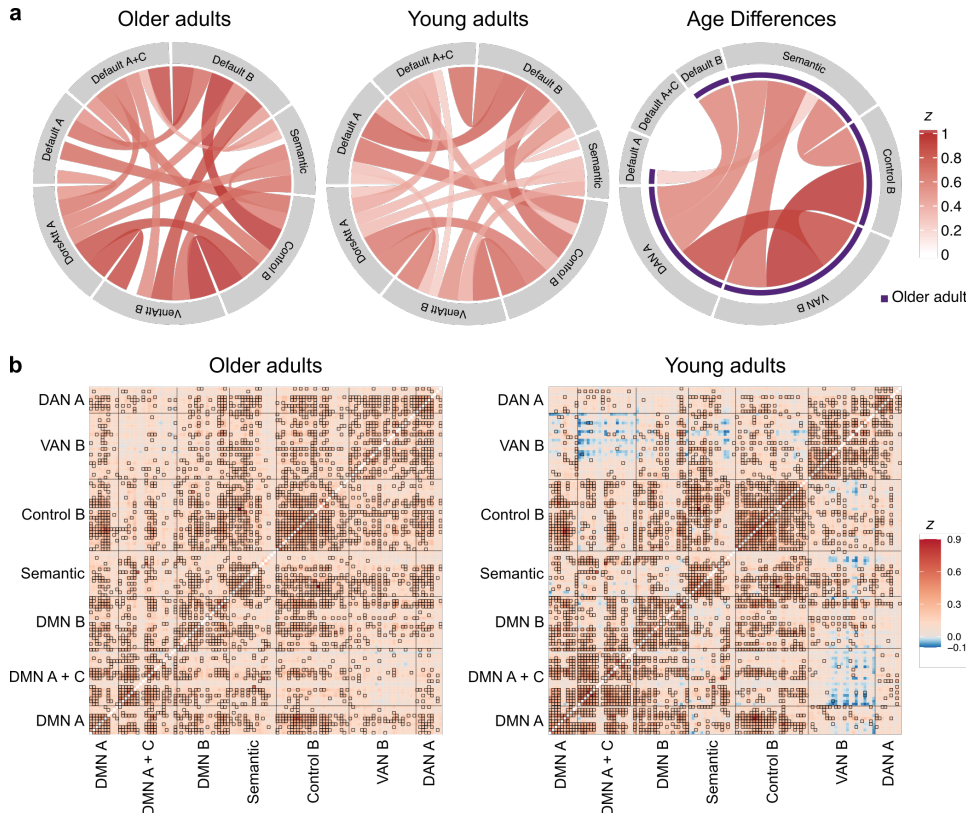
Figure S2. Comparison of within-group task effects for two different resampling procedures. Using the MNI standard template and a study-specific template. Results are FWE-corr. p < 0.05 at peak-level with a minimum cluster size of k = 10 voxels.

Figure S3 displays all 55 components resolved through our multivariate ICA analysis. Please see the Supplementary Material available online for all components: Link to
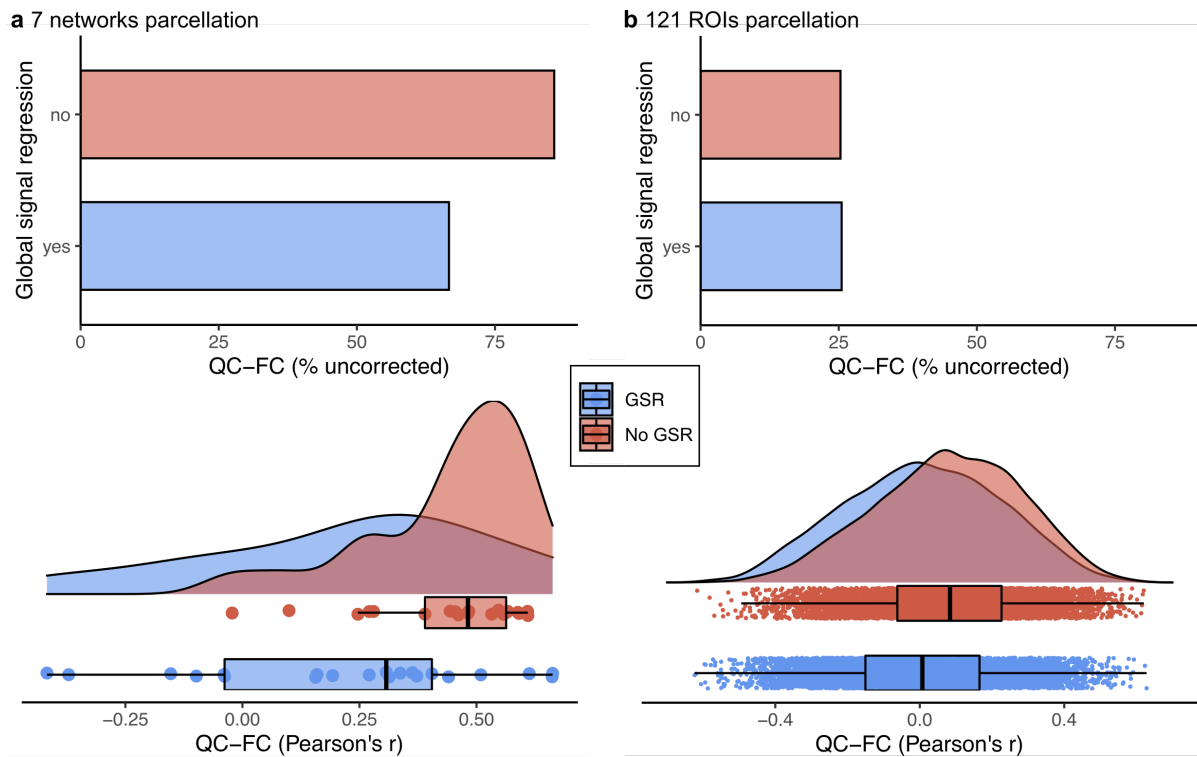
Supplementary Materials

Figure S4. Plots of global cost efficiency (GCE) against cost for different filtering options of graphs. We compared the GCE of two topological (minimum spanning tree (MST) and orthogonal minimum spanning tree (OMST)) and one proportional (5-20% strongest edge weights) edge filtering method in both age groups. Symbols indicate the average value in each group while densities display value distribution.
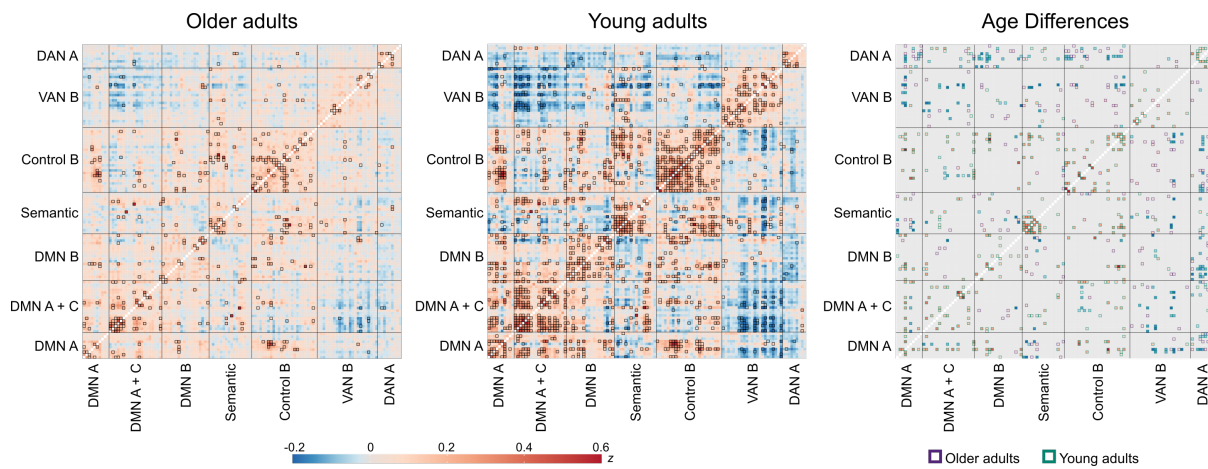
Figure S5. Within- and between-network functional connectivity results for denoising pipeline without global signal regression. (a) Chord diagrams display significant results of functional coupling for whole ICA-derived networks. Age differences were assessed using permutation testing in network-based statistics (cluster-forming threshold at p = 0.01, FWE-corrected significance threshold at p = 0.025 with 10,000 permutations). (b) Heatmaps show functional coupling between individual regions of interest (n = 121) of the seven networks. Note that there were no significant age differences at p = 0.025.

a 7 networks parcellation

b 121 ROIs parcellation

Figure S6. Comparison of denoising pipelines with global signal regression (GSR) and without for association between motion (mean FD) and functional connectivity (FC). The upper panels display the proportion of FC values that are correlated to mean FD at a threshold p < 0.05, uncorrected. The bottom panels show the distribution of all QC-FC correlations as smoothed kernel density estimates and boxplots with medians and interquartile ranges.

Supplementary Results

Older adults

Young adults

Age Differences

Figure S7. Heatmaps display significant results of functional coupling between the regions of interest (n = 121) of the ICA-derived networks. Connectivity values are Fisher-transformed partial correlations. Bold frames indicate significant values which are based on cPPI-derived significance values in the age groups while age differences were assessed using permutation testing in network-based statistics (cluster-forming threshold at p = 0.01, FWE-corrected significance threshold at p = 0.025 with 10,000 permutations).

Table S1. Behavioral results of mixed-effects models for accuracy and response time

Coefficient	Accuracy				Response time			
	Log-Odds	*CI*	*z-value*	*p*	*Estimates*	*CI*	*t-value*	*p*
Intercept	4.63	4.15 − 5.10	19.09	**<0.001**	6.43	6.39 − 6.47	326.96	**<0.001**
Age	-0.68	-1.13 − -0.23	-2.98	**0.003**	0.01	0.00 − 0.03	2.30	**0.021**
Condition	-3.16	-4.06 − -2.26	-6.90	**<0.001**	0.15	0.10 − 0.19	6.29	**<0.001**
Difficulty	2.01	1.50 − 2.51	7.76	**<0.001**	-0.07	-0.10 − -0.04	-4.71	**<0.001**
Education	-0.11	-0.24 − 0.01	-1.75	0.080	-0.01	-0.01 − 0.00	-1.88	0.060
Age * Condition	0.64	-0.18 − 1.46	1.53	0.125	0.08	0.06 − 0.10	8.94	**<0.001**
Age * Difficulty	-0.67	-1.08 − -0.26	-3.19	**0.001**	-0.00	-0.02 − 0.01	-0.39	0.695
Random Effects								
δ^2	3.29				0.09			
θ_{00}	0.19 Subj				0.01 Subj			
	0.29 Category				0.00 Category			
ICC	0.13				0.09			
Observations	19710				18877			
Marg R^2 / Cond R^2	0.495 / 0.559				0.065 / 0.148			

Note. Significant effects are marked in bold. Contrasts are sum coded. P-values were obtained via likelihood ratio tests. CI Confidence interval.

Table S2. Jaccard similarity coefficients with the 7-networks parcellation scheme

	IC06	IC09	IC13	IC16	IC18	IC45	IC52
Control	0.128	**0.287**	0.039	0.054	*0.194*	*0.161*	0.090
Default	**0.155**	*0.154*	**0.234**	**0.412**	0.133	0.133	0.043
Dorsal attention	0.073	0.089	0.067	0.022	0.139	0.059	**0.301**
Limbic	0.000	0.004	0.012	0.014	0.008	0.005	0.011
Ventral attention	0.039	0.045	0.025	0.039	0.053	**0.211**	0.097
Somatomotor	0.017	0.064	0.029	0.057	0.067	0.044	0.052
Visual	0.038	0.015	0.090	0.046	0.045	0.028	*0.177*
General semantic cognition	0.032	0.030	0.072	*0.194*	**0.201**	0.092	0.050
Semantic control	0.012	0.036	0.012	0.067	*0.153*	0.091	0.027

Note. The selected network labels for the respective independent components are shown in bold while all cognitive networks that showed a higher similarity coefficient than J = 0.15 are shown in italics.

Table S3. Significant clusters of task-relevant independent components

Anatomical structure	Hemi	*k*	*t*	*x*	*y*	*z*
IC 06						
Precuneus Cortex	R	1057	19.94	5	-71	35
Precuneus Cortex	L		17.67	-5	-66	38

Anatomical structure	Hemi	k	t	x	y	z
Cingulate Gyrus, posterior division	R		17.43	2	-41	35
Angular Gyrus	**L**	**242**	**14.56**	**-45**	**-64**	**46**
Angular Gyrus	L		13.29	-48	-56	44
Angular Gyrus	**R**	**289**	**14.31**	**47**	**-56**	**44**
Angular Gyrus	R		10.44	54	-51	41
Angular Gyrus	R		9.58	52	-54	33
Cingulate Gyrus, anterior division	**R**	**51**	**7.58**	**2**	**43**	**5**
Paracingulate Gyrus	R		6.17	5	46	-3
Paracingulate Gyrus	**L**	**25**	**6.96**	**-3**	**38**	**22**
Frontal Pole	**L**	**16**	**6.43**	**-23**	**66**	**5**

IC 09

Frontal Pole	**R**	**564**	**21.83**	**42**	**48**	**-9**
Frontal Pole	R		20.52	49	43	-9
Frontal Pole	R		19.22	29	56	5
Middle Frontal Gyrus	**R**	**810**	**21.33**	**49**	**31**	**33**
Middle Frontal Gyrus	R		18.52	37	21	55
Middle Frontal Gyrus	R		18.25	52	16	41
Angular Gyrus	**R**	**520**	**20.75**	**52**	**-51**	**44**
Angular Gyrus	R		20.72	57	-56	38
Angular Gyrus	R		20.26	39	-61	52
Middle Temporal Gyrus, posterior division	**R**	**104**	**18.62**	**62**	**-36**	**-12**
Middle Temporal Gyrus, temporooccipital part	R		16.94	59	-46	-12
Middle Temporal Gyrus, temporooccipital part	R		14.67	67	-39	-3
Superior Frontal Gyrus	**R**	**335**	**18.38**	**5**	**36**	**44**
Paracingulate Gyrus	R		18.04	7	26	46
Superior Frontal Gyrus	L		10.93	-5	33	46
Angular Gyrus	**L**	**364**	**15.31**	**-48**	**-54**	**55**
Angular Gyrus	L		12.43	-45	-61	52
Angular Gyrus	L		11.15	-38	-59	46
Frontal Pole	**L**	**231**	**14.18**	**-43**	**53**	**2**
Frontal Pole	L		13.29	-38	61	-1
Frontal Pole	L		10.39	-48	46	-12
Middle Frontal Gyrus	**L**	**200**	**10.80**	**-50**	**26**	**35**
Middle Frontal Gyrus	L		10.27	-48	21	44
Middle Temporal Gyrus, posterior division	**L**	**41**	**7.73**	**-63**	**-36**	**-9**
Superior Frontal Gyrus	**L**	**10**	**6.08**	**-23**	**18**	**57**

IC 13

Precuneus Cortex	**L**	**1459**	**32.20**	**-5**	**-59**	**19**
Precuneus Cortex	R		32.11	5	-59	27

Anatomical structure	Hemi	*k*	*t*	*x*	*y*	*z*
Precuneus Cortex	R		26.92	7	-54	16
Angular Gyrus	**L**	**525**	**20.64**	**-48**	**-71**	**30**
Angular Gyrus	L		18.65	-40	-66	27
Angular Gyrus	L		14.87	-38	-79	41
Parahippocampal Gyrus, posterior division	**L**	**207**	**18.74**	**-25**	**-31**	**-17**
Parahippocampal Gyrus, anterior division	L		10.87	-20	-22	-20
Lingual Gyrus	L		10.86	-25	-41	-6
Superior Frontal Gyrus	**L**	**228**	**16.63**	**-23**	**28**	**49**
Angular Gyrus	**R**	**461**	**15.89**	**52**	**-64**	**24**
Angular Gyrus	R		13.36	54	-69	35
Angular Gyrus	R		11.74	44	-54	22
Frontal Medial Cortex	**L**	**718**	**15.37**	**-5**	**51**	**-9**
Cingulate Gyrus, anterior division	R		13.77	2	33	-9
Frontal Medial Cortex	R		12.56	2	53	-6
Middle Temporal Gyrus, anterior division	**R**	**109**	**14.58**	**64**	**1**	**-17**
Parahippocampal Gyrus, posterior division	**R**	**133**	**11.99**	**27**	**-31**	**-17**
Parahippocampal Gyrus, anterior division	R		11.68	22	**-19**	-23
Superior Frontal Gyrus	**R**	**185**	**11.08**	**22**	**31**	**46**

IC 16						
Frontal Pole	**L**	**1390**	**23.11**	**-5**	**48**	**46**
Superior Frontal Gyrus	R		21.03	14	31	57
Paracingulate Gyrus	L		20.26	-5	53	19
Middle Temporal Gyrus, anterior division	**L**	**1382**	**23.08**	**-55**	**1**	**-20**
Middle Temporal Gyrus, posterior division	L		21.78	-58	-31	-3
Frontal Pole	L		19.89	-50	43	-12
Angular Gyrus	**L**	**356**	**22.67**	**-55**	**-59**	**30**
Supramarginal Gyrus, posterior division	L		14.15	-63	-49	41
Inferior Frontal Gyrus, pars triangularis	**R**	**313**	**17.26**	**52**	**31**	**-6**
Temporal Pole	R		12.61	37	23	-23
Frontal Orbital Cortex	R		11.27	44	23	-14
Temporal Pole	**R**	**238**	**16.84**	**52**	**16**	**-25**
Middle Temporal Gyrus, anterior division	R		16.64	52	3	-31
Temporal Pole	R		15.86	49	11	-34
Middle Temporal Gyrus, posterior division	**R**	**193**	**16.70**	**64**	**-29**	**-3**
Middle Temporal Gyrus, posterior division	R		15.08	54	-24	-6
Middle Temporal Gyrus, posterior division	R		14.76	67	-36	-1
Middle Frontal Gyrus	**L**	**151**	**16.01**	**-40**	**16**	**52**

IC 18						
Insular Cortex	**L**	**1554**	**28.83**	**-33**	**21**	**-1**

Anatomical structure	Hemi	k	t	x	y	z
Inferior Frontal Gyrus, pars triangularis	L		21.00	-48	28	19
Middle Frontal Gyrus	L		19.65	-50	21	33
Superior Frontal Gyrus	**L**	**511**	**22.76**	**-5**	**31**	**44**
Paracingulate Gyrus	L		19.99	-5	13	52
Paracingulate Gyrus	R		18.29	2	21	46
Inferior Temporal Gyrus, temporooccipital part	**L**	**984**	**18.99**	**-58**	**-49**	**-12**
Superior Temporal Gyrus, posterior division	L		10.54	-60	-31	5
Parahippocampal Gyrus, posterior division	L		9.82	-30	-31	-17
Angular Gyrus	**L**	**270**	**16.99**	**-35**	**-59**	**41**
Angular Gyrus	L		16.88	-30	-66	49
Angular Gyrus	L		16.52	-30	-71	41
Superior Frontal Gyrus	**L**	**50**	**11.92**	**-23**	**26**	**46**
Superior Frontal Gyrus	L		9.63	-15	36	46
Frontal Pole	L		8.39	-13	48	44
Temporal Fusiform Cortex, anterior division	**L**	**22**	**9.50**	**-38**	**-9**	**-28**
Superior Temporal Gyrus, anterior division	**R**	**32**	**9.14**	**59**	**-4**	**-1**
IC 45						
Frontal Pole	**L**	**583**	**23.44**	**-25**	**38**	**30**
Frontal Pole	L		21.05	-23	46	24
Frontal Pole	L		19.36	-30	53	24
Paracingulate Gyrus	**L**	**565**	**21.83**	**-5**	**31**	**33**
Cingulate Gyrus, anterior division	L		21.81	-5	31	22
Paracingulate Gyrus	R		21.76	14	28	27
Frontal Pole	**R**	**630**	**20.80**	**27**	**48**	**30**
Frontal Pole	R		20.35	27	41	24
Frontal Pole	R		18.56	37	43	30
Frontal Operculum Cortex	**L**	**225**	**16.57**	**-35**	**16**	**11**
Frontal Orbital Cortex	L		15.46	-33	26	-6
Inferior Frontal Gyrus, pars opercularis	L		15.04	-50	13	-3
Frontal Operculum Cortex	**R**	**280**	**16.15**	**47**	**18**	**-3**
Frontal Operculum Cortex	R		15.26	39	18	11
Frontal Orbital Cortex	R		14.28	39	18	-12
Supramarginal Gyrus, posterior division	**R**	**157**	**14.98**	**62**	**-44**	**27**
Supramarginal Gyrus, posterior division	R		13.20	67	-39	35
Supramarginal Gyrus, posterior division	R		5.93	62	-39	49
Superior Frontal Gyrus	**L**	**27**	**14.57**	**-13**	**3**	**68**
Superior Frontal Gyrus	L		12.61	-8	8	63
Supramarginal Gyrus, posterior division	**L**	**41**	**11.77**	**-60**	**-44**	**27**
Inferior Frontal Gyrus, pars opercularis	**R**	**22**	**8.01**	**52**	**11**	**11**

Anatomical structure	Hemi	k	t	x	y	z
Inferior Frontal Gyrus, pars opercularis	R		6.73	54	13	22
Frontal Pole	**L**	**27**	**7.76**	**-30**	**46**	**-14**
Inferior Frontal Gyrus, pars opercularis	**L**	**17**	**7.00**	**-50**	**11**	**11**
IC 52						
Angular Gyrus	**R**	**1860**	**22.56**	**27**	**-69**	**44**
Angular Gyrus	R		21.55	39	-76	27
Inferior Temporal Gyrus, temporooccipital part	R		20.54	52	-59	-12
Lateral Occipital Cortex, inferior division	**L**	**1437**	**21.63**	**-48**	**-66**	**2**
Angular Gyrus	L		21.17	-43	-81	16
Angular Gyrus	L		20.11	-28	-76	30
Temporal Occipital Fusiform Cortex	**L**	**24**	**12.07**	**-28**	**-51**	**-12**
Temporal Fusiform Cortex, posterior division	L		8.92	-30	-41	-12
Temporal Occipital Fusiform Cortex	**R**	**15**	**8.49**	**37**	**-44**	**-23**

Note. Results are based on one-sided t-tests and FWE-corrected $p < 0.05$ at peak level with a cluster extent threshold $k = 10$.

Table S4. Results for significant effects of cPPI connectivity for accuracy

	Accuracy				Accuracy			
Coefficient	*Log-Odds*	*CI*	*Statistic*	*p*	*Log-Odds*	*CI*	*Statistic*	*p*
Intercept	2.99	2.38 – 3.60	9.58	**<0.001**	3.19	2.58 – 3.80	10.21	**<0.001**
DMN A+C & VAN B	-0.93	-1.66 – -0.21	-2.52	**0.012**				
Age	-0.03	-0.28 – 0.22	-0.23	0.815	0.05	-0.28 – 0.38	0.31	0.754
Education	-0.12	-0.24 – 0.01	-1.80	0.072	-0.16	-0.29 – -0.02	-2.27	**0.023**
Motion RMSD	1.74	-1.46 – 4.94	1.07	0.286	-2.51	-5.39 – 0.36	-1.72	0.086
Age * DMN A+C & VAN B	2.01	0.89 – 3.13	3.51	**<0.001**				
VAN B & DAN A					-0.74	-1.91 – 0.43	-1.25	0.213
Age * VAN B & DAN A					-3.43	-5.20 – -1.65	-3.78	**<0.001**
Random Effects								
δ^2	3.29				3.29			
θ_{00}	0.18 sub				0.19 sub			
	1.71 Category				1.71 Category			
ICC	0.37				0.37			
Observations	9837				9837			
Marg R^2 / Cond R^2	0.012 / 0.373				0.013 / 0.374			

Note. Significant effects are marked in bold. Contrasts are sum coded. P-values were obtained via likelihood ratio tests. CI Confidence interval.

Table S5. Results for significant effects of cPPI connectivity for response time

	Response time				**Response time**			
Coefficient	*Estimates*	*CI*	*Statistic*	*p*	*Estimates*	*CI*	*Statistic*	*p*
Intercept	6.48	6.44 – 6.52	324.58	**<0.001**	6.48	6.44 – 6.53	297.98	**<0.001**
DMN A & SEM	-0.22	-0.30 – -0.14	-5.41	**<0.001**				
Age	0.07	0.05 – 0.10	5.40	**<0.001**	0.07	0.04 – 0.10	4.82	**<0.001**
Education	0.01	-0.00 – 0.02	1.25	0.211	-0.00	-0.01 – 0.01	-0.08	0.935
Motion RMSD	0.40	0.14 – 0.65	3.02	**0.003**	0.24	-0.01 – 0.49	1.87	0.061
Age * DMN A & SEM	0.69	0.55 – 0.83	9.54	**<0.001**				
DMN B & DAN A					-0.23	-0.31 – -0.14	-5.42	**<0.001**
Age * DMN B & DAN A					0.56	0.41 – 0.72	7.21	**<0.001**
Random Effects								
δ^2	0.11				0.11			
θ_{00}	0.01 sub				0.01 sub			
	0.00 Category				0.00 Category			
ICC	0.08				0.10			
Observations	9069				9069			
Marg R^2 / Cond R^2	0.032 / 0.113				0.020 / 0.118			

Note. Significant effects are marked in bold. Contrasts are sum coded. P-values were obtained via likelihood ratio tests. CI Confidence interval.

Table S5 cont. Results for significant effects of cPPI connectivity for response time

	Response time				**Response time**			
Coefficient	*Estimates*	*CI*	*Statistic*	*p*	*Estimates*	*CI*	*Statistic*	*p*
Intercept	6.53	6.49 – 6.57	302.80	**<0.001**	6.52	6.47 – 6.56	302.21	**<0.001**
Age	0.04	0.02 – 0.07	3.15	**0.002**	0.12	0.09 – 0.16	7.05	**<0.001**
Education	0.00	-0.01 – 0.01	0.28	0.783	0.00	-0.01 – 0.01	0.03	0.978
Motion RMSD	0.33	0.08 – 0.58	2.60	**0.009**	-0.29	-0.56 – -0.01	-2.05	**0.041**
SEM & VAN B	0.02	-0.05 – 0.09	0.47	0.642				
Age * SEM & VAN B	-0.57	-0.79 – -0.35	-5.12	**<0.001**				
VAN B & DAN A					-0.48	-0.60 – -0.35	-7.62	**<0.001**
Age * VAN B & DAN A					-0.44	-0.60 – -0.28	-5.37	**<0.001**
Random Effects								
δ^2	0.11				0.11			
θ_{00}	0.01 sub				0.01 sub			
	0.00 Category				0.00 Category			
ICC	0.09				0.10			
Observations	9069				9069			
Marg R^2 / Cond R^2	0.020 / 0.113				0.042 / 0.138			

Note. Significant effects are marked in bold. Contrasts are sum coded. P-values were obtained via likelihood ratio tests. CI Confidence interval.

Table S6. Results for linear mixed-effects model on the effect of age on brain system segregation

	Brain system segregation			
Coefficient	*Estimates*	*CI*	*Statistic*	*p*
Intercept	0.48	0.45 − 0.51	31.57	**<0.001**
Age	0.08	0.04 − 0.13	3.68	**0.001**
Motion RMSD	-0.76	-1.20 − -0.33	-3.52	**0.001**
Random Effects				
δ^2	0.00			
θ_{00} sub	0.00			
ICC	0.06			
Observations	58			
Marginal R^2 / Conditional R^2	0.523 / 0.553			

Note. Significant effects are marked in bold. Contrasts are sum coded. P-values were obtained via likelihood ratio tests. CI Confidence interval.

Table S7. Results for mixed-effects models on the effect of brain system segregation on accuracy and response time

	Accuracy				**Response time**			
Coefficient	*Log-Odds*	*CI*	*Statistic*	*p*	*Estimates*	*CI*	*Statistic*	*p*
Intercept	2.97	2.35 − 3.58	9.47	**<0.001**	6.55	6.49 − 6.60	242.95	**<0.001**
Global segregation	2.62	0.64 − 4.61	2.59	**0.010**	-1.31	-1.54 − -1.08	-11.29	**<0.001**
Age	0.08	-0.19 − 0.35	0.58	0.560	-0.02	-0.05 − 0.01	-1.57	0.116
Education	-0.14	-0.28 − -0.01	-2.08	**0.038**	0.02	0.01 − 0.04	3.50	**<0.001**
Motion RMSD	0.83	-2.15 − 3.81	0.55	0.584	-1.07	-1.41 − -0.73	-6.17	**<0.001**
Age * Glob Seg	-5.01	-8.17 − -1.85	-3.11	**0.002**	1.48	1.13 − 1.83	8.26	**<0.001**
Random Effects								
δ^2	3.29				0.11			
θ_{00}	0.17 sub				0.02 sub			
	1.71 Category				0.00 Category			
ICC	0.36				0.15			
Observations	9837				9069			
Marg R^2 / Cond R^2	0.010 / 0.370				0.050 / 0.193			

Note. Significant effects are marked in bold. Contrasts are sum coded. P-values were obtained via likelihood ratio tests. CI Confidence interval, Glob Seg Global Segregation.

Table S8. Results for linear mixed-effects model on the effect of age on global efficiency

	Global efficiency			
Coefficient	*Estimates*	*CI*	*Statistic*	*p*

Intercept	0.10	0.10 − 0.11	38.20	**<0.001**
Age	0.02	0.01 − 0.03	5.02	**<0.001**
Motion RMSD	-0.08	-0.16 − -0.00	-2.11	**0.040**
Random Effects				
δ^2	0.00			
θ_{00} sub	0.00			
ICC	0.16			
Observations	58			
Marginal R^2 / Conditional R^2	0.511 / 0.589			

Note. Significant effects are marked in bold. Contrasts are sum coded. P-values were obtained via likelihood ratio tests. CI Confidence interval.

Table S9. Results for mixed-effects models on the effect of global efficiency on accuracy and response time

	Accuracy				**Response time**			
Coefficient	*Log-Odds*	*CI*	*Statistic*	*p*	*Estimates*	*CI*	*Statistic*	*p*
Intercept	3.05	2.42 − 3.67	9.54	**<0.001**	6.47	6.43 − 6.52	296.92	**<0.001**
Global efficiency	13.53	4.33 − 22.73	2.88	**0.004**	0.55	-0.31 − 1.41	1.25	0.212
Age	0.13	-0.17 − 0.43	0.86	0.387	0.04	0.01 − 0.07	2.85	**0.004**
Education	-0.10	-0.23 − 0.04	-1.42	0.157	0.01	-0.01 − 0.02	1.05	0.293
Motion RMSD	0.96	-1.93 − 3.85	0.65	0.517	0.60	0.32 − 0.88	4.19	**<0.001**
Age * Glob eff	-13.71	-33.96 − 6.54	-1.33	0.185	-5.50	-7.23 − -3.76	-6.21	**<0.001**
Random Effects								
δ^2	3.29				0.11			
θ_{00}	0.24 sub				0.01 sub			
	1.71 Category				0.00 Category			
ICC	0.37				0.10			
Observations	9837				9069			
Marg R^2 / Cond R^2	0.009 / 0.378				0.018 / 0.112			

Note. Significant effects are marked in bold. Contrasts are sum coded. P-values were obtained via likelihood ratio tests. CI Confidence interval, Glob Eff Global Efficiency.

Table S10. Results for linear mixed-effects model on the effect of age on brain segregation as a function of network type

	Network segregation			
Coefficient	*Estimates*	*CI*	*Statistic*	*p*
Intercept	0.42	0.38 − 0.45	23.69	**<0.001**
Age	-0.11	-0.13 − -0.08	-7.09	**<0.001**

DMN A+C	0.22	0.18 − 0.26	10.67	**<0.001**
DMN B	0.06	0.02 − 0.10	2.82	**0.005**
SEM	0.02	-0.02 − 0.06	0.99	0.323
CONT B	0.13	0.09 − 0.17	6.43	**<0.001**
VAN B	0.17	0.13 − 0.21	8.30	**<0.001**
DAN A	0.31	0.27 − 0.35	14.86	**<0.001**
Motion RMSD	-0.67	-0.98 − -0.36	-4.24	**<0.001**
Random Effects				
δ^2	0.01			
θ_{00} sub	0.00			
ICC	0.10			
Observations	406			
Marginal R^2 / Conditional R^2	0.552 / 0.599			

Note. Significant effects are marked in bold. Contrasts are sum coded. P-values were obtained via likelihood ratio tests. CI Confidence interval.

Table S11. Results for mixed-effects models on the effect of network segregation on accuracy and response time

	Accuracy				Response time			
Coefficient	*Log-Odds*	*CI*	*Statistic*	*p*	*Estimates*	*CI*	*Statistic*	*p*
Intercept	2.93	2.32 − 3.54	9.37	**<0.001**	6.55	6.47 − 6.63	159.97	**<0.001**
DMN A	0.49	-0.27 − 1.26	1.26	0.208	0.62	0.52 − 0.72	12.02	**<0.001**
DMN A+C	-0.28	-1.67 − 1.12	-0.39	0.698	-0.24	-0.45 − -0.02	-2.12	**0.034**
DMN B	1.01	-0.18 − 2.20	1.67	0.095	0.21	0.04 − 0.38	2.41	**0.016**
SEM	-0.24	-1.19 − 0.71	-0.50	0.619	-0.59	-0.71 − -0.46	-9.17	**<0.001**
CONT B	1.75	0.15 − 3.34	2.15	**0.032**	-0.41	-0.67 − -0.15	-3.11	**0.002**
VAN B	1.15	0.06 − 2.24	2.07	**0.038**	-0.16	-0.31 − 0.00	-1.96	0.050
DAN A	-2.20	-3.46 − -0.94	-3.43	**0.001**	-0.31	-0.45 − -0.18	-4.49	**<0.001**
Age	-0.16	-0.52 − 0.20	-0.87	0.384	-0.10	-0.16 − -0.05	-3.60	**<0.001**
Education	-0.10	-0.24 − 0.04	-1.42	0.154	-0.02	-0.04 − -0.00	-2.45	**0.014**
Motion RMSD	4.34	0.87 − 7.81	2.45	**0.014**	-0.38	-0.90 − 0.13	-1.46	0.145
Age * DMN A	1.35	-0.10 − 2.80	1.82	0.068	-0.82	-1.01 − -0.64	-8.70	**<0.001**
Age * DMN A+C	-1.00	-3.66 − 1.67	-0.73	0.463	-0.29	-0.68 − 0.09	-1.50	0.133
Age * DMN B	-2.80	-5.17 − -0.42	-2.31	**0.021**	0.18	-0.15 − 0.51	1.07	0.284
Age * SEM	2.07	-0.29 − 4.44	1.72	0.086	0.37	-0.11 − 0.85	1.49	0.136
Age * CONT B	1.89	-0.78 − 4.57	1.39	0.165	0.73	0.38 − 1.07	4.11	**<0.001**
Age * VAN B	-5.00	-7.22 − -2.77	-4.40	**<0.001**	-0.13	-0.45 − 0.19	-0.80	0.425
Age * DAN A	-0.28	-3.02 − 2.46	-0.20	0.843	1.79	1.40 − 2.19	8.95	**<0.001**
Random Effects								
δ^2	3.29				0.10			
θ_{00}	0.07 sub				0.04 sub			

	1.71 Category	0.00 Category
ICC	0.35	0.30
Observations	9837	9069
Marg R^2 / Cond R^2	0.033 / 0.372	0.183 / 0.430

Note. Significant effects are marked in bold. Contrasts are sum coded. P-values were obtained via likelihood ratio tests. CI Confidence interval.

Table S12. Connector hubs in brain graphs of older adults

Network	Region of interest	Mean PC
DMN A	Lateral occipital cortex, superior division 1	0.55
DMN A	Angular gyrus 3	0.55
DMN A+C	Lateral occipital cortex, superior division 1	0.54
DMN A+C	Lateral occipital cortex, superior division 5	0.59
DMN B	Frontal pole 2	0.54
DMN B	Angular gyrus	0.55
DMN B	Middle temporal gyrus, posterior division 2	0.55
SEM	Superior frontal gyrus 1	0.54
SEM	Paracingulate gyrus 2	0.56
CONT B	Frontal pole 1	0.54
CONT B	Frontal pole 3	0.55
CONT B	Middle frontal gyrus 3	0.55
CONT B	Angular gyrus 1	0.56
CONT B	Angular gyrus 2	0.62
CONT B	Superior frontal gyrus 1	0.54
CONT B	Paracingulate gyrus	0.57
CONT B	Frontal pole 6	0.54

Note. PC participation coefficient.

Table S13. Connector hubs in brain graphs of young adults

Network	Region of interest	Mean PC
DMN A	Lateral occipital cortex, superior division 1	0.64
DMN A	Angular gyrus 3	0.63
DMN A+C	Lateral occipital cortex, superior division 1	0.53
DMN B	Angular gyrus	0.58
DMN B	Middle temporal gyrus, posterior division 4	0.52
SEM	Paracingulate gyrus 2	0.53

CONT B	Middle frontal gyrus 3		0.52
CONT B	Angular gyrus 1		0.59
CONT B	Angular gyrus 2		0.52
CONT B	Lateral occipital cortex, superior division 2		0.58
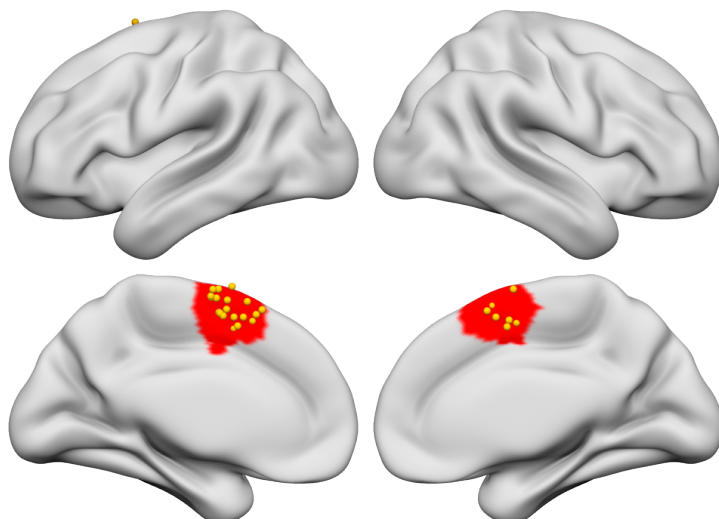
Note. PC participation coefficient.

Table S14. Significant age differences in participation coefficient
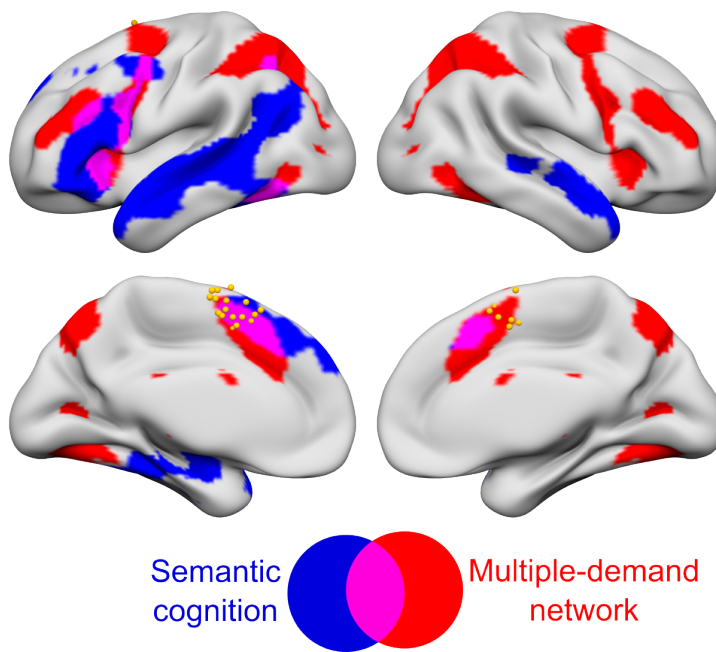
Network	ROI	Term	Estimate	SE	t-value	p-value	p corr
CONT B	Frontal pole 3	YA	-0.13	0.03	-3.70	0.001	0.049
CONT B	Pre-SMA	YA	-0.10	0.03	-3.75	0.001	0.043
SEM	Superior temporal gyrus	YA	-0.17	0.04	-4.69	0.001	0.002
DAN A	Fusiform cortex 1	YA	-0.20	0.04	-4.87	0.001	0.001
DAN A	Fusiform cortex 2	YA	-0.18	0.04	-4.05	0.001	0.016

Note. SE: standard error, p corr: p-value after correction for familywise error with Bonferroni-Holm method.

C Supplementary Material for Study 3

Figure S1. Individual stimulation sites within a pre-defined mask of the pre-SMA. The mask was taken from a freely available probabilistic cytoarchitectonic map (Ruan et al., 2018). Yellow nodes signify individual stimulation sites (n = 30).

Figure S2. Individual stimulation sites within the semantic cognition and the multiple-demand network. The map of the semantic cognition network was taken from (Jackson, 2021) and the multiple-demand network from Fedorenko et al. (2013).

Table S1. Model for DV Accuracy

Comparison	Model	Δ AIC	df
Random effects	**~ stim_type x condition + (1|sub)**	**0**	**10**
	~ stim_type x condition	71.4	9
Fixed effects	**~ stim_type x condition x congruency + age + (1|sub)**	**0**	**20**
	~ stim_type x condition + congruency + (1|sub)	55.6	11
	~ stim_type x condition + congruency + age + (1|sub)	57.6	12
	~ stim_type x condition + (1|sub)	131.6	10
	~ stim_type x condition + task + (1|sub)	131.6	10
	~ stim_type x condition + stim_order + (1|sub)	133.2	11
	~ stim_type x condition + age + (1|sub)	133.6	11

Note. Winning models are highlighted in bold; AIC Akaike Information Criterion

Table S2. Model for DV log(Response Time)

| Comparison	Model	Δ AIC	df
Random effects	**~ stim_type x condition + (1 + stim_type|sub) + (1|stimulus_audio)**	**0.0**	**17**
	~ stim_type x condition + (1 + stim_type|sub) + (1|stimulus_picture)	1058.4	17
	~ stim_type x condition + (1 + stim_type|sub)	1971.3	16
	~ stim_type x condition + (1|sub)	2644.0	11
	~ stim_type x condition	8421.5	10
Fixed effects	**~ stim_type x condition + congruency + age + (1 + stim_type|sub) + (1|stimulus_audio)**	**0**	**19**
	~ stim_type x condition + congruency + (1 + stim_type|sub) + (1|stimulus_audio)2	7.4	18
	~ stim_type x condition + age + (1 + stim_type|sub) + (1|stimulus_audio)	222.8	18
	~ stim_type x condition + (1 + stim_type|sub) + (1|stimulus_audio)	230.3	17
	~ stim_type x condition + task + (1 + stim_type|sub) + (1|stimulus_audio)	230.3	17
	~ stim_type x condition + stim_order + (1 + stim_type|sub) + (1|stimulus_audio)	232.3	18
Interactions	**~ stim_type x condition + congruency + condition x congruency + age + (1 + stim_type|sub) + (1|stimulus_audio)**	**0**	**21**

~ stim_type x condition + stim_type x congruency + condition x congruency + age + (1 + stim_type|sub) + (1|stimulus_audio)	2.1	23
~ stim_type x condition x congruency + age + (1 + stim_type|sub) + (1|stimulus_audio)	8.3	27
~ stim_type x condition + congruency + age + (1 + stim_type|sub) + (1|stimulus_audio)	302.5	19

Note. Winning models are highlighted in bold; AIC Akaike Information Criterion

Preprocessing of MRI data

Results included in this manuscript come from preprocessing performed using fMRIPrep 20.2.3 (Esteban, Markiewicz, et al. (2018); Esteban, Blair, et al. (2018)), which is based on Nipype 1.6.1 (Gorgolewski et al. (2011); Gorgolewski et al. (2018)).
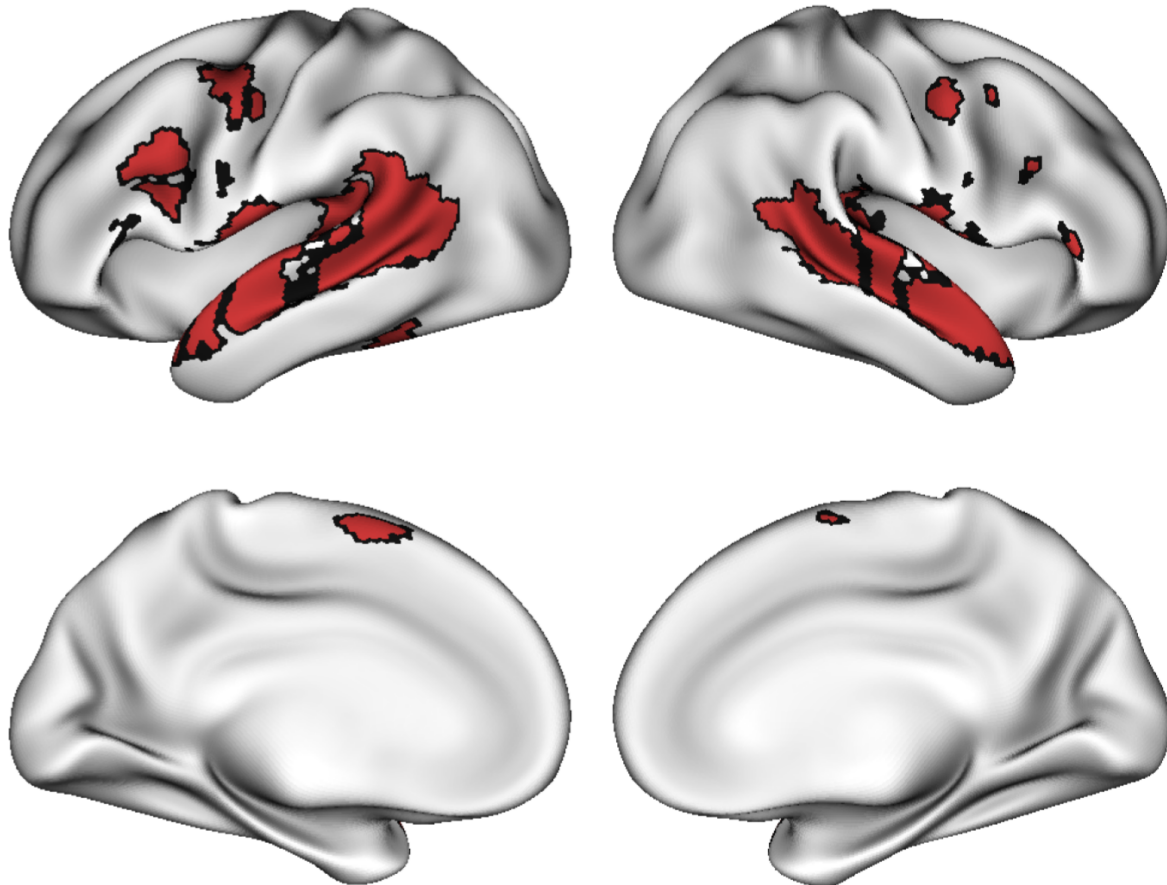
Anatomical data preprocessing A total of 1 T1-weighted (T1w) images were found within the input BIDS dataset. The T1-weighted (T1w) image was corrected for intensity non-uniformity (INU) with N4BiasFieldCorrection (Tustison et al. 2010), distributed with ANTs 2.3.3 (Avants et al. 2008), and used as T1w-reference throughout the workflow. The T1w-reference was then skull-stripped with a Nipype implementation of the antsBrainExtraction.sh workflow (from ANTs), using OASIS30ANTs as target template. Brain tissue segmentation of cerebrospinal fluid (CSF), white-matter (WM) and gray-matter (GM) was performed on the brain-extracted T1w using fast (FSL 5.0.9, Zhang, Brady, and Smith 2001). Brain surfaces were reconstructed using recon-all (FreeSurfer 6.0.1, Dale, Fischl, and Sereno 1999), and the brain mask estimated previously was refined with a custom variation of the method to reconcile ANTs-derived and FreeSurfer-derived segmentations of the cortical gray-matter of Mindboggle (Klein et al. 2017). Volume-based spatial normalization to two standard spaces (MNI152NLin6Asym, MNI152NLin2009cAsym) was performed through nonlinear registration with antsRegistration (ANTs 2.3.3), using brain-extracted versions of both T1w reference and the T1w template. The following templates were selected for spatial normalization: FSL's MNI ICBM 152 non-linear 6th Generation Asymmetric Average Brain Stereotaxic Registration Model [Evans et al. (2012); TemplateFlow ID: MNI152NLin6Asym], ICBM 152 Nonlinear Asymmetrical template version 2009c [Fonov et al. (2009); TemplateFlow ID: MNI152NLin2009cAsym],

Functional data preprocessing For each of the 8 BOLD runs found per subject (across all tasks and sessions), the following preprocessing was performed. First, a reference volume and its skull-stripped version were generated using a custom methodology of fMRIPrep. A B0-nonuniformity map (or fieldmap) was estimated based on two (or more) echo-planar imaging (EPI) references with opposing phase-encoding directions, with 3dQwarp Cox and Hyde (1997) (AFNI 20160207). Based on the estimated susceptibility distortion, a corrected

EPI (echo-planar imaging) reference was calculated for a more accurate co-registration with the anatomical reference. The BOLD reference was then co-registered to the T1w reference using bbregister (FreeSurfer) which implements boundary-based registration (Greve and Fischl 2009). Co-registration was configured with six degrees of freedom. Head-motion parameters with respect to the BOLD reference (transformation matrices, and six corresponding rotation and translation parameters) are estimated before any spatiotemporal filtering using mcflirt (FSL 5.0.9, Jenkinson et al. 2002). BOLD runs were slice-time corrected using 3dTshift from AFNI 20160207 (Cox and Hyde 1997). The BOLD time-series (including slice-timing correction when applied) were resampled onto their original, native space by applying a single, composite transform to correct for head-motion and susceptibility distortions. These resampled BOLD time-series will be referred to as preprocessed BOLD in original space, or just preprocessed BOLD. The BOLD time-series were resampled into standard space, generating a preprocessed BOLD run in MNI152NLin6Asym space. First, a reference volume and its skull-stripped version were generated using a custom methodology of fMRIPrep. Several confounding time-series were calculated based on the preprocessed BOLD: framewise displacement (FD), DVARS and three region-wise global signals. FD was computed using two formulations following Power (absolute sum of relative motions, Power et al. (2014)) and Jenkinson (relative root mean square displacement between affines, Jenkinson et al. (2002)). FD and DVARS are calculated for each functional run, both using their implementations in Nipype (following the definitions by Power et al. 2014). The three global signals are extracted within the CSF, the WM, and the whole-brain masks. Additionally, a set of physiological regressors were extracted to allow for component-based noise correction (CompCor, Behzadi et al. 2007). Principal components are estimated after high-pass filtering the preprocessed BOLD time-series (using a discrete cosine filter with 128s cut-off) for the two CompCor variants: temporal (tCompCor) and anatomical (aCompCor). tCompCor components are then calculated from the top 2% variable voxels within the brain mask. For aCompCor, three probabilistic masks (CSF, WM and combined CSF+WM) are generated in anatomical space. The implementation differs from that of Behzadi et al. in that instead of eroding the masks by 2 pixels on BOLD space, the aCompCor masks are subtracted a mask of pixels that likely contain a volume fraction of GM. This mask is obtained by dilating a GM mask extracted from the FreeSurfer's aseg segmentation, and it ensures components are not extracted from voxels containing a minimal fraction of GM. Finally, these masks are resampled into BOLD space and binarized by thresholding at 0.99 (as in the original implementation). Components are also calculated separately within the WM and CSF masks. For each CompCor decomposition, the k components with the largest singular values are retained, such that the retained components' time series are sufficient to explain 50 percent of variance across the nuisance mask (CSF, WM, combined, or temporal). The remaining components are dropped from consideration. The head-motion estimates calculated in the correction step were also placed within the corresponding confounds file. The confound time

series derived from head motion estimates and global signals were expanded with the inclusion of temporal derivatives and quadratic terms for each (Satterthwaite et al. 2013). Frames that exceeded a threshold of 0.5 mm FD or 1.5 standardised DVARS were annotated as motion outliers. All resamplings can be performed with a single interpolation step by composing all the pertinent transformations (i.e. head-motion transform matrices, susceptibility distortion correction when available, and co-registrations to anatomical and output spaces). Gridded (volumetric) resamplings were performed using antsApplyTransforms (ANTs), configured with Lanczos interpolation to minimize the smoothing effects of other kernels (Lanczos 1964). Non-gridded (surface) resamplings were performed using mri_vol2surf (FreeSurfer).

Many internal operations of fMRIPrep use Nilearn 0.6.2 (Abraham et al. 2014), mostly within the functional processing workflow. For more details of the pipeline, see the section corresponding to workflows in fMRIPrep's documentation.

Figure S3. Results of group-constrained subject-specific parcellation approach for language localizer task. The figure shows 25 regions of interest (ROIs) that were activated in at least 60% of participants for the contrast intact > degraded speech after data were parcellated using a watershed algorithm. To confirm that these parcels were indeed relevant to language processing, independent of the task, we entered them in a random-effects group-level analysis using the independent data set for the semantic judgment task at baseline. Results showed that all 25 parcels were significantly stronger activated for the language task relative to rest (see Table S3).

Table S3. Results of random-effects analysis semantic judgment > rest for 25 functional ROIs from localizer contrast

ROI	Hemi	Name	Avg. ROI size	Avg. Loc. Mask size	Overlap	*T*	*Df*	*P*
1	R	pMTG	473	132	1.00	11.21	27.08	0.001
2	R	MTG/STG	334	100	0.97	12.61	26.90	0.001
3	R	aMTG/ATL	705	195	1.00	13.05	27.20	0.001
4	L	MTG	581	157	1.00	13.40	28.35	0.001
5	L	ATL	204	52	0.97	13.35	26.86	0.001
6	R	Operculum	168	42	0.93	10.31	25.36	0.001
7	L	pMTG/AG/SMG	1045	258	1.00	13.49	27.97	0.001
8	L	pMTG/STG	86	24	0.97	12.81	26.63	0.001
9	L	Temporal pole	126	32	0.97	11.72	26.00	0.001
10	L	STG	16	5	0.93	15.05	25.36	0.001
11	L	pMTG	19	6	0.93	9.67	26.27	0.001
12	L	pMTG	14	4	0.80	6.51	22.38	0.001
13	L	Operculum	210	41	1.00	11.95	25.44	0.001
14	R	Operculum	252	52	0.87	12.32	21.76	0.001
15	L	Precentr. Gyrus	263	52	1.00	12.37	26.24	0.001
16	R	Precentr. gyrus	142	29	0.73	9.27	19.72	0.001
17	R	AG	97	18	0.77	2.57	20.11	0.009
18	L	IFG, pars op.	147	25	0.90	12.58	22.40	0.001
19	R	Cerebellum	113	21	0.70	8.81	18.79	0.001
20	L	IFG, pars op.	79	17	0.63	10.61	16.42	0.001
21	R	Cerebellum	129	22	0.90	9.13	23.09	0.001
22	L	Pre-SMA	73	14	0.77	11.87	18.97	0.001
24	R	IFG, pars tr.	130	23	0.87	7.31	21.50	0.001
25	L	IFG, pars tr.	59	11	0.70	8.97	18.18	0.001
29	L	IFG, pars tr.	35	6	0.70	6.27	18.02	0.001

Note. Df Degrees of freedom; p-value after FDR-correction q < 0.05.

Supplementary Results

Table S4. Results of mixed-effects models for accuracy and reaction time

	Accuracy				Reaction time			
Coefficient	*Log-Odds*	*CI*	*Statistic*	*p*	*Estimates*	*CI*	*Statistic*	*p*
Intercept	3.44	3.25 − 3.62	36.71	**<0.001**	6.90	6.85 − 6.96	242.35	**<0.001**
Session: baseline	-0.62	-1.03 − -0.21	-2.95	**0.003**	0.19	0.11 − 0.27	4.75	**<0.001**
Session: active	0.34	-0.10 − 0.78	1.52	0.128	-0.09	-0.13 − -0.04	-3.75	**<0.001**
Condition: WPM	3.04	2.51 − 3.57	11.22	**<0.001**	-0.30	-0.37 − -0.23	-8.54	**<0.001**
Condition: FPM	-2.12	-2.49 − -1.76	-11.33	**<0.001**	0.39	0.32 − 0.45	11.98	**<0.001**
Congruency: congruent	-0.64	-0.85 − -0.43	-6.05	**<0.001**	-0.04	-0.06 − -0.03	-6.36	**<0.001**
Age	0.00	-0.02 − 0.02	0.07	0.943				

	Estimate	CI	Statistic	p	Estimate	CI	Statistic	p
Condition WPM * Congruency congruent	0.63	-1.48 – 2.73	0.58	0.561	-0.14	-0.20 – -0.08	-4.48	**<0.001**
Condition FPM * Congruency congruent	-1.48	-3.67 – 0.72	-1.32	0.187	0.04	-0.02 – 0.10	1.30	0.195
Session baseline * Condition WPM	2.04	0.57 – 3.52	2.71	**0.007**	-0.08	-0.14 – -0.02	-2.51	**0.012**
Session active * Condition WPM	-1.22	-2.78 – 0.34	-1.54	0.124	0.06	-0.00 – 0.12	1.92	0.055
Session baseline * Condition FPM	0.70	-0.12 – 1.52	1.67	0.095				
Session active * Condition FPM	-0.36	-1.24 – 0.52	-0.81	0.417				
Age	-1.08	-2.14 – -0.02	-1.99	**0.046**	0.10	0.06 – 0.14	4.51	**<0.001**
Session: baseline * Congruency congruent	-1.59	-2.33 – -0.86	-4.25	**<0.001**	0.24	0.17 – 0.31	6.54	**<0.001**
Session: active * Congruency congruent	0.99	-3.20 – 5.18	0.46	0.643				
Session: baseline * Condition: WPM * Congruency congruent	1.69	-2.64 – 6.01	0.76	0.444				
Session: active * Condition: WPM * Congruency congruent	2.40	-0.54 – 5.35	1.60	0.110				
Session: baseline * Condition: FPM * Congruency congruent	-2.22	-5.32 – 0.87	-1.41	0.159				
Session: active * Condition: WPM * Congruency congruent					0.09	0.04 – 0.14	3.40	**0.001**
Random Effects								
σ^2	3.29				0.05			
τ_{00}	0.17 sub				0.01 stimulus_audio			
					0.02 sub			
τ_{11}					0.05 sub.stim_type1			
					0.01 sub.stim_type2			
ρ_{01}					-0.31 sub.stim_type1			
					0.30 sub.stim_type2			
ICC	0.05				0.45			
Observations	15750				15028			
Marginal R^2 / Conditional R^2	0.201 / 0.240				0.198 / 0.560			

Table S5. Univariate fMRI results

Anatomical structure	Hemi	k	t	x	y	z
WPM + FPM > Rest						
Superior temporal gyrus	L	19000	17.45	-57.66	-1.60	-3.25
Cerebellum	L		17.41	-20.34	-51.36	-19.75
Postcentral gyrus	R		15.33	51.82	-19.02	46.25
Supplementary motor area	R	1074	13.25	4.54	3.38	57.25
Presupplementary motor area	R		12.00	4.54	10.84	43.50
Supplementary motor area	L		11.69	-7.90	-1.60	60.00
Control Task > Rest						
Postcentral gyrus	R	17880	17.61	49.33	-21.50	46.25
Superior temporal gyrus	R		15.52	51.82	-21.50	7.75
Cerebellum	L		15.46	-17.85	-51.36	-19.75
Thalamus	L	13	10.55	-2.92	-26.48	-3.25
Precuneus	R	106	9.08	14.50	-66.29	46.25
Precuneus	R		6.91	14.50	-73.75	38.00
Frontal pole	L	129	9.03	-47.70	45.67	5.00
Middle frontal gyrus	L		8.84	-37.75	43.18	-0.50
Frontal pole	L		8.20	-42.73	55.62	2.25
Precuneus	R	11	7.10	4.54	-56.34	54.50
Thalamus	L	11	7.06	-12.87	-26.48	-6.00
WPM > FPM						
Superior temporal gyrus	L	56	7.63	-50.19	-19.02	5.00
Planum temporale	L		7.51	-55.17	-33.94	13.25
Superior temporal gyrus	L		6.16	-45.22	-26.48	5.00
Planum temporale	R	12	7.04	54.30	-21.50	10.50
Superior temporal gyrus	R		6.26	44.35	-26.48	10.50
FPM > WPM						
Middle frontal gyrus	L	483	10.48	-45.22	10.84	40.75
Inferior frontal gyrus, pars triangularis	L		10.24	-52.68	20.79	24.25
Inferior frontal gyrus, pars triangularis	L		9.09	-52.68	38.21	5.00
Middle temporal gyrus	L	166	9.73	-62.63	-51.36	-6.00
Middle temporal gyrus	L		8.56	-65.12	-46.38	2.25
Inferior temporal gyrus	L		8.41	-52.68	-58.82	-8.75
Inferior parietal lobe	L	156	9.45	-30.29	-78.73	43.50
Middle occipital gyrus	L		8.25	-27.80	-71.26	32.50
Superior parietal lobe	L		8.09	-30.29	-66.29	49.00
Supplementary motor area	L	122	7.96	-5.41	15.82	60.00
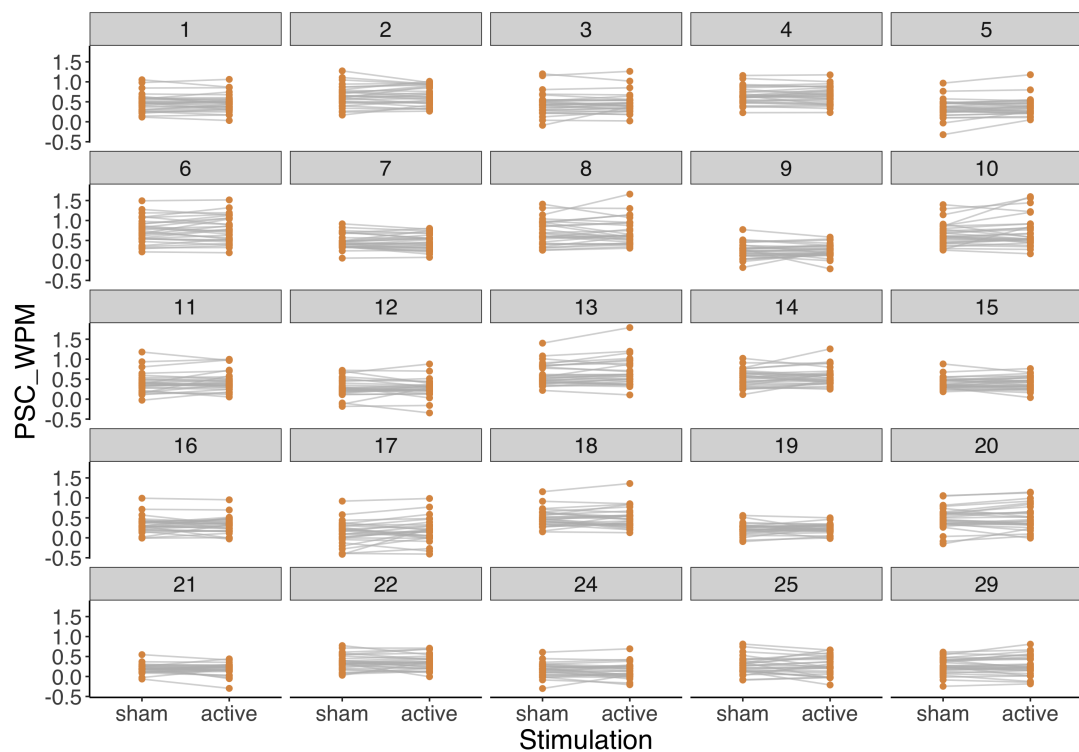
Anatomical structure	Hemi	k	t	x	y	z
Superior frontal gyrus	L		7.75	-5.41	33.23	46.25
Cerebellum	R	10	7.93	36.89	-66.29	-28.00
Middle frontal gyrus	L	42	7.87	-35.26	8.35	60.00
Superior frontal gyrus	L		7.73	-27.80	15.82	60.00
Middle frontal gyrus	L		6.49	-27.80	13.33	49.00
WPM + FPM > Control Task						
Fusiform gyrus	L	975	13.85	-37.75	-33.94	-22.50
Fusiform gyrus	L		12.10	-30.29	-36.43	-19.75
Fusiform gyrus	L		10.94	-32.78	-43.90	-17.00
Superior temporal gyrus	L	546	13.07	-60.14	-4.09	-6.00
Middle temporal gyrus	L		11.95	-65.12	-19.02	-0.50
Temporal pole	L		11.65	-52.68	13.33	-17.00
Fusiform gyrus	R	743	12.40	34.40	-38.92	-22.50
Fusiform gyrus	R		11.73	29.42	-46.38	-17.00
Fusiform gyrus	R		9.92	29.42	-31.46	-19.75
Precuneus	L	112	11.77	-5.41	-56.34	16.00
Posterior cingulate cortex	L		7.52	-0.43	-48.87	27.00
Amygdala	R	24	10.51	26.94	-4.09	-17.00
Inferior frontal gyrus, pars orbitalis	L	25	9.53	-37.75	35.72	-11.50
Temporal pole	R	176	8.95	56.79	5.86	-8.75
Temporal pole	R		8.66	54.30	8.35	-19.75
Superior temporal gyrus	R		8.57	61.77	-6.58	-6.00
Anterior cingulate cortex	L	50	8.67	-7.90	30.74	-11.50
Medial frontal gyrus	R		6.42	4.54	28.26	-14.25
Superior frontal gyrus	L	42	8.22	-5.41	58.11	29.75
Frontal pole	L		6.80	-5.41	63.09	18.75
Frontal pole	L		6.50	-7.90	53.14	40.75
Hippocampus	L	13	7.65	-20.34	-36.43	-0.50
Precuneus	L		6.74	-12.87	-38.92	2.25
Superior frontal gyrus	L	12	7.20	-17.85	35.72	54.50
Control Task > WPM + FPM						
Frontal pole	R	453	13.05	41.86	38.21	29.75
Frontal pole	R		11.05	39.38	53.14	13.25
Frontal pole	R		9.68	41.86	55.62	5.00
Precuneus	R	515	12.09	12.01	-66.29	46.25
Precuneus	R		11.31	4.54	-71.26	49.00
Precuneus	R		11.03	7.03	-76.24	40.75

Anatomical structure	Hemi	*k*	*t*	*x*	*y*	*z*
Middle frontal gyrus	R	222	11.62	34.40	8.35	57.25
Middle frontal gyrus	R		7.74	46.84	3.38	51.75
Superior frontal gyrus	R		7.59	19.47	10.84	60.00
Angular gyrus	R	699	11.36	54.30	-46.38	40.75
Angular gyrus	R		9.64	49.33	-53.85	38.00
Angular gyrus	R		9.53	41.86	-51.36	46.25
Middle frontal gyrus	L	94	11.29	-37.75	33.23	32.50
Middle frontal gyrus	L		9.27	-40.24	25.77	38.00
Insula	L	49	9.08	-30.29	15.82	7.75
Middle cingulate cortex	R	38	9.03	7.03	25.77	38.00
Cerebellum	L	63	8.85	-35.26	-63.80	-30.75
Cerebellum	L		7.27	-25.31	-66.29	-28.00
Inferior parietal lobe	L	181	8.29	-50.19	-51.36	38.00
Inferior parietal lobe	L		7.73	-42.73	-48.87	40.75
Angular gyrus	L		7.40	-40.24	-56.34	49.00
Cerebellum	R	15	7.95	34.40	-53.85	-30.75
Precentral gyrus	L	34	7.69	-32.78	-1.60	57.25
Superior frontal gyrus	L		6.27	-25.31	-6.58	51.75
Supplementary motor area	L	30	7.32	-7.90	-1.60	65.50
Cerebellum	L	50	7.14	-35.26	-51.36	-41.75
Cerebellum	L		7.13	-35.26	-63.80	-44.50
Insula	R	24	7.09	31.91	28.26	5.00
Cerebellum	L	11	6.93	-12.87	-71.26	-28.00
Inferior frontal gyrus, pars opercularis	R	21	6.88	46.84	13.33	13.25
Inferior frontal gyrus, pars opercularis	R		6.76	54.30	18.30	13.25
FPM > Control Task						
Superior temporal gyurs	L	531	13.63	-57.66	-1.60	-6.00
Temporal pole	L		11.56	-52.68	13.33	-17.00
Middle temporal gyrus	L		10.76	-62.63	-16.53	-3.25
Fusiform gyrus	L	900	13.15	-37.75	-33.94	-22.50
Fusiform gyrus	L		12.03	-30.29	-36.43	-19.75
Fusiform gyrus	L		10.07	-32.78	-43.90	-17.00
Fusiform gyrus	R	677	12.21	34.40	-38.92	-22.50
Fusiform gyrus	R		11.49	29.42	-46.38	-17.00
Parahippocampal cortex	R		10.45	29.42	-31.46	-19.75
Amygdala	R	21	10.31	26.94	-4.09	-17.00
Precuneus	L	62	10.29	-5.41	-56.34	16.00
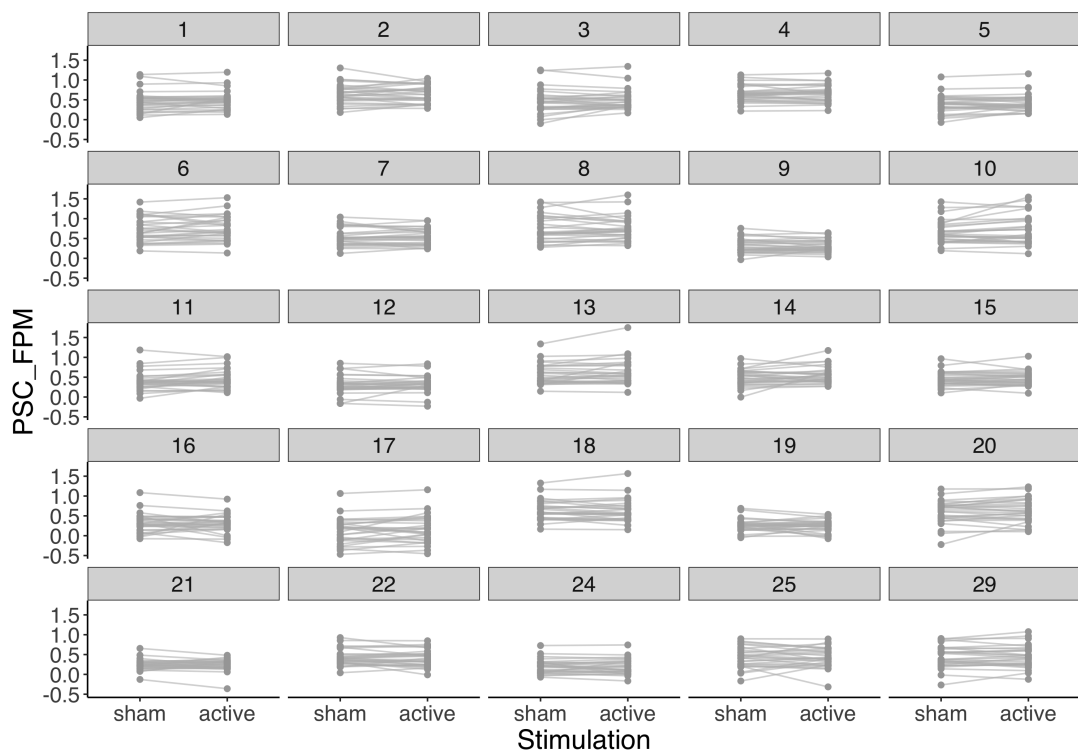
Anatomical structure	Hemi	k	t	x	y	z
Orbital cortex	L	41	10.28	-37.75	35.72	-11.50
Inferior frontal gyrus, pars triangularis	L		6.19	-47.70	28.26	-3.25
Temporal pole	R	148	9.24	56.79	5.86	-8.75
Temporal pole	R		8.67	54.30	8.35	-19.75
Temporal pole	R		8.15	51.82	15.82	-17.00
Frontal pole	L	59	8.13	-7.90	60.60	32.50
Frontal pole	L		7.30	-7.90	53.14	43.50
Frontal pole	L		7.21	-12.87	45.67	46.25
Pre-SMA	L	34	7.73	-2.92	30.74	-14.25
Pre-SMA	L		6.70	-0.43	40.70	-11.50
Posterior cingulate cortex	L	20	7.56	-17.85	-36.43	2.25
Thalamus	L		6.50	-10.38	-33.94	5.00
Inferior frontal gyrus, pars triangularis	L	21	7.19	-50.19	30.74	10.50
Control Task > FPM						
Precuneus	R	574.00	13.03	12.01	-66.29	49.00
Precuneus	R		12.49	4.54	-71.26	49.00
Precuneus	R		12.28	7.03	-76.24	40.75
Middle frontal gyrus	L	81.00	12.30	-37.75	33.23	32.50
Middle frontal gyrus	L		8.58	-40.24	25.77	38.00
Frontal pole	R	300.00	11.84	39.38	38.21	32.50
Frontal pole	R		10.79	41.86	43.18	24.25
Frontal pole	R		9.80	39.38	53.14	13.25
Angular gyrus	R	661.00	10.99	54.30	-46.38	40.75
Angular gyrus	R		9.20	41.86	-51.36	46.25
Angular gyrus	R		9.17	49.33	-46.38	24.25
Middle frontal gyrus	R	149.00	9.45	34.40	8.35	57.25
Precentral gyrus	R		7.39	51.82	-1.60	46.25
Precentral gyrus	R		7.34	46.84	3.38	51.75
Insula	L	43.00	9.18	-30.29	15.82	7.75
Cerebellum	L	48.00	8.71	-35.26	-63.80	-30.75
Cerebellum	L		7.03	-25.31	-66.29	-28.00
Inferior frontal gyrus, pars opercularis	R	27.00	8.60	56.79	15.82	5.00
Inferior frontal gyrus, pars opercularis	R		6.91	51.82	15.82	13.25
Supramarginal gyrus	L	100.00	8.10	-50.19	-51.36	38.00
Supramarginal gyrus	L		7.53	-60.14	-43.90	35.25
Supramarginal gyrus	L		7.16	-52.68	-43.90	40.75
Pre-SMA	L	34.00	7.77	-7.90	-1.60	65.50

Anatomical structure	Hemi	k	t	x	y	z
Cerebellum	L	10.00	7.23	-35.26	-48.87	-44.50
Middle frontal gyrus	L	17.00	7.13	-30.29	-1.60	57.25
Cerebellum	L	17.00	6.64	-35.26	-63.80	-44.50
Superior frontal gyrus	R	10.00	6.23	16.98	3.38	65.50
Superior frontal gyrus	R		6.21	14.50	-4.09	73.75
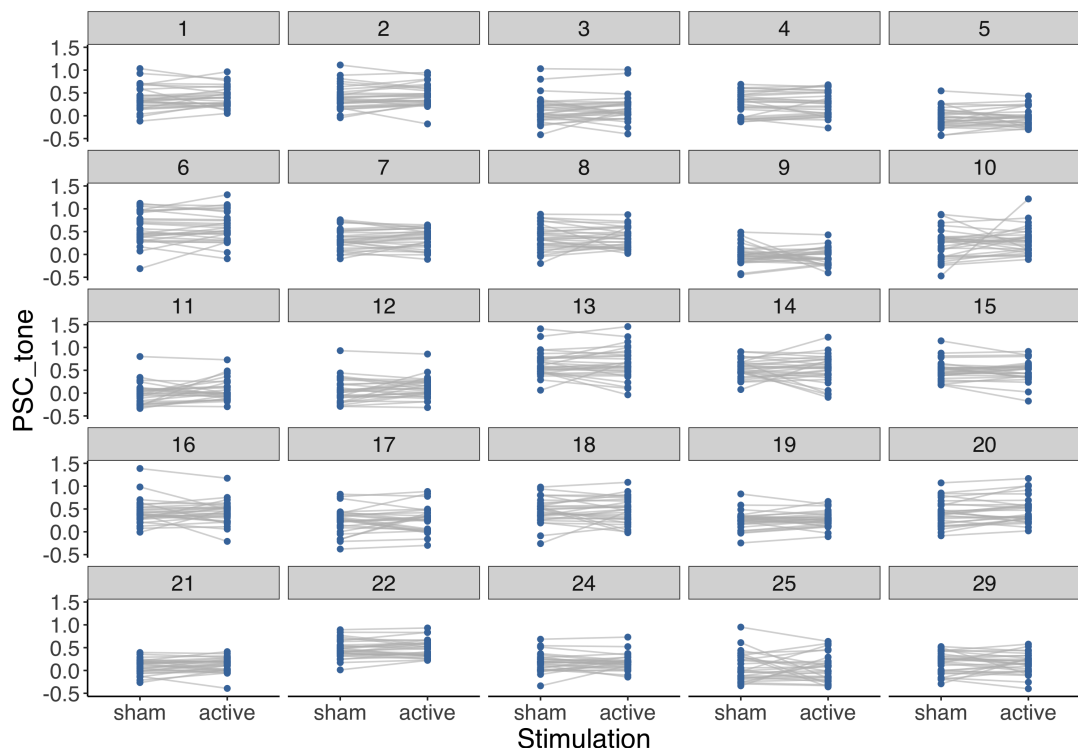
Note. Results are FWE-corrected at peak-level at $p < 0.05$. WPM: word-picture matching; FPM: feature-picture matching.
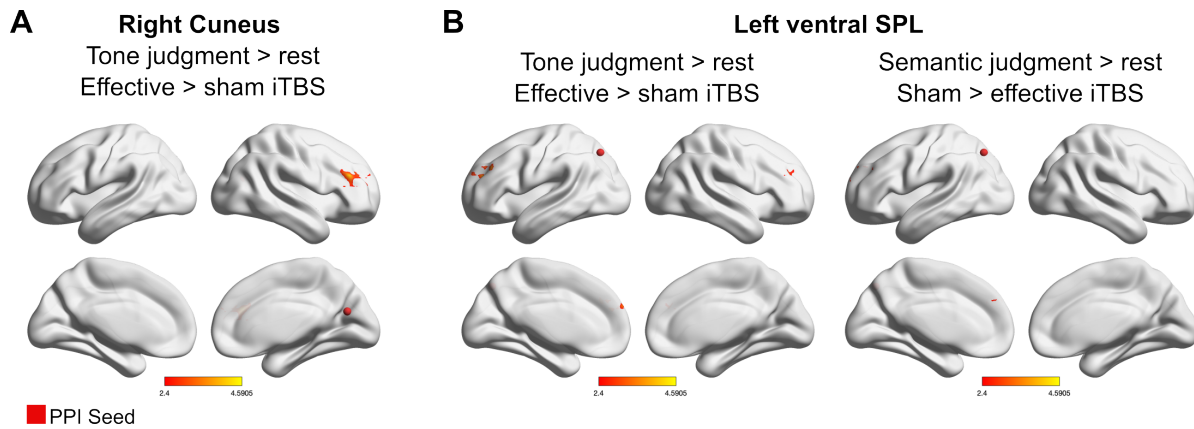
Figure S4. PSC in word-picture matching in 25 regions of interest according to subject-specific group parcellation for language localizer task.

Figure S5. PSC in feature-picture matching in 25 regions of interest according to subject-specific group parcellation for language localizer task.


Figure S6. PSC in tone judgment in 25 regions of interest according to subject-specific group parcellation for language localizer task.

A **Right Cuneus**
Tone judgment > rest
Effective > sham iTBS

B **Left ventral SPL**
Tone judgment > rest   Semantic judgment > rest
Effective > sham iTBS   Sham > effective iTBS

■ PPI Seed

Figure S7. (A) For the PPI seed in the right cuneus, stronger functional connectivity with a right prefrontal cluster after effective iTBS was driven by the tone judgment task. (B) For the PPI seed in the left ventral SPL, a cluster in left prefrontal cortex dissociated both tasks: It showed stronger coupling after effective iTBS for tone judgment and stronger decoupling for semantic judgment.

Table S6. Significant clusters – gPPI Effective < sham iTBS

Anatomical structure	Hemi	k	t	x	y	z
Seed: Left SPL [-22.8, -71.3, 54.5]						
Middle frontal gyrus	L	228	4.68	-22.82	35.72	29.75
Frontal pole	L		4.37	-35.26	38.21	29.75
Superior frontal gyrus	L		4.05	-7.90	45.67	35.25
Middle frontal gyrus	L		3.89	-25.31	28.26	32.50
Frontal pole	L		3.61	-10.38	58.11	18.75
Seed: Left SPL [-22.8, -71.3, 46.2]						
Frontal pole	L	1691	6.59	-22.82	38.21	29.75
Frontal pole	L		5.02	-37.75	38.21	29.75
Anterior cingulate gyrus	R		4.87	7.03	38.21	2.25
Middle frontal gyrus	L		4.79	-25.31	30.74	32.50
Anterior cingulate gyrus	L		4.78	-12.87	48.16	5.00
Superior frontal gyrus	R	299	5.14	24.45	-9.06	65.50
Pre-supplementary motor cortex	L		4.57	-0.43	-9.06	54.50
Superior frontal gyrus	R		4.29	12.01	-9.06	65.50
Middle frontal gyrus	R		3.87	39.38	0.89	60.00
Superior frontal gyrus	R		3.82	26.94	5.86	60.00
Superior parietal lobe	L	149	4.68	-42.73	-43.90	54.50
Supramarginal gyrus	L		3.69	-40.24	-38.92	40.75
Postcentral gyrus	L		3.06	-60.14	-26.48	43.50
Supramarginal gyrus	L		2.97	-52.68	-31.46	51.75
Postcentral gyrus	L		2.80	-45.22	-28.97	43.50

Precentral gyrus	L	188	4.00	-30.29	-14.04	71.00
Superior frontal gyrus	L		3.94	-20.34	-1.60	54.50
Superior frontal gyrus	L		3.69	-20.34	-6.58	71.00
Precentral gyrus	L		3.54	-42.73	-1.60	51.75
Precentral gyrus	L		3.36	-37.75	-9.06	65.50
Seed: Right Cuneus [9.5, -68.8, 21.5]						
Frontal pole	R	449	4.58	31.91	48.16	29.75
Middle frontal gyrus	R		4.33	41.86	55.62	2.25
Frontal pole	R		3.85	26.94	53.14	21.50
Frontal pole	R		3.79	29.42	63.09	2.25
Frontal pole	R		3.71	16.98	63.09	10.50

Note. Results are thresholded at p < 0.01 at peak level and FWE-corrected at p < 0.05 at cluster level.

Author Contributions

Contributions to the publication

"Age-related reorganization of functional network architecture in semantic cognition"

By Sandra Martin (SM), Kathleen Anne Williams (KAW), Dorothee Saur (DS), and Gesa Hartwigsen (GH)

Published in *Cerebral Cortex*, 2022

Contributions

Conceptualization: SM, KAW, GH, DS

Methodology: SM, KAW, GH

Investigation: SM

Data curation: SM

Formal analysis: SM, KAW

Visualization: SM

Writing – original draft: SM

Writing – review & editing: SM, GH, KAW, DS

_____ Sandra Martin

_____ Dorothee Saur

_____ Gesa Hartwigsen

Author Contributions

Contributions to the publication

"Age-dependent contribution of domain-general networks to semantic cognition"

By Sandra Martin (SM), Dorothee Saur (DS), and Gesa Hartwigsen (GH)

Published in *Cerebral Cortex*, 2022

Contributions

Conceptualization: SM, GH, DS

Methodology: SM, GH, DS

Investigation: SM

Data curation: SM

Formal analysis: SM

Visualization: SM

Writing – original draft: SM
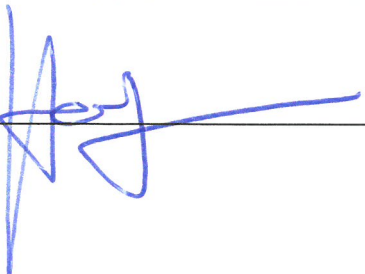
Writing – review & editing: SM, GH, DS

_____ Sandra Martin

_____ Dorothee Saur

_____ Gesa Hartwigsen

Author Contributions

Contributions to the publication

"Distinct effects of facilitatory stimulation of the pre-SMA on task-based activity and connectivity"

By Sandra Martin (SM), Regine Frieling (RF), Dorothee Saur (DS), and Gesa Hartwigsen (GH)
Published on bioRxiv as preprint, 2022

Contributions

Conceptualization: SM, GH, DS

Methodology: SM, GH, DS

Investigation: SM, RF

Data curation: SM, RF

Formal analysis: SM

Visualization: SM

Writing – original draft: SM

Writing – review & editing: SM, GH, DS
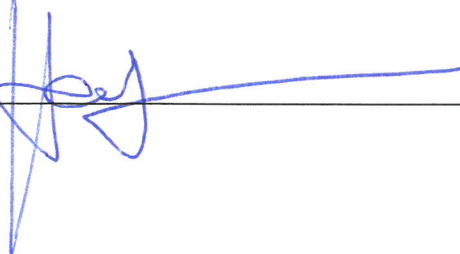
_____ Sandra Martin

_____ Dorothee Saur

_____ Gesa Hartwigsen

Declaration of Authenticity

Erklärung über die eigenständige Abfassung der Arbeit

Hiermit erkläre ich, dass ich die vorliegende Arbeit selbstständig und ohne unzulässige Hilfe oder Benutzung anderer als der angegebenen Hilfsmittel angefertigt habe. Ich versichere, dass Dritte von mir weder unmittelbar noch mittelbar eine Vergütung oder geldwerte Leistungen für Arbeiten erhalten haben, die im Zusammenhang mit dem Inhalt der vorgelegten Dissertation stehen, und dass die vorgelegte Arbeit weder im Inland noch im Ausland in gleicher oder ähnlicher Form einer anderen Prüfungsbehörde zum Zweck einer Promotion oder eines anderen Prüfungsverfahrens vorgelegt wurde. Alles aus anderen Quellen und von anderen Personen übernommene Material, das in der Arbeit verwendet wurde oder auf das direkt Bezug genommen wird, wurde als solches kenntlich gemacht. Insbesondere wurden alle Personen genannt, die direkt an der Entstehung der vorliegenden Arbeit beteiligt waren. Die aktuellen gesetzlichen Vorgaben in Bezug auf die Zulassung der klinischen Studien, die Bestimmungen des Tierschutzgesetzes, die Bestimmungen des Gentechnikgesetzes und die allgemeinen Datenschutzbestimmungen wurden eingehalten. Ich versichere, dass ich die Regelungen der Satzung der Universität Leipzig zur Sicherung guter wissenschaftlicher Praxis kenne und eingehalten habe.

Datum: 24.10.2022

Unterschrift:

Max Planck Institute for Human Cognitive and Brain Sciences
Lise Meitner Research Group Cognition & Plasticity
☎ +49 341 9940 2683
✉ martin@cbs.mpg.de

Sandra Martin

EDUCATION

PhD candidate
since 02/2018

MPI for Human Cognitive and Brain Sciences,
Lise Meitner Research Group Cognition and Plasticity
University Hospital Leipzig, Language and Aphasia Lab
Supervisors: PD Dr. Gesa Hartwigsen, Prof. Dr. Dorothee Saur

MSc Clinical Linguistics
2012 – 2014

University of Potsdam, Germany
University of Groningen, The Netherlands
Supervisors: PD Dr. Frank Burchert, Prof. Dr. Agnes Flöel
Thesis: Improving communication in aphasia: A comparison of naming- and discourse-based treatment, both facilitated by transcranial direct current stimulation
Grade: Excellent

BA Linguistics and Roman Philology
2007 – 2012

Humboldt-Universität zu Berlin, Germany
Grade: Very good
2009 – 2010 Erasmus exchange student at Université Aix-Marseille, France

PROFESSIONAL EXPERIENCE

Speech-Language Pathologist
2015 – 2017

Median Klinik Berlin Kladow, Clinic for neurological rehabilitation

Research Internship
2014 – 2015

NeuroCure Clinical Research Center, Charité Berlin
Advisors: Prof. Dr. Agnes Flöel, Dr. Marcus Meinzer

Student Assistantship
2012 – 2013

Center for Language and Cognition, University of Groningen, The Netherlands
Advisor: Prof. Dr. Roelien Bastiaanse

HONORS & AWARDS

PhD fellowship
Since 02/2018

German Academic Scholarship Foundation (Studienstiftung des deutschen Volkes)
Full stipend for graduate program

Poster prize
11/2020

64th Annual Meeting of the German Society for Clinical Neurophysiology and Functional Imaging (DGKN)

First prize at Science Slam
02/2019

20th Annual Meeting of the German Association of Speech-Language Therapy

Travel grant
2014

Erasmus Mundus program

Erasmus Mundus stipend 2012 − 2014
Erasmus Mundus Program European Union
Full stipend for Master's studies

DAAD PROMOS stipend 2011
German Academic Exchange Service

TEACHING

Data analysis with R 06/2021
Invited one-day workshop at the 5th Summer School of the PhDnet of the German Association of Speech-Language Therapy. I built an R package for the workshop:
gitlab.gwdg.de/sandra.martin/r-workshop-summer-school-2021

Introduction to fMRIPrep 05/2020
Introductory workshop at Neuropsychology department of MPI CBS how to run fMRIPrep for preprocessing fMRI data

Invited workshop at annual meeting of German Society for Aphasia Research 10/2019
Aphasia as a network disorder: Implications for speech-language therapy and the application of non-invasive brain stimulation methods for recovery from aphasia.

MENTORING & SUPERVISION

Master thesis
Katharina Polsterer (2022, University of Groningen)
Regine Frieling (2021, University of Cologne)

Interns / Student assistants
Caroline Duchow (2019, University of Erfurt)
Annika Dunau (2018, University of Leipzig)

OPEN SCIENCE

fMRI Preregistration template 2021
Co-author of current template. doi:10.23668/psycharchives.5121

Panelist at discussion on Research Data Management 05/2021
Invited speaker at panel discussion during the 4th research data management workshop organized by the Max Planck Digital Library. I was invited to represent the perspective of early career researchers on the handling and publication of research data.

Open Access Ambassador of the Max Planck Society 2019-2020
Including training at a 2-day conference on Open Access and Open Science, organized by the Max Planck Digital Library. Info: oambassadors.mpdl.mpg.de/ambassadors-2019

Doing Good − Scientific Practice under Review 11/2019
Organizer of a 2-day symposium on Open Science and Good Scientific Practice at MPI CBS, Leipzig. Info: cbs.mpg.de/doing-good

Open Science Initiative MPI CBS since 2018
Co-founder of the initiative. We organize workshops on Open Science-related topics, invite speakers for talks, and foster the implementation of good scientific practices at MPI CBS.
Info: cbs.mpg.de/de/cbs-open-science

SKILLS

Coding	R, Python, Matlab, Bash
Development	Git (Github, Gitlab)
Data analysis	fMRIPrep, SPM12, Brain Imaging Data Structure (BIDS), Nilearn, mixed-effects models, multivariate analysis, graph theory
Experimental programming	Presentation
Methods	Functional and structural magnetic resonance imaging, transcranial magnetic stimulation, transcranial direct current stimulation
Writing	LaTeX, Markdown, MS Office
Design	Inkscape
Languages	German (native), English (fluent), French (fluent), Hebrew (basic)

OUTREACH

- Workshop "Introduction to Programming in Neuroscience" at Girls' and Boys' Day 2022
- Article on our Cerebral Cortex paper in Leipziger Volkszeitung, 09/2021: Link to article
- Article about my research at MDR Wissen (in German), 09/2021: Link to article
- Co-author on the Blog Thinky & Brain by MPI CBS, 08/2020: Link to article
- Guest at the Orion Open Science Podcast, 11/2019: Link to episode

JOURNAL REVIEWING

Ad-hoc-reviewing	Brain, Cerebral Cortex, Brain & Language, Frontiers in Psychology
Co-reviewing	Journal of Cognitive Neuroscience, NeuroImage, NeuroImage Clinical

PROFESSIONAL MEMBERSHIPS

- Organization for Human Brain Mapping (OHBM)
- Society for the Neurobiology of Language (SNL)
- German Association of Academic Speech-Language Therapy

List of Publications

Publications

Martin, S., Frieling, R., Saur, D., & Hartwigsen, G. (2022). Facilitatory stimulation of the pre-SMA in healthy aging has distinct effects on task-based activity and connectivity. Preprint: https://www.biorxiv.org/content/10.1101/2022.10.21.513185v1

Martin, S., Williams, K., Saur, D., & Hartwigsen, G. (2022). Age-related reorganization of functional network architecture in semantic cognition. *Cerebral Cortex*. doi:10.1093/cercor/bhac387

Kuhnke, P., Chapman, C., Cheung, V., Turker, S., Graessner, A., **Martin, S.**, Williams, K., & Hartwigsen, G. (2022). The role of the angular gyrus in semantic cognition: a synthesis of five functional neuroimaging studies. *Brain Structure and Function.* doi:10.1007/s00429-022-02493-y

Martin, S., Saur, D., & Hartwigsen, G. (2021). Age-dependent contribution of domain-general networks to semantic cognition. *Cerebral Cortex*. doi:10.1093/cercor/bhab252

Darkow, R., **Martin, S.**, Burchert, F., Meinzer, M., & Flöel, A. (2015). Effekte von Benenntraining und Diskurstraining auf Spontansprache bei Aphasie: Ein Einzelfall unter transkranieller Gleichstromstimulation. *Sprache, Stimme, Gehör, 39*, 140-145. doi:10.1055/s-0035-1559656

Talks

About my research

Würzburger Aphasietage, virtual format   03/2022
Aphasia as neural network disorder

Psychologie und Gehirn (PuG), virtual format   06/2021
The role of domain-general networks in semantic processing in the young and the aging brain
Presented at symposium "Cognition and plasticity in the aging brain". I also organized and chaired the symposium.

German Academic Scholarship Foundation, virtual format   03/2021

Domain-general networks in semantic processing in the aging brain

Presented at annual meeting for doctoral students of the German Academic Scholarship Foundation (Studienstiftung des deutschen Volkes).

Clinic Christophsbad, Göppingen, Germany   04/2019

The application of non-invasive brain stimulation techniques in neurorehabilitation

Invited talk at colloquium of rehabilitation clinic.

German Society for Aphasia Rehabilitation, Freiburg, Germany   11/2014

Expressing your own intentions with aphasia: A comparison of a naming and a discourse treatment, both enhanced by transcranial direct current stimulation

About Open Science

Colloquium at MPI for Human Cognitive and Brain Sciences, virtual format 01/2022

Advancing the responsible conduct of research at the MPI CBS

Invited talk to present a recommendations paper I wrote together with other researchers from MPI CBS (available here: osf.io/9n2at/)

Research Interactions Symposium by Wiley, virtual format   06/2021

Trust in science: How early career researchers benefit from open and transparent research practices

Invited talk at symposium organized by Wiley.

Conference proceedings & posters

Martin, S., Saur, D., & Hartwigsen, G.   06/2021

Age-dependent contribution of domain-general networks to semantic cognition

Organization for Human Brain Mapping (OHBM), virtual edition

Martin, S., Saur, D., & Hartwigsen, G.   11/2020

The multiple-demand network in language processing of the young and the aging brain

Clinical Neurophysiology 131(4):e201-e202

van Scherpenberg, C., **Martin, S.**, Hartwigsen, G., Obrig, H., & Beese, C.   09/2019

Age-related decline of semantic inhibition despite the preservation of semantic memory

PaePsy, Leipzig, Germany

Martin, S., Saur, D., & Hartwigsen, G.   08/2019

The multiple-demand network in language processing: Its role in the aging brain

11. Annual Meeting of the Society for the Neurobiology of Language (SNL), Helsinki, Finland

Martin, S., Darkow, R., Burcher, F, Meinzer, M., & Flöel, A.   09/2014
Improving communication in aphasia: A comparison of naming- and discourse based treatment,
both facilitated by transcranial direct current stimulation (tDCS)
Science of Aphasia, Venice, Italy

Darkow, R., Meinzer, M., **Martin, S.**, Würtz, A. & Flöel, A.   12/2013
Transcranial direct current stimulation and aphasia
German Society for Neurorehabilitation, Berlin, Germany

Acknowledgments

This thesis marks the end of a journey that was full of instructive, fun, surprising, occasionally insecure and challenging, but at most times grateful moments. Being faced with a pandemic, brought unforeseen challenges to my PhD but for every issue there was a solution because of the amazing people I work with. This thesis would not have been possible without the endless support of so many people.

First and foremost, I want to express my deepest gratitude to PD Dr. Gesa Hartwigsen for supervising and mentoring my research. Thank you for always motivating and sharing your ideas with me. Your continued guidance, your enthusiasm and supervision were the foundation of my dissertation. I am deeply grateful for all the time you invested in this research and your excellent support in all intellectual and everyday matters. I am also very grateful to my supervisor Prof. Dr. Dorothee Saur for her continuous guidance and the opportunity to work together with her and the Language & Aphasia Lab.

I am deeply grateful for all the support I received from former and current members of the MPI for Human Cognitive and Brain Sciences. Along the way, I have met many inspiring researchers and committed colleagues, who made my work possible. Special thanks to my colleagues and friends from the Cognition & Plasticity Lab: Working with you during the past years made my dissertation experience fun and memorable. I would like to particularly thank my lab mates Jana Klaus, Stan van der Burght, Kathleen Williams, Ole Numssen, Philipp Kuhnke, Astrid Graessner, Anna Rysop, Laura Nieberlein, Curtiss Chapman, Pei-Ju Chien, and Sabrina Turker. Sharing thoughts, ideas, and coffees with you in the past years—both virtually and in person—kept me motivated. I would also like to thank my colleagues from the Neuropsychology department where I started my PhD journey. Sharing the office with my two Claras, Clara Kühn and Clara Eckerdt, along with the guidance of Caroline Beese gave me the best arrival possible. You made sure I knew what I was getting into and your unlimited knowledge about the MPI made the beginning of my PhD so much easier.

I also want to thank all the people who supported and continue to support all things Open Science at the MPI and invest their time and energy for the greater cause of good scientific practice. A special thanks goes to my dear friend Cornelia van Scherpenberg, my partner in crime of "Doing Good". Your shared enthusiasm for open and responsible research made the organization of a whole symposium next to our everyday PhD work possible. Thank you for continuing to be such a great friend.

I am deeply grateful to all my friends who do not necessarily always understand what and

why I am doing research but who nonetheless support me and are always next to me to keep me sane and make me laugh. Special thanks to two of my closest and oldest friends, Christopher Izgin for all our shared nerdy academic moments, and Josefine Andronic for reminding me that academia is only a small part of my life. I am deeply grateful to my close friends Sasha Khakalo, Yael Farhy, and Liesa Didoff. Endless nights with Weißweinschorle and Paloma along with runs on the field and even some gardening work made the past years wonderful, and I am so lucky to have such great friends in my life.

I am also very grateful to all the student assistants and interns who supported my research and helped me through the stressful moments of data acquisition. I owe my deepest gratitude to the participants of my experiments, without whom none of these projects would exist and whose curiosity and belief in science makes them endure at times boring or exhausting experimental set-ups. I am very grateful to the Studienstiftung des deutschen Volkes for funding my research at the MPI and making my PhD possible.

And finally, last but by no means least, I want to thank my family for all your love and for always encouraging me. My parents, for having unlimited trust in my choices and my abilities, and my sister Anne for always supporting me from far, and helping me to keep my spirit up. Words can hardly describe my gratitude to my partner Nir: Thank you so much for joining me on this roller coaster ride called PhD, your limitless support and for always being next to me, no matter how strong the doubts. Thank you for anchoring me in love and laughter.